Assessing the remaining life of the Hollandsche IJssel storm surge barrier

H. Vader

TU Delft

Deltares

Assessing the remaining life of the Hollandsche IJssel storm surge barrier

by

Hidde Vader

to obtain the degree of

Master of Science
in Civil Engineering

at the Delft University of Technology,
to be defended publicly on Friday 5 November 2021 at 4:00 PM.

Student number:	4494741	
Project duration:	9 November 2020 – 5 November 2021	
Thesis committee:	Prof. dr. ir. S.N. Jonkman,	TU Delft
	Dr. ir. A.M.R. Bakker,	TU Delft
	Dr. ir. M. van den Boomen,	TU Delft
	Ir. E.S. van Baaren,	Deltares
	Dr. ir. F.L.M. Diermanse,	Deltares

An electronic version of this thesis is available at `http://repository.tudelft.nl/`.

Cover photo: The Hollandsche IJssel barrier (Rijkswaterstaat, 2018a)

TU Delft Delft University of Technology

Deltares

Preface

For the sake of nostalgia, I could say that my interest in civil engineering begun at a young age while playing with building-block toys such as Lego or building sandcastles on the beach. That would make a nice story, but unfortunately it is not true. The choice for civil engineering was a pragmatic one that I made to bridge the time until I was eligible for a different study programme and out of interest in mathematics and physics. As I continued with the study, I became more fascinated by the field of civil engineering. It interested me so much that I decided to pursue a master's degree in hydraulic engineering, which culminated in the completion of this thesis.

The process of writing this thesis has been challenging, though not in the way I expected beforehand. As an engineering student, you may struggle with comprehending abstract science concepts or solving complex equations. However, I found that the most difficult part of the research was to accept that sometimes a relatively simple analysis suffices. The quality or level of the study is not always determined by the appearing complexity, and the inverse, simplicity, does not necessarily mean doing easy work. It is this realisation that I hope to keep in mind for the future.

Although working on this thesis has mostly been an individual process, I could not have made it to this point without the contribution, help, and support of a number of people. First of all, I would like to express my gratitude towards Alexander Bakker for your enthusiasm and help when I lost track of the big picture. I enjoyed our sometimes diverging discussions. I also have to thank Bas Jonkman for chairing my committee and investing time and effort in this research. Furthermore, I would like to thank Martine van den Boomen, your constructive criticism, especially at the start, provided much-appreciated guidance during the research. A special thanks also to Esther van Baaren and Ferdinand Diermanse of Deltares for offering the opportunity to conduct my research at Deltares and the supportive feedback during the project.

Finally, I would like to thank my friends and family for taking my mind off my studies from time to time. I am particularly grateful to my parents for the unconditional support and for enabling me to broaden my horizon. The periods abroad were undoubtedly the best experiences of the past six years.

Hidde Vader
Cruquius, November 2021

Abstract

Monday 22 October 2018 marked the 60th anniversary of the Hollandsche IJssel storm surge barrier. This structure is expected to last another 40 years, but replacement or renovation may be needed sooner than anticipated due to factors such as climate change and societal developments. Yet, there is relatively little known about what factors and how these factors influence the remaining life of the storm surge barrier, and methods that can be used to estimate the remaining life of the barrier are lacking. This thesis aims to identify the dominant factors and associated uncertainties affecting the remaining life and to provide a method for the estimation of the remaining life of the Hollandsche IJssel storm surge barrier. The focus of the study is on the functional and technical life of the storm surge barrier as the economic life is not expected to be governing for this kind of structure with enormous investment costs.

First, the functions and structural components of the storm surge barrier were identified. For each function, requirements were formulated to support the evaluation of the impact of the external drivers. The physical decomposition of the storm surge barrier was needed to identify the dominant deterioration mechanisms, such as carbonation of concrete and steel corrosion, and external drivers influencing these mechanisms. The analysis of the deterioration mechanisms revealed that none of the mechanisms result in the end of the technical life of non-replaceable components, which led to the conclusion that the technical life is not dominant for the total remaining life of the Hollandsche IJssel barrier. Therefore, the focus should mainly be on the functional life in the further analysis of the lifespan of the storm surge barrier.

Next, the impact of external drivers on the functional performance or technical state of the storm surge barrier was assessed by a semi-quantitative analysis in which scenarios with the projected changes were used to evaluate the impact of the respective drivers. The external drivers were grouped into physical drivers, such as sea level rise, precipitation and land subsidence, and societal developments. The latter was further subdivided into socio-economic changes and policy changes. For the majority of the drivers, with the exception of sea level rise, future changes were found to be too small to be of importance, or the impact on the functional performance or technical state of the barrier was argued to be limited. Sea level rise was found to be the most important external driver because of the potentially large future changes and far-reaching consequences, which are mostly caused by the associated increase in the number of closures.

As the remaining life of the storm surge barrier was found to be governed by functional aspects and largely dominated by sea level rise, methods or models were proposed to relate the functional performance to sea level rise. The functions for which methods were discussed include flood protection, navigation, and water management. The other functions of the storm surge barrier were not considered due to a lack of quantitative requirements. The approach for the flood protection function comprises the comparison of extreme water levels (return period of 30,000 years) for various amounts of sea level rise with an assessment water level ("beoordelingspeil") to estimate the critical amount of sea level rise for which the functional performance is no longer sufficient. The assessment water level corresponds to the water level with a 30,000-year return period and a non-closure probability of 1/200 (or 1/1,000) per closure. The second non-closure probability is set to be achieved in 2030 according to the Delta Programme, and thus included to anticipate for the future policy change. This approach with assessment water levels assumes that the remaining life of the storm surge barrier with respect to flood protection is zero years for the non-closure probability that was used for the assessment water level (1/200 or 1/1,000 per closure). This assumption is justified since extensive dike reinforcement are currently required to comply with the flood protection standards. Without these dike reinforcements the end of functional life would thus indeed have been reached if the non-closure probability is not reduced. For the navigation function, the number of closures and total yearly duration of the closures were calculated as a function of sea level rise using water level measurements of the past 50 years. The probability of a “maalstop”, the situation in which the discharge of water from the pumping stations into the Hollandsche IJssel has to be ceased, was calculated for several scenarios of sea level rise to evaluate the performance of the water management function. The resulting probabilities of a “maalstop” were deemed sufficiently small for the function to be non-critical. Another aspect to consider is that local water authorities may have the possibility to release water into other waterways than the Hollandsche IJssel to reduce the likelihood of a "maalstop". For this reason, the water management function was excluded from the further analysis of the remaining life of the Hollandsche IJssel barrier.

Estimates of the remaining life of the storm surge barrier were then obtained by combining the required performance levels for the flood protection and navigation function expressed as critical amounts of sea level rise with various sea level rise projections. Multiple sea level rise projections were considered to deal with the deep uncertainty associated with the projections. This deep uncertainty was also reflected in the estimates of the remaining life by wide uncertainty ranges and differences between the estimates for separate sea level rise projections.

One of the key findings in relation to the remaining life of the Hollandsche IJssel barrier is that even for moderate sea level rise scenarios, the end of life of the storm surge barrier could be reached within 20 years based on the median values for the most stringent assessment water level for the flood protection function (NAP +2.90 m) and the most stringent requirement for the navigation function (nine closures per year). However, these estimates are uncertain, and a considerably longer lifespan cannot be ruled out. Furthermore, the results suggest that the estimates of the remaining life of the barrier are greatly influenced by the choice for the assessment water level, the non-closure probability, and the acceptable number of closures. The choice for one of the two assessment water levels depends on the desired conservatism in the evaluation of the remaining life, but may also have practical implications since extensive dike reinforcements are currently required to comply with the flood protection standards of the dike trajectories along the Hollandsche IJssel. Reducing the probability of non-closure of the storm surge barrier was found to be an effective measure to lengthen the remaining life with respect to the flood protection function, and could be a measure to reduce the required dike reinforcements. For instance, an extension of the lifespan in the range of eight to 40 years could be achieved by reducing the non-closure probability of the storm surge barrier from 1/2,000 to 1/5,000 per closure. Similar extensions of the lifespan with respect to the navigation function could be obtained by accepting 15 or 30 closures per year instead of nine, though this would result in more hindrance to shipping.

Ultimately, the essence of this study is to illustrate how the complex issue of the remaining life of a hydraulic structure, such as the Hollandsche IJssel barrier, could be approached in a systematic manner in which the external drivers or factors that may affect the remaining life in terms of the functional performance or deterioration of components are identified first. The subsequent focus on only the most important or dominant drivers turns the problem into a more manageable one. The second part of the study, the estimation of the remaining life, is then optional if one wishes to not just identify the most important drivers, but also assess the impact on the remaining life of the structure. In this case, possible approaches to assess the impact of sea level rise on the remaining life of the Hollandsche IJssel barrier have been presented. As mentioned before, the results reveal that there is a significant probability that the end of life of the Hollandsche IJssel barrier will be reached earlier than previously anticipated. Accordingly, it is recommended to investigate possible measures to lengthen the lifespan and determine the best moment in time to implement these measures. A more system-oriented approach is recommended for this kind of analysis since modifications to a certain object could impact other elements within the system, e.g. dike reinforcements affect the required closure reliability of the storm surge barrier. In addition, economic considerations should be included as the decision to implement specific measures will be dependent on the costs and benefits. Finally, a more general recommendation is to perform similar studies for other critical structures as the remaining life of those structures may also be reached sooner than anticipated if, for example, functional aspects are taken into account.

List of Figures

List of Tables

Nomenclature

Acronyms

CLO	Environmental Data Compendium (Compendium voor de Leefomgeving)
CPB	Bureau for Economic Policy Analysis (Centraal Planbureau)
e-EOL	End of economic life
f-EOL	End of functional life
HIJK	Hollandsche IJssel barrier
IPCC	Intergovernmental Panel on Climate Change
KNMI	Royal Netherlands Meteorological Institute (Koninklijk Nederlands Meteorologisch Instituut)
KNMI'06	Climate change scenarios for the Netherlands 2006
KNMI'14	Climate change scenarios for the Netherlands 2014
KWA	An alternative route for the supply of fresh water to the areas that normally take in water from the Hollandsche IJssel in case the extraction from the Hollandsche IJssel is ceased due to high chloride concentrations (Klimaatbestendige WaterAanvoer)
MHWS	Governing high water level (Maatgevende Hoge Waterstand)
MLK	Maeslant barrier
NAP	Amsterdam Ordnance Datum (Normaal Amsterdams Peil)
PBL	Netherlands Environment Assessment Agency (Planbureau voor de Leefomgeving)
RCP	Representative Concentration Pathway
RMD	Rhine-Meuse delta
SLR	Sea level rise
SROCC	Special Report on the Ocean and Cryosphere in a Changing Climate
t-EOL	End of technical life
WBI	Statutory Assessment Tools (Wettelijk Beoordelingsinstrumentarium)
WLO	Socio-economic scenarios for the Netherlands, which are called Prosperity and the Living Environment (Welvaart en de Leefomgeving)

List of Terms

Assessment (water) level	Water level used to evaluate the functional performance with respect to flood protection (Beoordelingspeil). The assessment water level corresponds to the 1/30,000-year water level and a non-closure probability of the Hollandsche IJssel barrier of 1/200 (or 1/1,000) per closure.

Deep uncertainty	A situation in which parties cannot agree upon (1) methods or models to describe the system, (2) the probability distributions to represent the uncertain key variables and parameters of the models, and/or (3) how to value the desirability of alternative outcomes (Lempert et al., 2003).
Delta Programme	A national programme of the Dutch government in which strategies and plans are developed to protect the Netherlands from flooding, ensure a sufficient supply of fresh water, and achieve a climate-proof and water-resilient Netherlands by 2050 (Deltaprogramma, 2020).
Economic life	The time period over which the costs of owning and operating an asset are still less than the costs of equivalent alternatives.
Functional life	The time period during which an asset complies with the functional requirements. The end of the functional life could be reached due to changing physical conditions, societal developments, or altering functional requirements.
Hydra-NL	A probabilistic model to derive the hydraulic boundary conditions for flood defences in the Netherlands.
Maalstoppeil	Water level at which the discharge of water from the pumping stations into the Hollandsche IJssel is ceased.
Remaining useful life	The remaining time period that an asset is expected to be used or in service (ISO, 2019; Sullivan et al., 2019).
Sea Level Rise Knowledge Programme	A joint research programme of many parties that aims to gain better insight into sea level rise and the associated uncertainties, assess the impact of a rising sea level on flood risk management and freshwater supply in the Netherlands, and explore long-term strategies to ensure the Netherlands is well-prepared to cope with the consequences of sea level rise (Ministerie van Infrastructuur en Waterstaat, 2019).
Storm surge barrier	A fully or partly moveable barrier than can be closed temporarily to limit the extreme water levels in the hinterland and thereby provide protection against flooding.
Technical life	The time period until an asset is no longer able to fulfil its functions according to the original functional requirements due to deterioration of non-replaceable components or the use of outdated technologies.
Unavailability	Total average yearly duration of closures of the storm surge barrier.

Contents

1

Introduction

1.1 Replacement and renovation of major hydraulic structures

As in other developed economies, many Dutch infrastructure assets date back to the early 20th century or were constructed in the second half of the 20th century. With much of these structures nearing the end of their design life in the coming decades, major replacement and renovation tasks will have to be carried out. However, it is not just these older assets that are in need of replacement or renovation. Changing demands, intensified utilisation, and climate change accelerate the ageing and make that even relatively new structures may have to be replaced soon. This replacement and renovation demand poses an enormous challenge to Rijkswaterstaat from the planning as well as the financial perspective. The estimated required investments are in the order of hundreds of millions of Euros a year, €672.8 million per year for the period 2031-2040 and €757.7 million per year for 2041-2050 (Klatter et al., 2019). The projected funding causes the replacement and renovation programme to be a serious issue for Rijkswaterstaat and the Ministry of Infrastructure and Water Management.

A substantial part of the replacement and renovation programme concerns assets that are part of waterways, regulate water levels, provide flood protection, or enable the crossing of waterways, i.e. structures in the wet infrastructure (Rijkswaterstaat, 2017b). Many of these structures were also built before or in the first decades after the second world war. As a result, more than 200 wet infrastructure assets are reaching the end of their design life in the next 40 years (Bles et al., 2015).

Storm surge barriers are an example of wet infrastructure assets that may have to be replaced within several decades. These massive, moveable flood defences were commissioned in the second half of the last century and the early 21st century, between 1958 and 2002. Given the age of the structures, replacements can be expected for the older barriers, but, as said before, changing functional requirements and uncertainties in external conditions could potentially have a large effect on the actual remaining life (Tosserams, 2014; Van der Vlist et al., 2016). Take, for instance, the Maeslant barrier, which became operational in 1998. It was expected that the barrier could be in use until the end of the century since the design life is 100 years, but sea level rise could shorten the life drastically. During the design of the barrier, a sea level rise of 0.25 m over a period of 50 years was accounted for (Ministerie van Verkeer en Waterstaat & Bouwkombinatie Maeslant kering, 1989), and according to current climate projections, this value could be reached as early as 2030 in case of extreme sea level rise projections or as late as the end of this century for the most moderate scenario (IPCC, 2019; Le Bars et al., 2017; Van den Hurk et al., 2014). The high-end sea level rise scenarios could thus more than half the useful life of the barrier. The example of the Maeslant barrier and sea level rise clearly shows why it is insufficient to rely only on the design lifespan for the management of the assets. To obtain a more accurate overview of the total replacement demand for the coming decades and to reserve the required funds, it is vital to gain better insight into the time period that these structures are expected to be used, i.e. remaining useful life (ISO, 2019; Sullivan et al., 2019).

1.2 Lifespan concepts

Every infrastructure asset has a lifespan that ends at a certain point, but what is actually meant by the lifespan of structures? It is a somewhat vague term as researchers and asset managers interpret the concept in different ways depending on the disciplinary perspective. For this study, the lifespan is referred to as the time

period that an asset is expected to be used (ISO, 2019; Sullivan et al., 2019). The asset could be considered to have reached the end of life when it has to be replaced due to inadequate performance. The evaluation of the performance could be based on technical grounds, i.e. structural state of the asset, technological developments, regulatory standards, economic considerations, or societal values (Lemer, 1996). Ferry and Flanagan (1991) distinguish the functional, physical, technological, economic, and social/legal life. This classification of lifespans was also adopted by Woodward (1997) and the Royal Institution of Chartered Surveyors (RICS) (2016). However, more often the distinction is made between only three lives: the technical, functional, and economic life. Yet, authors are still inclined to use different definitions for these three concepts. In the next sections, some definitions of the three lifespans are presented. This discussion is by no means a complete overview of the concepts, it is merely to illustrate the diffuse terminology used by people and to establish the definitions used in this study.

Technical life

Hermans (1999) defines the technical life as the period over which an asset is expected to physically exist until major renovation or replacement is required. A limitation of this definition is the imprecise phrase "physically exist". A better definition should include criteria for the physical performance. Such a definition is used by Rijkswaterstaat in their report *Staat van Infra RWS* (2020b): "the end of the technical life is reached when - with regular maintenance - the prescribed safety levels or required technical performance levels cannot be met". Similar definitions are given by other authors (Bles et al., 2015; de Jonge et al., 2018; Wilkinson et al., 2014). According to these definitions, the end of the technical life could be reached either by degradation of the structure (strength deterioration or ageing of technologies) or higher performance requirements associated with increased loads. The latter aspect could cause difficulties in discerning the difference between technical life and functional life. For instance, flood protection structures are designed to retain water; it is their primary function. With time, the asset ages and the strength decreases, this clearly affects the technical life. At the same time, the design water level could increase (due to sea level rise) up to a point that the structure is not able to withstand the loads. From one point of view, one could say that the structure has reached the end of its technical life as the strength is insufficient to cope with the increased loads, but from another perspective, the functional life of the asset has ended since it is no longer able to perform its water-retaining function. To overcome this ambiguity, the following definition is proposed for the technical life:

> *The time period until an asset is no longer able to fulfil its functions according to the original functional requirements due to deterioration of non-replaceable components or the use of outdated technologies.*

As a consequence of this definition, only the deterioration and ageing is analysed for the end of the technical life. The increase of loads is seen as an external change that is considered when studying the functional life.

Functional life

Van den Boomen et al. (2019) state that the end of the functional life is reached when an asset can no longer fulfil its original functions; Hermans (1999) and Klatter and Van Noortwijk (2003) give similar definitions. However, by including the term "original", the possibility of assigning new functions to an asset that could influence the end of life decision is disregarded. For instance, due to sea level rise, the boundary between salt and fresh water might shift more inland at the expense of the quality of the water that is used for other purposes, such as irrigation or drinking water. The decision could then be made that the asset should also limit this salt intrusion, albeit this need was not considered in the original functional requirements. A more comprehensive definition would therefore be one that accounts for dynamic functional requirements. Such a definition is provided by several authors (J. Bakker et al., 2016; de Jonge et al., 2018; Wilkinson et al., 2014) and is also adopted for this study:

> *The time period during which an asset complies with the functional requirements. The end of the functional life could be reached due to changing physical conditions, societal developments, or altering functional requirements.*

Economic life

Assessing the economic life often involves an evaluation of the costs and benefits of an asset. Following this idea of balancing costs and benefits, de Jonge et al. (2018) and Wilkinson et al. (2014) define the economic life as the period during which the benefits of the asset outweigh the costs. The flaw of this definition is that

it does not consider the possibility of lower-cost alternatives. Some structures could have a positive benefit-cost ratio, but other options might be economically more attractive. A second issue is that if the terms costs and benefits are not well specified, the difference between functional life and economic life could be a large grey area. For example, more frequent closure of a storm surge barrier causes more hindrance to navigation, thereby increasing the incurred costs or reducing the benefits of a barrier. The additional costs or deprived benefits could be used to express the functional performance of the barrier, but these costs could also be incorporated in the assessment of the economic life. For this reason, some researchers do not separate functional and economic life (PIANC, 2008; Van Veelen, 2016). To make a better distinction between functional and economic life, one could restrict the definition to the costs of owning and operating the asset (Hermans, 1999; Hertogh et al., 2018; Sullivan et al., 2019). Thus, the economic life is defined as:

> *The time period over which the costs of owning and operating an asset are still less than the costs of equivalent alternatives.*

1.3 Prior research on the lifespan of infrastructure assets

The anticipated replacement and renovation challenge has meant that quite some research is now aimed at better determining the residual life of structures. Besides the highly simplified approach of the design life, the technical, functional, and economic performance are increasingly considered. A number of interesting studies are listed in Table 1.1 and discussed below.

Table 1.1: Overview of relevant studies related to the lifespan of infrastructure.

Study	Type of lifespan	Research approach	Focus area
Kallen et al. (2014), Nicolai and Klatter (2015)	Technical life	Statistical analysis of lifespan of assets using a Bayesian model ("DISK Pro") and lifespan data	Lifespan of groups of structures, both hydraulic structures as well as road infrastructure
Gaal (2004)	Technical life	Literature study to develop physical models	Prediction of chloride-induced deterioration and carbonation of concrete bridges
Heutink et al. (2004), Nicolai et al. (2007)	Technical life	Review of stochastic model using inspection results	Prediction of the corrosion of steel gates, in particular the gates of the Haringvliet sluices
de Groot-Wallast and Van Twuiver (2019)	Functional life	Literature study, interviews	Functional life of hydraulic structures in general
Von Meijenfeldt et al. (2017)	Functional life	Quantitative analysis using WBI2017 guidelines and expert judgements	Impact of sea level rise on the flood protection function of Eastern Scheldt (storm surge barrier)
Op 't Landt (2018)	Functional life	Quantitative risk analysis using probabilistic models and expert judgements	Impact of sea level rise on the flood protection function of the Maeslant barrier and Eastern Scheldt barrier
Welsink (2013)	Functional life	Development of new design for the Hollandsche IJssel barrier	A large part of the study focuses on the structural strength of the storm surge barrier for the current and future situation with sea level rise
J. Bakker et al. (2016)	Economic life	Review of an earlier developed tool	Economic evaluation of life cycle costs of existing structures
Van den Boomen (2020)	Economic life	Development of replacement models using case studies	Economic optimisation of the replacement of infrastructure assets

The deterioration of structures has been the subject of several studies. Rijkswaterstaat developed a method to generate statistical estimates of the remaining technical life of structures (Kallen et al., 2014; Nicolai & Klatter, 2015). The method, called "DISK Pro", provides a first estimate of the end of life for groups of similar structures (e.g. navigation locks, movable bridges) using Bayesian inference. The lifespan is represented by a Weibull distribution and lifetime data of existing and demolished structures are used to derive the posterior prediction of the lifespan of the group of structures. Unfortunately, the results for individual structures cannot

be used due to too large uncertainties in the end of life estimate. Moreover, it was not possible to apply this statistical analysis to the storm surge barriers due to the limited number of barriers (Klatter et al., 2019). Apart from these limitations, one could question whether such a method gives a good indication of the technical lifespan because the data used for the distributions only include the lifetime of structures and not the reason why a structure reached the end of its life. Structures could still be in good condition but be replaced because of a capacity problem or as part of a new development plan for the area.

Other approaches to assess the technical life of individual structures include applying physical models to study the deterioration processes or using stochastic models without describing the exact physical process but using expert judgement or inspection data to predict the deterioration. The first approach was adopted by Gaal (2004) to predict the deterioration of concrete bridges by modelling the reinforcement corrosion with physical models based on Fick's laws of diffusion. This method for concrete deterioration modelling can be used for other structures as well, but the quality of the results is largely determined by the input parameters, which can be very case-specific. The second approach using expert judgement or inspection data has been applied to the storm surge barriers several times. An example in which stochastic models were applied, is the case of corrosion of the steel gates at the Haringvliet sluices (Heutink et al., 2004; Nicolai et al., 2007). Inspection data were used to estimate the parameters of the gamma process or the Brownian motion process that were used to describe the expected deterioration of the steel. Often, the approaches discussed above were aimed at modelling the deterioration of specific elements to improve maintenance strategies and thereby prevent the structure from reaching the end of its technical life rather than estimating the technical life.

In the past, the need for replacement was based on the technical state of an asset and the functional life was not really considered in the discussion of replacement or renovation. However, changing demands and changes in the spatial environment, cause the determination of the functional life to be more relevant (Klatter et al., 2019). Recently, the Method Functional Lifetime ("Methode Functionele Levensduur") has been developed (de Groot-Wallast & Van Twuiver, 2019). This method consists of five steps: (1) provide a description of the infrastructure asset, (2) describe the functions of the asset and how well the asset is performing on these functions, (3) identify future scenarios, e.g. the Delta scenarios, (4) specify the current and future requirements for the asset, and (5) assess the future functioning of the structure based on the input obtained from the previous steps in a qualitative or quantitative matter. How to perform the quantitative assessment of step 5 is still a topic of discussion. One option is to include existing models that are already applied to analyse water management issues and water flows (SOBEK), to assess the flood defences (Riskeer, Hydra-NL), or to perform network analyses for the inland waterway transport sector (BIVAS). This method is a first step to assess the functional life of structures. The method provides a framework and an overview of the existing models that could be used in the assessment of the functional life. More research is required to identify appropriate models and their added value, the uncertainties in different parts of the method, and how these uncertainties affect the estimated functional life (Breedeveld & Kramer, 2019).

A few studies have looked at the functional performance of storm surge barriers. For example, Von Meijenfeldt et al. (2017) studied the consequences of sea level rise on the flood protection system of the Eastern Scheldt, including the Eastern Scheldt barrier. It was found that the effects of sea level rise on the flood protection system of the Eastern Scheldt are limited up to 2050 (assuming 22 cm of sea level rise w.r.t. 2017). Improvements to the dikes mainly arise from the new, stricter flood protection standards of 2017. Between 2050 and 2100, more issues are expected. For example, the structural strength of the Eastern Scheldt barrier and the dike revetments may be insufficient. A second major issue is an increase in the number of closures. The closure frequency increases to 10 per year for 60 cm sea level rise and to almost 100 per year for 125 cm sea level rise. The thesis by Op 't Landt (2018) described the impact of sea level rise scenarios on the Maeslant barrier and the Eastern Scheldt barrier. Critical aspects for Maeslant barrier were found to be the structural strength and the current closure procedure. The loads on the ball joints become too high for 30 cm sea level rise. Adjustments to the closing procedure and closure reliability could extend the lifespan to 61 cm sea level rise. The limiting factor for the Eastern Scheldt barrier is the storage capacity in the Eastern Scheldt. The leakage volume during closures may result in exceedance of the storage capacity with 90 cm sea level rise or more. Reducing the leakage opening and modifying the moment of closure could extend the lifespan to 130 cm sea level rise. Finally, Welsink (2013) looked at adaptations to the structure of the Hollandsche IJssel barrier to improve flood protection and cope with sea level rise and salt intrusion. In his study, Welsink (2013), proposes to lower the closure level of the barrier from NAP +2.25 m to NAP +1.75 m. This change would require modifications to the steel gate of the barrier. The newly designed gate would be able to cope with 50 cm sea level rise. The conclusions of Welsink (2013) should, however, be interpreted with caution as an allowable head difference of 1.9 m was assumed for the current structure, whereas a head difference of 4.5 m was

reported for the design of the barrier (Rijkswaterstaat Deltadienst, 1957). In addition, Welsink (2013) did not study the effects of the lower closure level in terms of hindrance to shipping. The study is mainly concerned with the effects on the flood protection function.

For the economic life of assets, Rijkswaterstaat developed the Economic End of Life Indicator (EELI). This tool compares the life-cycle cost of maintaining an asset and replacing it in a statistically expected replacement year with the life-cycle cost of direct replacement and subsequent maintenance (J. Bakker et al., 2016). The EELI is a simple indicator that provides a clear statement of whether a structure should be replaced or not. However, the tool does not provide an indication of the end of the economic life according to the definition given above. It merely states whether an asset should be replaced at a given moment in time based on economic considerations. The tool does not compare earlier or later replacement moments that could be economically more beneficial. Van den Boomen (2020) provides a more dedicated analysis of the economic life by looking at different optimisation models based on the life cycle cost. One of the main findings of this study was the unsuitability of the classical net present value method for replacement optimisation since it often leads to suboptimal results. The research presents six other economic optimisation models for the life-cycle cost of infrastructure and evaluates the applicability of these models for different types of replacement challenges. Yet, the classical method (comparison of the net present value) remains attractive as the knowledge about the other optimisation methods is still very limited within organisations.

To summarise, several studies have looked at the technical, functional, or economic life of storm surge barriers, and structures in general. The deterioration of structures, relevant to both the technical and economic life, has been the subject of several studies, though these studies were predominantly aimed at modelling the deterioration of specific elements to improve current maintenance strategies. The functional life has not been given much attention in the past, and only in recent years, several studies have looked at the consequences of sea level rise on the functional performance of storm surge barriers with respect to flood protection. Only one study (Van den Boomen, 2020) was found that examined the economic life of infrastructure assets in detail. However, an evaluation of the storm surge barriers on economic grounds has not been performed yet.

Besides the assessment of the technical, functional and economic life, the role of external factors or structural properties and their uncertainties influencing the performance of the storm surge barriers have not been studied extensively. An overview of how and to what extent these factors play a role is lacking. For example, consider the external driver sea level rise. Sea level rise impacts a multitude of aspects related to the performance of a storm surge barrier. It influences the loads on the structure, the number of closures, but also the navigational and ecological function. Therefore, it is important to obtain a better overview of what aspects are exactly impacted by sea level rise. Apart from these factors themselves, their uncertainties have to be accounted for. The impact of sea level rise is usually studied by adopting only an upper percentile value of a certain climate scenario, but the role of sea level rise uncertainties on the performance of storm surge barriers have to be considered as well since the future should not simply be captured in some deterministic value. Besides sea level rise, more factors could potentially impact the performance of storm surge barriers, but not all factors are equally important. Hence, to gain better insight into the remaining life of structures it is also important to determine the dominant mechanisms or factors that lead to the end of life decision.

In short, there is a need for an alternative method to assess the remaining life of storm surge barriers because the existing approach using the design life is inadequate to timely arrange the required funding for replacement and renovation of the storm surge barriers. This alternative method should consider the technical, functional and economic performance, provide insight into the dominant factors that impact the performance of the barrier and incorporate the uncertainties in these factors.

1.4 Research focus

The previous sections show that knowledge on the technical, functional, and economic performance is required to gain better insight into the remaining life of storm surge barriers. However, the question is whether the economic life, as defined in Section 1.2, can be determined for storm surge barriers. Storm surge barriers are structures with a very long lifespan (100 years) and very high investment costs compared to the operational costs. So, especially under the assumption that the utilisation remains the same, it is unlikely that opting for the replacement asset will lead to lower costs. Even if the utilisation increases, replacing the barrier will not be favourable as the new storm surge barrier will run into the same problems as the old barrier. For example, changing circumstances may lead to an increase in the number of closures resulting in faster

deterioration and higher maintenance costs, but replacing the barrier does not resolve this issue as the deterioration of the components of the new barrier is accelerated as well. The technical state and functional performance will likely be governing for the remaining life of the storm surge barrier. Therefore, this study looks at the technical and functional life of the storm surge barriers.

Although all storm surge barriers serve the purpose of reducing the extreme water levels in the hinterland, each barrier is unique. These structures are tailor-made to the conditions at a particular location and the demands of stakeholders. The Maeslant barrier was designed with entirely different requirements than the Eastern Scheldt barrier. This uniqueness makes it quite challenging, if not impossible, to develop a generic method that can be used to estimate the remaining life of each storm surge barrier. Hence, this study focuses on a single storm surge barrier. The barrier chosen for the case study is the Hollandsche IJssel barrier. This is the oldest storm surge barrier in the Netherlands, and it will reach the end of its design life by the year 2058. As storm surge barriers typically have a lead-time (time for planning and implementation) of 20 to 40 years (Haasnoot et al., 2020; Hallegatte, 2009), it is particularly relevant to obtain better insight into the remaining life of this structure.

1.5 Research objective and questions

The lack of knowledge on the remaining useful life of the storm surge barriers is addressed in this study. This study seeks to assist in gaining more insight into the factors affecting the remaining life of the Hollandsche IJssel storm surge barrier and the remaining life of the barrier itself. Hence, the aim of this study is as follows:

> *(1) To identify the dominant factors and associated uncertainties affecting the remaining life and (2) to provide a method for the estimation of the remaining life of the Hollandsche IJssel storm surge barrier considering the uncertainties affecting the technical and functional lives.*

To achieve the research the main research questions, the following sub-questions are formulated:

1. What are the main functions of the Hollandsche IJssel barrier and their desired performance level?
2. What are the main physical components of the barrier and their mechanisms of deterioration?
3. What are the major external drivers affecting the functional performance and deterioration mechanisms, and thereby the residual life of the barrier?
4. What methods can be deployed to estimate the residual life of the barrier?
5. What is the remaining life of the Hollandsche IJssel barrier?

1.6 Research approach

The study can broadly be divided into two phases. In the first phase, factors or external drivers that could impact the remaining life of the Hollandsche IJssel barrier are identified. This phase is related to the first three research questions. The second phase is concerned with the last two research questions and the estimation of the remaining life of the storm surge barrier, for which the results of the first phase are used. For both phases, different methods are applied.

A literature study forms the basis for the first phase of the research. Literature, ranging from scientific studies to design reports, is collected to obtain better insight into the determining factors and how these factors can lead to the end of life. However, in some cases, when qualitative assessments are insufficient, quantitative methods have to be applied. The assessment of external drivers could thus be viewed as a semi-quantitative analysis. The relevant information from literature, information from interviews with the asset managers and other experts with knowledge on the Hollandsche IJssel barrier, and the results of quantitative assessments are used in a careful, systematic analysis leading to the identification of the dominant factors. The steps of this analysis can be derived from Figure 1.1. This approach starts with the definitions of the lifespan concepts that were given in Section 1.2. Then the functions and related requirements are identified. At the same time, the physical components of the structure and associated deterioration mechanisms are identified. The results of this step can be used in the final step of this phase in which the external drivers are analysed. The advantage of using this top-down approach is that it provides the desired systematic way for identifying what and how external drivers could affect the lifespan of the storm surge barrier. In case one would start by listing possible external drivers, there is a chance that important interactions or functions are overlooked as one could get mired in details.

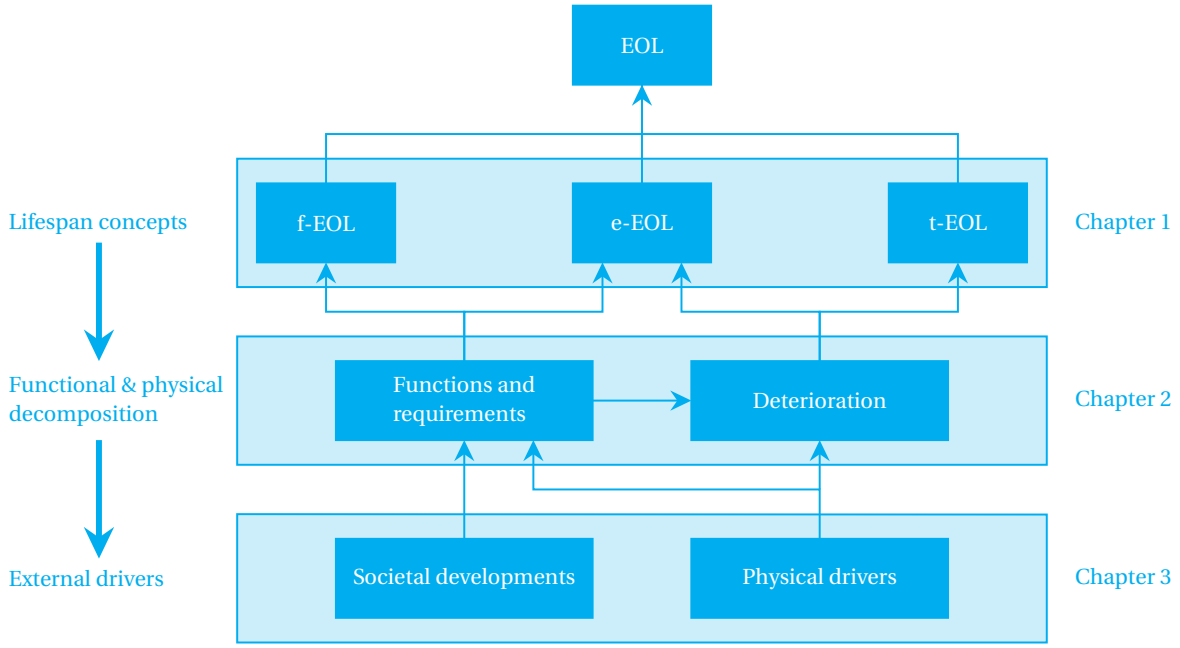

Figure 1.1: Relations between elements that result in the end of life of an asset. f-EOL = end of functional life, e-EOL = end of economic life, and t-EOL = end of technical life.

The second phase concerns the estimation of the remaining life of the Hollandsche IJssel barrier. Methods and models are explored to assess the functional and/or technical performance of the storm surge barrier. The choice for a specific method depends on whether models are available and suitable for the purpose. For example, the probabilistic model Hydra-NL is a widely applied model to derive the hydraulic boundary conditions for flood defences in the Netherlands. A new version has even been developed specifically for the Hollandsche IJssel. Hence, it makes sense to use this model to derive the hydraulic loads. The results can then be used to calculate the failure probabilities for different failure mechanisms in a different model. However, certain limitations to a model may also prohibit the use of the model. The applicability of specific models or approaches must therefore be carefully assessed. In all cases, the methods used to evaluate the performances should be sufficiently flexible, transparent, and fast to allow for a wide range of scenarios to be studied, but also take into account the uncertainties in the external drivers and properties of the structure.

1.7 Thesis outline

In Chapter 2, the Hollandsche IJssel storm surge barrier is introduced, its functions are analysed, and a physical decomposition is performed. The results of this chapter are used in the next two chapters. Chapter 3 focuses on the external drivers and their impact on the functional performances and technical state of the Hollandsche IJssel barrier. Chapter 4 presents the methods that are used for the estimation of the remaining life of the storm surge barrier. The results regarding the estimation of the remaining life can be found in Chapter 5. Chapter 6 discusses the outcomes, limitations, and implications of this study. Finally, in Chapter 7, conclusions are presented and recommendations for potential further research are stated.

2

Hollandsche IJssel barrier

The Hollandsche IJssel barrier is one of the seven storm surge barriers in the Netherlands (see Appendix A for a brief overview of all storm surge barriers). The barrier was built after the North Sea flood of 1953 (in Dutch referred to as the "Watersnoodramp") as part of the Dutch Delta Works. This chapter gives an introduction to this unique structure, describes the functions, and provides an overview of the main components of the storm surge barrier. Requirements are established for each of the functions, and the dominant deterioration mechanisms of the structural components are identified. These requirements could be used in the evaluation of the remaining functional life of the barrier. The identification of important deterioration mechanisms is relevant to the technical (and economic life). The chapter thus addresses the following research questions:

1. What are the main functions of the Hollandsche IJssel barrier and their desired performance level?
2. What are the main physical components of the barrier and their mechanisms of deterioration?

First, an introduction of the area in which the Hollandsche IJssel barrier is situated is given in Section 2.1. This area analysis produces valuable information for the functional analysis of Section 2.2, in which functions and corresponding requirements are identified. The next section (Section 2.3) focuses on the technical life rather than the functional life, as the main components of the barrier and their deterioration mechanisms are analysed. Finally, a summary of the findings of the previous sections and answers to the addressed research questions are provided in Section 2.4.

2.1 Introduction to the area

The Hollandsche IJssel storm surge barrier is located in the south-western part of the Netherlands, protecting one of the most low-lying parts of the country. The ground level in the hinterland is as low as NAP -6.76 m (Rijkswaterstaat, n.d.-b). The barrier closes off the Hollandsche IJssel, a tidal river that is of importance to shipping between the Port of Rotterdam and inland terminals, recreational navigation, and water management of the surrounding areas. The tidal river and the location of the Hollandsche IJssel system in the Netherlands are shown in Figure 2.1.

Figure 2.1: The Hollandsche IJssel situated in the south-west of the Netherlands.

2.1.1 Water system

The Hollandsche IJssel used to be a distributary of the river Lek until a dam was constructed near Nieuwegein in 1285 (de Nijs, 2008; van Groningen, 1996). The damming was intended to reduce the occurrence of floods and improve the drainage of peatlands, but it also caused the river to silt up as the influence of the tide was enhanced. The siltation was detrimental to the navigation on the river and flooding was again a threat. In the 19th century (1853-1860), the decision was made to canalise the Hollandsche IJssel from Nieuwegein to Gouda, where the Waaier lock was built. This second major intervention resulted in two separate waterways, which are now called the Hollandsche IJssel and Canalised Hollandsche IJssel. As a result of the construction of the Waaier lock and later the Juliana locks, the Hollandsche IJssel is now only under the influence of the sea through the river New Meuse for roughly the first 19 km. This tidal influence makes it a unique freshwater tidal river of high ecological value.

Besides the tide, the water level in the Hollandsche IJssel is affected by the presence of storm surge barriers, discharge of the river Rhine, spillage of water through the Waaier lock, and the many pumping stations along the river. Further downstream of the New Meuse, where it continues as the Scheur and later the Nieuwe Waterweg, the Maeslant barrier and Hartel barrier are located. These barriers lower the extreme water levels in the hinterland. The Hollandsche IJssel barrier further reduces the extreme water levels in the Hollandsche IJssel by limiting the flow of water from the New Meuse into the Hollandsche IJssel.

The discharge of the river Rhine is especially relevant for salt intrusion in the river. If the discharge of the Rhine falls below 1100-1200 m^3/s, salt water from the sea could reach the mouth of the Hollandsche IJssel and even reach further upstream. The water authorities speak of salt intrusion if the chloride concentration at the mouth is 50 mg/l higher than the background concentration in the Rhine at Lobith two days prior (Ministerie van Verkeer en Waterstaat et al., 2005). The ongoing supply of water to the surrounding areas could further increase the problem as the salt water is pulled further upstream. But even without large water withdrawal, the salt water could reach Gouda. Salt intrusion may put significant pressure on the freshwater supply of the region since the inlet near Gouda is the largest inlet in the area. In order to avoid the extraction of salt water, withdrawal at the pumping stations of the water authority Schieland en de Krimpenerwaard is ceased when the chloride concentration reaches 200 mg/l at the measuring point near Krimpen aan den IJssel. The water authority Rijnland stops the intake of water at the inlet near Gouda (pumping station Pijnacker-Hordijk) and shifts to the KWA (Klimaatbestendige WaterAanvoer) when a chloride concentration of 200-250 mg/l is reached, the Rhine discharge is lower than 1100 m^3/s and it is expected to last for some time (HydroLogic, 2016). The KWA ensures a certain amount of fresh water for the water authorities that normally take water

from the Hollandsche IJssel. Through the KWA, which more or less comes into force when a chloride concentration of about 250 mg/l is reached, Rijnland receives 6.9 m^3/s of fresh water through the lock at Bodegraven (originating from the Amsterdan-Rijn Canal and river Lek) of which 2.9 m^3/s is transferred to the water authority Delfland, which in turn transfers 1.0 m^3/s to the water authority Schieland en de Krimpenerwaard (Ministerie van Verkeer en Waterstaat et al., 2017). The KWA route is shown in Figure 2.2.

Figure 2.2: Freshwater supply to the water authorities through the KWA (HydroLogic, 2016; Provincie Zuid-Holland, 2018).

The KWA is considered an emergency measure and is insufficient for the long-term supply of fresh water to the water authorities. One of the decisions of the Delta Programme 2015 was to increase of the capacity of the KWA to 15 m^3/s. This KWA+ strategy entails an increase of the supply by the lock near Bodegraven to 10.5 m^3/s and the creation of a freshwater buffer near Gouda by letting water in from the Canalised Hollandsche IJssel through the Waaier lock. This expansion of the KWA capacity is planned for 2021 (HydroLogic, 2020; Ministerie van Verkeer en Waterstaat et al., 2017).

The spillage of water through the Waaier lock and the many pumping stations along the river serve the purpose of draining water from the polders as well as supplying fresh water to the surrounding areas. The fresh water is used to maintain the water levels in the vulnerable peat areas, for drinking water purposes, and it is a dominant source for the agricultural activities in Central Holland. Hence, the strict requirements regarding the chloride concentration in the Hollandsche IJssel.

2.1.2 Flood protection system

In 2017, the *Waterwet* was amended following a more risk-based approach to flood protection. This recent change means that most reports on the flood protection system include the old safety standards. Information referring to the old or new safety standards is treated separately in the next paragraphs to avoid any confusion for the reader.

Old safety standards

Before 2017, dikes were assessed based on the exceedance probability of a certain water level. The flood defences should be able to withstand certain hydraulic loads, which can be seen as an approach based on design loads (Jonkman, Voortman, et al., 2018). The conditions of the primary flood defences are investigated in safety assessments that were carried out every five years since 1996. In 2012, the interval was changed to 12 years to provide more time to complete reinforcement projects before the next assessment round (Jonkman, Jorissen, et al., 2018). The latest assessment round finished in 2011. This third national assessment showed

that significant segments of both dikes along the Hollandsche IJssel and the Hollandsche IJssel barrier failed to meet the standards. In fact, the safety level of the entire 19 km dike on the side of Capelle aan den IJssel was deemed inadequate (Kraaijenbrink, 2010). The dikes were susceptible to inner or outer slope instability and insufficient in height over large stretches of the dikes. For the storm surge barrier, the closure reliability was found to be insufficient (Witteveen+Bos, 2010).

New safety standards

The new safety standards are expressed as a probability of flooding rather than a probability of exceedance, following a risk-based approach. A second change concerns the use of the term dike trajectories. A trajectory is a segment of a dike ring for which the consequences of flooding are similar (Jonkman, Jorissen, et al., 2018). Following this definition, two trajectories of the same dike ring can have different safety standards, whereas the entire dike ring had the same probability of exceedance according to the old safety standards. The Hollandsche IJssel flows between two dike trajectories, 14-1 and 15-3. Dike trajectory 14-1 protects parts of the Randstad, a densely populated region of high economic importance. Hence, the high safety standard for the probability of flooding of 1/10,000 per year (signal value[1] is 1/30,000 per year). Trajectory 15-3 protects the polder Krimpenerwaard and has a safety standard of 1/3,000 per year (signal value of 1/10,000 per year). The Hollandsche IJssel barrier has to comply with two standards. The first one is similar to the safety standards of the dikes and is related to the loss of the water-retaining function. The second requirement prescribes the acceptable probability of non-closure. The failure probability in terms of loss of the water-retaining function equals 1/30,000 per year (signal value is 1/100,000 per year), and the prescribed probability of non-closure is 1/200 per closure. These safety standards are defined in the new law that came into effect in 2017 (Slootjes & Van der Most, 2016a). For more information on the new safety standards, see Section 3.6.

Reinforcement programmes

Several reinforcement programmes were set-up after the results of the conditions of the dikes along the Hollandsche IJssel were published in 2011. The most urgent sections of trajectory 14-1, near Capelle aan den IJssel and Moordrecht, were reinforced in recent years (Maronier, 2014). The reinforcement project of trajectory 14-1 started in 2014 and, as a consequence, the design was based on the old safety standards. Furthermore, the water authority Hoogheemraadschap Schieland en de Krimpenerwaard initiated the project Krachtige IJsseldijken Krimpenerwaard (KIJK), in which 10.51 km of trajectory 15-3 is strengthened to ensure that it will meet the safety standards by the year 2026 (Hoogheemraadschap van Schieland en de Krimpenerwaard, 2018). A third reinforcement project for trajectory 14-1, Capelle-Zuidplas, is planned for the near future. This project encompasses the reinforcement of 2.28 km of the dike west of the Hollandsche IJssel (HWBP, 2018).

Apart from dike reinforcement programmes, the possibility of increasing the closure reliability, i.e. reducing the non-closure probability, of the storm surge barrier has been investigated. Expensive dike reinforcements could be avoided by improving the reliability of the barrier. According to the Delta Programme, the non-closure probability of the Hollandsche IJssel barrier should be reduced from 1/200 to 1/1,000 per closure event by 2030 and a further reduction to 1/2,000 per closure event is strived for in later years (DRPD, 2020). The effects of such improvements on the water levels behind the barrier are significant as a study by HKV showed (Rongen & Maaskant, 2019). The water levels in the Hollandsche IJssel from Krimpen to Gouda for different closure reliabilities are presented in Figure 2.3.

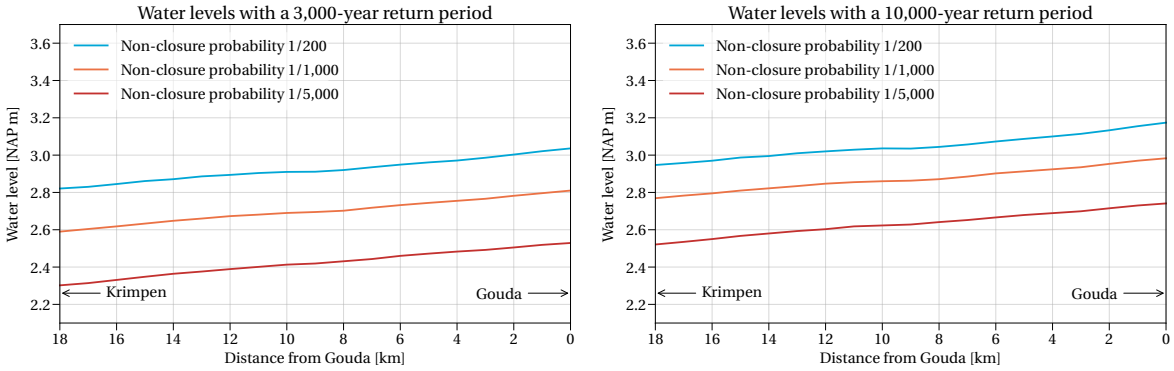

Figure 2.3: Water levels in the Hollandsche IJssel for two return periods neglecting the discharge of pumping stations, adapted from Rongen and Maaskant (2019).

[1] The signal value indicates the moment at which reinforcement works should be prepared (Jonkman, Jorissen, et al., 2018).

2.1.3 Navigation locks

Two lock complexes can be found in the upstream part of the tidal river near Gouda. The first one, the Waaier lock, marks the transition to the Canalised Hollandsche IJssel, and north of the Juliana lock complex, the waterway continues as the Gouwe canal. The Waaier lock was constructed in 1854-1856 as part of the canalisation project of the Hollandsche IJssel (van Groningen, 1996). It is one of the few locks of its kind and hence it has a monumental status (Rijksdienst voor Cultureel Erfgoed, 2020b). The lock is relatively small with the top of the sill being at NAP -2.80 m, a length of 24.5 m, and a width of 6.0 m (Rijkswaterstaat, n.d.-a). Due to the limited dimensions, the lock is predominantly used by recreational vessels; less than 400 commercial vessels and over 8000 recreational boaters passed the lock in 2002 (Jansen et al., 2010).

The Juliana lock complex, the older part to be more precise, dates back to the 1930s (1932-1935) and is a monument as well (Rijksdienst voor Cultureel Erfgoed, 2020a). The old lock chamber is 110 m in length, has a minimum width of 12 m, and the top of the sill lies between NAP -3.40 m and NAP -4.00 m (Rijkswaterstaat, n.d.-a). A second lock chamber was deemed necessary considering the potential growth of the inland waterway transport. The construction of this chamber was finished in 2014. The second chamber also improves the availability of the complex because one of the lock chambers can still be used if the other one is undergoing maintenance or suffers from a malfunction (Van de Sandt, 2014). The new chamber is 5 m longer (115 m), 2 m wider (14 m), and the top of the sill is at a slightly larger depth (NAP -4.40 m). Based on the lock dimensions and the depth of the waterway, vessels of CEMT class IV are able to pass the lock (Rijkswaterstaat, n.d.-a).

2.1.4 Storm surge barrier complex

The Hollandsche IJssel or Algera barrier (Figure 2.4) was constructed after the flood of 1953, which exposed the vulnerability of the dikes along the Hollandsche IJssel. Instead of extensive reinforcements of the dikes or damming the river, a storm surge barrier was built. The storm surge barrier would have the least impact on navigation, the discharge of water into the Hollandsche IJssel by the water authorities, and it would preserve the unique freshwater tidal environment. The barrier consists of two 80 metres wide vertical lifting gates made of steel and four 45 meters high concrete towers (Rijkswaterstaat, 2018b). The towers and the first gate were commissioned by the year 1958, but the second gate was put in place almost 20 years later in 1976 due to the high costs of the structure (Deltares et al., 2018).

Figure 2.4: The Hollandsche IJssel barrier (Rijkswaterstaat, 2018a).

It is generally stated by Rijkswaterstaat (2018b) and several other authors (Deltares et al., 2018; Mooyaart & Jonkman, 2017) that the barrier is closed when the expected water level at Krimpen aan den IJssel exceeds NAP +2.25 m, but a more formal closure strategy is documented in the *Waterakkoord* (Ministerie van Verkeer en Waterstaat et al., 2005; Rongen & Maaskant, 2019):

- If the expected water level at Hoek van Holland is between NAP +2.00 m and NAP +3.00 m and the discharge of water from the Rijnland polders into the IJssel is less than 100 m^3/s, the barrier closes at a moment such that the water level at Krimpen aan den IJssel does not exceed NAP +2.25 m.

- If the expected water level at Hoek van Holland is between NAP +2.00 m and NAP +3.00 m and the discharge of water from the Rijnland polders into the IJssel is more than 100 m^3/s, the barrier closes at low water slack prior to the storm surge.
- If the expected water level at Hoek van Holland exceeds NAP +3.00 m, the barrier closes at low water slack prior to the storm surge.

In short, a distinction can be made between closures based on the critical water level and slack water closures. For the closures at the critical water level, one of the gates is initially lowered from NAP +12.0 m to NAP -3.5 m with a speed of 0.02 m/s. In the final stage when the gate is 3 m above the sill (at NAP -6.5 m), the speed is reduced to 0.005 m/s and the closure is done in ten steps with a three-minute pause between each step to limit the formation of translatory waves. In total, such a closure would take approximately one hour. The benefits of the other type of closure, closure at slack water, is a larger storage capacity behind the barrier after closure and smaller translatory waves. In that case, the gate could be lowered within 25 minutes with a speed of 0.012 m/s. The barrier is opened once the water levels on both sides are equal. When, in closed condition, the outside water level is lower than the water level in the Hollandsche IJssel, e.g. in between two periods of high tide, water could be flushed from the Hollandsche IJssel (Van Balen et al., 2010). The barrier closes about three to four times a year due to expected high waters and once a month in the storm season (1 October to 15 April) for a test closure (Rijkswaterstaat, 2018b). If the barrier is closed due to a storm, the next planned closure is cancelled, but only if the storm closure is within two weeks of the test closure (Van der Graaf & Van Voorst, 2016). Consequently, the total number of closures per year fluctuates between six and nine closures and the ratio between test closures and storm closures could vary by year.

Next to the barrier, the Algera lock was constructed to enable vessels to pass when the barrier is closed (for water levels up to NAP +2.50 m) or the vertical clearance is insufficient. This navigation lock has a chamber width of 23.9 m, and the top of the sill is at NAP -5.20 m. The chamber length varies due to the tidal nature of the river and the use of mitre gates. During high tide, the chamber length is 139 m and during ebb the length is 120 m (Rijkswaterstaat, n.d.-a). Consequently, the lock is suitable for vessels up to CEMT class Va.

Together with the construction of the storm surge barrier, a bridge was built to connect the Krimpenerwaard to the city of Rotterdam. This bridge is part of the regional road N210 and was completed at the same time as the storm surge barrier, but the entire road N210 was only opened for traffic in 1965. The bridge has one lane in each direction and a reversible lane to improve the traffic flow in one of the directions. Nevertheless, the corridor over the Algera bridge is characterised by highly congested traffic (Studio Bereikbaar, 2019).

2.2 Functional analysis

The most recognisable function of storm surge barriers is to provide protection against flooding. However, these structures never fulfil only one function as less expensive solutions would then be implemented. Other functions could follow from requirements of the area in which the barrier is situated. For example, if a barrier is located in an important shipping channel, it should also facilitate navigation. The main functions of the Hollandsche IJssel barrier are listed in Table 2.1. These functions are introduced and discussed below. Requirements for these functions are also formulated based on the description of the functions. These requirements are essential for the determination of the remaining life of the barrier.

Table 2.1: Functions of the Hollandsche IJssel barrier.

Function category	Function
Flood protection	Reduce extreme water levels in the hinterland
Navigation	Facilitate navigation
Water management	Provide storage capacity for and discharge of “polder water” from the pumping stations into the Hollandsche IJssel
	Supply fresh water to the polders
	Prevent salt intrusion[a]
Ecology	Allow tidal flow in the Hollandsche IJssel
Road traffic	Provide a road connection between Krimpen a/d IJssel and Capelle a/d IJssel
Monument	Provide iconic value

[a] function that is currently not assigned to the storm surge barrier.

2.2.1 Reduce extreme water levels in the hinterland

The fundamental function of the Hollandsche IJssel barrier is to retain high water and thereby limit the extreme water levels in the Hollandsche IJssel. The storm surge barrier was designed for an outer water level of NAP +4.5 m and the retaining height of the gates is NAP +5.0 m (Van der Graaf & Van Voorst, 2016).

The retaining height has an impact on the head difference over the structure and thus the probability of failure due to piping or structural failure. For the design of the barrier, three different conditions were considered (Rijkswaterstaat Deltadienst, 1957):

1. Outer water level: NAP +4.50 m and inner water level: NAP 0 m
2. Outer water level: NAP +2.50 m and inner water level: NAP -2.00 m
3. Outer water level: NAP -1.95 m and inner water level: NAP +0.30 m

The barrier was thus designed to withstand a positive head difference of 4.5 m. The maximum negative head difference the barrier is able to withstand is 2.25 m, based on the third case with a water level of NAP +0.30 m in the Hollandsche IJssel and NAP -1.95 m in the New Meuse. This negative head difference is mainly relevant for situations in which the barrier fails to open or when the barrier is used to prevent salt intrusion.

The retaining height and head difference are of importance for the probability of loss of the water-retaining function. Another important aspect for the assessment of the flood protection function is the closure reliability. The closure reliability influences the probability of extreme water levels behind the barrier. The closure reliability is expressed as the failure probability per closure event. For both probabilities (loss of water-retaining function and non-closure), the requirement is stipulated in the law that came into effect in 2017 (Slootjes & Van der Most, 2016a). The probability of loss of the water-retaining function of the Hollandsche IJssel barrier is 1/30,000 per year and the acceptable non-closure probability is 1/200 per closure (Slootjes & Van der Most, 2016b). Strictly speaking, these probabilities are the only requirements for the function reducing extreme water levels in the hinterland.

2.2.2 Facilitate navigation

The Hollandsche IJssel is navigated by both commercial and recreational vessels. Therefore, relevant aspects of both types are discussed in the following paragraphs.

Commercial vessels

The governing vessel class of the Hollandsche IJssel is CEMT class Va. The classification system of CEMT is useful to determine the accessibility for vessels of different sizes, but even if waterways have the same CEMT class, local characteristics, such as structures and water level regulations, could govern the maximum size of the ships that are permitted to navigate on that waterway. More detailed information about the maximum vessel size for the Hollandsche IJssel can be found in the online database *Vaarweginformatie* (Rijkswaterstaat, n.d.-a). According to the information in this database, the maximum dimensions of vessels that can sail along the river are a length of 110 m, a beam of 11.4 m, and a draught of 3.6-4.7 m (with respect to NAP 0 m), which corresponds to the characteristic vessel *Groot Rijnschip*. It is, however, expected that most vessels are of class IV or smaller due to the dimensions of the Gouwe canal, which is on the other side of the Juliana locks. The Hollandsche IJssel and the Gouwe canal are important waterways for ships between the port of Rotterdam and the inland shipping terminal Alpherium in Alphen aan den Rijn, which is one of the largest inland terminals in the Netherlands (de Graaf & Steensma, 2019). The Gouwe canal is accessible for vessels up to CEMT class IV, with dimensions limited to 90 × 9.5 (L × B) and a draught of 2.8 m with respect to NAP -0.70 m (Rijkswaterstaat, n.d.-a).

Recreational vessels

The Hollandsche IJssel is also part of the *staande mast route Vlissingen-Delfzijl*, a series of waterways from Vlissingen to Delfzijl of which the vertical clearance must be at least 30 m (Rijkswaterstaat, 2020a). This route was established with sailing boats in mind, hence, the Hollandsche IJssel is frequently navigated by recreational vessels, especially during the summer. The *staande mast route Vlissingen-Delfzijl* also runs through the Gouwe and most of the recreational boats are also expected to continue on the Gouwe after passing the Hollandsche IJssel barrier. These sailing boats will have to pass the barrier through the lock where the bridge can be opened.

Required width and vertical clearance

The required width of a waterway or navigation lock for a specific vessel class can be found in the *Richtlijnen Vaarwegen* (Rijkswaterstaat, 2020a). The minimum width for straight waterways in inland regions (the Hollandsche IJssel is on the edge of the division between the inland and coastal region) accessible to CEMT class Va vessels of 110 m in length is 51.1 m. The 80 m wide storm surge barrier is thus certainly sufficient. The Algera lock is 23.9 m wide and has a minimum chamber length of 120 m, which means that one CEMT Va vessel or two CEMT IV vessels could fit in the lock chamber each lock cycle.

Whether vessels can pass the storm surge barrier under the 80 m wide gates and the bridge is determined by the CEMT class of the vessel, its loading condition, and the water level. The vertical clearances for vessels of class IV and V are 7.0 m and 9.1 m, respectively, according to the *Richtlijnen Vaarwegen*. These values are based on the 10% exceedance height of unloaded motor vessels. As mentioned before, the Hollandsche IJssel is an important waterway for container vessels because of the inland container terminal near Alphen aan den Rijn. The vertical clearance required for container vessels is linked to the number of layers of containers that can be stacked on a ship: two, three, or four layers. Measurements on the river Rhine showed that container vessels are actually higher than the values described in the *Richtlijnen Vaarwegen*, see Table 2.2.

Table 2.2: Required vertical clearance for container vessels according to guidelines and measurements performed in 2012 (Brolsma, 2013).

CEMT class	*Richtlijnen Vaarwegen (CEMT standard)*	Measurements 2012 (10% exceedance)
III (2 layers)	5.25 m	5.80 m
IV (3 layers)	7.00 m	8.50 m
V (4 layers)	9.10 m	10.85 m

One of the reasons for the differences between the prescribed vertical clearances and the ones based on measurements is the emergence of high cube containers. These containers have a height of 9 feet and 6 inches, which makes them approximately 30 cm larger in height compared to the conventional containers (8 ft 6 in). The effect of high cube containers on the required vertical clearance is illustrated in Table 2.3.

Table 2.3: Required vertical clearances for different layers of conventional and high cube containers (Brolsma, 2013).

CEMT class	Average loaded[a]		Fully loaded[b]		Empty loaded[c]	
	Conventional	High cube	Conventional	High cube	Conventional	High cube
III (2 layers)	4.75 m	5.36 m	4.20 m	4.81 m	5.04 m	5.65 m
IV (3 layers)	7.06 m	7.97 m	4.20 m	7.14 m	7.51 m	8.43 m
V (4 layers)	9.20 m	10.42 m	7.96 m	9.18 m	9.88 m	11.10 m

[a] 65% of vessel's container capacity is utilised with 65% loaded containers (and 35% empty containers).
[b] 100% of vessel's container capacity is utilised with 100% loaded containers.
[c] 100% of vessel's container capacity is utilised with 0% loaded containers..

High cube containers are expected to become the standard in the coming decades, with serious consequences for the required vertical clearance for waterways, as Table 2.3 shows. However, several cost-benefit analyses showed that heightening structures across waterways above the CEMT standards is not cost-effective. Hence, the current CEMT standards remain in place (Kst-31409-239, 2019). Seaport areas are excluded from this decision. The Minister of Infrastructure and Water Management could specify additional requirements for seaport areas and for four main transport corridors. Neither of those cases apply to the Hollandsche IJssel.

The above described vertical clearances are relative to the governing high water level ("Maatgevende Hoge Waterstand", MHWS). The governing high water levels for various types of waterways are also included in the *Richtlijnen Vaarwegen*. For tidal rivers, the MHWS is equal to the limit level ("grenspeil"), the water level that is on average exceeded once every two years. The limit levels can be found in the storm surge reports of Rijkswaterstaat. A map with the limit levels at several locations is included in Appendix 6 of the report of the storm surge of 21 March 2008 (Rijkswaterstaat, 2008). The limit level for the Hollandsche IJssel is NAP +2.60 m. The Algera bridge deck is at NAP +8.5 m (NAP +7.5 m for the movable bridge), which means that the vertical clearance (8.5 – 2.6 = 5.9 m) is formally insufficient for unhampered passage of all navigating vessel classes. However, the limit level is somewhat meaningless for navigation on the Hollandsche IJssel because

the barrier is closed when the forecasted water level exceeds NAP +2.25 m and passage at the navigation lock is halted at a water level of NAP +2.50 m (Rijkswaterstaat, 2011). The mean high water level is NAP +1.24 m (NAP +1.36 m at spring tide and NAP +1.08 m at neap tide), so in most situations vessels up to CEMT class IV should be able to navigate under the barrier. The container vessels of the type *Gouwenaar*, specifically designed for transport to the Alpherium, can sail under bridges with a vertical clearance of 7 m with three layers of empty high cube containers through the use of an innovative ballast tank system (Hoek, 2012, 2019).

Ship passages

Unfortunately, data on the number of vessels passing the storm surge barrier complex were not available. However, vessel passages are recorded at the Juliana locks near Gouda. As this lock complex is also part of the route to the inland container terminal and the *staande mast route*, these numbers provide a good indication of the traffic intensity on the Hollandsche IJssel. Data on passages at the Juliana locks have been presented in several reports for other projects. For instance, a consortium comprising Buck Consultants International, Witteveen+Bos, and Henk van Laar advies en projectbureau included the figures of 2013 in their report *Effectberekening verbetermaatregelen rond De Gouwe* (Buck Consultants International et al., 2014). They reported that about 8,200 commercial and 13,000 recreational vessels passed the locks in 2013. Figure 2.5 shows that the number of commercial vessels is relatively stable year-round, fluctuating between 500 and 900 passages a month. Recreational navigation, on the other hand, is characterised by strong seasonal variation.

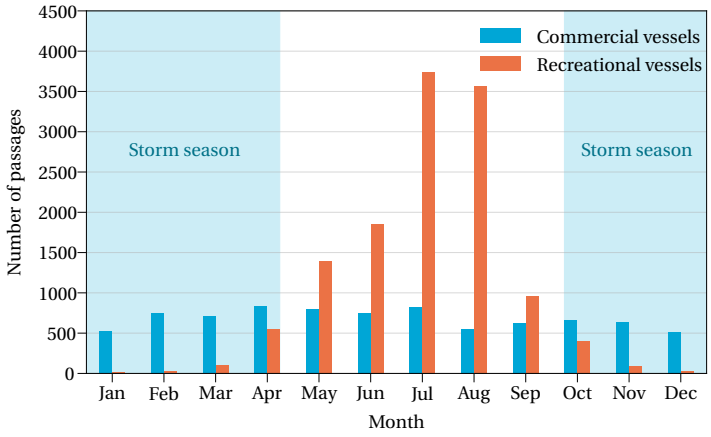

Figure 2.5: Monthly vessel passages at the Juliana locks in 2013, data from Buck Consultants International et al. (2014).

It should be noted that considering only the data of 2013 may not give a proper depiction of the navigation intensity on the Hollandsche IJssel. Other sources were looked for to conclude whether these numbers are representative. For the project *Beter Bereikbare Gouwe*, Royal HaskoningDHV presented the recorded number of ship passages over the years 2006-2017 (Ammerlaan et al., 2019). These numbers are less detailed than the data in *Effectberekening verbetermaatregelen rond De Gouwe*; only yearly values were reported (Figure 2.6).

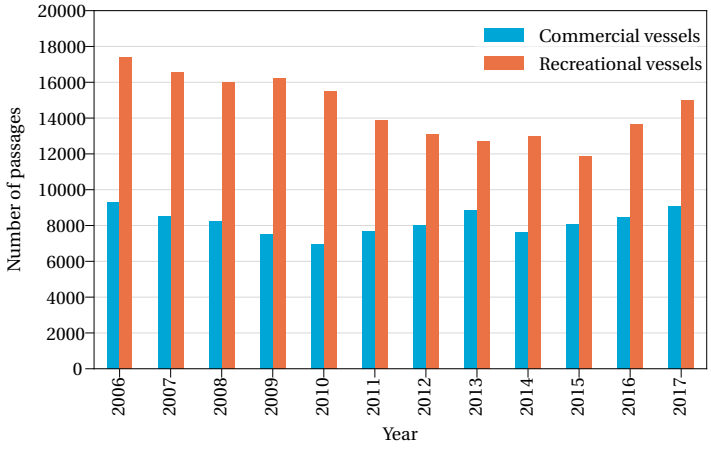

Figure 2.6: Annual vessel passages at the Juliana locks for 2006-2017, data from Ammerlaan et al. (2019).

A more detailed inspection of this figure reveals that the number of commercial vessels passing the lock in 2013 is higher than the number in the report *Effectberekening verbetermaatregelen rond De Gouwe* (8,800 vs. 8,200). The number of recreational vessels is about the same, 13,000. It is difficult to explain this difference based on the presented numbers alone, but a plausible explanation lies in the definition used for commercial vessels. The report *Effectberekening verbetermaatregelen rond De Gouwe* probably only considers freight carrying vessels, while Royal HaskoningDHV includes both freight carrying and non-freight carrying vessels, such as tugboats and passenger ships. This conclusion could be inferred from a more in-depth look at the number of passages in the years 2006-2008 of Figure 2.6. Rijkswaterstaat provided an elaborate decomposition of the types of vessels that pass the navigation locks in the main waterways for the years 2005-2008 in their publication *Scheepvaartinformatie Hoofdvaarwegen Editie 2009* (Rijkswaterstaat, 2009a). The number of passages from 2006 to 2008 that are shown in Figure 2.6 match the sum of freight carrying and non-freight carrying vessels in the *Scheepvaartinformatie Hoofdvaarwegen Editie 2009*. The number of non-freight carrying vessels is on average 566 (over 2005-2008), which corresponds to the difference of approximately 600 vessels between the number of passages presented in the reports *Effectberekening verbetermaatregelen rond De Gouwe* (Buck Consultants International et al., 2014) and *Beter Bereikbare Gouwe* (Ammerlaan et al., 2019).

The average number of vessels over the years 2006-2017 is about 8,200 commercial and 14,500 recreational vessels. The number of commercial vessels has been relatively stable since 2006. The opening of the inland container terminal Alpherium in 2009 has not translated into significant changes in the absolute number of commercial vessels or the amount of tonnage passing through the Juliana locks. Instead, there has been a shift to more container transport and the use of larger ships (de Graaf & Steensma, 2019). It should be noted that a significantly higher number of vessels passed the lock complex in 2018. In 2018, the number of passages was 11,639 (Binnenvaartcijfers, n.d.), more than 40% higher than the average over the period 2006-2017. It is unknown what caused this surge as only the total number of passages was reported. It remains to be seen whether this number is a one-time outlier or part of a trend. For this study, the figures over the period 2006-2017 were used as these are more detailed (decomposed into commercial and recreational) and considered more robust.

Hindrance due to closure of the barrier

The main conclusion that could be drawn from the data on ship passages is that recreational navigation shows strong seasonal variation, with the number of boats peaking during the summer. This seasonal swing implies that commercial vessels are predominantly hindered by a closure of the Hollandsche IJssel barrier since closures generally take place in the storm season (1 October to 15 April). The barrier closes on average six to nine times times a year due to storm surges or for testing procedures. So apparently, nine closures are still deemed acceptable for the navigation industry. However, there is a difference in terms of hindrance between test closures and unforeseen closures due to storms. Test closures can be communicated well in advance and parties could plan their activities better to limit the negative consequences of an obstructed waterway or road. Storm closures are announced a few days prior to the expected time of closure and it is more difficult for stakeholders to take them into account in the planning of their activities. As clearly defined requirements regarding the acceptable number of closures are lacking, nine closures may still be a good first value to evaluate the remaining life in terms of the number of closures.

An alternative way to obtain an indication of the acceptable hindrance is to use the required availability of navigation locks as a reference. Primary navigation locks have to be available for 98% of the operational hours (Brasser, 2021; Willems et al., 2018). If the storm surge barrier is assumed to be in operation for 100% of the time, then the acceptable hindrance to shipping is $0.02 \cdot 8670 = 175.2$ hours a year.

In conclusion, the following requirements can be formulated with respect to facilitating navigation:

- Vessels of CEMT class Va with dimensions 110 m × 11.4 m (L × B) and a draught of 3.6-4.7 m (with respect to NAP 0 m) must be able to pass the lock and sail along the Hollandsche IJssel (follows from the waterway dimensions).
- The minimum length and width of the lock must be 120 m and 23.9 m, respectively, in order to accommodate one CEMT Va or two CEMT IV vessels (follows from the guidelines and current dimensions of the lock).
- The minimum navigational width at the storm surge barrier must be 51.1 m (follows from the guidelines for CEMT Va vessels).

- The minimum water depth must be 4.2 m in the lock (follows from the guidelines for CEMT Va vessels)
- The guaranteed vertical clearance must be 7.0 m under normal conditions (based on free passage of the container vessels and CEMT IV vessels).
- The maximum number of closures for which no further cost analysis is required is 9 (follows from the current number of closures). In addition, the availability requirement for navigation locks can be used. In that case, the storm surge barrier is allowed to be unavailable for navigation for 175.2 hours a year.

2.2.3 Provide storage capacity for and discharge of “polder water” from the pumping stations into the Hollandsche IJssel

The Hollandsche IJssel is crucial for the water management in the area. The water authorities discharge water from the polders into the Hollandsche IJssel to regulate the water levels and groundwater table in the polders. But when the barrier is closed, the pumping stations have to stop discharging water after the water level at Krimpen aan den IJssel reaches NAP +2.60 m ("maalstoppeil"). Whether this water level will be reached depends on the closure strategy and the amount of discharged water. A closure at low water slack results in lower water levels in the basin and reducing the discharges slows down the water level rise. The effect of both variables is shown in Table 2.4. The time until the "maalstoppeil" is reached was calculated using the data on the surface area in Appendix C of the operations manual belonging to the *Waterakkoord* (Ministerie van Verkeer en Waterstaat et al., 2006). The surface area varies with the water level and this dependency is included in the calculations. The computed durations until a water level of NAP +2.60 m is reached correspond well with previous calculations performed by HKV (Rongen & Maaskant, 2019).

Table 2.4: Duration until the "maalstoppeil" (NAP +2.60 m) is reached [hours].

Closure level [NAP m]	Discharge [m^3/s]			
	45	60	75	90
0.5	33.7	25.3	20.2	16.9
1.0	26.0	19.5	15.6	13
1.5	18.3	13.7	11.0	9.1
2.0	10.3	7.7	6.2	5.2

Pausing the pumping stations for a certain period of time has undesirable effects. The main consequences manifest in flooding of basements or water in the streets, i.e. unfortunate situations that should be prevented. The water authorities have never had to stop the discharge of water into the Hollandsche IJssel in the past since the critical water level was never reached during closures (HydroLogic, 2016). The requirement for the function providing storage capacity could be formulated as an acceptable probability of exceedance of the critical water level NAP +2.60 m. According to the operations manual (Ministerie van Verkeer en Waterstaat et al., 2006), the pumping has to be stopped about once every 200 years. So this probability of 1/200 per year is currently deemed acceptable and could be used as a requirement.

Under normal conditions, the regional water authorities discharge water into the river through several pumping stations. Additionally, water could both enter and leave the Hollandsche IJssel from the Canalised Hollandsche IJssel through the Waaier lock or the pumping station next to the lock in case of high water levels in the Hollandsche IJssel (Ministerie van Verkeer en Waterstaat et al., 2005). The capacities of the discharge points are summarised in Table 2.5 and their locations are shown in Figure 2.7. The capacities of most pumping stations were obtained from the *Waterakkoord* (Ministerie van Verkeer en Waterstaat et al., 2005). The data were verified and updated if necessary by searching the online database of the Dutch Pumping Stations Foundation ("Nederlandse Gemalen Stichting") since some stations were renovated in recent years, e.g. Verdoold (Nederlandse Gemalen Stichting, n.d.).

Table 2.5: Capacities of the discharge points along the Hollandsche IJssel.

Discharge location	Capacity [m^3/s]	Water authority
Pumping station Abraham Kroes	14.2	HH Schieland en de Krimpenerwaard
Pumping station Middelwatering	1.5	HH Schieland en de Krimpenerwaard
Pumping station Hitland	1.3	HH Schieland en de Krimpenerwaard
Pumping station Oostgaarde	0.8	HH Schieland en de Krimpenerwaard
Pumping station Johannes Veurink	5.0	HH Schieland en de Krimpenerwaard
Pumping station De Nesse	0.7	HH Schieland en de Krimpenerwaard
Pumping station Stolwijkersluis	1.2	HH Schieland en de Krimpenerwaard
Pumping station Verdoold	7.5	HH Schieland en de Krimpenerwaard
Pumping station Kromme, Geer en Zijde	Out of use	HH Schieland en de Krimpenerwaard
Pumping station Mallegat	1.3	HH Rijnland
Pumping station Hanepraai	1.2	HH Rijnland
Pumping station Willens Goejanverwelledijk (WG)	0.9	HH Rijnland
Pumping station Pijnacker-Hordijk	40	HH Rijnland
Waaier lock / pumping station Waaier lock	14 / 7.5	HH De Stichtse Rijnlanden
Wastewater treatment plants	0.7	
Total	90.2 / 83.7	

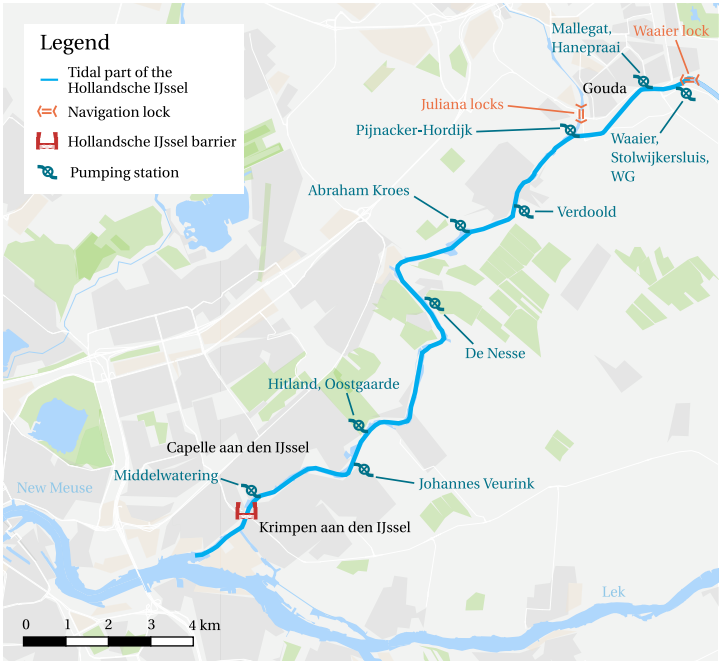

Figure 2.7: Locations of the discharge points along the Hollandsche IJssel (HydroLogic, 2016; Nederlandse Gemalen Stichting, n.d.)

The discharge of water is considered not to be limiting for the functional life of the Hollandsche IJssel barrier. The maximum discharge of the outlets is 90 m^3/s, while on average 730 m^3/s flows through the river New Meuse downstream of the Hollandsche IJssel (Vellinga et al., 2014). Moreover, Mooyaart et al. (2014) reported an estimated peak tidal flow rate of 350 m^3/s in the Hollandsche IJssel using a simple formula. The peak tidal flow rate is thus 4 times larger than the maximum discharge of the outlets. Therefore, no requirements with respect to discharge of "polder water" into the Hollandsche IJssel that could be of importance for the assessment of the remaining life were formulated.

2.2.4 Supply fresh water to the polders

The water of the rivers in the region is used to maintain the water levels in the vulnerable peat areas, for drinking water purposes, and for agricultural activities in Central Holland. The water authorities use water from the river Lek, Amsterdam-Rijn Canal, and (Canalised) Hollandsche IJssel. For the Hollandsche IJssel, most of the inlets are either located next to or part of the pumping stations where water is discharged from the polders into the river. The inflow of fresh water mainly takes place through gravitational flow, thus the supply varies depending on the water level difference. The inflow capacity per location is listed in Table 2.6. The capacities were obtained from the *Waterakkoord* (Ministerie van Verkeer en Waterstaat et al., 2005) and these values were checked with the capacities summarised in the report *Slim Watermanagement Hollandsche IJssel* (HydroLogic, 2016).

Table 2.6: Capacity of inlet points along the Hollandsche IJssel.

Discharge location	Capacity [m^3/s]	Water authority
Pumping station Abraham Kroes	14.2	HH Schieland en de Krimpenerwaard
Snelle Sluis	2.5	HH Schieland en de Krimpenerwaard
Pumping station De Nesse	0.3	HH Schieland en de Krimpenerwaard
Pumping station Verdoold	0.8	HH Schieland en de Krimpenerwaard
Inlet Gouda (Pumping station Pijnacker-Hordijk)	35	HH Rijnland
Waaier lock / pumping station Waaier lock	5[a]	HH De Stichtse Rijnlanden
Total	43.6	

[a] average daily intake through the Waaier lock.

As for the function discharge of water, supply of fresh water is assumed not to be restrictive for the functional life of the Hollandsche IJssel barrier. Under normal conditions, the barrier is open and sufficient fresh water can flow into the Hollandsche IJssel. During storm conditions, the water authorities are more concerned with pumping out water from the polders to prevent flooding of streets or land, and the storage capacity of the river basin becomes more important, see Section 2.2.3. For dry periods, the KWA could be invoked to provide fresh water to the surrounding areas. The barrier could possibly be used to stop salt water from flowing into the river and thereby guarantee the availability of a certain amount of fresh water for the water authorities, but that is viewed as a separate function that is treated in the next section. Therefore, no requirements with respect to the freshwater supply that could be of importance for the assessment of the remaining life were formulated.

2.2.5 Prevent salt intrusion

In the past, the Hollandsche IJssel barrier was closed to stop the salt intrusion in the Hollandsche IJssel. However, this option is considered undesirable. The main reason is that low river discharges and the associated salt intrusion could last for multiple days or even weeks. The barrier would then have to be closed for a prolonged time, while only a limited amount of fresh water can be stored in the river basin. Other sources of fresh water will be needed to meet the demand of the water authorities. Eventually, the barrier has to be opened again and the salt water that accumulated in front of the barrier could still flow into the river. The net effect could be that the salt intrusion is worse compared to the situation in which the barrier is kept open (Ministerie van Verkeer en Waterstaat et al., 2006). Additionally, the hindrance to shipping and road traffic will be significant since all vessels have to go through the Algera lock. Only under extraordinary conditions, such as extreme wind set-up at sea and low river discharges, the authorities could close the barrier for one tidal period, but this situation is still undesirable and the effect on the prevention of salt intrusion is minimal (Ministerie van Verkeer en Waterstaat et al., 2006).

As long as the Hollandsche IJssel barrier is not part of official strategies to cope with salt intrusion, there are no requirements concerning the function prevent salt intrusion. If the barrier is nonetheless used to prevent salt intrusion, one may formulate the requirement that the barrier must only be closed for one tidal cycle (12 hours and 25 minutes).

2.2.6 Allow tidal flow in the Hollandsche IJssel

The Hollandsche IJssel river is a unique freshwater tidal river and besides a navigational motive, the preservation of this tidal influence was also one of the reasons to construct the storm surge barrier instead of a dam (Deltares et al., 2018). The tidal variation is clearly visible in Figure 2.8, which shows the water level between 7 and 15 February 2020. These water level measurements at the Hollandsche IJssel barrier have been recorded since 1971 and are available on the Rijkswaterstaat website *Waterinfo* (https://waterinfo.rws.nl). For Gouda, measurements since 1981 are available. Notice the storm surge on 10-12 February and the effect of the subsequent closure on the water level behind the barrier. This was the last time the Hollandsche IJssel barrier was closed due to high water levels (Rijkswaterstaat, 2020c).

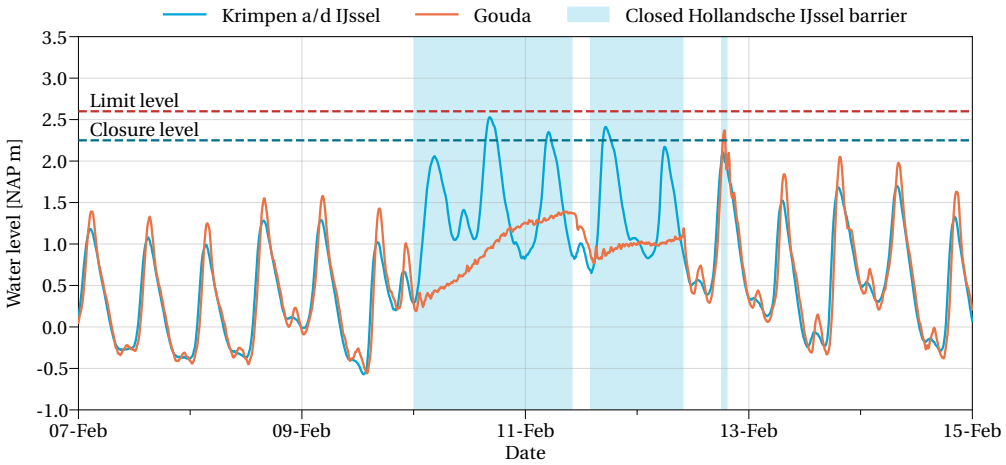

Figure 2.8: Water level between 7 and 15 February 2020, data from *https://waterinfo.rws.nl*.

Over the last 20 years, the mean water level at high tide near Krimpen aan den IJssel was NAP +1.21 m and the mean water level at low tide was NAP -0.26 m. At Gouda, the water level varied between NAP +1.43 m and NAP -0.32 m at high tide and low tide, respectively. So the tidal range is on average 1.47 m near Krimpen and 1.75 m near Gouda, slightly smaller than the 1.50 m and 1.84 m reported in the operations manual of the *Waterakkoord* (Ministerie van Verkeer en Waterstaat et al., 2006). The tide is relevant for the water quality as flushing of the river reduces the concentration of pollutants and is beneficial for the oxygen levels, and it creates a unique environment for specific flora and fauna, such as the streambank bulrush (Schoenoplectus triqueter), a specific marsh marigold (Caltha palustris araneosa) and mudwort (Limosella aquatica) (Emond et al., 2018). The impact of changes in the tidal regime on the water quality or the flora and fauna would require a separate study.

According to the reassessment of the Preferential Strategy for the Rhine Estuary-Drechtsteden region (DRPD, 2020), the tidal system should be maintained for the coming decades. Once replacement of the storm surge barrier is deemed necessary (expected in the second half of this century), this requirement will be dropped and options that permanently close off the river will also be considered. This decision could be interpreted as preserving the tidal nature as long as small interventions that postpone the replacement of the barrier are still possible.

2.2.7 Provide a road connection between Krimpen a/d IJssel and Capelle a/d IJssel

The road N210 runs across the Algera bridge, which is part of the storm surge barrier complex. This regional road is the only connection between the Krimpenerwaard and the city of Rotterdam. The area is thus strongly dependent on this road for the daily commute, visitation of friends or family, and access to public services. The importance of the road connection is evidenced by the almost 45,000 motorised vehicles that cross the bridge every day. However, the road is heavily congested, especially during rush hours, and an easily accessible alternative route is not available (Studio Bereikbaar, 2019). The bottlenecks of the Algera corridor [2] are located where two lanes continue as one lane, e.g. on the bridge, and near junctions, see Figure 2.9.

[2] The Algera corridor is defined as the road segment between the Kralingseplein and Krimpenerbosweg-C.G. Roosweg.

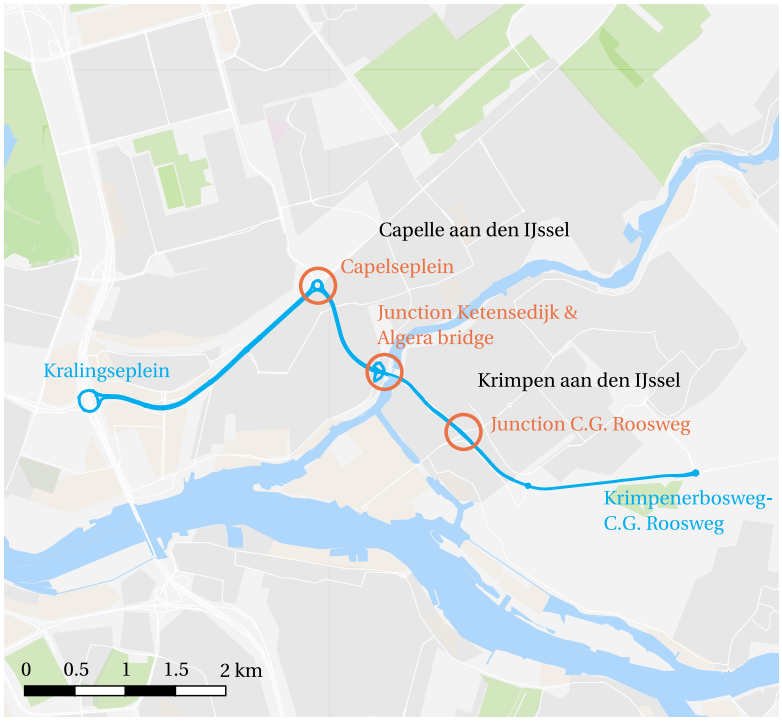

Figure 2.9: Algera corridor and the bottlenecks (Studio Bereikbaar, 2019).

The capacity deficit results in considerable delays for traffic on the road. For example, the travel time along the Algera corridor during the normative rush hour (evening, in the direction of Krimpen a/d IJssel) is 10.5 minutes, 2.2 times the free-flow travel time (5th percentile of the travel time outside rush hour), while the target value is two times the free-flow travel time (Studio Bereikbaar, 2019). The capacity problem of the Algera corridor has been addressed in the regional project *Oeververbindingen regio Rotterdam* (Gemeente Rotterdam et al., 2020). Within this project, a strategy, comprising both short-term and long-term measures, has been developed. The effects of the suggested measures have been studied using traffic simulation models in which the WLO scenarios (socio-economic scenarios) for 2030 have been incorporated. Short-term measures (realisation within 5 years) include adjustments to the junction C.G. Roosweg-Nieuwe Tiendeweg, relocation of the Park and Ride (P+R), and a new technology for the bicycle traffic light system ("groenvoorspellers"). These measures are currently being prepared and implemented (Gemeente Rotterdam et al., 2020; Studio Bereikbaar, 2019). For the long-term, two sets of measures have been developed. The first set of measures is aimed at increasing the use of public transport and bicycles instead of cars. A new cycling bridge and expansion of the public transport network should encourage people to leave their cars at home. The second set of measures aims to improve the traffic flow in quite the opposite manner. By upgrading the bridge to a four-lane road (two in each direction) and a separate cycling bridge, the bottleneck near the bridge should be resolved (Gemeente Rotterdam et al., 2020; Studio Bereikbaar, 2019). It is likely that, rather than implementing one of the sets of measures, a combination of both sets will be chosen. The study of Studio Bereikbaar (2019) was a first step in the development of possible solutions, but a detailed study on the effectiveness of the measures and the development of the preferred strategy have yet to be performed (Gemeente Rotterdam et al., 2020).

The capacity problem is assumed to be resolved by the project *Oeververbindingen regio Rotterdam*, but besides the capacity, the performance in terms of reliability and availability is relevant. The reliability is evaluated based on the steadiness of the travel time and the availability is related to the fraction of time the corridor can be used by road traffic. The reliability is explicitly considered in the development of strategies and measures for the Algera corridor by defining a norm for the ratio between planned travel time and actual travel time (Studio Bereikbaar, 2019). For the availability, the interaction between navigational traffic and road traffic is relevant. Figure 2.10 shows that the operating hours of the bridge are quite well tailored to the intensity of road traffic. The operating hours are rather restrictive in terms of availability for waterway vessels, though the hours are extended during closures of the storm surge barrier. During closures, the navigation lock is only unavailable during rush hours (6:45-9.00 and 15:30-18:30) (Gemeente Krimpen aan den IJssel, n.d.).

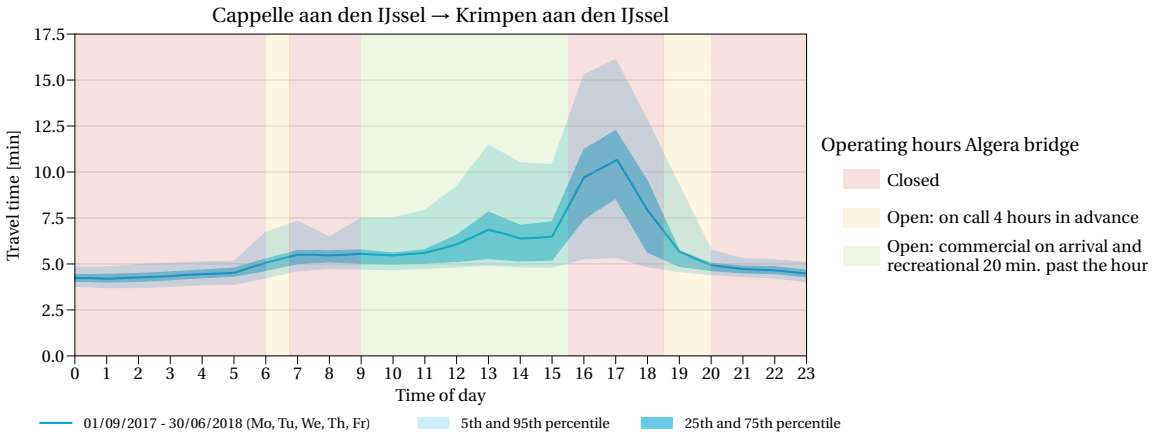

(a) Travel time from Capelle aan den IJssel to Krimpen aan den IJssel.

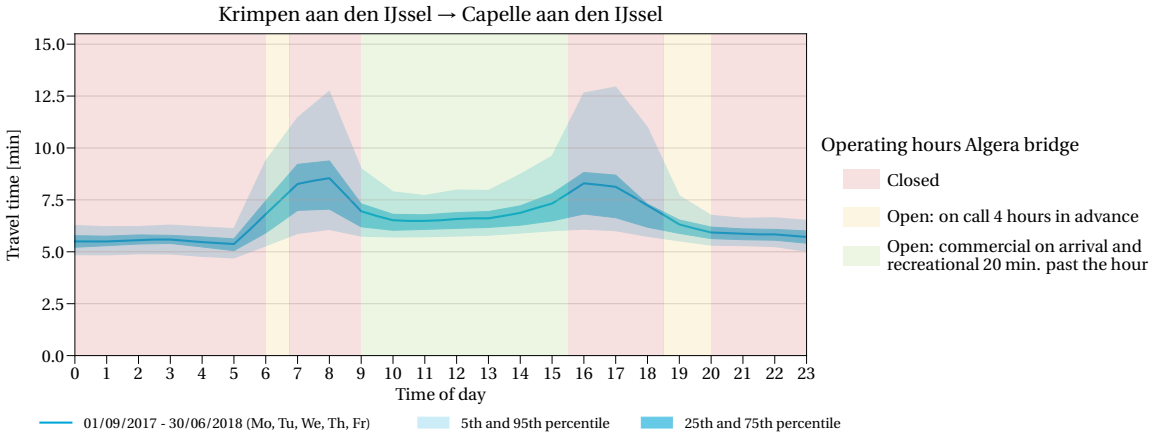

(b) Travel time from Krimpen aan den IJssel to Capelle aan den IJssel.

Figure 2.10: Travel time on the Algera corridor, adapted from Studio Bereikbaar (2019), operating hours were obtained from the municipality (Gemeente Krimpen aan den IJssel, n.d.).

In conclusion, the function provide a road connection is considered not to be limiting for the functional life of the Hollandsche IJssel barrier because of the planned improvements of the road connection within the project *Oeververbindingen regio Rotterdam* (Gemeente Rotterdam et al., 2020). Hence, no requirements were formulated.

2.2.8 Provide iconic value

The Hollandsche IJssel barrier was awarded the status of monument in 2018. The storm surge barrier is considered to be a milestone in the field of hydraulic engineering. It is an example of the flood protection developments of the post-war era with large historic and reminiscent value being the first Delta Work built after the “Watersnoodramp” (Rijksdienst voor Cultureel Erfgoed, 2018). The designation as a monument means that adjustments to the complex or replacements of components require a permit, which complicates the maintenance of the structure. Furthermore, the status of monument could play a role in the future decision to replace the barrier. How this aspect will affect the replacement decision is unknown. Nevertheless, the iconic value of the structure has to be taken into account in the decision.

2.2.9 Overview of functions and requirements

In the previous sections, the functions of the Hollandsche IJssel barrier were described, together with requirements for these functions. These requirements will be applied in future stages to assess the functional lifespan. The functions and requirements of the storm surge barrier are summarised in Table 2.7.

Table 2.7: Functions and requirements for the Hollandsche IJssel barrier. Official or formal requirements and requirements derived from official guidelines are written with a regular font-weight and assumed requirements are written in italics.

Function category	Function	Requirements
Flood protection	Reduce extreme water levels in the hinterland	– The probability of loss of water-retaining function must be less than or equal to 1/30,000 per year. – The closure reliability must be less than or equal to 1/200 per closure.
Navigation	Facilitate navigation	– Vessels of CEMT class Va with dimensions 110 m × 11.4 m (L × B) and a draught of 3.6-4.7 m (with respect to NAP 0 m) must be able to pass the lock and sail along the Hollandsche IJssel. – The minimum length and width of the lock must be 120 m and 23.9 m, respectively, in order to accommodate one CEMT Va or two CEMT IV vessels. – The minimum navigational width at the storm surge barrier must be 51.1 m. – The guaranteed vertical clearance must be 7.0 m under normal conditions. – The minimum water depth in the lock must be 4.2 m. – *The maximum number of closures of the storm surge barrier is 9 per year.* – *The storm surge barrier is allowed to be unavailable for navigation for 175.2 hrs / yr.*
Water management	Provide storage capacity for and discharge of "polder water" from the pumping stations into the Hollandsche IJssel	*The probability of occurrence of the "maalstoppeil" must be less than or equal to 1/200 per year.*
	Supply fresh water to the polders	No requirements, see Section 2.2.4.
	Prevent salt intrusion[a]	*Undesirable to use storm surge barrier, if used only for one tidal cycle (12 hours and 25 minutes).*
Ecology	Allow tidal flow in the Hollandsche IJssel	The tidal regime must be preserved as long as reasonably possible in accordance with the reassessment of the Preferential Strategy for the Rhine Estuary-Drechtsteden region (DRPD, 2020)
Road traffic	Provide a road connection between Krimpen aan den IJssel and Capelle aan den IJssel	*No requirements, capacity after improvement of Algera corridor is assumed sufficient, see Section 2.2.7.*
Monument	Provide iconic value	*Monumental status must be taken into consideration in renovation/replacement programme.*

[a] function that is currently not assigned to the storm surge barrier.

2.3 Structural components and their deterioration

The deterioration of the storm surge barrier and its components determine the technical state and required maintenance of the structure. Each element of the barrier has its own function and is made of a certain material which makes them suffer from various material or element specific deterioration processes. By decomposing the storm surge barrier into different components relevant deterioration mechanisms and external drivers influencing these mechanisms can be identified.

2.3.1 Physical decomposition

The physical decomposition is performed to identify the important components of the barrier. The components usually have different replacement periods and specific elements are more subject to external influences than others, which means that renovation programmes could range from replacing only a few components to a complete replacement of the structure. The decomposition of the structure aims to assist in differentiating between components with a relatively long lifespan and ones with a relatively short lifespan to determine whether the end of life is actually reached or the issues could be resolved by replacing several elements.

Some of the components can already be recognised from Figure 2.11, but other parts are either submerged or incorporated in the visible elements. A more extensive overview of the components is provided in Figure 2.12. In the decomposition, a first classification is made based on three types of components: fixed structures, movable parts, and electrical installations. This subdivision follows from the typical lifespan of the components and the ageing mechanisms that play a role. Fixed structures, such as the concrete towers, foundation or lock heads, generally have a lifespan of 100 to even 200 years. Movable components, such as gates and the drive mechanism, last for up to 50 years, sometimes 100 years. The category electrical installations include the control system, the communication system, as well as software. Those parts typically have to be replaced within 5, 10 or 30 years (Voortman & Veendorp, 2011).

Figure 2.11: Overview of several elements of the Hollandsche IJssel barrier, picture by Van Houdt (2008).

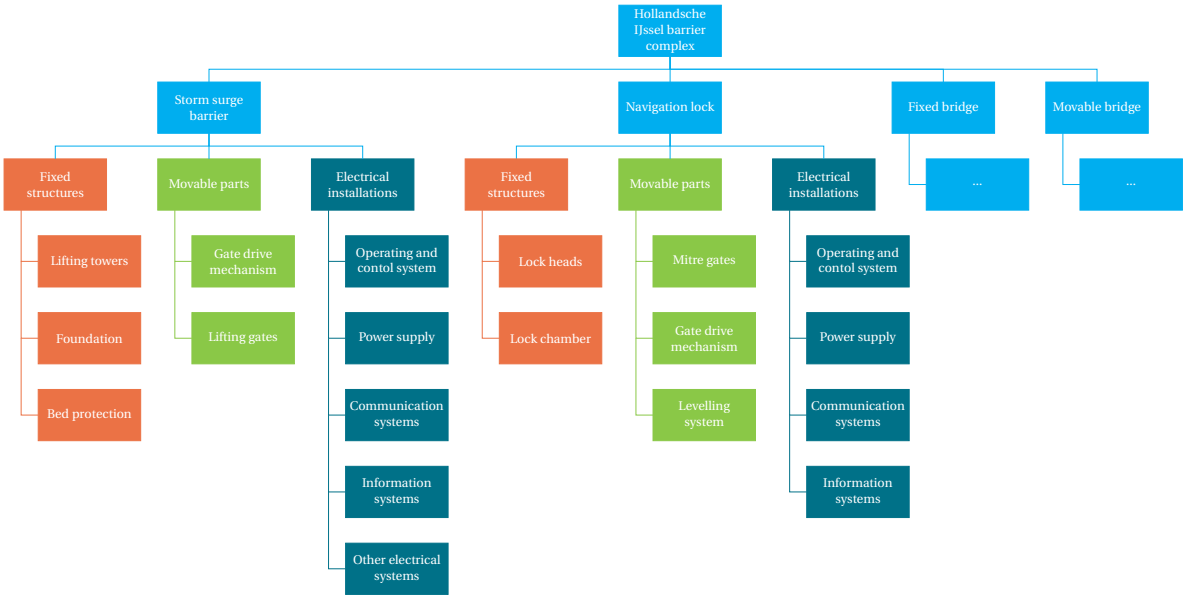

Figure 2.12: Relevant components of the Hollandsche IJssel barrier.

The decomposition of the complex (Figure 2.12) is restricted to elements of the storm surge barrier and the navigation lock because the Algera bridge is already subject of the project *Oeververbindingen regio Rotterdam* (Gemeente Rotterdam et al., 2020). This project aims to resolve the traffic congestion issues on the Algera corridor and renovation of the bridge or even construction of a new bridge is among the options that will be investigated (Zeeman, 2019).

Fixed structures

The fixed structures of the Hollandsche IJssel barrier complex treated here comprise the lifting towers of the storm surge barrier, the lock heads and chamber, the foundation, and the bed protection. These fixed structures are discussed below.

- Lifting towers

  The most distinctive fixed structural elements of the Hollandsche IJssel barrier are the lifting towers. Four 44.75 m high concrete towers were constructed to hold the two gates in position. All four towers were finished in 1958. Besides the steel gates and the required guiding wheels, the gate drive mechanisms, counterweights, emergency control systems (only present in three of the four towers), and power distribution systems can be found in the towers. These towers form the backbone of the storm surge barrier; once the towers reach the end of their life the entire storm surge barrier will probably have to be replaced.

- Lock heads

  The lock heads are concrete structures that hold the gates and other components necessary for the opening and closing of the lock. They transfer the loads from the gates or walls to the foundation, retain water, and prevent seepage around the structure. The outer lock head contains a set of flood gates, a set of ebb gates, and a set of storm gates. The inner lock head is equipped with a set of flood gates and a set of ebb gates. As the lock heads are made of concrete, the same deterioration mechanisms as for the towers are relevant, and the lifespan is also similar.

- Lock chamber

  The lock chamber consists of concrete walls and a concrete floor. The chamber is, next to the lock heads, one of the main structural elements of the lock. The chamber is constructed to retain soil and water and accommodate vessels during passage. The lock chamber is 23.9 m wide, has a length of 120 m, and the sill is at NAP -5.20 m.

- Foundation

  The concrete abutments of the Hollandsche IJssel barrier are founded on reinforced concrete piles (steel piles for the sills), which makes the structure relatively insensitive to settlements. About 90% of the piles are batter piles since the barrier has to be able to resist large horizontal forces (Rijkswaterstaat Deltadienst, 1957).

- Bed protection

  Large flow velocities underneath the gates or pressure differences could lead to erosion of the bed, which could undermine the stability of the barrier. Therefore, concrete sills were constructed for the gates to rest on and to protect the river bed against the strong flows during opening and closing. The sills have a width of 7.50 m and a special shape that was developed to reduce the scour of the river bed (Rijkswaterstaat Deltadienst, 1957). The unique shape of the sills turned out to be insufficient to limit the scour as the bed protection around the storm surge barrier complex was reinforced recently. Fascine mattresses with rubble mound on top were placed near the sills and sides of the waterway. The rubble mound was filled with concrete to improve the stability of the stones (Van der Graaf & Van Voorst, 2016).

Movable parts

The movable components of the storm surge barrier include the large steel gates and their drive mechanisms. For the navigation lock, one can think of the mitre gates, their drive mechanism, and the levelling system when it comes to the movable parts.

- Steel gates

  Two 81.2 m wide and 11.5 m high steel gates hang in between the lifting towers. The steel gates consist of arched truss girders with rectangular front plates. The southern gate was already put in place in 1958, while the second gate was added in 1976. The southern gate was replaced in 1998 after a ship collision. The original southern gate was made of riveted steel, but the newly placed gate was welded, just as the northern gate that was placed in 1976. The use of welded steel made the gate roughly 200 tons lighter (B. Visser, personal communication, 9 September 2021).

- Gate drive mechanism of the storm surge barrier

  The gate drive mechanism is vital for the functioning of the storm surge barrier. A failure of the drive mechanism means that the gate cannot be lowered and not fulfil its protection function. The drive mechanism, present in all four towers, is an electromechanical drive system that consists of two large gear wheels powered by four electric motors; two for the initial stage of closure (from NAP +12.0 m to NAP -3.5 m) and two for the final stage (from NAP -3.5 m to NAP -6.5 m). The gear wheels are connected to a wire rope drum around which the hoisting cables of the gates are wound. Relevant for the maintenance is the requirement that the gear wheels have to be lubricated after every closure. The hoisting cables are lubricated during two of the six test closures (Van der Graaf & Van Voorst, 2016). Lubrication is required to control friction and limit wear of the components (Daniel & Paulus, 2019).

- Mitre gates

  The navigation lock has 10 identical gates in total, one set of storm gates, two sets of flood gates, and two sets of ebb gates. The steel gates are mitre gates, which means that they can only retain water in one direction, hence the double execution at every lock head.

- Gate drive mechanism of the navigation lock

  Although both the drive mechanism of the lock gates and the drive mechanism of the gates of the flood barrier are electromechanical drives, the operating machinery is different. While the lifting gates of the storm surge barrier are operated through a hoisting mechanism with wire ropes, the drive system of the navigation lock consists of a rod or strut that connects the mitre gate to a sector gear, referred to as Panama wheel, which is powered by an electric motor.

- Levelling system

  The levelling or filling and emptying system of the lock is of the simplest kind. The system does not use pumps or culverts. Instead, water is let in or out through valves in the gates. The lock is used to pass the barrier in case of insufficient air draught or when the barrier is closed (only when the water level is lower than NAP +2.50 m). Hence, the water level differences that have to be overcome are in the order of 1 to 2 m. Under those conditions, the system with valves in the gates is the recommended and most economical type (Glerum & Vrijburcht, 2000). Because the filling and emptying system is of the gate opening type, it is not really a component on its own, but rather part of the lock gates.

Electrical installations

The barrier complex incorporates several electrical components that are required for the functioning of the complex. Examples are the operating and control system, the communication system, and of course the power supply system. These systems are relevant for the maintenance plan of the complex since they generally have a shorter lifespan than the structural elements and thus have to be replaced several times during the entire life of the structure.

- Operating and control system

  The complex incorporates several operating and control systems: a main system, a local system, and an emergency control system. The main system is used to control the gates of the barrier and lock as well as the movable bridge. In case the main system malfunctions, the local system could be used to close

the northern gate of the barrier and the gates of the inner lock head. When the local control system fails as well, the operators could resort to the emergency control of the barrier gates and storm gates of the lock.

- Power supply system

  The power supply of the complex comprises a regular and emergency power supply system to prevent outages of the control system. The regular system uses electricity from the grid of Krimpen aan den IJssel and the emergency system consists of a diesel generator and electricity from the grid of Capelle aan den IJssel (Van Voorst & Van der Graaf, 2016).

- Communication systems

  The Hollandsche IJssel barrier complex incorporates several communication systems. Examples are telephones, marine VHF radio, CCTV, fire alarms, et cetera. These systems are required to inform relevant parties in case of closures or when levelling operations are carried out at the lock. The systems are also convenient for the coordination during manual closures when the regular closure operation fails.

- Information systems

  The term information system could be perceived as being the same or similar to a communication system, but information system is used here to refer to installations used for water level and ship passage measurements. These installations are required for, amongst other things, the closure operation of the complex.

- Other electrical systems

  Several electrical components are grouped under other electrical systems. Those systems are for the comfort and well-being of operators and other people present at the complex. For instance, climate control systems, such as central heating, cooling, and ventilation systems. These installations are included for the sake of completeness.

2.3.2 Deterioration mechanisms

The three types of components (fixed, movable, electrical) distinguished in the previous section suffer from various material or element specific deterioration processes. Concrete structures are subject to completely different processes than steel structures or the drive mechanisms. Moreover, the consequences of ageing differ for each component. If replacement of the lifting towers is required, it is very likely that the end of life of the structure has been reached, whereas replacement of the operating and control system is purely a matter of maintenance. The deterioration or ageing mechanisms typical for each type of component and the expected consequences are described below.

Fixed structures

The deterioration mechanisms and maintenance activities for the fixed structures are as follows:

- Lifting towers

  The lifting towers are made of concrete, which makes them susceptible to various deterioration mechanisms such as sulfate attack, alkali-aggregate reactions, and corrosion of the reinforcement due to carbonation or chloride-ingress. These mechanisms have been described extensively in scientific literature and a more detailed description can be found in Appendix B. The most important deterioration processes of concrete structures are the ones related to the reinforcement corrosion: carbonation and chloride-ingress. These mechanisms are also the ones focused on in the asset management document on storm surge barriers (*Objectbeheerregime Stormvloedkeringen*) (Rijkswaterstaat, 2019). Maintenance activities that are carried out to repair concrete structures that are subject to carbonation or chloride-ingress include removal of the carbonated or chloride-contaminated concrete and replacing it with new concrete or adding a new concrete cover. These activities are usually carried out every 25 to 35 years (Rijkswaterstaat, 2019).

- Lock heads and chamber

  The lock heads and lock chamber are also concrete structures and thus subject to the same deterioration mechanisms as the lifting towers. These elements are regularly inspected and maintenance, e.g. replacing the concrete or adding a new cover, is carried out every 25 to 35 years (Rijkswaterstaat, 2019).

- Foundation

  The main threat to foundations is (differential) settlement, but since the structure is founded on piles, the risk of settlements is deemed insignificant. The condition of the foundation is unknown because neither inspections nor maintenance can be carried out.

- Bed protection

  The bed protection is susceptible to erosion due to large flow velocities. Monitoring activities are carried out on a yearly basis to detect possible scour holes and intervene in early stages. If the gullies or scour holes are too deep, the bed protection could be reinforced by dumping more stones or placing a slab of underwater concrete. This is a form of corrective maintenance, and because of the inspection interval it is expected that deterioration can be repaired relatively easily. Given the recent reinforcement of the bed, scour holes are not expected to develop soon.

Movable parts

The movable components of the storm surge barrier are almost exclusively made of steel for which processes such as corrosion and fatigue are relevant, see Appendix B for more information on these two processes.

- Steel gates

  The gates are protected from corrosion by a paint coating. The gates are regularly inspected to review the condition of the protective coating. The coating is locally repaired every 15-20 years and provided with a new coating every 20-30 years. Full replacement of the gates is expected to be needed after 100 years (Rijkswaterstaat, 2019). Fatigue does not seem to be an issue for the gates due to the infrequent usage (de Jong, 2021). This may change in the future if the closure frequency increases. The risk of ship collision may also increase due to more frequent closures, which could lead to earlier replacements of a gate.

- Gate drive mechanism of the storm surge barrier

  The gate drive mechanism is susceptible to wear and fatigue. Restoration or replacement of components of the gate drive system takes place every 15-20 years. The protective coating against corrosion is renewed after about 20 years. The entire drive system is replaced after 50 years (Rijkswaterstaat, 2019).

- Mitre gates

  The mitre gates are subject to the same deterioration processes as the lifting gates of the storm surge barrier. These gates are easier to replace due to their relatively common size. The maintenance intervals are assumed to be the same as for the gates of the barrier. Local repair of the coating every 15-20 years, application of a new coating every 20-30 years, and complete replacement of the gate after 100 years. Additionally, there is a risk of ship collision which could lead to the replacement of a gate.

- Gate drive mechanism of the navigation lock

  The drive mechanism consists of a rod or strut connected to the mitre gates. This type of operating machinery that was often applied in the past (Glerum & Vrijburcht, 2000) is also sensitive to wear and fatigue, but the loads are considerably smaller compared to the drive mechanism of the lifting gates. Gate drive mechanisms have a lifespan of 50 years (Glerum & Vrijburcht, 2000). Hence, the same maintenance requirements as for the machinery of the lifting gates are assumed. Restoration or replacement of components every 15-20 years, coating renewal after 20 years, and complete replacement of the drive system after 50 years (Rijkswaterstaat, 2019).

Electrical installations

The electrical installations of the barrier are prone to regular wear and tear and have to be replaced every 15 years (Rijkswaterstaat, 2019). Hardware and software generally have a shorter lifespan, not because the parts do not function anymore, but to keep up with external developments of the technologies. The deterioration process of these components is thus related to obsolescence: the component is outdated, no longer manufactured, or repair service has become unavailable. The hardware and software are renewed about every eight years (Siemens, 2021).

2.3.3 Overview of deterioration mechanisms

The information on the deterioration processes and consequences of the deterioration of the components is summarised in Table 2.8. The maintenance activities and intervals were primarily obtained from the asset management document on storm surge barriers (*Objectbeheerregime Stormvloedkeringen*) (Rijkswaterstaat, 2019).

Table 2.8: Structural components and their deterioration mechanisms.

Component	Dominant deterioration mechanisms	Consequence	Maintenance interval
Lifting towers	Concrete deterioration	Removal of contaminated concrete Application of new concrete cover	25-35 years
Lock heads	Concrete deterioration	Removal of contaminated concrete Application of new concrete cover	25-35 years
Lock chamber	Concrete deterioration	Removal of contaminated concrete Application of new concrete cover	25-35 years
Foundation	Settlements	Technical end of life, but structure is founded on piles	No inspection or maintenance
Bed protection	Erosion	Reinforced by dumping more stones or placing a slab of underwater concrete	Yearly inspection, repair if necessary
Steel gates (SSB)	Corrosion	Local repair of coating Coating renewal Replacement	15-20 years 20-30 years 100 years
	Fatigue	Maintenance (replacement)	No inspection or maintenance
	Ship collision	Replacement	–
Gate drive mechanism (SSB)	Mechanical wear and fatigue	Restoration or replacement of parts Coating renewal Replacement	15-20 years 20 years 50 years
Steel mitre gates (lock)	Corrosion	Local repair of coating Coating renewal Replacement	15-20 years 20-30 years 100 years
	Fatigue	Maintenance (replacement)	No inspection or maintenance
	Ship collision	Replacement	–
Gate drive mechanism (lock)	Mechanical wear and fatigue	Restoration or replacement of parts Coating renewal Replacement	15-20 years 20 years 50 years
Electrical installations	General ageing and obsolescence	Replacement of electrical components Replacement of hardware and software	15 years 8 years

Table 2.8 shows that essentially all dominant deterioration mechanisms lead to (increased) maintenance. None of the mechanisms results in the end of the technical life of non-replaceable components. Deterioration of components is a matter of additional costs and thus relevant to the economic life of the storm surge barrier. As a consequence, the technical life can be considered not to be governing for the remaining life of the Hollandsche IJssel barrier.

2.4 Conclusions

This chapter has introduced the Hollandsche IJssel storm surge barrier and relevant site-specific information. These elements were described to serve the main purpose of this chapter, which was to identify the functions and physical components of the Hollandsche IJssel barrier. Hence, the core part of this chapter comprises the functional analysis and physical decomposition.

The functional analysis was performed to establish requirements that could be used to assess the remaining functional life of the storm surge barrier. The identified functions of the barrier were grouped into six

different categories: flood protection, navigation, water management, ecology, road traffic, and monument. Where possible, requirements were formulated for each function. Some of these requirements are not formal requirements. The number of closures, for example, was based on the current situation, and the unavailability of the waterway was derived from a general requirement for navigation locks.

The physical decomposition was conducted to identify the dominant deterioration mechanisms of the different components of the barrier. The analysis showed that none of the deterioration mechanisms leads to the end of the technical life of the storm surge barrier. Therefore, it was concluded that the technical life is not dominant for the total remaining life of the Hollandsche IJssel barrier. The results of the functional analysis and the physical decomposition are used in Chapter 3 to assess the impact of the external drivers.

3

Effect of external drivers on the barrier's remaining life

The functional performance and deterioration processes of the Hollandsche IJssel barrier that were described in the previous chapter are influenced by several external drivers. How and to what extent these drivers impact the functional performance and deterioration processes is studied in this chapter. In doing so, the chapter provides an answer to the following research question:

3. What are the major external drivers affecting the functional performance and deterioration mechanisms, and thereby the residual life of the barrier?

In an attempt to answer this research question, the external drivers are first divided into physical and societal developments. The physical drivers are described in the Sections 3.1 to 3.5. The physical drivers are treated in multiple sections as a distinction is made between climate change related drivers (Section 3.1 and Section 3.2) and other physical drivers such as land subsidence (Section 3.3). Although sea level rise, changes in storm surge characteristics, and river discharge changes are also climate change induced, they are examined in a separate section (Section 3.4) as the interaction between these three factors influences the water levels. Because of the large number of physical drivers, a summary of the impacts is provided in Section 3.5. The societal developments include policy changes (Section 3.6) and socio-economic developments (Section 3.7). The chapter concludes, in Section 3.8, with a summary of the findings and an answer to the question above.

3.1 Climate change scenarios

Climate change is among the most important and uncertain factors affecting the lifespan of assets. It manifests itself in many ways of which the increase in global temperature and sea level rise are well-known examples. Future changes in these variables are included in climate change scenarios. Two sets of scenarios that can be used to evaluate the impact on the Hollandsche IJssel barrier are briefly discussed in the next sections.

3.1.1 IPCC scenarios

Approximately every six to seven years, the Intergovernmental Panel on Climate Change (IPCC) publishes Assessment Reports about the current state of knowledge on climate change, its causes, potential impacts, and response options. The fifth Assessment Report (AR5)[1] includes four scenarios of future climate change based on Representative Concentration Pathways (RCPs). These RCPs describe plausible pathways of greenhouse gas (GHG) emissions and atmospheric concentrations, air pollutant emissions, and land use/cover for the 21st century (IPCC, 2014; Moss et al., 2010). The pathways follow from developments of factors such as economic and population growth, technology, and climate policy. The pathways are named after the amount of radiative forcing that will be reached in 2100 (IPCC, 2014). Positive radiative forcing implies a net heating of the Earth and negative radiative forcing corresponds to cooling of the planet. RCP2.6 represents a scenario that is likely (66% probability or more) to keep the global temperature rise below 2 °C and the most extreme scenario RCP8.5 corresponds to very high GHG emissions.

[1]The first part of the sixth Assessment Report, Climate Change 2021: The Physical Science Basis, was released in August 2021 (IPCC, 2021).

3.1.2 KNMI scenarios

The KNMI has developed climate change scenarios for the Netherlands based on the global scenarios of the IPCC supported by model calculations of KNMI's own climate models (Klein Tank et al., 2015; Van den Hurk et al., 2014). The climate change scenarios of the KNMI are classified by the resulting global mean temperature rise and changes in air circulation pattern. The four scenarios are named G_L, G_H, W_L, and W_H. The increase in global mean surface temperature is expressed as either Moderate (G) or Warm (W) and the changes in air circulation pattern are either Low (L) or High (H). In the G scenarios, the global mean temperature rise equals 1 °C by 2050 and 1.5 °C in 2085. The W scenarios result in an increase in global mean temperature of 2 °C by 2050 and 3.5 °C in 2085. In the H scenarios, summers are warmer and drier and winters are mild and more humid compared to the L scenarios. The scenarios of the KNMI are not one-to-one related to the four scenarios of the IPCC because the KNMI uses different drivers than the RCPs to develop climate change scenarios. The KNMI uses the global mean temperature and air circulation change as drivers of climate change. The differences between the IPCC scenarios and the scenarios of the KNMI can best be illustrated by looking at the global mean temperature rise for the scenarios. Figure 3.1 shows that the G scenarios of the KNMI correspond to the lower part of RCP4.5 and RCP6.0 and the W scenarios match the upper part of RCP8.5.

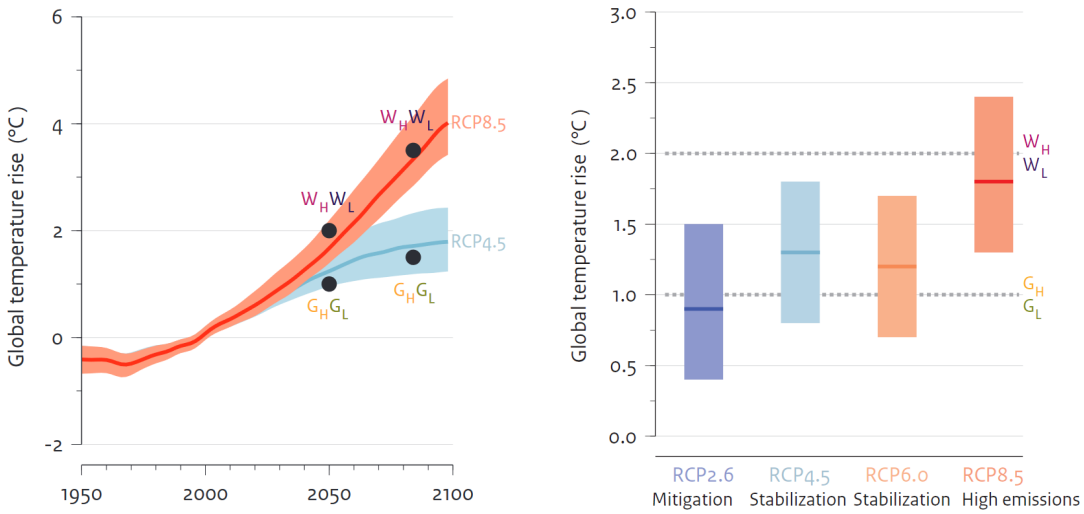

(a) Global temperature rise relative to 1981-2010.

(b) Global temperature rise around 2050 relative to 1981-2010.

Figure 3.1: Comparison of global temperature rise for IPCC and KNMI climate change scenarios (Klein Tank et al., 2015).

3.2 Local climate

Although climate change occurs on a global scale, the effects and risks can vary strongly on a regional scale. For example, the Arctic region is warming more rapidly than the global mean temperature, and sea level rise is greatest in the Southern Ocean between South America, South Africa and Australia (IPCC, 2014, 2019). Regarding the risks, it is clear that coastal systems and low-lying areas are more at risk from sea level rise than mountainous areas. The impact of climate change thus has to be assessed on a local scale. The effects and consequences of climate change in the Netherlands are discussed in the following sections. Each section starts with a discussion on how the specific climate variable could affect the remaining life. This introduction to the potential impact of the variable is followed by an analysis of the observed and future changes, and finally, the impact of the variable assessed. The KNMI'14 climate change scenarios and the climate variables described therein serve as a starting point for the evaluation of the impact.

3.2.1 Temperature

Potential impact of temperature rise

Changes in temperature as a result of climate change can impact different aspects of the storm surge barrier. Both the functional performance and the deterioration processes of components may be affected. High temperatures result in the expansion of structural elements of the Hollandsche IJssel barrier. This thermal expansion could result in additional stresses in the materials or even frustrate the closure operation of the

barrier. In that case, the changes in extreme temperatures are important. The changes in mean temperature are particularly relevant for the deterioration since the corrosion and carbonation rates will increase with rising temperatures.

Observed changes

The global temperature has been rising for more than a century. The globally averaged combined land and ocean surface temperature rose by 0.85 °C over the period 1880 to 2012 (IPCC, 2014). For the Netherlands, the average temperatures in de Bilt increased by 1.8 °C between 1901 and 2013. The majority of this increase, 1.4 °C, took place in the years after 1951. The fact that land masses generally warm faster than the oceans explains the difference between the warming in the Netherlands and the global temperature rise. Changes in the average temperature were also observed for the seasons. More frequent westerly winds have led to milder temperatures in the winter, and the increase in solar radiation, mainly due to a reduction in air pollution, has resulted in warmer summers (Van den Hurk et al., 2014).

Extreme temperatures have increased as well. Figure 3.2 depicts the observed maximum and minimum temperature over the past century. The maximum temperature has increased by about 4.2 °C since 1905, according to the trend analysis by the Environmental Data Compendium (Compendium voor de Leefomgeving, CLO) (2020b). This trend was determined using the Integrated Random Walk (IRW) model. For more information on the model, see Visser (2004). A similar increase has been observed for the annual minimum temperature.

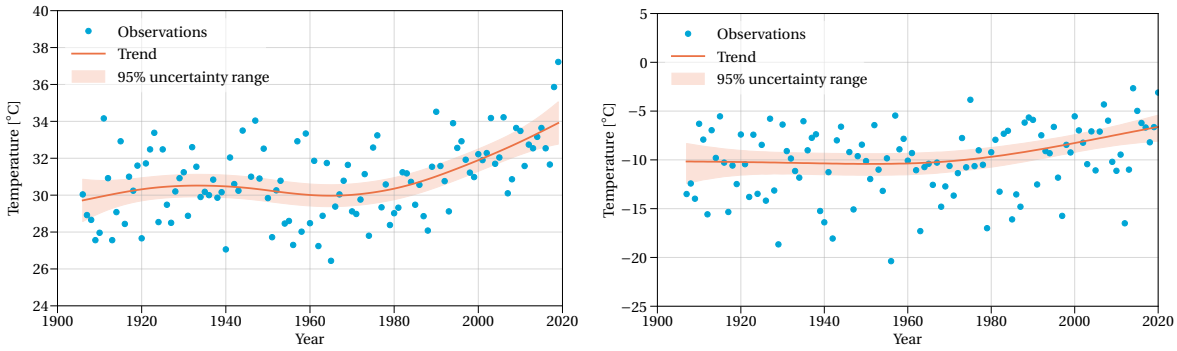

(a) Annual maximum temperature.

(b) Annual minimum temperature.

Figure 3.2: Observed changes in extreme temperatures, analysis by the CLO (2020b).

High temperatures occur more often as well. The average number of summer days (days with a maximum temperature at or above 25 °C) for the period 1981-2010 is almost twice as high compared to the average value over the previous 30 years (1951-1980). On the other hand, the average number of frost days (days with a minimum temperature below 0 °C) decreased by 4 days over the same periods (Klein Tank et al., 2015).

Future changes

This trend of global warming will continue in the future, though the rate is dependent on the emission scenario. In general, winters will become milder and the probability of having very cold winters will decrease. Summers will become warmer and the occurrence of warm extremes will become more likely. The number of days with a maximum temperature at or above 25 °C increases from 21 days to more than 40 days for both W scenarios (Klein Tank et al., 2015). The projections of the temperature changes for each scenario are provided in Table 3.1.

Table 3.1: Temperature changes for the different KNMI'14 scenarios (Klein Tank et al., 2015).

Variable	Ref. period	2050				2085			
	(1981-2010)	G_L	G_H	W_L	W_H	G_L	G_H	W_L	W_H
Mean annual temperature	10.1 °C	+1 °C	+1.4 °C	+2.0 °C	+2.3 °C	+1.3 °C	+1.7 °C	+3.3 °C	+3.7 °C
Mean winter temperature	3.4 °C	+1.1 °C	+1.6 °C	+2.1 °C	+2.7 °C	+1.3 °C	+2.0 °C	+3.2 °C	+4.1 °C
Mean summer temperature	17.0 °C	+1 °C	+1.4 °C	+1.7 °C	+2.3 °C	+1.2 °C	+1.7 °C	+3.2 °C	+3.7 °C
Coldest winter day per year	−5.9 °C	+2.0 °C	+3.6 °C	+3.9 °C	+5.1 °C	+2.7 °C	+4.1 °C	+5.6 °C	+7.3 °C
Warmest summer day per year	24.7 °C	+1.4 °C	+1.9 °C	+2.3 °C	+3.3 °C	+2.0 °C	+2.6 °C	+4.2 °C	+4.9 °C
Number of days with min. temp < 0 °C	38	−30%	−40%	−50%	−60%	−35%	−50%	−70%	−80%
Number of days with max. temp ≥ 25 °C	21	+22%	+35%	+40%	+70%	+30%	+50%	+100%	+130%

Evaluation of the impact of temperature rise

The high temperatures that cause the thermal expansion of structural elements are generally associated with easterly winds and these winds do not lead to severe storm surges along the Dutch coast. The north-westerly winds cause the highest storm surges and these occur mostly in the storm season during which the temperature is not very high. The direct impact of the more frequent occurrence of high temperatures on the closure operation of the barrier is therefore negligible. A similar conclusion can be drawn for the movable bridge of the barrier in relation to shipping. Heat waves in the summer and the associated thermal expansion could lead to difficulties in the opening and closing of the bridge, but the water levels during these warm periods are generally lower than in the winter and vessels are more likely to be able to pass under the storm surge barrier. A third effect of high temperatures is the possible overheating of electrical systems. Overheating could damage the components or cause system disruptions. However, these consequences can be mitigated by proper maintenance of the systems.

Changes in mean temperature affect the deterioration of structural elements of the storm surge barrier. The corrosion rates will increase with rising temperatures, which is relevant for the deterioration of both the steel and concrete elements of the barrier. The steel gates are covered by a protective painting and thus the effect of increasing temperatures on the deterioration and maintenance is assumed negligible. For the concrete elements, a temperature rise also leads to an increase in the diffusivity of CO_2 and chloride ions which accelerates the processes of carbonation and chloride ingress; the two most important mechanisms of concrete deterioration, see Appendix B.

For the Hollandsche IJssel barrier, carbonation is probably the dominant deterioration mechanism as the barrier is not exposed to a saline environment. Whether an acceleration of the carbonation process will really impact the deterioration and associated maintenance, is another question. The rate of carbonation may increase significantly in a relative sense but if the critical levels are still not reached in between maintenance intervals or even during the lifespan of the structure, then the absolute impact is limited. A probabilistic calculation of the carbonation depth was performed to determine whether the temperature rise would affect the concrete deterioration process. The calculation method is based on carbonation tests under standardised environmental conditions (65% RH, 20 °C, natural CO_2 concentration). The method corrects for the relative humidity and CO_2 concentration, but it was considered safe to neglect the effect of temperature since the mean temperatures in Europe lie below the 20 °C used in the tests. The method is described in detail in Appendix B. For now, it suffices to present how the carbonation depth develops over time, see Figure 3.3. This figure shows that despite the large uncertainty in the carbonation depth, the critical level, i.e. the moment the carbonation front reaches the reinforcement, is reached after about 110 years (95th percentile). The concrete cover depth is estimated to be 40 mm based on the cover depths of the structural elements of six concrete structures in the Netherlands included in the study by Polder and De Rooij (2005). The estimate of 110 years until the carbonation front reaches the reinforcement is likely to be extremely pessimistic. The study by Polder and De Rooij (2005) reviewed the results of site investigations on six concrete structures in the

Netherlands, including the Haringvliet sluices and the Eastern Scheldt barrier, and they found carbonation depths of 2 to 5 mm for these structures with ages between 18 to 41 years. Therefore, it is assumed that the rise in temperature does not lead to significant acceleration of the concrete deterioration.

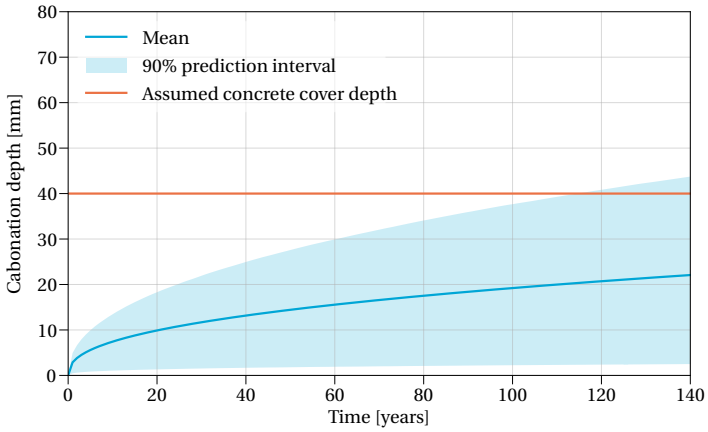

Figure 3.3: Mean value and 90% prediction interval of the carbonation depth.

3.2.2 CO_2 concentration

Potential impact of changes in CO_2 concentration

Atmospheric CO_2 concentration is an important driver for the reinforcement corrosion of concrete structures. An increase in the CO_2 concentration may increase the rate of carbonation-induced corrosion. Stewart, Wang, and Nguyen (2011) studied the impact of climate change factors relevant to the deterioration of concrete (CO_2 concentration, temperature, relative humidity) for the Australian cities of Darwin and Sydney. It was found that the results were most sensitive to increases in atmospheric CO_2, especially for inland arid or temperate climates the risk of carbonation-induced corrosion increased significantly. For this reason a separate section is dedicated to changes in the atmospheric CO_2 concentration.

Observed changes

Since the start of the Industrial Revolution at around 1750, the amount of carbon dioxide in the atmosphere has risen by more than 40%. In 1750, the global atmospheric CO_2 concentration was about 280 ppm, and in 2020, a concentration of 412.5 ppm was measured (NOAA, 2021). Despite the COVID-19 pandemic, which lead to a reduction of about 7% in global carbon emissions, the measured concentrations were higher than at any point in the past 800,000 years. A large part of the total increase, about 50%, took place in the last 40 years (Figure 3.4).

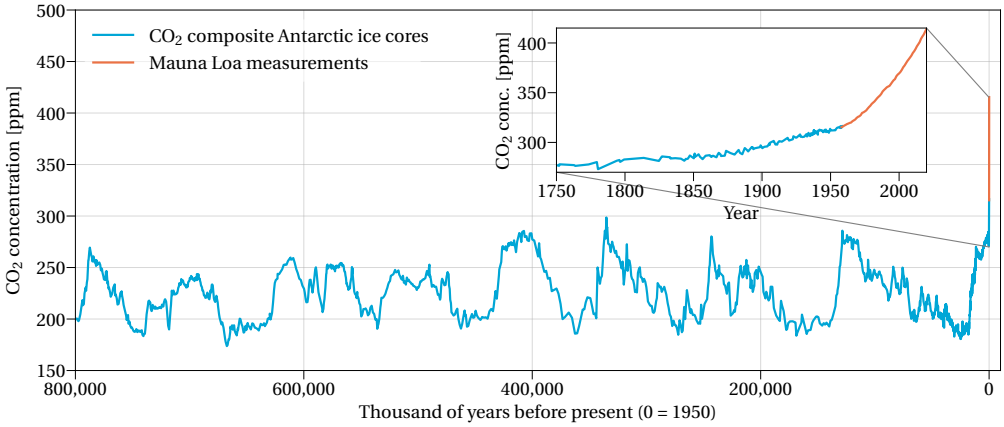

Figure 3.4: Long-term trend in atmospheric CO_2 concentrations. Data before 1958 was obtained from the study by Bereiter et al. (2015), which includes the construction of a composite of the CO_2 concentrations from Antarctic ice cores. Annual mean concentrations from 1959 onwards come from the Mauna Loa observatory. This station has the longest running record of atmospheric CO_2 concentrations, see website of the Scripps CO_2 Program (*https://scrippsco2.ucsd.edu*) and Keeling et al. (2005).

Future changes

The concentration is expected to continue to grow in the future. Van Vuuren et al. (2011) studied the trends in the concentrations of greenhouse gases in the RCPs adopted by the IPCC. All four pathways project a rise in the coming decades, but the scenarios start to deviate after 2050. RCP8.5 shows a rapidly increasing CO_2 concentration that reaches about 950 ppm by 2100. In RCP6.0 and RCP4.5, the concentrations stabilise at 625 ppm and 540 ppm, respectively, at the end of the century. RCP2.6 shows a decline after 2050 to about 420 ppm by 2100 (Figure 3.5).

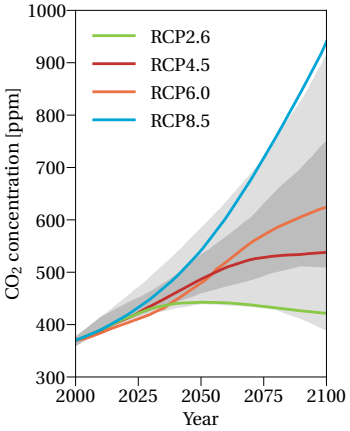

Figure 3.5: Trends in the global atmospheric CO_2 concentration for the 21st century. Grey area indicates the 98th and 90th percentiles (light/dark grey) of the EMF-22 study by Clarke et al. (2009), adapted from Van Vuuren et al. (2011).

Evaluation of the impact of changes in CO_2 concentration

The CO_2 concentration more than doubles in RCP8.5. The effect of this increase on the reinforcement corrosion can be assessed by performing the same calculation as discussed Section 3.2.1, but for a CO_2 concentration of 950 ppm. Note that use of this concentration is quite conservative as it is not expected to be reached until around 2100. The calculated carbonation depth is shown in Figure 3.6. The moment the carbonation front reaches the reinforcement has shifted from about 100 years to 55 years for the 95th percentile. Again, the 95th percentile is probably very conservative. Von Greve-Dierfeld and Gehlen (2016c) proposed to use the mean values multiplied with a partial safety factors of up to 1.25 to obtain design conditions. This approach would give a carbonation depth of 40 mm after 125 years. Secondly, the carbonation depth only signifies the initiation corrosion, the moment the carbonation front reaches the reinforcement, after which the actual corrosion process starts. There is ample time to execute repair works before the reinforcement is damaged.

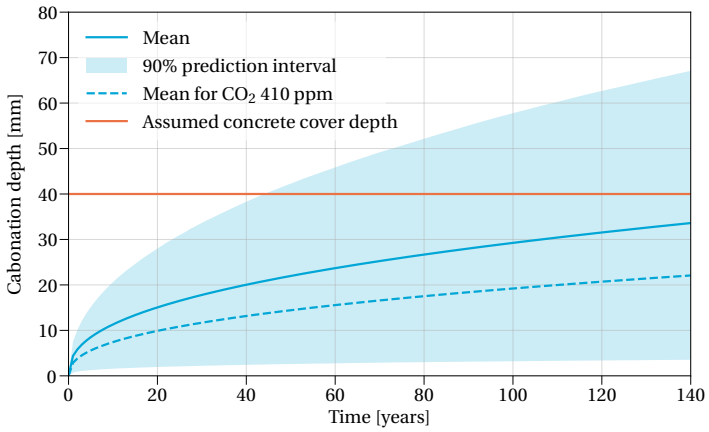

Figure 3.6: Mean value and 90% prediction interval of the carbonation depth for a CO_2 concentration of 950 ppm.

3.2.3 Precipitation

Potential impact of changes in precipitation

More extreme rainfall puts pressure on the water management system in the area. Larger quantities of water will have to be discharged into the Hollandsche IJssel to prevent flooding of the polders. When the storm surge barrier is closed during those rainfall events, the water level in the river will rise and loads on the flood defences will increase. Changes in rainfall are also closely linked to the variation in discharges in the rivers. If the occurrence and intensity of long-lasting rainfall increases, higher river discharges can be expected, resulting in an increase in the water levels in the rivers. The opposite is true for long periods of drought as a result of rainfall deficits. Next to the impact on the functional performance, changes in the precipitation pattern will impact several deterioration mechanisms. For instance, a wetter environment results in increased corrosion rates, while longer periods of drought accelerate the carbonation process.

Observed changes

The annual precipitation in the Netherlands increased by 26% over the period 1910 to 2013 and all seasons except the summer have become wetter. Most of this change in precipitation took place after 1951. Between 1951 and 2013, the annual precipitation rose by 14% (Van den Hurk et al., 2014). The increase in precipitation is primarily caused by the increase in water vapour in the atmosphere associated with higher temperatures. Both the number of winter days with at least 10 mm precipitation and the number of summer days with at least 20 mm have increased, whereas the total number of wet days (days with precipitation above 0.1 mm) has not changed (Van den Hurk et al., 2014). This observation indicates that the rainfall has become more severe.

The observed changes in extreme precipitation are even greater. The number of days with more than 50 mm precipitation at any of the 102 homogenised stations has increased by 76% from 5.3 days in 1951 to 9.0 days in 2019, according to the IRW trend analysis by the CLO (2020a). These heavy rainfall events are problematic in the sense that they could cause traffic disruptions or flooding of streets, but the effect on the river discharges is limited as long as the events are of short duration, i.e. several days.

Future changes

Since the temperature will continue to rise in the future for all KNMI'14 scenarios, the mean precipitation will increase as well, except for the summer. Only the scenarios W_L and G_L show a small increase in the mean precipitation during the summer in 2050, see Figure 3.7. For 2085, the changes are more pronounced, the precipitation during the winter increases significantly for the W_H scenario, and the same scenario exhibits a strong reduction of the precipitation in the summer.

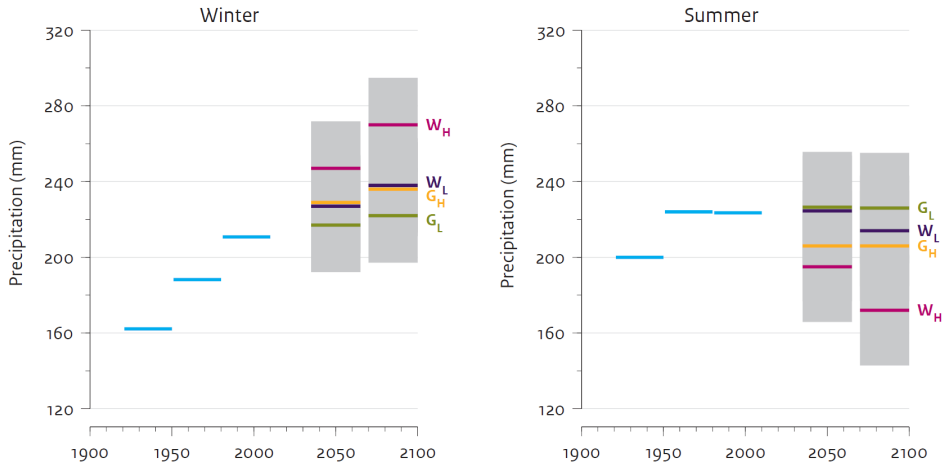

Figure 3.7: Precipitation: observations (30-year averages) and KNMI'14 scenarios for 2050 and 2085 (Klein Tank et al., 2015).

Regarding the precipitation extremes, all scenarios display an increase of the extremes throughout the whole year, even the G_H and W_H scenarios that are characterised by drier summers. Rainfall extremes in the summer are typically caused by rain showers, which have a relatively short duration, in the order of hours. Winter extremes are usually a result of frontal precipitation that occurs when warm air meets cooler air. The intensity

of frontal rainfall is generally lower than during showers, but the rain can last several days and across a larger area. The discharge peaks of the rivers are also related to these events (KNMI, n.d.). The distinction between both types of rainfall is not always clear-cut; often a combination of both types occurs.

The changes in the extremes for each of the KNMI'14 scenarios were studied by HKV and the KNMI on behalf of STOWA, the centre of expertise of the regional water managers (Beersma et al., 2019). Because of additional uncertainties in the rainfall extremes associated with rain showers, which are not well resolved in the climate models, three sub-scenarios were included for each KNMI'14 scenario. These sub-scenarios are denoted as "lower", "centre", and "upper". For each of these sub-scenarios, the amount of rainfall for different durations and return periods were derived. The annual rainfall statistics, which are virtually equivalent to the summer statistics, show a significant increase in the maximum extreme rainfall, up to 41% for the W scenarios in 2085. The changes in rainfall extremes during the winter are less severe (a maximum increase of about 29% for the W scenarios in 2085). The larger increase in the summer is probably due to stronger changes in the extremes of rain showers. According to a rule of thumb mentioned by the KNMI, the intensity typically increases by about 7% per degree warming, but in the summer, there is a much larger uncertainty and the increase could be between 2% and 14% per degree warming (KNMI, n.d.). Illustrative for the large uncertainties associated with the rainfall extremes is that the sub-scenario "upper" of the moderate G scenarios overlap with the sub-scenario "lower" of the W scenarios for both the annual and winter statistics. Another difference between the sub-scenarios includes the opposite behaviour of the "lower" sub-scenarios to the "centre" and "upper" sub-scenarios. In the "lower" sub-scenarios, the relative changes in intensity increase with longer rainfall durations and return periods, whereas the opposite occurs for the "centre" and "upper" sub-scenarios. These findings can also be observed from the 24-hour winter rainfall for different return periods as shown in Table 3.2. Variations in the rainfall during the winter were chosen to be shown since these changes are most relevant to the storm surge barrier.

Table 3.2: Increase in extreme 24-hour winter rainfall in percentages, based on data from meteobase.nl as explained in (Beersma et al., 2019).

Return period	**Current climate**	**2050**				**2085**			
[years]	**(2014)**	G_L	G_H	W_L	W_H	G_L	G_H	W_L	W_H
0.5	22 mm	-2% to 1%	1% to 5%	3% to 8%	5% to 12%	1% to 5%	2% to 7%	6% to 15%	11% to 22%
1	26 mm	-2% to 2%	0% to 5%	3% to 9%	4% to 12%	0% to 5%	2% to 7%	6% to 17%	10% to 23%
2	30 mm	-2% to 2%	0% to 5%	3% to 10%	4% to 12%	0% to 5%	2% to 7%	6% to 19%	9% to 24%
5	36 mm	-2% to 2%	0% to 5%	3% to 11%	3% to 13%	0% to 5%	1% to 7%	7% to 20%	9% to 24%
10	41 mm	-2% to 2%	0% to 5%	3% to 12%	3% to 13%	0% to 6%	1% to 7%	7% to 21%	8% to 25%
20	46 mm	-2% to 3%	0% to 5%	3% to 12%	3% to 13%	0% to 6%	1% to 7%	7% to 22%	8% to 25%
25	47 mm	-2% to 3%	0% to 5%	3% to 12%	3% to 13%	-1% to 6%	1% to 7%	7% to 22%	8% to 25%
50	53 mm	-2% to 3%	0% to 5%	3% to 13%	3% to 13%	-1% to 6%	1% to 7%	7% to 22%	8% to 26%
100	59 mm	-2% to 3%	0% to 6%	3% to 13%	3% to 13%	-1% to 6%	1% to 8%	7% to 23%	8% to 26%
200	64 mm	-2% to 3%	0% to 6%	3% to 13%	2% to 14%	-1% to 6%	0% to 8%	7% to 23%	8% to 26%
250	66 mm	-2% to 3%	0% to 6%	3% to 13%	2% to 14%	-1% to 6%	0% to 8%	7% to 23%	8% to 26%
500	73 mm	-2% to 3%	0% to 6%	3% to 13%	2% to 14%	-1% to 6%	0% to 8%	7% to 24%	7% to 26%
1000	80 mm	-2% to 3%	0% to 6%	3% to 14%	2% to 14%	-1% to 6%	0% to 8%	7% to 24%	7% to 27%

Evaluation of the impact of changes in precipitation

The increase in drought caused by larger precipitation deficits in the summer for the G_H and W_H scenarios leads to lower discharges in the river and accelerated land subsidence. Low river discharges could negatively affect the shipping on the rivers because it poses restrictions to the maximum draught, but this is not related to the functional performance of the Hollandsche IJssel barrier. Another consequence of the decrease in summer precipitation and low discharges is the intrusion of seawater that could pose problems for the freshwater supply. The Hollandsche IJssel barrier could be closed to stop the salt intrusion in the Hollandsche IJssel as was done in the past, but this action is undesirable, and the KWA has been developed to cope with periods of drought. Therefore, the impact of reduced summer precipitation and low river discharges on the functional performance of the barrier is assumed to be negligible. Land subsidence will hardly affect the storm surge barrier since it is founded on piles. The dikes, on the other hand, are subject to subsidence. The rates and consequences of subsidence are treated as a separate external driver in Section 3.3.

The increase in precipitation intensity poses challenges to the water management of the polders surrounding the Hollandsche IJssel. The pumping stations have a maximum capacity that could be insufficient during heavy rainfall events. The critical situations of capacity shortage are more likely to be achieved during

the summer half year in which the more intense, short rain showers occur. These situations are less problematic for the storm surge barrier as it is virtually always open during the summer half year. However, even if the capacity of the pumping stations is sufficient during the winter half year, a long closure in combination with high discharges of water from the polders could result in the declaration of a "maalstop". According to HydroLogic (2016), the probability of a closure coinciding with maximum discharge into the river is relatively small, but exact figures were not mentioned. Rongen and Maaskant (2019) state that on average 1/3 of the closures are closures at slack water due to high discharges from the polders. Hence, they assume that the probability of having a discharge of 75 m^3/s is 1/3. A discharge of 75 m^3/s instead of the maximum capacity of 90 m^3/s was used because the water authorities, in particular HH Rijnland, are able to discharge water into waterways other than the Hollandsche IJssel.

A second consequence of the increase in precipitation, especially during the winter, is higher river discharges. An increase in river discharges results in higher water levels and thus an increased risk of flooding. The higher water levels could lead to more frequent closures of the storm surge barrier affecting both the functional performance as well as deterioration of the closure elements, such as the gate drive mechanism. The impact of the changes in precipitation, and the KNMI'14 scenarios in general, on the river discharges have been studied by Sperna Weiland et al. (2015) and have been included in the databases for the probabilistic model Hydra-NL. This model, which can be used to derive local water levels for a range of return periods, is also used in this study.

The impact of future variations in the precipitation on the deterioration of the structure is considered to be negligible. More wet days in the winter could lead to accelerated corrosion of steel elements, but the scenarios show a decrease in the number of wet days in the summer which may cancel out the effect of wetter winters. Moreover, the steel gates are covered by a protective painting that has to degrade first before corrosion starts. A similar conclusion can be drawn for the deterioration of the concrete. Longer dry periods are favourable for carbonation, but the wetting of concrete during rain events slows down this process (Bertolini et al., 2013).

3.2.4 Other climate variables

In addition to the already described effects of climate change, there are also changes in other climate variables such as wind, humidity, solar radiation, and droughts. The changes and possible influence of each of these climate variables are only briefly discussed below because either the expected changes are small or the direct impact on the functional performance or technical state of the Hollandsche IJssel barrier is limited.

- Wind

  The wind field has experienced large (interannual) variations over the past century. Wind speeds over the North Sea were relatively high at the beginning and end of the 20th century, but lower values were observed mid-century and in recent years. Despite the variations on a decadal scale, no clear trend could be discerned in the observations (Klein Tank et al., 2015; Van den Hurk et al., 2014). Wind speeds over land, on the other hand, show a decrease since the early 1960s. This decrease may partly be due to urbanisation that results in an increase in surface roughness (Klein Tank et al., 2015).

  The projected changes in wind speed in the KNMI'14 scenarios are small and within the natural variation range. The G_H and W_H scenarios do show an increase in the number of days with southerly and westerly winds, but these winds do not cause the highest storm surges. Based on the small changes in the wind field in the KNMI'14 scenarios, one may conclude that higher storm surges and wind set-up are not expected. However, in order to assess whether changes in storm surges indeed do not have to be considered, studies that have specifically looked at the effects of climate change on storm surges along the European coasts are analysed in Section 3.4.

- Humidity

  Although the rising temperature results in more atmospheric water vapour, the relative humidity has decreased over the past decades. This decrease is the result of the difference in the warming of oceans and land. Land masses warm more quickly than oceans and the capacity to hold water vapour increases with temperature. Atmospheric water vapour over land masses can thus be higher than over the ocean surface. At the same time, the majority of atmospheric water vapour (~85%) is evaporated from the oceans, where the water-holding capacity of the air is smaller. The net result is a decrease in relative humidity because the evaporation rate cannot keep up with the increased capacity of the air over land masses. Other processes such as changes in air circulation and reduced moisture availability may also affect the relative humidity (Willett et al., 2014).

Lower relative humidities (and higher temperatures) result in higher evaporation rates over land since the capacity for evaporation is increased. Higher evaporation rates could in turn exacerbate the imbalance between precipitation and evaporation resulting in drought. The fact that relative humidity is mostly relevant to drought-related issues may be the reason why the KNMI'14 climate change scenarios only report changes in relative humidity for the summer months. The global trend of a decreasing relative humidity described by Willett et al. (2014) is reflected in the projections of the KNMI, though the projected changes are in the order of several percentages at most (-3% for W_H). These changes in relative humidity could affect the deterioration processes of components, but because the changes are small the impact is assumed negligible.

- Solar radiation

  Solar radiation is the energy source of the Earth's climate system. The amount of radiation decreased between 1950 and 1980, but widespread brightening has occurred since 1980 (IPCC, 2013). This increasing trend in solar radiation has also been observed by the KNMI, which reports a 9% increase over the period 1981 to 2013 (Klein Tank et al., 2015). The KNMI attributes this increase partly to a more transparent atmosphere due to the reduction in air pollution.

  The KNMI'14 scenarios indicate that more solar radiation will reach the Earth in the future, but the changes fall within the range of natural variability. The increase is only significant, yet small (max. 9.5%), for the summertime radiation in the G_H and W_H scenarios in which the more easterly winds result in a decrease in summer cloudiness (Klein Tank et al., 2015). The ultraviolet component of solar radiation could have a damaging effect on materials, yet the impact is assumed negligible due to the small changes. The additional warming due to the increase in solar radiation, which could also affect the deterioration of materials, is accounted for in the temperature changes in the scenarios.

- Drought conditions

  As temperature rises, evaporation rates increase and, in combination with a lack of precipitation, there is a higher risk of droughts. As prolonged periods of high temperatures and low precipitation generally occur during the summer, only the changes in evaporation in summer are often considered. The KNMI uses the Makkink formula to calculate the potential evaporation during the summer months. Potential evaporation is defined as the evaporation taking place if sufficient water is available, and between 1951 and 2013, this potential evaporation increased by about 12% (Klein Tank et al., 2015).

  The potential evaporation is expected to increase in the future as all scenarios project rising temperatures and increasing solar radiation. The increase in the amount of evaporation in 2085 varies between 3% and 15% for the G_L and W_H scenarios, respectively (Klein Tank et al., 2015). The greater amounts of evaporation have a negative impact on the precipitation deficit, which is an indicator of drought. Prolonged periods without precipitation may further aggravate the situation. Drought is relevant to water management related issues, such as sufficient availability of freshwater resources for drinking water and irrigation. The Hollandsche IJssel barrier does facilitate the supply of fresh water, but it is not part of any strategy to cope with droughts. Besides causing freshwater shortages, dry periods could also threaten the stability of peat dikes, but failure due to drought is unrelated to the functioning of the storm surge barrier. In the future, the barrier may, however, be used to maintain a certain water level in the river to avoid the drying out of the (peat) dikes. The drawback of using the barrier during periods of drought is that salt water could accumulated in front of the barrier, as discussed in Section 2.2.5. In addition, fresh water cannot be extracted from the river as only a limited amount of fresh water can be stored in the river basin. This implies that the risk of instability of the dikes has to be weighed against the risks of salt intrusion and freshwater shortages before a decision can be made on whether to deploy the storm surge barrier during periods of drought. For now, drought aspects are not taken into account in the assessment of the remaining life of the storm surge barrier as the water authorities concluded that it is also undesirable to use the Hollandsche IJssel barrier to prevent salt intrusion.

3.3 Land subsidence

Land subsidence is another important driver that could affect the remaining life of the Hollandsche IJssel barrier. Land subsidence is discussed in a different section than climate change because the processes that lead to subsidence are independent of climate change. However, climate change may accelerate some of these processes, such as oxidation or compaction.

Potential impact of land subsidence

Land subsidence could cause damage to structures and leads to increased flood vulnerability as the relative height of flood defences is reduced. The Hollandsche IJssel barrier is founded on piles and land subsidence is less relevant, but the dikes along the Hollandsche IJssel are subject to subsidence. As a result, the risk of flooding may increase while the barrier still functions properly according to the requirements.

Observed changes

In the Netherlands, land subsidence is an ongoing process of which the primary causes are (1) salt mining and gas extraction, (2) low groundwater tables in peatlands due to drainage, and (3) expansion of built-up areas and infrastructure on soft soil layers (Van den Born et al., 2016; Stouthamer et al., 2020). The western part of the Netherlands (where the Hollandsche IJssel barrier is located) is characterised by peat and clay soils. In those areas, subsidence is mainly due to peat oxidation, shrinkage, and compaction of the soft soil layers as a result of drainage (Van den Born et al., 2016). In addition, the area around the Hollandsche IJssel used to be a peat mining area in previous centuries (Erkens et al., 2016). These excavation activities further lowered the ground level. The subsidence varies considerably across the polders surrounding the Hollandsche IJssel. Over the past 30 years, areas in the western part of the Krimpenerwaard have experienced settlements of up to 30 cm, while some areas in the east have not settled at all (Hoogheemraadschap van Schieland en de Krimpenerwaard, 2021). Such specific data were not available for the polder on the other side of the Hollandsche IJssel (Schieland), but recent subsidence rates (0.5-1.0 cm/year) indicate that the subsidence in Schieland has been of a similar order of magnitude (Hoogheemraadschap van Schieland en de Krimpenerwaard, 2019).

Future changes

The main causes of subsidence are all related to human activities, which makes land subsidence dependent on socio-economic developments. In addition, climate change could accelerate the subsidence as higher temperatures and longer periods of drought lead to more peat oxidation (Van den Born et al., 2016). The complicated interactions between climate change, low groundwater levels, and greenhouse gas emissions due to peat oxidation make future subsidence inherently uncertain (Stouthamer et al., 2020). Nevertheless, Deltares, TNO, and Wageningen Environmental Research (WEnR) developed subsidence maps for the Netherlands for the period 2020-2100. These maps are part of the Climate Impact Atlas (Klimaateffectatlas) and show the expected subsidence for two climate change scenarios, a low and a high scenario. The low scenario corresponds to the G_L scenario of the KNMI'14 climate change scenarios, and the high scenario shows the projected subsidence for the scenario W_H. The projections primarily include two processes: subsidence due to oxidation of organic matter, such as peat, and subsidence due to compaction of soft soil layers. The projections thus mainly focus on subsidence as a result of drainage. Subsidence due to salt mining and gas extraction are also taken into account in the projections (Erkens et al., 2021).

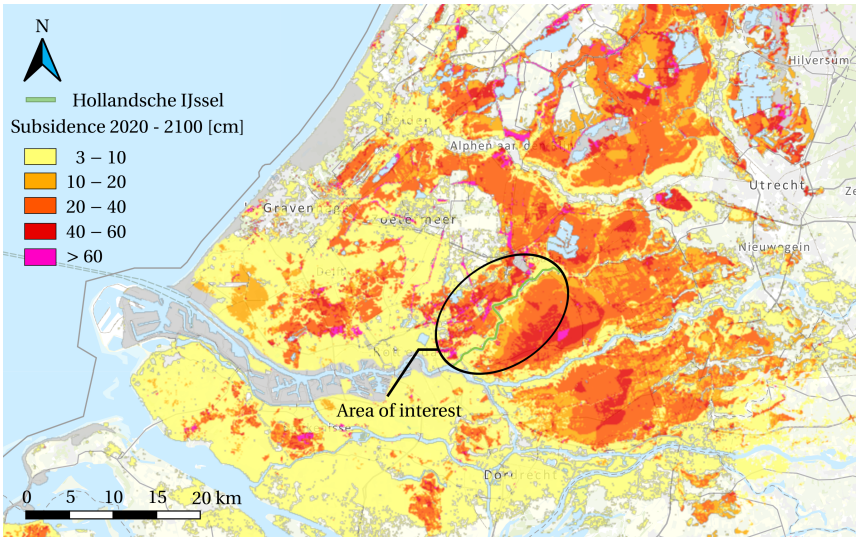

Figure 3.8: Projected subsidence in the south-west of the Netherlands over the period 2020-2100 for the low scenario (G_L of KNMI'14) (Klimaateffectatlas, n.d.).

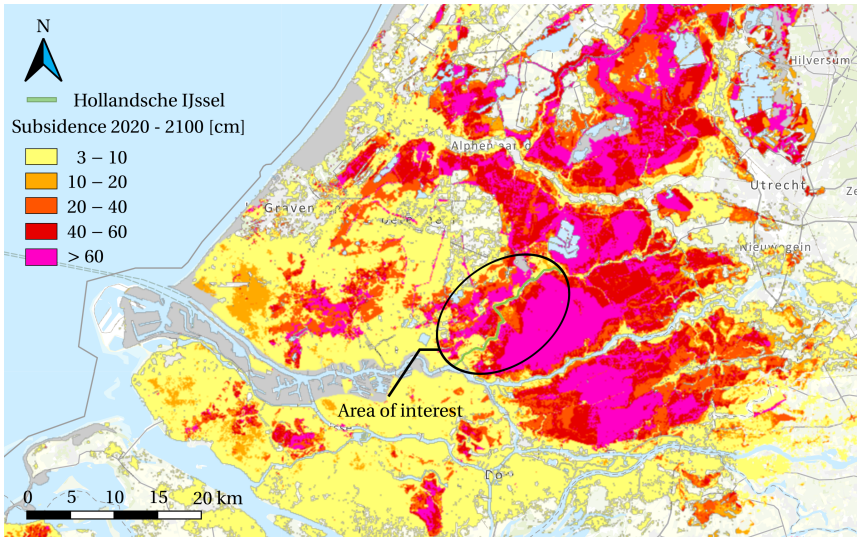

Figure 3.9: Projected subsidence in the south-west of the Netherlands over the period 2020-2100 for the high scenario (W_H of KNMI'14) (Klimaateffectatlas, n.d.).

As becomes apparent from Figure 3.8 and Figure 3.9, the area around the Hollandsche IJssel is one of the regions most strongly affected by land subsidence, though there is a large variation. On the eastern side of the river, the subsidence ranges from 3-10 cm (0.38-1.25 mm/year) to 40-60 cm (5-7.50 mm/year) for the low scenario. Under the high scenario, a subsidence of more than 60 cm (> 7.50 mm/year) is projected for most parts of the Krimpenerwaard polder. West of the river, the projected subsidence is roughly of the same order of magnitude. However, these subsidence values generally apply to the more low-lying areas rather than the dikes along the river. For the dikes, values in the order of 3-10 cm (0.38-1.25 mm/year) and 10-20 cm (1.25-2.50 mm/year) are projected for the low scenario. Under the high scenario, the projected subsidence of certain dike stretches is in the order of 40-60 cm (5-7.50 mm/year).

Evaluation of the impact of land subsidence

The effect of land subsidence is considered minimal for the Hollandsche IJssel barrier itself because of its foundation on piles. On the other hand, the dikes behind the storm surge barrier will settle, which leads to a decrease in the storage capacity. So while the structure itself is hardly affected by subsidence the functional performance of the barrier with respect to flood protection and water management could decline. Fortunately, subsidence is accounted for in previous and ongoing reinforcement programmes following the assessment in 2011. The designs of the dike sections of trajectory 14-1, near Capelle aan den IJssel and Moordrecht, include a subsidence of 25 cm over 50 years for the earthen solution and 40 cm over 100 years for the structural solution (sheet piles) (Maronier, 2014). These values are lower than the expected subsidence, especially for the longer time period of 100 years, but probably sufficient given the fact that the earthen solution was adopted for most parts of the dike trajectory, and thus the possibility of having to carry out reinforcement works within 50 years has already been accounted for regardless of the subsidence. Within the project Krachtige IJsseldijken Krimpenerwaard (KIJK), in which 10.51 km of trajectory 15-3 is strengthened, the engineers are also aware of the impact of subsidence. The preferred strategy includes solutions with a lifespan of 20 years, which suits well with the maintenance interval of the road structure and enables a better response to the uncertainties in the subsidence (Hoogheemraadschap van Schieland en de Krimpenerwaard, 2018). This solution, however, has been chosen for only a small stretch of the trajectory. For most parts (6.89 km), a structural solution with a lifespan of 50 years is the preferred option. How this solution accounts for land subsidence is not explicitly mentioned, but since the designers have shown to be aware of the subsidence, it was assumed that this solution also deals sufficiently with the land subsidence.

Another possible consequence of land subsidence is an increase in the discharge of water from the polders into the river to regulate the groundwater table. This increase could lead to more frequent occurrences of a "maalstop". However, the discharge that is needed to regulate the groundwater table may temporarily be decreased during a closure of the barrier to compensate for the effect on the frequency of a "maalstop". In that case, the increase of discharge due to land subsidence will only become problematic if the barrier has to be closed so often and for so long that the discharge during normal conditions (when the barrier is open) is insufficient to regulate the groundwater table.

In conclusion, the impact of land subsidence on the Hollandsche IJssel barrier itself is negligible. It is mainly a threat to the dikes behind the barrier, but the ongoing reinforcement programmes that followed the third assessment round, incorporate subsidence sufficiently in their designs. The effect of an increased discharge to adjust the groundwater table was also assumed to be limited. Therefore, subsidence is deemed to be of minor importance for the lifespan of the Hollandsche barrier and it is not considered any further.

3.4 Hydraulic boundary conditions

Changes in the local water levels are actually the result of a combination of external drivers. Hence, these drivers are discussed in one section. The most important external drivers determining the local water levels are sea level rise, storm surges, and river discharges.

Sea level rise

The global mean sea level rose by 0.19 (0.17 to 0.21) m between 1901 and 2010 according to the IPCC in their fifth assessment report (AR5) (IPCC, 2014). The average rate of global sea level rise was 1.7 (1.5 to 1.9) mm/year over the period 1901-2010 and accelerated to 3.2 (2.8 to 3.6) mm/year between 1993 and 2010. These figures were slightly updated in the IPCC's Special Report on the Ocean and Cryosphere in a Changing Climate (SROCC) as part of the IPCC's AR6 cycle (IPCC, 2019). The SROCC estimates a global mean sea level rise of 0.16 (0.12 to 0.21) m between 1902 and 2015, with rate of 1.4 mm/year for most part of the 20th century (1901-1990). The rate increased to 2.1 mm/year for 1970-2015 and then to 3.6 mm/year for 2006-2015, about 2.5 times the rate for 1901-1990. The acceleration in sea level rise in recent decades can be attributed to the increasing rates of ice loss from the Greenland and Antarctic ice sheets (IPCC, 2019). Other global sources of sea level rise include ocean thermal expansion, glacier mass loss, and changes in land water storage.

The IPCC projected a global mean sea level rise of 0.26-0.98 m by the year 2100 in their fifth assessment report. The upper limit of 0.98 m was adjusted to 1.1 m in the SROCC (IPCC, 2019). These estimates are presented as a likely range (66% probability or more) as the IPCC acknowledged the limited understanding of the behaviour of the large ice sheets of Greenland (GIS) and Antarctica (AIS) under climate change (IPCC, 2014). Several studies have sought to quantify the contribution of these ice sheets, in particular the contribution of the Antarctic ice sheet. The results show large deviations in the estimated contribution of the AIS, ranging from several centimetres up to more than one metre. These differences follow from model assumptions and the choices for including certain processes in the models (A. M. R. Bakker et al., 2017; Jevrejeva et al., 2019). Especially the inclusion of processes such as hydrofracturing and marine ice cliff instability results in a considerable contribution of the AIS (DeConto & Pollard, 2016). The conservatism of the projections of the IPCC and also the large uncertainty in sea level rise are reflected in the results of studies on future sea level rise that have been published over the past decades. The evolution of the sea level rise projections for the high emission scenarios is shown in Figure 3.10.

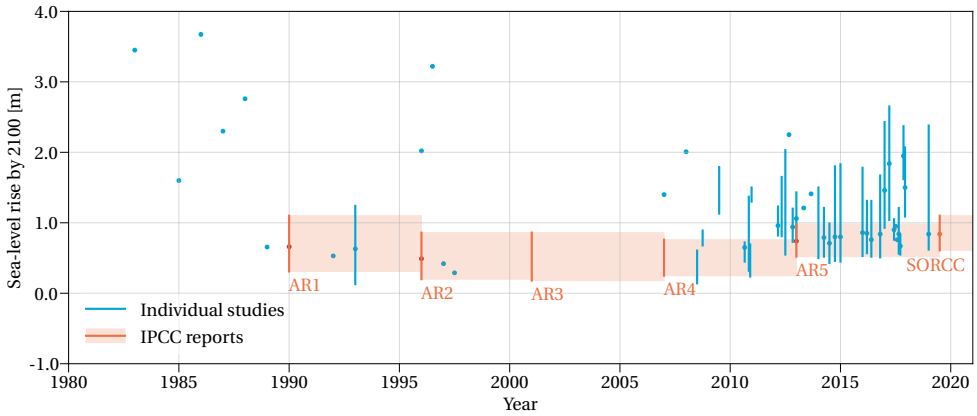

Figure 3.10: Evolution of sea level rise projections for 2100 under high emission scenarios, based on data from Garner et al. (2018). The projections for the high emission scenario of Bamber et al. (2019) and the SROCC report of the IPCC (IPCC, 2019) were added. The dots represent central sea level rise projections and the bars indicate the lower (5th percentile) and upper (95th percentile) values of the individual projections. The orange-shaded regions display the Low to High range of the projections for the high emission scenarios of AR1 (scenario A: Business-as-Usual) and AR2 (scenario IS92a), the range of all AOGCMs projections for the high emission scenario of AR3 (scenario A1FI), the 5-95% range of the projections for the high emission scenario of AR4 (scenario A1FI), and the likely ranges of the projections for the high emission scenarios of AR5 (scenario RCP8.5) and SROCC (scenario RCP8.5).

On a regional scale, additional processes that redistribute the water around the oceans play a role. These processes comprise changes in the gravitational field and rotation of the Earth caused by the redistribution of mass, local land subsidence, and atmosphere/ocean dynamics, e.g. changes in current circulation patterns (Horton et al., 2018; Le Bars et al., 2019; Slangen et al., 2014). These regional effects, except land subsidence, are included in the sea level rise projections of KNMI'14. These projections were made for the G and W climate change scenarios; no distinction was made between the L and H scenarios as changes in air circulation pattern over Europe have limited effect on the sea level changes (Klein Tank et al., 2015). The future sea level changes for both scenarios are shown in Figure 3.11a. The upper values (95th percentile) are 0.75 m and 1.0 m in the G and W scenarios, respectively. However, these values should be interpreted as conservative estimates similar to the likely range of the IPCC (A. M. R. Bakker et al., 2017; Van den Hurk & Geertsema, 2020).

Apart from these relatively conservative scenarios, Haasnoot et al. (2020) constructed high-end sea level rise projections for the Netherlands based on global projections of Le Bars et al. (2017), which included the results of DeConto and Pollard (2016) on the possible contribution of the Antarctic ice sheet to future sea level rise. These high-end scenarios have low probabilities but potentially severe consequences. The sea level rise estimates of the high-end scenarios deviate strongly from the values of the KNMI'14 scenarios, as can be seen in Figure 3.11b. The 95th percentile value for RCP8.5 is 3.17 m in 2100.

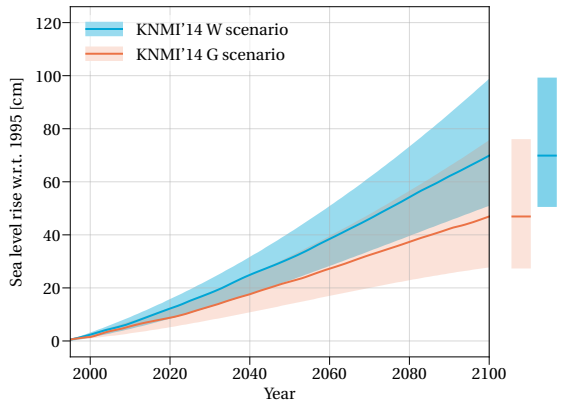

(a) Sea level rise projections under the KNMI'14 scenarios, based on a third order polynomial fit through the ensemble members of the scenarios by Van den Hurk et al. (2014).

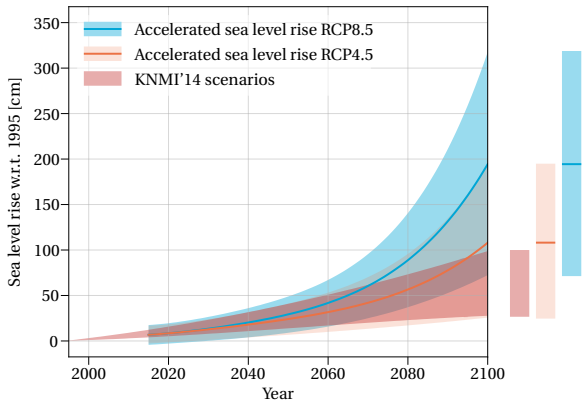

(b) Sea level rise projections under the KNMI'14 scenarios and high-end scenarios (Haasnoot et al., 2020), which were based on the global projections of Le Bars et al. (2017).

Figure 3.11: Sea level rise projections along the Dutch coast.

Storm surge characteristics

A storm surge is a temporary increase of the water level due to the combination of wind set-up associated with strong onshore winds and a lowered atmospheric pressure (Bosboom & Stive, 2015). Changes in the wind field due to climate change could thus affect the height and duration of storm surges along the Dutch coast. Several studies have modelled the meteorological conditions in the North Sea and the impact on the storm surge characteristics for various climate change scenarios (Gaslikova et al., 2013; Howard et al., 2014; Sterl et al., 2009; Vousdoukas et al., 2016). Two of those studies mention the conditions along the Dutch coast. Sterl et al. (2009) report a small increase in the maximum wind speed due to a more frequent occurrence of south-westerly winds, but this increase lies within the range of natural variability. Besides, the highest storm surges in the Netherlands are reached for north-westerly wind whereas south-westerly winds have limited effect on the storm surge characteristics (Sterl et al., 2009). A more recent study (Howard et al., 2014) that investigated the storm surge changes along the European coasts also found no significant changes in the storm surge characteristics along the Dutch coast. It should be noted that both studies consider the SRES A1B emission scenario, a scenario that corresponds best to RCP6.0 (Van Vuuren & Carter, 2014). Secondly, these studies do not take into account the increased probability of hurricane formation due to global warming. Remnants of these hurricanes could reach the North Sea and lead to more frequent and intense storms (Haarsma et al., 2013). There is, however, a large uncertainty regarding this change in extreme storm conditions and the effect on storm surges and wave heights might be moderate since the fetch of these storms is relatively short (Van den Hurk et al., 2014). This process is also not considered in the KNMI'14 scenarios, which indicate minor changes in the wind field and storm surges as well (Van den Hurk et al., 2014).

River discharges

The third factor affecting the local water levels is the changes in the river discharges. The Dutch river system constitutes of two major rivers: the Rhine and the Meuse. The river Rhine is fed by rainfall and meltwater from the Alps and enters the country from Germany. The average discharge is 2200 m^3/s at Lobith where it enters the Netherlands. Near the border with Germany, it bifurcates into three branches: Waal (2/3), Nederrijn/Lek (1/3) and IJssel (1/9) (Klijn et al., 2019). During low water conditions, the discharge distribution is changed and more water is directed to the Nederrijn/Lek to facilitate shipping (Kind et al., 2019). The Meuse is a rain-dominated river showing a larger discharge fluctuation over the year (Liefveld & Postma, 2007). It has a substantially lower average discharge (230 m^3/s) and is not split at any point. The Meuse flows, together with the majority of the Rhine discharge (8/9), through the Rhine-Meuse delta (RMD), where three of the five storm surge barriers, including the Hollandsche IJssel barrier, are located.

The effects of climate change on the discharges of the Rhine and Meuse are a larger variability over the year and more extreme discharges (Sperna Weiland et al., 2015). The stronger seasonal variation in discharges manifests itself stronger for the Meuse due to its rainfed character and relatively small basin area. The extreme discharges increase for both the Meuse and the Rhine. For both rivers, the differences in extreme discharges are relatively small for 2050, but there is a large spread in the projections for 2085 (Figure 3.13). This large spread is caused by differences in the expected precipitation under the various scenarios. For the Rhine, an additional contribution is possible from snowmelt in the Alps due to the increase in temperature. The wide ranges of extreme river discharges in 2085 for both rivers illustrate the uncertainties related to the impact of climate change on the river discharges. Additional uncertainties arise from changes in the upstream river system, e.g. flood mitigation measures or policy changes in Germany, and physical characteristics such as the size of retention areas and hydraulic roughness (Hegnauer et al., 2015; Prinsen et al., 2015).

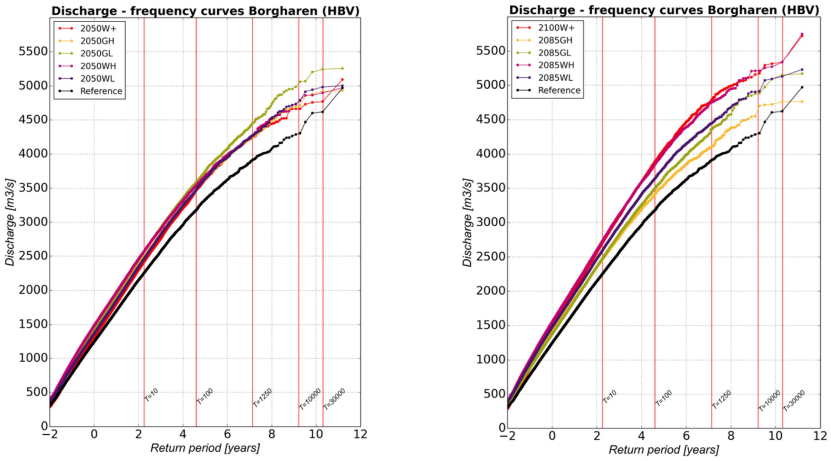

Figure 3.12: Discharge-frequency curves for the Meuse at Borgharen for the KNMI'14 scenarios and years 2050 and 2085 (Sperna Weiland et al., 2015).

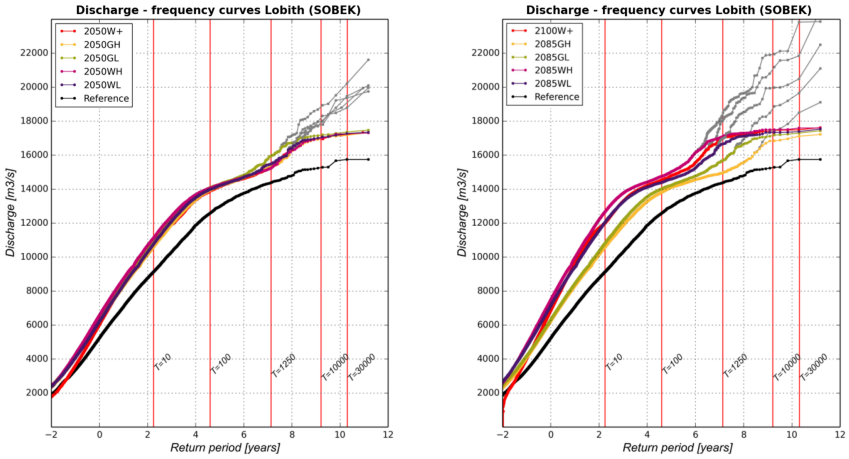

Figure 3.13: Discharge-frequency curves for the Rhine at Lobith for the KNMI'14 scenarios and years 2050 and 2085 (Sperna Weiland et al., 2015).

Evaluation of the impact of the three drivers

The extent to which these three factors influence the water levels depends on the location in the Rhine-Meuse delta. The delta can be separated into different sub-areas in which either one or a combination of the factors are dominant. The division into sub-areas is shown in Figure 3.14.

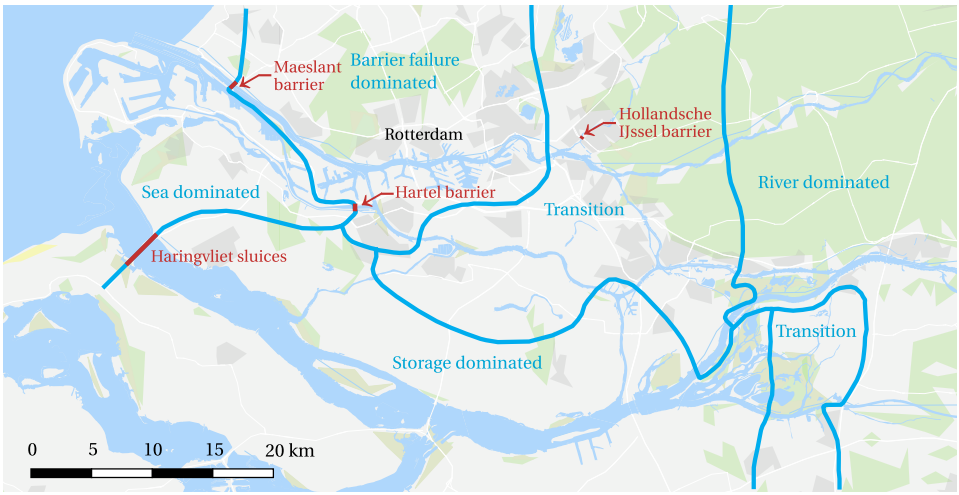

Figure 3.14: Sub-areas of the Rhine-Meuse delta, based on the map by De Goederen (2014).

The area seaward of the Maeslant barrier and Haringvliet sluices is fully dominated by the water level at sea and thus by sea level rise and the height of storm surges. The most eastern sub-area is entirely determined by the river discharges. The storage capacity is important for the sub-area behind the Haringvliet sluices, which in turn depends on the river discharges and the duration of the storm surges. The water levels in the area east of the Maeslant barrier and Hartel barrier are strongly dependent on failure of the storm surge barriers. Since the failure probability is given per closure and the closure frequency increases with a rising sea level, it can be said that sea level rise is the dominant factor in this area. The governing water levels in the remaining areas are determined by a combination of these factors.

The Hollandsche IJssel barrier is located in the transition area in which the design water levels are determined by a combination of failure of the seaward storm surge barriers and high river discharges. This would mean that both sea level rise and the changes in extreme river discharges are important for future water levels near the barrier. The relative importance of these factors can be studied through a number of calculations with Hydra-NL, in which the sea water level and river discharges are varied on the basis of the KNMI'14 climate change scenarios. The results are shown in Figure 3.15.

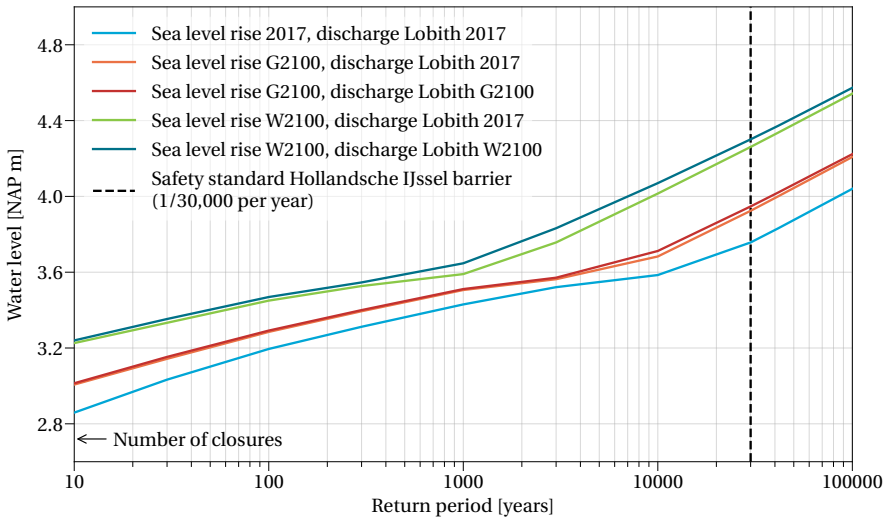

Figure 3.15: Impact of sea level rise and river discharges on the water levels at the Hollandsche IJssel barrier.

Figure 3.15 shows that for the climate change scenarios G (25 cm sea level rise compared to 2017) and W (75 cm sea level rise compared to 2017) the associated changes in river discharges do have some influence on the water levels at the Hollandsche IJssel barrier, but this influence is fairly limited. The maximum difference between the water levels for scenario G with the associated discharge and the current discharge is 2.6 cm. For scenario W, a maximum difference of 6.4 cm was found. Moreover, these differences occur at return periods that are irrelevant to the performance of the barrier. The flood protection standard of the barrier is based on a return period of 30,000 years and for this return period the differences are very small. The number of closures per year and the closure duration are important for the functional performance with respect to navigation and the degradation mechanisms of the storm surge barrier. The water level at which the barrier closes occurs several times per year and in that case the rise in the sea level is probably dominant, also because the sea level rise translates into a higher average water level, which could mean that closures will occur more frequently and it will take longer for the water level to fall below the closure level again. These findings show that sea level rise is the most important factor in assessing both the functional performance and the deterioration of the barrier. Therefore, when it comes to the consequences of climate change on the water levels, the remainder of this study focuses on the influence of sea level rise.

The consequences of higher water levels have already been discussed several times. An apparent effect is higher loads on the gates during closures. The most extensive consequence is, however, more frequent and longer closures. An increase in the closure frequency and duration leads to:

- Increase in the frequency of events in which the barrier should be closed but closure of the barrier fails. This increase in the frequency of non-closures affects the probability of extreme water levels in the hinterland (functional).
- More hindrance to shipping (functional).
- Increase in the probability of reaching the “maalstoppeil” (functional).
- Greater disruption of the tidal regime (functional).
- Faster deterioration of the closure elements due to wear and fatigue (technical/economic).
- More frequent exposure of the bed protection to large flow velocities (technical/economic).

3.5 Summary of the impacts of physical drivers

The previous sections describe the effects of physical drivers that could potentially influence the remaining life of the Hollandsche IJssel barrier. These effects were evaluated, mostly qualitatively and based on climate change projections of the KNMI, to gain better insight into how climate change could impact the functional performance or technical state of the storm surge barrier. The results are summarised in Table 3.3 and Table 3.4. The first table gives an overview of the effects of climate change on the functional performance of the barrier, whereas the latter summarises the effects on the technical state of the barrier and its components. Note that the tables only provide an overview of the impacts in relation to the storm surge barrier. For instance, changing river discharges will have an impact on the maximum load-carrying capacity or maximum draught of vessels, or an increase in the mean temperature or the occurrence of heatwaves may alter the ecosystem in the area of the Hollandsche IJssel barrier. In both cases, these consequences of climate change are not related to the operation of the storm surge barrier, and therefore not included in the table. The tables show that the consequences of sea level rise are by far the most extensive. Hence, sea level rise is the most relevant external driver to focus on when it comes to climate change.

Table 3.3: Overview of the impacts of physical drivers on the functional performance of the Hollandsche IJssel barrier. Whether the variable has an impact is indicated by the colour of the cell; coloured cells indicate that the variable has an impact. The magnitude of the impact is indicated by the font style; impacts that are either limited or already accounted for in future designs or models are written in italics, and the most serious impacts are written in bold.

Function category	Temperature	Precipitation	Land subsidence	Sea level rise	High river discharges	Low river discharges	Drought	CO_2 conc.
Flood protection		*Increase in river discharges causing higher water levels*	*Lower dike heights results in a higher probability of flooding*	**Increase in the probability of extreme water levels**	*Limited effect on the probability of extreme water levels*		*May pose a risk to the stability of the dikes, but the storm surge barrier is not part of any strategy to cope with droughts*	
Navigation				**More frequent closures leads to more hindrance to shipping**		*Lower water levels affect the navigability of the river but this is unrelated to the functioning of the storm surge barrier*		
Water management		Increased or more frequent discharge of water from the polders into the river may increase the frequency of a "maalstop"	*Lower dike heights may incite water authorities to adjust the "maalstoppeil", or the frequency of a "maalstop" may increase when more water has to be discharged to regulate the groundwater table*	**Increase in the probability of reaching the "maal-stoppeil"**			*May pose a risk to the supply of fresh water or increase the salt intrusion, but the storm surge barrier is not part of any strategy to cope with droughts*	
Ecology				**More frequent closures leads to increased disruption of the tidal regime**				
Road traffic				*Vessels will have to use the navigation lock more often. However, based on the operating hours of the bridge, road traffic is given priority*				
Monument								

Table 3.4: Overview of the impacts of physical drivers on the technical state of the Hollandsche IJssel barrier and its components. Whether the variable has an impact is indicated by the colour of the cell; coloured cells indicate that the variable has an impact. The magnitude of the impact is indicated by the font style; impacts that are either limited or already accounted for in future designs or models are written in italics, and the most serious impacts are written in bold.

Component	Temperature	Precipitation	Land subsidence	Sea level rise	High river discharges	Low river discharges	Drought	CO_2 conc.
Lifting towers	*Negligible effect on deterioration of concrete (carbonation)*	*Negligible effect on deterioration of concrete (carbonation)*						*Acceleration of the carbonation process, but consequences are still limited*
Lock heads	*Negligible effect on deterioration of concrete (carbonation)*	*Negligible effect on deterioration of concrete (carbonation)*						*Acceleration of the carbonation process, but consequences are still limited*
Lock chamber	*Negligible effect on deterioration of concrete (carbonation)*	*Negligible effect on deterioration of concrete (carbonation)*						*Acceleration of the carbonation process, but consequences are still limited*
Foundation			*Negligible effect since structure is founded on piles*					
Bed protection				**Increase in number of closures leads to more frequent exposure of the bed protection to large flow velocities**				
Steel gates (SSB)	*Accelerated corrosion, but protected by coating*	*Accelerated corrosion, but protected by coating*		**Elements are exposed to larger forces due to higher water levels (and waves)**	*Limited effect on water levels (and waves)*			
Gate drive mechanism (SSB)				**Faster deterioration (wear and fatigue) due to more frequent use**				
Steel mitre gates (lock)	*Accelerated corrosion, but protected by coating*	*Accelerated corrosion, but protected by coating*		**Elements are exposed to larger forces due to higher water levels (and waves)**	*Limited effect on water levels (and waves)*			
Gate drive mechanism (lock)				**Faster deterioration (wear and fatigue) due to more frequent use**				
Electrical installations	*Damage to electrical systems may effect failure frequency, can be mitigated by appropriate maintenance*							

3.6 Policy changes

Besides the physical changes due to climate change, changes in policies or laws could affect the remaining life of the storm surge barrier. Several factors can give rise to legislative or regulatory revisions. These factors include political decisions, newly gained information or knowledge, societal values, socio-economic developments, and unexpected disasters. An example of a policy change that impacted the storm surge barriers and all other flood defences in the Netherlands is the revision of the safety standards.

Prior to 2017, the safety standards were based on exceedance probabilities of water levels for which the flood defences were designed. Although the standards took into account the economic value and population size of flood-prone areas, the method only provided a global insight into the flooding consequences. The method focused on dike rings and flooding scenarios due to different breach locations in the dike ring were not considered. Large economic growth and an increase in the number of people in flood-prone areas, together with new insights into the failure mechanisms of flood defences and the consequences of flooding were the motivation for a new, more risk-based approach (Jonkman, Voortman, et al., 2018; Slootjes & Van der Most, 2016a). These new standards focus on the consequences of flooding instead of resisting a certain design load. The standards are expressed in terms of acceptable probabilities of flooding and they are defined per dike trajectory, which can be considered as sections of a dike ring subject to similar loads and with similar consequences of a dike breach. The probabilities are obtained from the acceptable risk levels, where risk is expressed as the product of probability and consequence. Three measures of risk are included in the safety standards:

- individual risk: the annual probability of a person dying due to a flood.

  The individual risk may not be higher than 10^5 per year. This risk measure represents the basic flood protection standard for people in the Netherlands. It is in fact the product of the probability of flooding, the percentage of people that are unable to be evacuated, and the mortality from a flood (Slootjes & Van der Most, 2016a).

- societal risk: the annual probability of a flood with many fatalities (Jonkman, Jorissen, et al., 2018).

  This criterion was introduced to account for densely populated areas and evacuation possibilities. For example, the western part of the country has a relatively low evacuation fraction of 0.15. This rate is a result of the population density, available evacuation routes, and the available time before arrival of the floodwater. The time to respond to a flood is longer for the eastern part of the country were the main threat arises from river floods and these floods are better predictable (Jonkman, Jorissen, et al., 2018).

- economic risk: the expected annual economic damage.

  The economic risk follows from a cost-benefit analysis. The costs of reinforcements are compared to the gained reduction of the risk of flooding. In the analysis for the flood protection standards, economic damages in year 2050 and costs of interventions have been considered to obtain the optimal protection levels for the various flood defences (Jonkman, Jorissen, et al., 2018).

In general, the most stringent risk criterion will determine the safety standard (Jonkman, Voortman, et al., 2018). An even stricter safety standard could be assigned to certain regions if it concerns vital and vulnerable infrastructure of national interest, e.g. the nuclear power plant near Borssele (Slootjes & Van der Most, 2016a).

An overview of both the old and new safety standards is given in Figure 3.16. The old standards are expressed as a probability of exceedance of design load and the new standards refer to the maximal acceptable failure probability of a flood defence.

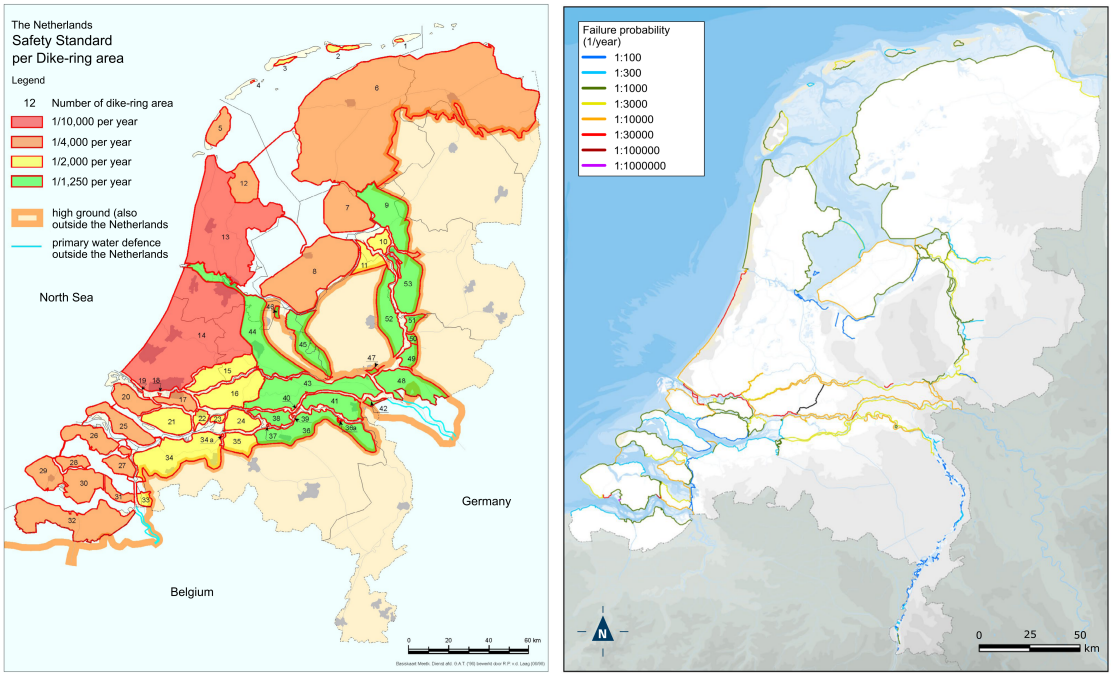

(a) Old safety standards (public information from Rijkswaterstaat).

(b) New safety standards (Slootjes & Van der Most, 2016a).

Figure 3.16: Safety standards for the flood defences in the Netherlands.

There are still reinforcement projects going on or planned to guarantee that the flood defences meet the current safety standards. The aim is to comply with the new standards at every dike trajectory by 2050. A revision of these standards similar to the one of 2017 is therefore not expected in the near future. However, the safety standards of dike trajectories could become more or less stringent, for example, due to large population shifts in regions or economic developments. These developments are not considered as policy changes since the legislation is not adjusted. They are categorised as socio-economic developments, which are treated in the next section.

3.7 Socio-economic developments

Future socio-economic conditions are important for the assessment of a structure's lifespan, especially for the functional and economic life. Fast growth of the population in flood-prone areas and economic growth might make policy-makers decide that reinforcement works will have to be carried out as the flood defences are not up to the required safety standards. The economic growth also affects the costs of measures, availability of resources, and technological advancements. Shipping on the waterways can also be heavily influenced by socio-economic developments. The total amount of cargo transshipment in a particular region shows a strong relationship with the economic product (Gross Domestic Product, or GDP) and economic developments drive changes in the inland waterway transport sector (Van Dorsser, 2012).

3.7.1 Scenarios

Socio-economic scenarios have been developed by the Bureau for Economic Policy Analysis (Centraal Planbureau, CPB) and the Netherlands Environmental Assessment Agency (Planbureau voor de Leefomgeving, PBL) (Wolters et al., 2018). These socio-economic scenarios, called Prosperity and the Living Environment (Welvaart en Leefomgeving, WLO), are incorporated in the Delta Scenarios. The Delta Scenarios were drawn up for the Delta Programme and aim to provide a coherent view of future climate and socio-economic developments, the associated uncertainties, and the implications for the water management in the Netherlands (Wolters et al., 2018). The four Delta Scenarios were last updated in 2017 after the new KNMI'14 and WLO scenarios were published, and a variant (DRUK-Parijs) on one of the four scenarios was added to reflect the consequences of the Paris Climate Agreements. A schematic overview of the scenarios and relevant socio-economic developments are presented in Figure 3.17. The climate change related developments are not included in the figure as these were already discussed in Section 3.1.

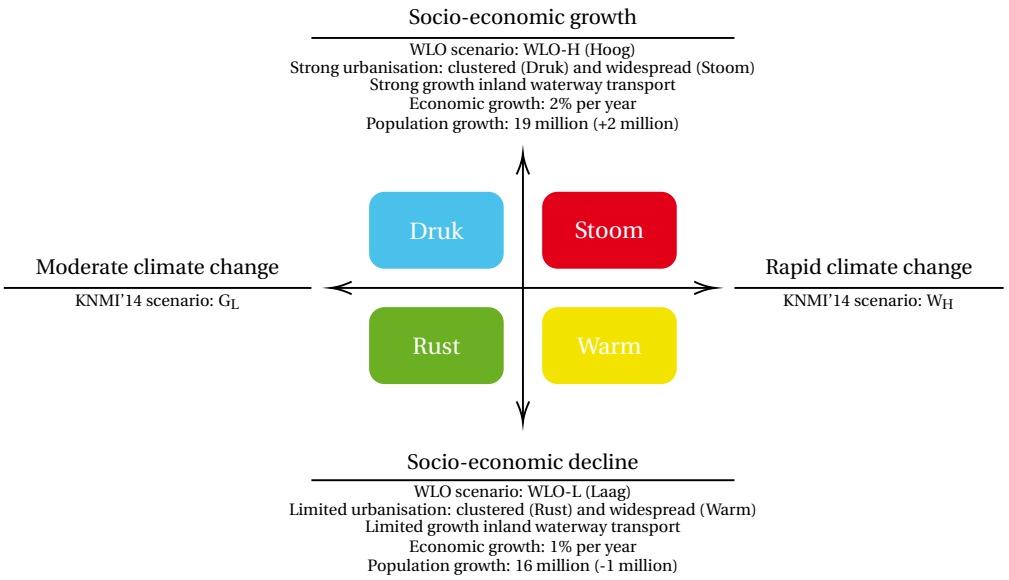

Figure 3.17: Overview of the Delta Scenarios. Growth figures apply to the year 2050 (Wolters et al., 2018).

The variant DRUK-Parijs is very similar to the main scenario DRUK, but incorporates measures to reduce the greenhouse gas emissions. These measures translate into more natural grasslands and forests compared to the scenario DRUK and increased subsurface drainage to mitigate land subsidence in peatlands. On all other aspects, the figures of DRUK were adopted.

The WLO scenarios only give projections up to 2050 and socio-economic projections beyond 2050 are not available. Usually, the scenarios are extrapolated to obtain estimates for the end of the century. This practice increases the uncertainty in the projections. However, the scenarios do not pretend to offer predictions, they merely present plausible ranges of future developments to provide more insight into future challenges and help select promising policies or strategies, for example, through a cost-benefit analysis (Wolters et al., 2018).

3.7.2 Flood protection

Dike trajectories are allocated to a safety standard class based on the acceptable failure probability that follows from the risk criteria (individual, societal, and economic). These classes range from 1/100 per year up to 1/30,000 per year (1/300 - 1/100,000 per year for the signal value) and differ a factor 3 (see Figure 3.16). The dike trajectory near the nuclear power plant of Borssele is a special case with a signal and limit value of 1/1,000,000 per year. The classes and the range of failure probabilities that are assigned to a certain class are shown in Table 3.5. Note that this table shows the classes for the signal value as this was for a long time the only considered value in the development of the new safety standards (Slootjes & Van der Most, 2016a).

Table 3.5: Allocation of failure probabilities to a safety standard class (signal value) (Slootjes & Van der Most, 2016a).

Safety standard [1/year]	Interval [1/year]		
1/300	0	-	550
1/1,000	550	-	1,700
1/3,000	1,700	-	5,500
1/10,000	5,500	-	17,000
1/30,000	17,000	-	55,000
1/100,000	55,000	-	170,000

An increase in the population in the region near the Hollandsche IJssel barrier or strong economic growth may lead to the situation in which the consequences of flooding are such that the protection against flooding is insufficient with the current safety standards. In that case, the dikes along the Hollandsche IJssel will fall into a stricter class. The result is that either the dikes have to be reinforced or the closure reliability of the Hollandsche IJssel barrier has to be improved in order to reduce the probability of extreme water levels.

The likelihood of imposing stricter safety standards depends on the margin within the current safety standard class. Some trajectories have a failure probability that lies near the lower end of the range and thus the consequences or damages have to increase substantially before the standards becomes more stringent. For other trajectories it is the other way around. How much the damage may increase before a trajectory is allocated to another class was studied by Kind et al. (2019). In the development of the new standards, the total damage has been defined as economic damage, damage to those affected, and fatalities. The latter two consequences have been monetised by using a value of €12,500 for the damage to property of victims and €6.7 million for the cost of a fatal casualty (Slootjes & Wagenaar, 2016). The analysis by Kind et al. (2019) was performed for the dike trajectories in the Rhine-Meuse delta and assumed that the ratio between these three categories of damage remains the same. So only the allowable increase in the total damage was examined. The damages as a result of a dike breach in trajectory 14-1 and 15-3 have to increase by a factor 2.15 and 2.18, respectively. The damages may thus double before the trajectories fall into a more stringent class. It is deemed unrealistic that the damages will increase to such an extent, especially since the damage figures already account for an economic growth of 1.9% per year (Kind et al., 2019). This value is only slighly smaller than the growth figure of the WLO scenario Hoog (Wolters et al., 2018). Some critical remarks regarding the calculations can be made. For instance, the study only looks at the effect of economic growth on the economic risk requirement. Effects on the individual risk or societal risk due to population shifts were not included. However, an increase in the population in the region could lead to a higher number of potential fatalities, which impacts the societal risk. The second effect of population growth is a reduction in the evacuation fraction, affecting both the individual and societal risk. However, the areas where societal risk plays an important role already have a high number of potential victims, and an increase due to housing projects is relatively low (Kind et al., 2019). Regarding the individual risk, the area near the Hollandsche IJssel already falls into the lowest evacuation fraction category. Hence, an increase in the regional population does not affect the individual risk.

In conclusion, it is considered unlikely that the dikes along the Hollansche IJssel will be assigned a stricter safety standard. The damages have to increase to such a degree that even for the highest economic growth rate of the WLO scenarios, the current safety standards can be maintained.

3.7.3 Navigation

Developments in the inland waterway transport sector are another type of socio-economic developments. Although these developments are relevant to the navigation function of the Hollandsche IJssel barrier, they mainly serve as input for the analysis of the costs associated with the hindrance to shipping, which is not part of this study. Projections of the shipping intensity may also be used to assess the capacity of an asset or waterway, which is relevant to the functional performance of the storm surge barrier. However, the functional analysis in Section 2.2 indicated that capacity problems would first arise at the Juliana locks upstream of the storm surge barrier due to the smaller dimensions. Insufficient capacity of the storm surge barrier in terms of vessel passage could therefore also be neglected, and developments in the inland waterway transport sector do not have to be discussed in detail. For the interested reader, an exploration of the range of future developments in the inland navigation sector is included in Appendix C anyway.

3.8 Conclusions

The potential impacts of external drivers on the remaining life of the Hollandsche IJssel barrier have been analysed in this chapter. A distinction was made between physical drivers and societal developments. The physical drivers comprise climate change related drivers and land subsidence, and societal developments include policy changes and socio-economic developments. The evaluation of the impacts of these drivers generally involved qualitative judgements based on information obtained from other studies, though, in some cases, quantitative assessments were needed.

The main finding was that sea level rise is the most important or dominant driver affecting the remaining life. In part, this is because of the potentially large future changes in sea level, but also due to the widespread consequences. Sea level rise leads to an increase in the number of closures which affects the probability of extreme water levels, hindrance to shipping, the probability of reaching the “maalstoppeil”, and several other aspects. For most of the other physical drivers, the effects can be disregarded in the further assessment of the remaining life for three reasons. First, future changes of the variable are small. Second, the impact on the functional performance or technical state of the barrier is limited. Third, the consequences can be resolved relatively easily or are already accounted for, e.g. in the case of land subsidence.

A similar conclusion was drawn for the societal developments. For the policy changes, the likelihood of new flood protection standards was examined. A complete revision of the standards was deemed unlikely for the near future since not even all dike trajectories meet the current standards that were introduced in 2017; the authorities aim to comply with these standards by 2050. The possibility of more stringent standards within the current legislation was considered to be a socio-economic development as the decision to impose stricter standards is prompted by an increase in the potential damage of flooding. This development was also considered unlikely because the damages have to increase to such a degree that, even for the highest economic growth rate of the WLO scenarios, the current safety standards can be maintained. The second type of socio-economic developments that was considered were developments in the inland waterway transport sector. However, these developments are not essential for this study since the navigational requirements are independent of the shipping intensity and only related to the functioning of the storm surge barrier. Essentially, the future developments in the inland navigation sector were only mentioned for the sake of completeness and hence briefly discussed.

Following the outcome that the remaining life of the Hollandsche IJssel barrier is largely dominated by sea level rise, this study proceeds by exploring methods to incorporate sea level rise into the estimation of the remaining life of the barrier in Chapter 4.

4

Methodology for the quantitative analysis of the remaining life

The previous chapter indicates that sea level rise is the dominant external driver affecting the remaining life of the Hollandsche IJssel barrier, and the question is now how to estimate the remaining life of the barrier. This chapter describes the data, tools, and methods used to quantify this remaining life. The following research question is thus treated in this chapter:

4. What methods can be deployed to estimate the residual life of the barrier?

Because sea level rise is the main driver impacting the residual life, methods or models are proposed to relate the functional performance to sea level rise, i.e. as a function of sea level rise. The technical life of the barrier is not considered in the discussion of the methodology since the analysis of the deterioration mechanisms in Chapter 2 already indicated that the technical life is unlikely to be governing for the end of life decision of the storm surge barrier.

The chapter starts with an analysis of the local water level statistics to examine a possible relationship between sea level rise and a rise in the local water levels. The water level statistics in front of and behind the barrier are discussed in separate sections, Section 4.1 and Section 4.2, respectively, as the statistics at these two locations are different due to the influence of the storm surge barrier. Section 4.3 focuses on the increase in closure frequency of the barrier as a result of sea level rise. The closure frequency is analysed in a separate section because of the broad consequences of changes in the number of closures. In the next section, Section 4.4, the analysis of the functional life of the barrier is described. Methods or models that can be used to relate the functional performance to sea level rise are presented. The overall result of this chapter is an overview of the functional performance as a function of sea level rise for the various functions of the barrier, which, combined with sea level rise projections, can provide estimates of the remaining life of the Hollandsche IJssel barrier. The structure of the chapter and the purpose of each section is further clarified in Figure 4.1.

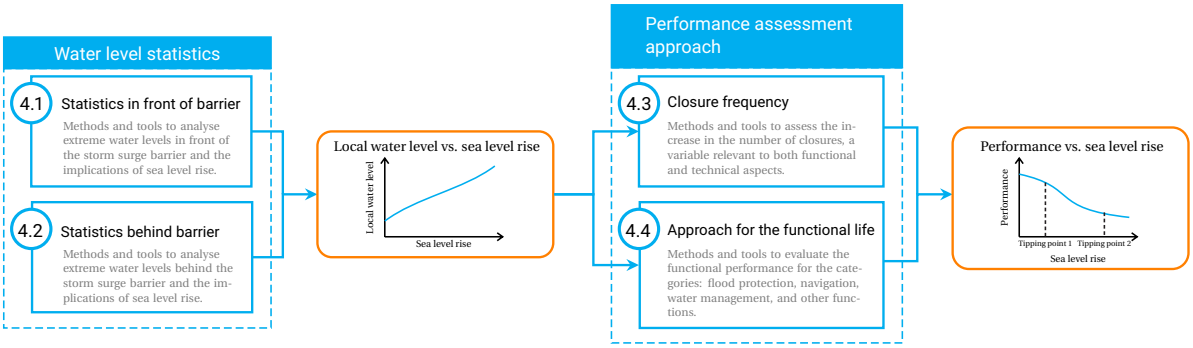

Figure 4.1: Illustration of the structure of Chapter 4. Water level statistics in front of and behind the barrier are analysed to relate a rise in the local water levels to sea level rise. The results of this analysis are used in the methods or models that are proposed to express the functional performance as a function of sea level rise. By expressing the required performance levels as critical amounts of sea level rise, the tipping points, i.e. moments at which the performance is insufficient and measures or adaptations have to be considered, can be identified. These tipping points can be expressed as moments in time when the values are incorporated in sea level rise scenarios.

4.1 Analysis of water levels in front of the barrier

For the analysis of the water levels in front of the Hollandsche IJssel barrier, a distinction was made between water levels with a low frequency of occurrence and water levels with a high occurrence frequency. For the low-frequency water levels, a probabilistic model called Hydra-NL was used. This program is included in the Wettelijk Beoordelingsinstrumentarium (WBI2017), a set of tools and guidelines used for the assessment of flood defences in the Netherlands (Ministerie van Infrastructuur en Milieu, 2016). Water levels with a short return period (< 10 years) are required for the estimation of the closure frequency of the storm surge barrier, but these high-frequency water levels cannot be calculated with the model. Instead, water level measurements at the barrier were used to determine the return periods of relatively low water levels. Both approaches are treated in the next sections. The effects of sea level rise are also discussed as sea level rise is considered to be the most important climate change related driver.

4.1.1 Low-frequency water levels

The probabilistic model Hydra-NL calculates the hydraulic loads at a specific location and with a certain return period by combining the statistical properties of global load variables (river discharge, sea level, wind speed, etc.) with databases in which the influence of those variables on the local hydraulic loads is collected. These databases are created using hydrodynamic models (WAQUA or SOBEK) and wave models (SWAN). The Hydra-NL model requires several user defined parameters which need to be clarified in order to guarantee the reproducibility of the results of this study. These variables include the non-closure probabilities of the storm surge barriers, uncertainties in the hydraulic loads, sea level rise, and whether or not the river discharge should be capped at a certain value. The applied settings are explained in more detail in Appendix D.

Implications of sea level rise

The Hollandsche IJssel barrier is located more inland than other storm surge barriers, such as the Maeslant barrier and the Eastern Scheldt barrier. Because of this location sea level rise does not translate one-on-one to higher water levels locally. To quantify the effect of sea level rise, the water level statistics as a function of sea level rise were calculated in Hydra-NL (see Figure 4.2). These results should be interpreted with care, especially the values for large amounts of sea level rise. In Hydra-NL, sea level rise is modelled as an additional storm surge under daily conditions instead of a rise in all water levels. This way of modelling implies that 50 cm of sea level rise together with a storm surge of 150 cm is treated as equivalent to 0 cm of sea level rise and a surge of 200 cm, while in reality, these situations are quite different. This conceptual error has to be accepted for now as other methods to model the effects of sea level rise on the water level statistics are lacking.

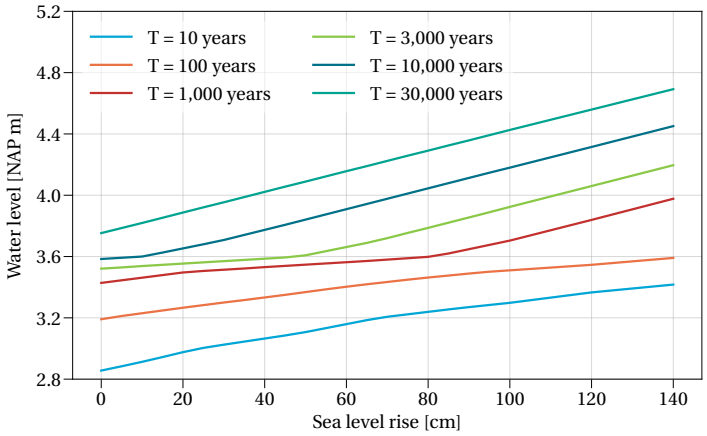

Figure 4.2: Water levels at the Hollandsche IJssel barrier for six return periods as a function of sea level rise.

As Figure 4.2 indicates, the extent to which sea level rise leads to a rise in the local water levels depends on the water levels themselves. For water levels above approximately NAP +3.6 m (water levels with the longest return periods), the trend is linear and 1 m sea level rise results in an increase of approximately 67 cm in the local water level. The kink around NAP +3.6 m and the linear trend for higher water levels can be explained by the fact that for these higher water levels the open condition of the Maeslant barrier[1] (failing storm surge

[1] The Maeslant barrier and Hartel barrier are modelled in Hydra-NL using a single failure probability, but the failure probability of the Hartel barrier has a limited effect on the water levels in the Rhine-Meuse delta (De Deugd, 2007).

barrier), in which the local water level rises with the sea water level, becomes dominant. The flood protection standard of the barrier is 1/30,000 years (lower limit value), which means that this linear relationship between the rise of the local water level and the rise in sea level could be used for the flood protection function.

4.1.2 High-frequency water levels

Water level measurements can be used to estimate the water levels with a return period of less than 10 years. Measurements of the water level at the Hollandsche IJssel barrier have been recorded since 1971 and are available at the website *Waterinfo* of Rijkswaterstaat (*https://waterinfo.rws.nl*). The water level measurements between 1971 and 2020 were downloaded from this website. Inspection of the dataset reveals that data is missing between 1 February 1989 and 6 September 1993 and between 9 October 2020 and 16 November 2020. Including the measurements of these incomplete years may result in lower return periods of the maximum water levels or an underestimation of the number of closures, especially when sea level rise is incorporated. Therefore, only the complete years were included in analysis, resulting in a time series of 44 years.

The return period can be calculated from the cumulative distribution function $F(x)$ (Coles, 2001):

$$T = \frac{1}{1 - F(x)} \tag{4.1}$$

An estimate of the cumulative distribution function can be obtained empirically from the water level measurements. This empirical cumulative distribution function $\tilde{F}(x)$ can be defined as (Coles, 2001):

$$\tilde{F}(x) = \frac{i}{n+1} \quad \text{for } x_i \leq x < x_{i+1} \tag{4.2}$$

where $n+1$ is used to avoid having a value of 1 for $\tilde{F}(x)$, which would lead to an infinite return period.

Before the water level measurements can be used to estimate the return periods, a correction for sea level rise has to be applied. The rise in sea level along the Dutch coast over the past decades was analysed in the *Zeespiegelmonitor 2018* (Baart et al., 2019). The sea level rose by about 24 cm (1.86 mm/year) between 1890 and 2017. For station Hoek van Holland, the measuring station closest to the storm surge barriers, the report mentions a trend of 2.3 mm/year for the period 1890-2017. This value was used to correct the measurements.

Besides the trend, a reference year had to be selected for the correction. The reference year for the current assessment round of the flood defences is 2023. So this year could be adopted to correct the measured water levels. However, the small rise in sea level between 2017 and 2023 is either ignored, or the applied values in previous versions of Hydra-NL were overestimates since the reported values in Hydra-NL version 2.7 for the period 1990-2017 do not differ from the values in Hydra-NL version 2.8 for 1990-2023 (Duits, 2019, 2020). In this study, 2017 is the year used to correct the measured water levels in order to be on the safe side, and because the trend of 2.3 mm/year was determined for the years up to 2017. The effect of the correction for sea level rise is illustrated in Figure 4.3. This correction is on the high side since sea level rise does not necessarily translate one-on-one to higher water levels at the Hollandsche IJssel barrier. However, the differences between the corrections when assuming a one-on-one relationship or the 0.67 : 1.0 ratio used for the low-frequency water levels are in the order of a few centimetres.

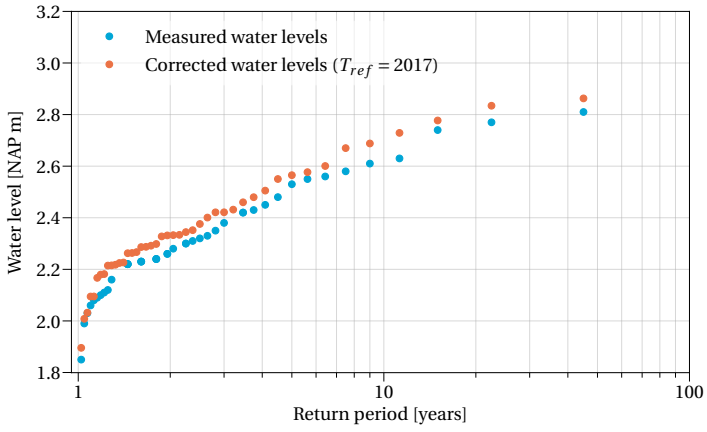

Figure 4.3: Return period of the annual maximum water level at the Hollandsche IJssel barrier.

Implications of sea level rise

Ideally, one would prefer to run hydrodynamic simulations with the changing sea level as a boundary condition to estimate how sea level rise translates into an increase in the local water levels. These simulations are time-consuming and less practical for this study in which a range of sea level rise scenarios is considered. A more pragmatic approach, similar to the one chosen for the low-frequency water levels, was adopted instead. By running Hydra-NL simulations with an open Maeslant barrier (failure probability of 1) for several values of sea level rise, an estimate of the rise in the local water level under daily conditions could be retrieved. The results of these simulations are shown in Figure 4.4.

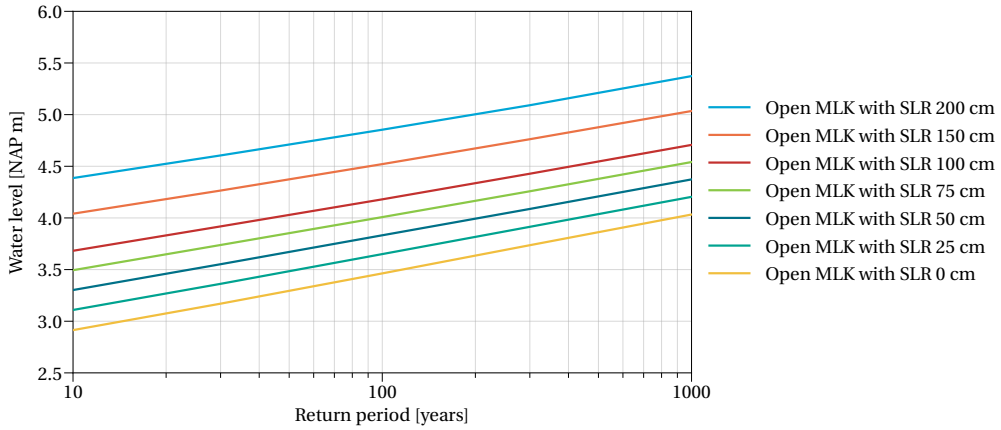

Figure 4.4: Return period of water levels at the Hollandsche IJssel barrier for various amounts of sea level rise and an open Maeslant barrier (MLK). Note that the water levels for the longer return period, for which the Maeslant barrier is normally closed, are not relevant as the results are used to estimate the rise in the local water level under daily conditions. These longer return periods are only plotted to illustrate the linear trend.

Figure 4.4 displays a fairly linear relationship between the rise in sea level and the rise in the local water level. To illustrate this relationship more clearly, the relative increases are depicted in Figure 4.5.

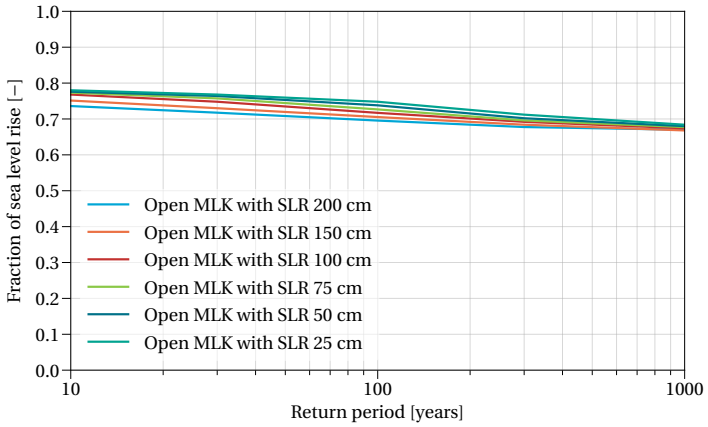

Figure 4.5: Rise in the local water level at the Hollandsche IJssel barrier as a fraction of sea level rise with an open Maeslant barrier (MLK).

From Figure 4.5, one could conclude that there is indeed a linear relationship between sea level rise and local water level rise for most return periods and values of sea level rise. It is important to stress that the figures do not present the actual water levels in front of the Hollandsche IJssel barrier. The “true” water levels expected to occur with a certain return period will be lower than the water levels depicted in Figure 4.4 because the Maeslant barrier is closed at about NAP +3.0 m. The relatively simple analysis was merely performed in an attempt to determine a relationship between sea level rise and the increase in the local water levels under daily conditions (for which the Maeslant barrier is not closed).

Based on the results discussed above, the assumption was made that 1 m sea level rise results in an increase in the local water level of about 80 cm. This relationship was used to raise the local water levels with a return period shorter than 10 years. These water levels are important for the estimation of the number of closures and duration of closures.

4.2 Analysis of water levels behind the barrier

The extreme water levels in the Hollandsche IJssel are reduced by the storm surge barrier. This influence is included in Hydra-NL, and thus this program is generally well suited for the determination of the water levels behind the Hollandsche IJssel barrier. The only issue with applying Hydra-NL to the Hollandsche IJssel is related to the model uncertainty in the water levels. This model uncertainty used to be linked to the state of the Maeslant barrier, but this link was changed in the latest version of Hydra-NL (version 2.8.2) since it would be more logical to relate the uncertainty to the state of the Hollandsche IJssel barrier when deriving the water levels in the Hollandsche IJssel. This adjustment implies that a decision has to be made whether the same values as for the Rhine-Meuse delta can be used or new values are required. This decision has not yet been taken, and thus appropriate values for the model uncertainty remain undetermined. In addition, the currently adopted uncertainty parameters for the Rhine-Meuse delta seem to be an overestimation (Rongen & Maaskant, 2019). This overestimation is less problematic for the Hollandsche IJssel barrier itself because of the robust design of the structure. But the consequences are more severe for the water levels behind the barrier. The closure level (NAP +2.25 m) is relatively close to the "maalstoppeil" (NAP +2.60 m) and the height of the dikes (NAP +3.2 m to NAP +4.3 m), which makes the margins on the Hollandsche IJssel smaller and accurate estimates of the parameters imperative. Therefore, Rongen and Maaskant (2019) recommend deriving uncertainty parameters for the water levels in the Hollandsche IJssel. As new values have not yet been derived, model uncertainty was neglected when calculating the water levels behind the barrier with Hydra-NL.

Implications of sea level rise

The presence of a second storm surge barrier further increases the difficulty of deriving a proper relationship between sea level rise and an increase in the local water levels. A second complication is the coupling between wind speed and sea water level for the Hollandsche IJssel in Hydra-NL. As a result, sea level rise leads to higher wind speeds in the model, and thereby higher water levels. Rongen and Botterhuis (2018) and Rongen and Maaskant (2019) avoided this issue by performing additional SOBEK simulations with 25 cm and 75 cm sea level rise (W+ scenario of KNMI'06 for the years 2050 and 2100, respectively). However, when dealing with a large number of scenarios or probabilistic projections of sea level rise, as is the case in this study, running additional SOBEK simulations to generate new databases for Hydra-NL is infeasible, and thus a more practical approach had to be adopted.

By studying the water levels in the Hollandsche IJssel for the sea level rise scenarios for which the hydrodynamic simulations were performed (current climate, 25 cm and 75 cm sea level rise), a relationship between sea level rise and an increase in the water levels in the Hollandsche IJssel was sought. This analysis of the water levels for various return periods and the sea level rise scenarios can be found in Appendix E. The analysis shows that the water levels are dominated by the situation with an open Hollandsche IJssel barrier (failing storm surge barrier). Water levels with a 1,000-year return period or longer are even completely determined by an open Hollandsche IJssel barrier. As a result, the exceedance probability of water levels behind the storm surge barrier $P_{bb}(h)$ may be approximated by multiplying the exceedance probability of the water levels in front the barrier $P_{fb}(h)$ by the non-closure probability of the barrier P_{nc}:

$$P_{bb}(h) = P_{nc} \cdot P_{fb}(h) \tag{4.3}$$

According to Equation (4.3), the water level statistics behind the storm surge barrier are dependent on the water level statistics in front of the barrier and the non-closure probability. This simple relationship implies that the water level statistics can be estimated for a range of closure reliabilities and sea level rise scenarios without having to run additional hydrodynamic simulations as there is no coupling between wind speed and sea water level for the Rhine-Meuse delta databases that are used for the water level statistics in front of the Hollandsche IJssel barrier (G. Rongen, personal communication, 7 June 2021). The validity of Equation (4.3) was assessed by comparing the water level statistics that follow from this relationship with the water level statistics obtained from Hydra-NL for which the hydrodynamic simulations were performed (current climate, 25 cm and 75 cm sea level rise). This analysis is also included in Appendix E and the comparison for the current climate and 75 cm sea level rise for 2100 are shown in Figure 4.6. The results show that the water levels calculated with Equation (4.3) match the water levels obtained from Hydra-NL well for return periods that are relevant to flood protection (> 10,000 years). As sea level rises, the open condition becomes more dominant, and the correspondence also increases for shorter return periods. Moreover, the increase in water levels upstream in the Hollandsche IJssel due to wind set-up is more or less constant for rising sea levels (see Appendix E). This means that deriving the water level at one location is sufficient to assess the effects of sea level rise on the water levels in the Hollandsche IJssel.

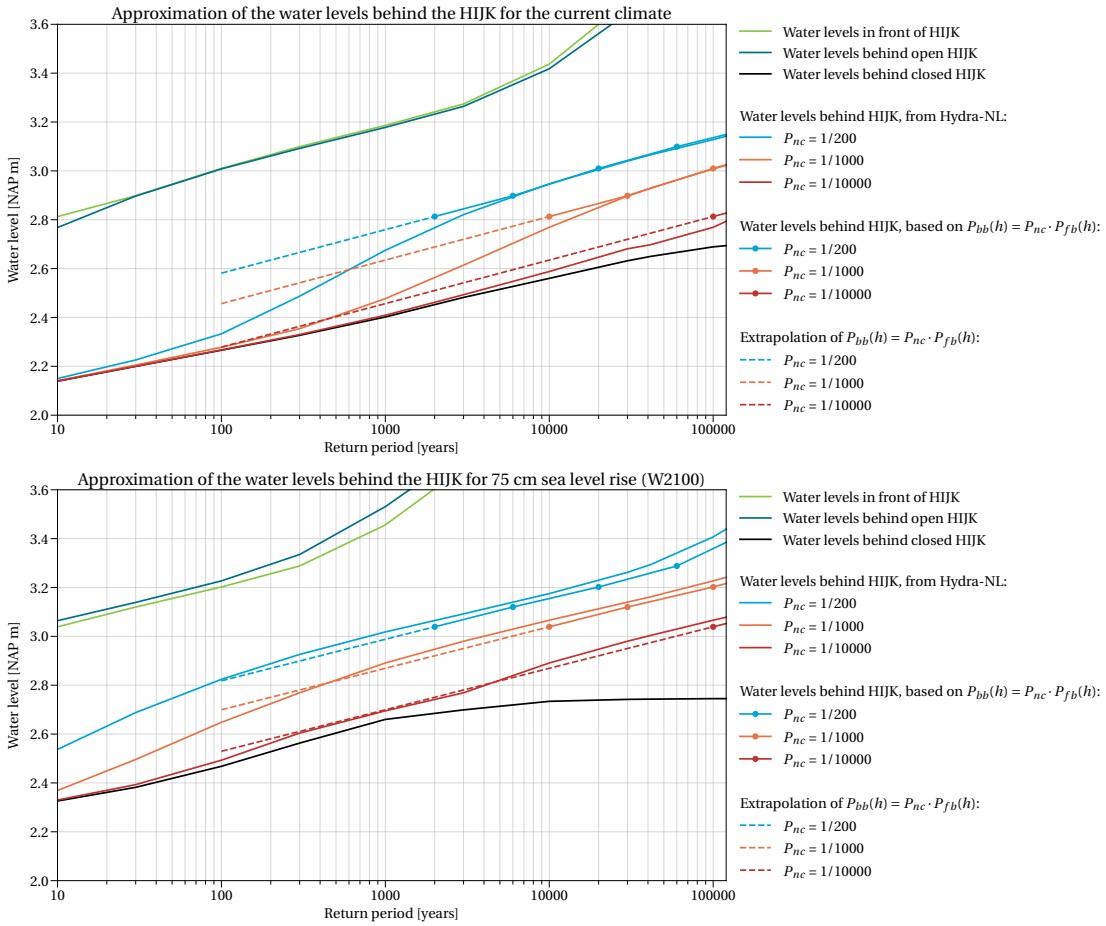

Figure 4.6: Comparison of the approximated water level statistics behind the Hollandsche IJssel barrier (HIJK) using Equation (4.3) with the water level statistics obtained from Hydra-NL.

Using Equation (4.3), the water levels directly behind the storm surge barrier as a function of sea level rise are plotted in Figure 4.7. Because the water levels derived with the relationship in Equation (4.3) correspond well with the water levels from Hydra-NL for the longer return periods in particular, only the water levels for the return periods 10,000 years and 30,000 years are depicted in Figure 4.7. The water levels for a different non-closure probability (1/1,000 per closure) are also plotted to illustrate how the relationship could be used to assess the effectiveness of improvements to the closure reliability of the barrier. The fact that any non-closure probability could be inserted into Equation (4.3) makes the simple approach quite useful for the evaluation of the flood protection function.

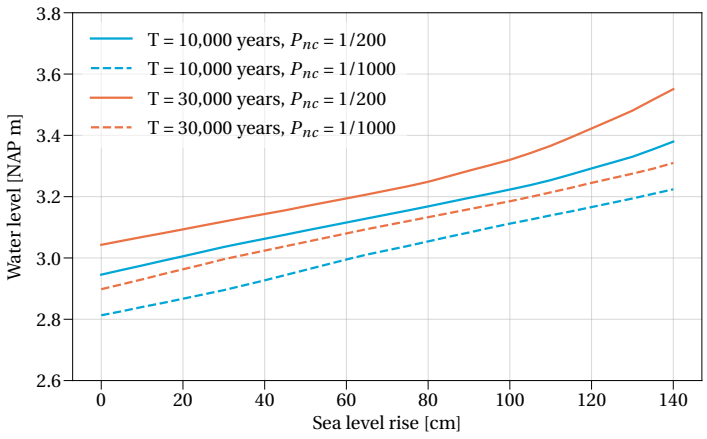

Figure 4.7: Water levels behind the Hollandsche IJssel barrier for two return periods as a function of sea level rise.

4.3 Closure frequency with rising sea level

Changes in the closure frequency have a broad range of impacts that is not limited to any type of lifespan. An increase in the number of closures impacts both the functional performances and deterioration of several components of the storm surge barrier. Hence, a distinct section is dedicated to the closure frequency.

The water level measurements at the Hollandsche IJssel barrier combined with a critical water level at which the barrier closes would provide an estimate of the number of closures per year. This critical water level could be the design closure level, which is NAP +2.25 m. However, this design closure level means that the barrier must be in closed condition when the water level in the Hollandsche IJssel reaches NAP +2.25 m. The barrier is thus closed earlier and using NAP +2.25 m results in an underestimation of the number of closures. Another option is to look at the water levels at which the barrier was closed in the past. Between 2000 and 2016, the barrier was closed for water levels varying between NAP +1.95 and NAP +2.10 m (Hoogheemraadschap van Schieland en de Krimpenerwaard, 2018). Adopting a closure level of NAP +2.10 m as closure level leads to 3.5 closures a year under the current climate, which is in line with the current number of closures of three to four a year (Rijkswaterstaat, n.d.-b).

The relationship between sea level rise and an increase in the local water level, derived in Section 4.1.2, was used to study the impact of sea level rise on the number of closures per year. So, for a sea level rise of 1 m, the water level measurements at the Hollandsche IJssel barrier were raised by 80 cm. This approach is depicted in Figure 4.8 for the storm of February 2020 and 100 cm sea level rise.

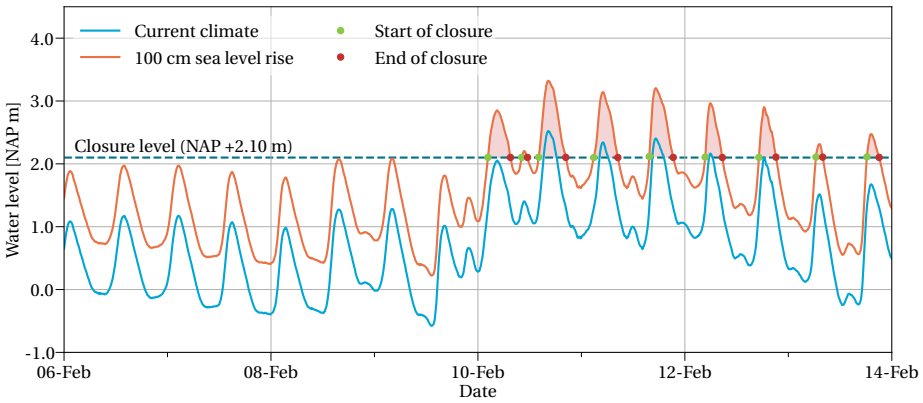

Figure 4.8: Example of how the number of closures were determined using the water level measurements at the storm surge barrier.

Figure 4.8 also shows that an additional processing step is required to obtain a more precise indication of the closure frequency. The closure events displayed in the figure were solely based on the crossing of the critical water level without looking at previous closure events, while, in reality, the barrier will not be opened to facilitate navigation if the next moment of closure is within several hours. Three approaches were considered to account for rapidly succeeding closure events: (1) a required time difference of 12 hours between the start of closures, (2) a required time difference of 6 hours between the end of a closure and the start of the next closure, and (3) considering only the daily maxima of the water levels. The third approach implies that the time between the considered water levels is about 12 hours or more as the maximum water level is likely to occur during high tide. The third option is also the fastest solution as timestamps do not have to be compared, but the drawback is that the second high tide of the day is neglected resulting in an underestimation of the number of closures. The difference of 12 hours in the first approach was chosen to include the possibility of an additional closure during the second high tide of the day. The second approach, comparing start and end, followed from the assumption that if the time until the next closure is more than 6 hours, it is worthwhile to open the barrier to let vessels pass the barrier. The effect of the different options on the number of closures is illustrated in Figure 4.9.

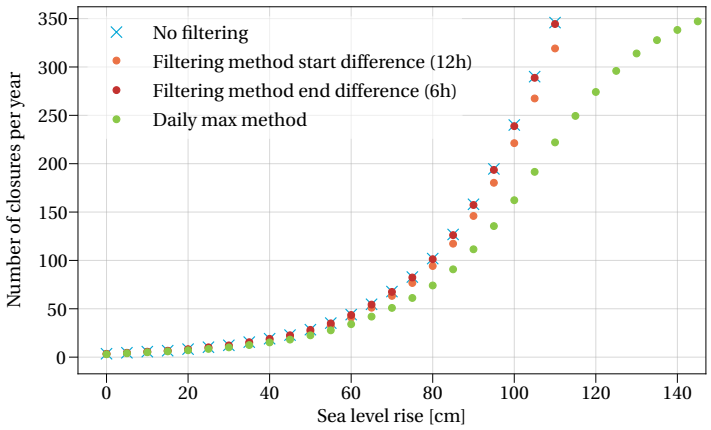

Figure 4.9: Number of closures as a function of sea level rise, determined with four different approaches.

As depicted in Figure 4.9, the closure frequency increases approximately exponentially with sea level rise. The differences between the approaches are small for low values of sea level rise, only the method using the daily maxima results in a considerably lower closure frequency, and starts to deviate from the exponential trend around 1 m sea level rise. The number of closures calculated with the second approach, which compares the end of a closure with the start of the next closure, was used in the remainder of the analysis of the lifespan of the Hollandsche IJssel barrier since the decision to open the barrier is probably motivated by waterway traffic. However, using the results of the approach that compares the starts of closures, or the results without any filtering, would be almost equally appropriate since the differences are small, especially for a sea level rise of less than 50 cm.

4.4 Approach for the functional life

The functional analysis of Section 2.2 shows that the Hollandsche IJssel barrier has multiple functions. This section discusses the proposed methods to evaluate the functional performance for each of these functions. For the flood protection function, standardised methods or tools described in guidelines were adopted, but for other functions new methods were devised. The reason being that flood protection has been a matter of great concern to the government for a long time. This has lead to a number of regulations and guidelines in order to prevent flooding. Such standardised methods are lacking for other functions, and thus alternative approaches have to be developed.

4.4.1 Flood protection

The flood protection function can be evaluated by considering the failure mechanisms of hydraulic structures described in the WBI2017 guidelines. Although these mechanisms are described for hydraulic structures in general, some mechanisms are applicable to the storm surge barriers as well. These mechanisms could be used as guidance for the evaluation of the flood protection function. The four main failure mechanisms of hydraulic structures described in the guidelines are (’t Hart et al., 2018):

- Failure due to overtopping/overflow.
- Failure due to piping.
- Structural failure due to a lack of strength or stability (from a functional point of view).
- Failure due to non-closure.

These failure mechanisms consist of several sub-mechanisms. Some of these sub-mechanisms (or even the entire mechanism) have a negligible contribution to the probability of flooding or can be neglected due to the local conditions and characteristics at the Hollandsche IJssel barrier. The next paragraphs elaborate on the main failure mechanisms and their sub-mechanisms to find out whether a mechanism should be taken into account or can be neglected.

Overtopping/overflow

The failure mechanism overtopping/overflow is related to the height of the structure. If the height and storage capacity behind the barrier are insufficient, the amount of water flowing over the structure could be such that the critical water levels in the hinterland are exceeded. Besides exceedance of the storage capacity, overtopping/overflow could cause erosion of the bed protection. The subsequent formation of scour holes may lead to the collapse of the structure. The third effect of overtopping/overflow is the occurrence of vibrations. High discharges could cause heavy vibrations in the gate, which could lead to failure of the gate. This type of failure could also be considered a structural failure and is therefore included in that category of failure mechanisms.

The amount of overtopping can be calculated using the equations in the guidance manual for overtopping/overflow (*Schematiseringshandleiding hoogte kunstwerk*) developed for the WBI2017 (Rijkswaterstaat WVL, 2021):

$$q_{os} = m_{os} \cdot \sqrt{g \cdot (H_{m0})^3} \cdot e^{\left(-3 \cdot \frac{h_{kr}-h}{H_{m0}} \cdot \frac{1}{\gamma_\beta \cdot \gamma_n}\right)} \tag{4.4}$$

where m_{os} [−] is the model factor for overtopping, g [m/s^2] is the gravitational acceleration, H_{m0} [m] is the significant wave height, h_{kr} [m] is the retaining height of the structure, h [m] is the outer water level, and γ_β [−] and γ_n [−] are influence factors for oblique wave attack and the presence of a wave return wall/bullnose, respectively.

For water levels exceeding the retaining height of the structure, overflow occurs as well. In that case, a formula combining overtopping and overflow can be used (Rijkswaterstaat WVL, 2021):

$$q_{ol+os} = m_{ol} \cdot 0.55 \cdot \sqrt{-g\,(h_{kr} - h)^3} + m_{os} \cdot \sqrt{g \cdot H_{m0}^3} \tag{4.5}$$

where m_{ol} [−] is the model factor for overflow, similar to m_{os} in Equation (4.4).

The guidance manual for overtopping/overflow recommends values for the parameters in Equation (4.4) and (4.5). These values are presented in Table 4.1.

Table 4.1: Values and statistical distributions of the parameters in Equation (4.4) and (4.5) (Rijkswaterstaat WVL, 2021).

Parameter	Unit	Distribution	Mean	CV or SD	Remark
m_{ol}	[−]	Normal	μ = 1.1	σ = 0.05	
m_{os}	[−]	Lognormal	μ = 0.09	σ = 0.06	
g	[m/s^3]	Deterministic	9.81		
H_{m0}	[m]	Deterministic	Input		
h_{kr}	[m]	Normal	Input	σ = 0.05	
h	[m]	Deterministic	Input		
γ_β	[−]	Deterministic	1		The factor is assumed to be 1 as a pessimistic assumption
γ_n	[−]	Deterministic	1		The factor is equal to 1 because the structure does not have a bullnose

The overtopping quantities for a range of water levels and a significant wave height H_{m0} of 1.53 m were calculated to obtain an indication of the expected overtopping quantities for the present and future conditions, see Table 4.2. The calculation consisted of a straightforward Monte Carlo simulation using the values in Table 4.1. The maximum considered water level was NAP +5.0 m. This water level corresponds to a return period of 100,000 years and 1.4 m sea level rise (about 1.5 m with respect to 1995). The wave height of 1.53 m was chosen because this value also corresponds a return period of 1/100,000 years. Other wave heights were not considered because the simulations in Hydra-NL showed that the wave height does not change significantly with sea level rise, which can be considered as a change in the water level. Note that the selected conditions are very extreme. It is quite realistic that by the time the sea level has risen by 1.4 m, the current situation is not sustainable anymore. The Hollandsche IJssel barrier might have to close several times a week during the storm season and the Maeslant barrier will probably also function completely differently. However, the purpose of the overtopping calculation, of which the results are shown in Table 4.2, is not to assess the likelihood of situations, but to determine whether a (sub-)mechanism should be considered in the assessment. In that case, the use of the most extreme condition is useful as the calculations may indicate that, even under pessimistic assumptions, the mechanism is not relevant.

Table 4.2: Overtopping quantities for various water levels and wave height H_{m0} = 1.53 m.

Water level [NAP m]	Overtopping [$m^3/s/m$]		
	5th percentile	Median	95th percentile
3.0	0.00	0.01	0.02
3.5	0.01	0.02	0.06
4.0	0.02	0.06	0.17
4.5	0.06	0.17	0.46
5.0	0.16	0.44	1.22

The results of the quick assessment of this failure mechanism show that the sub-mechanisms related to the erosion of the bed protection are not relevant. Erosion of the bed protection can occur due to a horizontal flow caused by overtopping or by a jet caused by water spilling over the gates. The situation of overflow will not occur because the retaining height (NAP +5.0 m) is larger than or equal to the considered water levels, and thus the second situation with a jet is irrelevant. The other mechanism of horizontal flow can be neglected as well. The flow velocity due to overtopping is likely to be very low because of the relatively large water depth behind the barrier. This presumption can be verified by computing the flow velocity that follows from the maximum amount of overtopping. This flow velocity can be estimated by dividing the overtopping discharge by the total water depth (Rijkswaterstaat WVL, 2021). The maximum overtopping discharge is q_{os} = 1.22 $m^3/s/m$ (95th percentile for a water level of NAP +5.0 m). This discharge leads to a flow velocity of about 0.16 m/s for an inner water level of NAP +1.0 m. The smallest critical flow velocity at which an unprotected sand bed starts to erode is 0.10-0.30 m/s, depending on the grading of the sand (Rijkswaterstaat WVL, 2021). However, the bed can be exposed to considerably higher flow velocities since a rubble mound bed protection is present. Therefore, erosion of the bed protection resulting from overtopping/overflow does not have to be considered any further.

The values in Table 4.2 also suggest that exceedance of the storage capacity could be neglected. The total amount of overtopping over the entire width of the storm surge barrier complex (80 + 24 = 104 m) is 1.22·104 ≈ 127 m^3/s. Given this discharge, the surface area of the Hollandsche IJssel, and the closure level, the time until a critical water level is reached could be calculated, similar to the calculation in Section 2.2.3 in which the duration until a "maalstop" (a water level of NAP +2.60 m) was calculated for various pumping discharges. For a discharge of 127 m^3/s and a closure level of NAP +2.0 m, it takes about 3.7 hours before a water level of NAP +2.60 m is reached. It takes more than 9 hours for a closure level of NAP +1.0 m, which is the average closure level at low water slack (Rongen & Maaskant, 2019). If one includes an additional and continuous discharge of 75 m^3/s from the pumping stations, the duration reduces to 2.3 and 5.8 hours for a closure level of NAP +2.0 m and NAP +1.0 m, respectively. The duration of 5.8 hours is more realistic since the operators will prefer a closure at low water slack if the water authorities discharge such amounts of water into the Hollandsche IJssel. Closures may last longer than 5.8 hours, yet exceedance of the storage capacity could also be considered irrelevant for a number of reasons:

1. The discharge of 1.22 m^3/s is already high as a result of the choice for a return period of 100,000 years and the applied conservatism in the calculation of the overtopping discharge. For instance, the reducing effect of oblique wave attack was neglected.
2. The maximum overtopping discharge only arises for a fraction of the total closure duration. During a storm, water levels rise, wind speeds develop, et cetera. As a result, the amount of overtopping attains its maximum only at the peak of the storm.
3. During very long closures, there is the opportunity to raise the gates slightly to spill water to lower the water levels behind the barrier.
4. After reaching the "maalstop" level, the water levels behind the barrier may still rise several decimetres before the critical water levels for the dikes are reached.

In conclusion, the entire failure mechanism overtopping/overflow does not have to be considered when assessing the functional performance with respect to flood protection.

Piping

Piping is a failure mechanism that is driven by hydraulic gradients in the subsurface. These hydraulic gradients are the result of head differences over the structure. When the hydraulic gradients are sufficiently high,

erosion of soil particles on the landside starts. This erosion process may continue upstream forming networks of erosion channels, the so-called pipes. These pipes could undermine the stability of the structure leading to collapse. Since piping is a progressive failure mechanism, the soil erosion process does not always result in failure of the structure. The head difference needs to be high enough and persist for a sufficient amount of time to sustain the erosion process.

The failure mechanism is dependent on the head difference over the structure as well as soil characteristics. The changes in the latter are expected to be limited in the future, whereas the head difference increases due to the increasing outer water levels associated with sea level rise. Hence, the assessment of the relevance of piping under future conditions could be based on changes in the head difference.

The maximum head difference the barrier can withstand is 4.5 m (see design conditions in Section 2.2.1). This head difference of 4.5 m means that the outer water level has to be NAP +5.5 m for piping to become a risk since the water level in the Hollandsche IJssel is approximately NAP +1.0 m after a closure at low water slack (Rongen & Maaskant, 2019). The occurrence of this extreme water level is deemed unrealistic because the 1/100,000 year water level for a sea level rise of 1.4 m is about NAP +5.0 m, still 0.5 m lower. Therefore, the failure mechanism piping could be neglected.

Structural failure due to a lack of strength or stability

Failure due to a lack of strength or stability occurs if either structural components lose their load-carrying capacity or the structure as a whole becomes unstable. These situations could be the result of an increase in the loads or deterioration of the structure. The first case is associated with the functional end of life while the latter is related to the technical life of the structure. As this assessment focuses on the functional life, only an increase in the loads is implied when referring to the failure mechanism structural failure due to a lack of strength or stability. The likelihood of structural failure can be assessed by comparing the forces exerted on the storm surge barrier during extreme conditions with the loads considered for the design. When considering static forces, the design head difference of 4.5 m may be used. For dynamic forces, the overtopping discharge is more relevant. Unfortunately, it is unclear what amount of overtopping the storm surge barrier has been designed for. As an alternative, the Guidelines for Designing Water-retaining Structures (*Werkwijzer Ontwerpen Waterkerende Kunstwerken*) (van Breem et al., 2018) could be used. The guidelines suggest a maximum overtopping discharge of 1.0 $m^3/s/m$ to guarantee the structural integrity. In case of higher discharges, dynamic aspects may start to play a role, and the stability of water-retaining components has to be proven. Based on these design guidelines, which apply to hydraulic structures in general, it was assumed that dynamic forces would not lead to failure as long as the overtopping discharge remains less than 1.0 $m^3/s/m$.

Next to the mechanisms overtopping/overflow and piping, structural failure can be neglected as well. As for piping, a head difference of 4.5 m implies that, in order to endanger the structural integrity, the outer water level has to be NAP +5.5 m, which is deemed unrealistic because, as mentioned before, the 1/100,000 year water level for a sea level rise of 1.4 m is about NAP +5.0 m. The corresponding dynamic loads, on the other hand, may pose a risk to the structural integrity. For a water level of NAP +5.0 m, the overtopping discharge is 1.22 $m^3/s/m$ (Table 4.2), which is significantly higher than the critical value of 1.0 $m^3/s/m$. However, this value is probably too extreme since the barrier already has to close at every high water for 1.2 m sea level rise. For a rise in sea level of 1.2 m, the overtopping discharge is 0.89 $m^3/s/m$, well below the critical value, and thus structural failure due to dynamic forces is also not expected.

The fact that structural failure (and overtopping/overflow) is irrelevant is probably the result of the situation at the time of construction in combination with the more inland location of the storm surge barrier. When the Hollandsche IJssel barrier was built, the Hollandsche IJssel was still in open connection with the sea, with the result that quite high water levels were considered in the design of the barrier. The construction of the Maeslant barrier has lead to a reduction in the extreme water levels, while the Hollandsche IJssel barrier has remained unchanged. As a result, extreme loads (and amounts of overtopping/overflow) rarely occur.

Non-closure

The closure operation may fail due to several reasons, such as software failure, technical failure or human failure. If the closure operation is unsuccessful, it does not mean that failure due to non-closure occurs. Failure of the closure operation can be seen as the initiation step of the failure mechanism. The structure actually fails if either high flow velocities associated with the inflow through the opening damage the bed protection causing instability of the entire structure, or if the critical water levels behind the barrier are exceeded. Failure of the bed protection due to non-closure is unlikely for the Hollandsche IJssel barrier since the bed was

designed for significantly higher flow velocities, which arise during closure operations. Hence, exceedance of critical water levels after a non-closure is the dominant sub-mechanism.

Failure due to non-closure is a special failure mechanism for storm surge barriers as storm surge barriers are the only structures for which an acceptable non-closure probability has been prescribed. This non-closure probability follows from a fault-tree analysis in which the possible causes that could lead to failure of the closure operation, e.g. failure of the operating and control systems, failure of the gate drive mechanisms, and human failure, are included. This given failure probability of the closure operation simplifies the analysis of the failure mechanism failure due to non-closure considerably. Still, evaluating the failure mechanism remains quite complex as the maximum allowable probability of non-closure of the storm surge barrier is related to the failure of flood defences in the hinterland. The probability should be such that these flood defences meet the prescribed safety standards. However, for the analysis with varying amounts of sea level rise, it is not feasible to perform a detailed analysis from which the required probability of non-closure follows. Instead, an approach similar to the one used for the Eastern Scheldt barrier was applied (Rijkswaterstaat, 2017a). In this approach, the occurring water levels ("prestatiepeilen") are compared with an assessment water level ("beoordelingspeil") in order to assess whether the storm surge barrier meets the performance requirements.

The occurring water levels can be obtained using Hydra-NL, but, as discussed in Section 4.2 and Appendix E, Hydra-NL is only suitable for specific scenarios of sea level rise (this holds only for the Hollandsche IJssel). Therefore, the relationship described by Equation (4.3) was used instead. This equation gives the water levels directly behind the barrier. Appendix E shows that the increase in water levels upstream in the Hollandsche IJssel is almost constant for all return periods and the considered values of sea level rise, which means that the water level directly behind the barrier is sufficient to assess the performance. An additional benefit of using Equation (4.3) is that the water levels could easily be determined for various probabilities of non-closure.

The assessment water level ("beoordelingspeil") can be calculated with Hydra-NL because this water level is independent of sea level rise. As for the occurring water levels, only the water level directly behind the barrier has to be calculated. The chosen assessment water level is the water level corresponding to a 30,000-year return period and a non-closure probability of 1/200 per closure. The water level corresponds to the signal value of the most stringent safety standard of the dikes behind the Hollandsche IJssel barrier (dike trajectory 14-1), and 1/200 per closure is the acceptable non-closure probability stipulated in the law. However, a lower non-closure probability (1/1,000 per closure) is set to be achieved by 2030 (DRPD, 2020). This reduction is larger than the reduction required to compensate for sea level rise, based on the current rate of 2.3 mm/year (Baart et al., 2019). This lower probability of non-closure can therefore be interpreted as a more stringent requirement and was included to anticipate for the future policy change. Figure 4.7 shows that the assessment water level is NAP +3.04 m for a 30,000-year return period and a non-closure probability of 1/200 per closure. The assessment water level corresponding to a 30,000-year return period and a non-closure probability of 1/1,000 per closure is NAP +2.90 m.

Figure 4.10 shows for what amount of sea level rise the end of functional life is reached for various non-closure probabilities and the two assessment levels. The results are also listed in Table 4.3. The values in this table were used to estimate the remaining functional life with respect to flood protection.

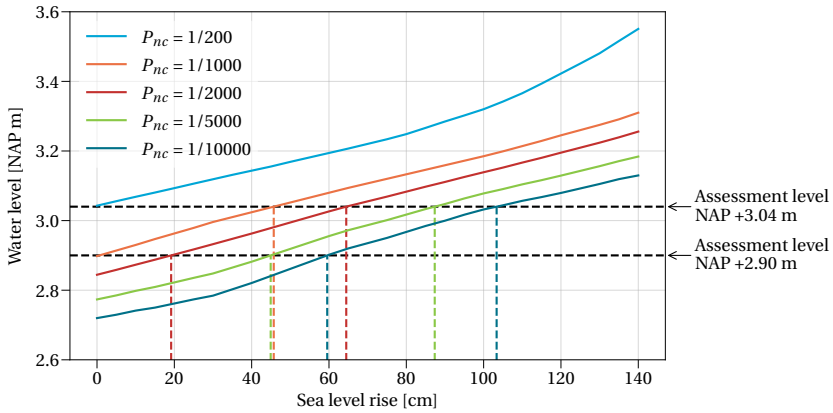

Figure 4.10: End of functional life for the failure mechanism failure due to non-closure in terms of sea level rise for various probabilities of non-closure P_{nc} [per closure] and the two assessment water levels ("beoordelingspeilen").

Table 4.3: Sea level rise values corresponding to the requirements for flood protection. The values were corrected for the sea level rise between 1995 and 2017 using a rate of 2.3 mm/year, as mentioned in the *Zeespiegelmonitor 2018* (Baart et al., 2019).

Indicator	Functional requirement	Performance requirement	Sea level rise w.r.t. 2017 [cm]	Sea level rise w.r.t. 1995 [cm]
Non-closure probability [per closure]	Assessment level NAP +3.04 m	1/1,000	46	51
		1/2,000	64	70
		1/5,000	87	92
		1/10,000	103	108
	Assessment level NAP +2.90 m	1/2,000	19	24
		1/5,000	45	50
		1/10,000	60	65

The approach discussed above relies on the important assumption that the functional performance in terms of flood protection is just sufficient for the non-closure probability that is used for the assessment water level (1/200 or 1/1,000 per closure). Any amount of sea level rise would imply the end of the functional life if the probability of non-closure of the storm surge barrier is not reduced. The duration of the remaining functional life of the barrier is thus a matter of how much the non-closure probability can be reduced. This assumption can be justified by the fact that currently substantial reinforcement works are required to comply with the flood protection standards, see for example the reinforcement programme KIJK. Without these dike reinforcements, the end of the functional life would thus indeed have been reached if the non-closure probability is not reduced.

Conclusion on relevant failure mechanisms

The review of the failure mechanisms indicates that three of the four mechanisms have a negligible effect on the functional performance of the Hollandsche IJssel barrier with respect to flood protection. The structure is sufficiently robust to resist the loads, even for future conditions with more than 1 m sea level rise. The only relevant failure mechanism is non-closure of the storm surge barrier, for which the closure reliability or probability of non-closure of the barrier is the governing parameter. This failure mechanism was assessed by an approach comparable to the one used for the Eastern Scheldt barrier. In this approach, the water levels with a 30,000-year return period (signal value of dike trajectory 14-1) determined for different scenarios of sea level rise are compared with an assessment water level, which is defined as the water level with a return period of 30,000 years for a non-closure probability of 1/200 or 1/1,000 per closure. The chosen probability of non-closure depends on the preferred conservatism in the calculation. This approach assumes that the remaining life of the storm surge barrier with respect to flood protection is zero years for the current non-closure probability. This assumption is justified since extensive reinforcement works are currently required to comply with the flood protection standards of the dike trajectories along the Hollandsche IJssel if the non-closure probability is not reduced.

4.4.2 Navigation

For the navigation function, the number of closures of the Hollandsche IJssel barrier is an important parameter. The number of closures for various amounts of sea level rise was already analysed in Section 4.3. The results of this analysis could also be used to assess the functional performance with respect to navigation. In addition, the duration of the closures, which provides an indication of the unavailability of the waterway, is relevant.

Regarding unavailability, a distinction was made between partial and complete unavailability of the waterway. This differentiation is necessary because, in the event of a closure, vessels could still make use of the adjacent lock to pass the Hollandsche IJssel barrier. However, levelling operations are ceased when the water level reaches NAP +2.50 m, and the waterway becomes completely blocked. The waterway is thus partially unavailable when the water level exceeds the closure level (assumed at NAP +2.10 m) and fully unavailable when a water level of NAP +2.50 m is reached.

As for the estimation of the number of closures, the water level measurements at the Hollandsche IJssel barrier were used in the assessment of the unavailability. A limitation of the measurement data is, however, the presence of different time resolutions. The data before 1994 include hourly water level measurements, and the data after 1994 consist of measurements taken every 10 minutes. This inconsistency means that

the time for which the water level is above the critical level can only be determined in whole hours for the years before 1994, whereas for the years after 1994, the unavailability with a resolution of 10 minutes could be obtained. Hence, the measurements prior to 1994 and around the critical water level (and higher) were interpolated to obtain a time series with a resolution of 10 minutes as well. After this interpolation step, the cumulative duration of the closures was calculated by summing up the intervals in which the water level exceeds the critical level (NAP +2.10 m or NAP +2.50 m). If the start of a closure is within 6 hours after the end of the previous closure, the events were combined and considered as one closure event. The total number of hours was then divided by the number of years of the time series to obtain an estimate of the unavailability. In addition, two hours were added to each closure event to account for the time between the start or end of a closure operation and the waterway being available for traffic again. These extra hours could also serve as some sort of correction for closures at slack water that generally take place earlier and last longer than the closures based on the critical water level. The yearly unavailability as a function of sea level for both a critical level of NAP +2.10 m and NAP +2.50 m is shown in Figure 4.11.

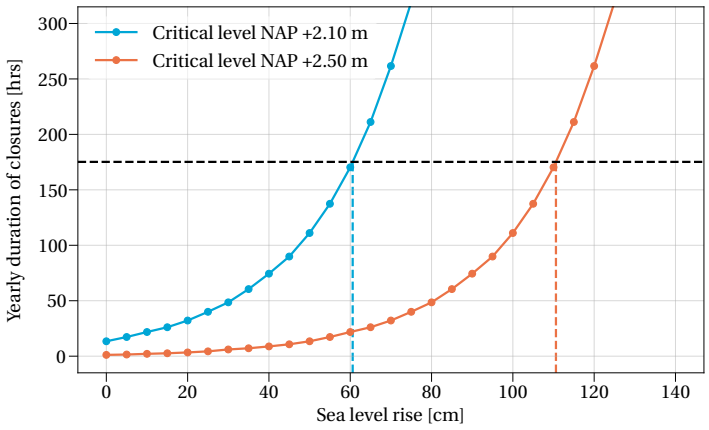

Figure 4.11: Total average yearly duration of closures (unavailability) as a function of sea level rise for a critical level of NAP +2.10 m and NAP +2.50 m.

In the functional analysis of Section 2.2, several requirements were formulated to restrict the hindrance to shipping. These requirements were summarised in Table 2.7. For the number of closures, a maximum of nine closures per year was defined. This value is reached when the sea level rises by about 20-25 cm, according to the analysis in Section 4.3. Two other closure frequencies were added to study the effectiveness of increasing the acceptable number of closures. The two values are 15 and 30 closures. The first number roughly corresponds to two closures per month during the storm season and the second one resembles four closures per month, or one closure a week. These numbers are averages, and thus it should be kept in mind that multiple closures a week could also occur, especially in case of the second additional closure frequency. For the second performance indicator, the unavailability, a maximum of 175.2 hours (2% of 8760 hours) was formulated. This unavailability criterion is exceeded for a sea level rise of about 61 cm or 111 cm, depending on the critical water level (NAP +2.10 m or NAP +2.50 m). The functional performance of the Hollandsche IJssel barrier with respect to navigation is thus governed by the number of closures. The requirements and corresponding amounts of sea level rise for both performance indicators are summarised in Table 4.4.

Table 4.4: Sea level rise values corresponding to the requirements for navigation. The values were corrected for the sea level rise between 1995 and 2017 using a rate of 2.3 mm/year, as mentioned in the *Zeespiegelmonitor 2018* (Baart et al., 2019).

Indicator	Functional requirement	Performance requirement	Sea level rise w.r.t. 2017 [cm]	Sea level rise w.r.t. 1995 [cm]
Number of closures [per year]	–	9	22	27
		15	34	39
		30	51	56
Unavailability	NAP +2.10 m	175.2 hours	61	66
	NAP +2.50 m	175.2 hours	111	116

4.4.3 Water management

The only function in the category water management that may influence the remaining life of the Hollandsche IJssel barrier is providing storage capacity for “polder water” in closed condition. In case the barrier is closed, the water levels in the Hollandsche IJssel will rise as a result of the discharge of water from the polders into the Hollandsche IJssel. The discharge will have to be ceased ("maalstop") if the water level reaches NAP +2.60 m ("maalstoppeil"). The halt of the pumping operations may have undesired consequences such as submerged basements or destruction of agricultural crops due to an abundance of water. Although the effects are less severe than the consequences of dike breaches, these situations should still be prevented.

For the calculation of the frequency of a "maalstop", only the closed situation may be considered because for an open Hollandsche IJssel barrier water can flow freely downstream. Moreover, in case of failure of the storm surge barrier, the "maalstoppeil" is exceeded to such an extent that the value becomes meaningless. Because only the closed situation is relevant, Hydra-NL is the preferred tool to calculate the frequency of a "maalstop". By setting the non-closure probability of the Hollandsche IJssel barrier to 0, the frequency curves of the water levels in closed condition could be obtained. The frequency (or return period) of a "maalstop" then follows from the return period of the water level NAP +2.60 m. The resulting return periods are listed in Table 4.5 and depicted in Figure 4.12. Rongen and Maaskant (2019) performed an identical analysis and their results are also included in Table 4.5.

Table 4.5: Return period of the "maalstoppeil" for the considered scenarios. $P_{Q_{pump}}$ indicates the probability of having a discharge of Q_{pump} = 75 m^3/s, e.g. a probability of 1/3 implies a discharge of 75 m^3/s during one in three closures of the Hollandsche IJssel barrier.

Scenario	**Return period [years]**	
	This study	Rongen and Maaskant (2019)
Current climate, $P_{Q_{pump}}$ = 1/3	18 000	20 000
Current climate, $P_{Q_{pump}}$ = 1	6000	7000
W2050, $P_{Q_{pump}}$ = 1/3	2200	3000
W2050, $P_{Q_{pump}}$ = 1	730	1200
W2100, $P_{Q_{pump}}$ = 1/3	450	600
W2100, $P_{Q_{pump}}$ = 1	150	200

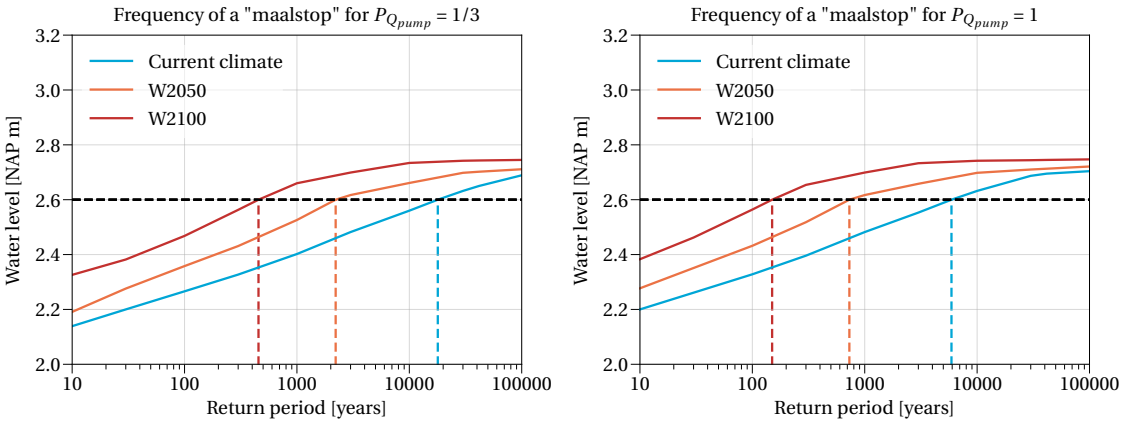

Figure 4.12: Estimates of the frequency of a "maalstop" based on the water levels behind a closed Hollandsche IJssel barrier. The left figure shows the estimates for the situation in which the probability of having a discharge of Q_{pump} = 75 m^3/s is 1/3. The figure on the right shows the estimates for the situation in which the same amount is discharged into the river during every closure.

Figure 4.12 suggests that there is a maximum to the water levels behind the Hollandsche IJssel barrier. This is because the increase in the water levels directly behind the storm surge barrier is mainly determined by the discharge of water from the pumping stations into the Hollandsche IJssel. Other factors that may influence the water levels, such as wind set-up and failure of the storm surge barrier, have little to no effect since the water levels were derived for the location directly behind the barrier and for the situation with a closed storm surge barrier. The rise in the water level will slow down soon after the "maalstoppeil" (NAP +2.60 m) is reached as the pumping stations stop discharging. Water levels that are substantially higher than this "maalstoppeil" will therefore not occur.

The differences between the return periods of the “maalstoppeil” in this study and the ones of Rongen and Maaskant (2019) are a result of the computational settings in Hydra-NL. The return periods in this study were calculated with repaired water levels. Repairing of the water levels implies that Hydra-NL ensures that the water levels are monotonously increasing in relation to increasing wind speed, discharge, lake level, or sea water level (Duits, 2020). This is standard practice for the wind speed, but it is an option for river discharge and sea water level. Rongen and Maaskant (2019) chose not to repair the water levels along the river discharge and sea water level. However, since the water levels are repaired by default when Hydra-NL is used for the assessment of the flood defences, the water levels are also repaired in the calculation of the frequencies of a “maalstop” in this study. Usually, the choice to repair has limited effects on the water levels. But because only the closed situation, the situation for which the water levels are most often repaired, is considered when calculating the frequencies of a "maalstop", the differences are visible. Yet, the choice to repair the water levels or not does not have major consequences for the evaluation of the functional performance as the calculated frequencies are well above the critical frequency of a "maalstop" of 1/200 per year for most of the scenarios, except for a sea level rise of 75 cm and a maximum discharge (Q_{pump} = 75 m^3/s) into the Hollandsche IJssel during every closure event ($P_{Q_{pump}} = 1$).

Another issue related to the use of Hydra-NL is that the frequency of a "maalstop" could only be calculated for the scenarios shown in Figure 4.12 (current climate, 25 cm and 75 cm sea level rise) due to the coupling between wind speed and sea water level (see Section 4.2). However, as already mentioned before the acceptable probability of reaching the "maalstoppeil" of 1/200 per year is only exceeded for the most extreme scenario considered (75 cm of sea level rise and a discharge of 75 m^3/s into the Hollandsche IJssel during every closure event). For this amount of sea level rise, the non-closure probability has to be reduced to values lower than 1/10,000 per closure to safeguard the flood protection function (Figure 4.10), and the barrier has to be closed multiple times a week (Figure 4.9), which leads to inadmissible hindrance to shipping. Moreover, the water authorities, especially HH Rijnland, could release water into other waterways to reduce the likelihood of a "maalstop". The discharge of water into alternative watercourses is also an option to cope with future increases in precipitation and the associated discharge demand. Based on these considerations, the water management function is considered not to be governing for the remaining life of the Hollandsche IJssel barrier.

It should be noted that the above-described analysis of the frequency of the "maalstop" with Hydra-NL does not include the model uncertainty in the water levels for the reasons explained in Section 4.2. The impact of the model uncertainty on the frequencies may be significant because of the small margin between the closure level and "maalstoppeil". This margin could be increased by closing the barrier at low water slack instead of using the closure criterion based on a critical water level. But as the sea level rises, the water level at slack water increases too, and the difference between the water level directly after a closure and the "maalstoppeil" decreases. In view of a future with rising sea levels, accurate estimates of the model uncertainty in the water levels behind the Hollandsche IJssel barrier are therefore deemed necessary. However, since official values for the model uncertainty have not yet been determined, the conclusions based on the calculations without model uncertainty were maintained and the water management function was excluded from the remainder of the lifespan analysis.

4.4.4 Other functions

The remaining functions or function categories (ecology, road traffic, and monument) are not included in the analysis of the remaining life as no quantitative requirements were formulated in Section 2.2. The fact that these requirements are not suitable for a quantitative assessment of the remaining life of the Hollandsche IJssel barrier does not mean that the associated functions should not be taken into account when considering replacement or renovation of the storm surge barrier. Therefore, it is advised to include these functions in the discussions on measures to extend the lifespan of the structure or when studying alternative solutions for the flood protection of the area.

4.5 Conclusions

Methods and tools for the assessment of the remaining life of the Hollandsche IJssel barrier have been discussed in this chapter. As sea level rise was found to be the most important external driver (see Chapter 3), methods/approaches have been described that relate the functional performance to sea level rise. But before the functional performance could be linked to sea level rise, relationships between the water levels at the bar-

rier and sea level rise had to be derived because of the more inland location of the Hollandsche IJssel barrier. Based on analyses of the water levels with Hydra-NL, a sea level rise of 1 m was found to result in an 80 cm increase in the water level at the barrier under daily conditions, i.e. the conditions under which the Maeslant barrier is open. For the extreme water levels (water levels > NAP +3.6 m), the same amount of sea level rise leads to an increase of 67 cm. The latter relationship is less relevant since the results of Hydra-NL could also be used directly when water levels with a return period longer than 10 years are considered.

The three functions or function categories for which methods were introduced are flood protection, navigation, and water management. The functional performance with respect to flood protection was assessed by comparing the 1/30,000-year water level behind the storm surge barrier for a specific value of sea level rise and probability of non-closure with an assessment water level (NAP +2.90 m and NAP +3.04 m). These water levels follow from the probabilistic model Hydra-NL and a simple relationship between the water levels in front of and behind the Hollandsche IJssel barrier (Equation (4.3)). For navigation, water level measurements at the barrier were used to derive the closure frequency and unavailability (total average duration of closures per year) of the storm surge barrier as a function of sea level rise. Hydra-NL was also applied to evaluate the performance with respect to water management, but this function turned out not to be governing, and therefore it does not have to be considered any further in the assessment of the remaining life of the barrier. The remaining functions (ecology, road traffic, monument) were also disregarded since the performance could not be evaluated due to a lack of quantitative requirements.

The output of the performance assessment approaches are tables with the required performance levels as a function of sea level rise. These tables, combined with sea level rise projections, provide estimates of the remaining life of the Hollandsche IJssel barrier. The selected sea level rise projections and estimates of the remaining life are presented in the next chapter (Chapter 5).

5

Evaluation of the remaining life of the Hollandsche IJssel barrier

In Chapter 3, sea level rise was identified as the dominant factor affecting the remaining life of the Hollandsche IJssel barrier. Hence, methods to relate the functional performance of the barrier to sea level rise were presented in Chapter 4. In this chapter, sea level rise projections are combined with the results from the approaches described in Chapter 4 in order to estimate the end of life or remaining life of the Hollandsche IJssel barrier. The chapter thus seeks to answer the following research question:

5. What is the remaining life of the Hollandsche IJssel barrier?

The chapter is divided into four sections. First, in Section 5.1, sea level rise projections are discussed. Multiple projections or studies on sea level rise are considered to deal with the deep uncertainty[1] that characterises sea level rise projections. Section 5.2 describes how the estimates of the remaining life of the storm surge barrier could be derived using these sea level rise projections. In Section 5.3, the resulting estimates of the remaining life for each function are presented. Finally, in Section 5.5, the findings of the previous sections are summarised and an answer to the addressed research question is provided.

5.1 Analysis of sea level rise projections

The estimated sea level rise ranges of the KNMI'14 climate change scenarios are among the most-well known projections in the Netherlands. These projections are incorporated in the Delta Scenarios, which are used within the Delta Programme, a national programme of the Dutch government in which strategies and plans are developed to protect the Netherlands from flooding, ensure a sufficient supply of fresh water, and achieve a climate-proof and water-resilient Netherlands by 2050 (Deltaprogramma, 2020). Even though the scenarios form the basis of the Dutch Delta Programme, they may provide an incomplete picture of the future sea level rise as the large differences in the projections in Figure 3.11 in Section 3.4 show. The KNMI'14 climate change scenarios are closely related to the scenarios of the IPCC, for which there are several limitations. For instance, the IPCC scenarios focus on the likely range (66% probability or more) and on approaches for producing information on future sea level rise about which consensus among researchers exists. This preference for consensus among scientists may lead to overconfident projections that do not necessarily provide a good basis for long-term decision making or risk management (Hinkel et al., 2015, 2019). As the KNMI'14 climate change scenarios are based on the global IPCC scenarios, the KNMI'14 projections may be overconfident as well.

As an alternative to the sea level rise projections of the KNMI'14 climate change scenarios, probabilistic projections could be used to represent a wider range of possible scenarios of sea level rise, including high-end scenarios. Unfortunately, there is no single unambiguous probability distribution of sea level rise. Sea level rise projections are deeply uncertain, and different yet all reasonable methods or assumptions could lead to widely divergent probabilistic projections (A. M. R. Bakker et al., 2017).

[1] a situation in which parties cannot agree upon (1) methods or models to describe the system, (2) the probability distributions to represent the uncertain key variables and parameters of the models, and/or (3) how to value the desirability of alternative outcomes (Lempert et al., 2003)

One of the most important sources of uncertainty in these projections is related to the (dynamic) response of the ice sheets, in particular the West Antarctic ice sheet, to future global warming (Bamber et al., 2019; Horton et al., 2018; IPCC, 2019; Jevrejeva et al., 2019). The contribution of the Antarctic ice sheet in 2100 under RCP8.5 could be a few centimetres (5th percentile of Levermann et al. (2014) is 0.01-0.04 cm) or, on the other end of the spectrum, exceeding 1 m (95th percentile of DeConto and Pollard (2016)). The process that is responsible for the large contribution of the Antarctic ice sheet in the study of DeConto and Pollard (2016) is Marine Ice-Cliff Instability (MICI). Although the validity of this process remains unproven, it is the primary driver of deep uncertainty in sea level rise projections (Kopp et al., 2019). A reasonable approach to account for the deep uncertainty in the projections would therefore be to consider several studies that incorporate the contribution of the (Antarctic) ice sheets differently. This way the large uncertainty within the projections is also be demonstrated.

For this study, the projections of the KNMI'14 climate change scenarios (Van den Hurk et al., 2014), Kopp et al. (2017), Le Bars et al. (2017), and Bamber et al. (2019) were selected. The studies by Kopp et al. (2017) and Le Bars et al. (2017) incorporate the projections of the Antarctic ice sheet model by DeConto and Pollard (2016), but adopted different approaches. Kopp et al. (2017) used the ensemble values of DeConto and Pollard (2016) directly, whereas Le Bars et al. (2017) fitted a normal distribution to these values. The study by Bamber et al. (2019) was also considered as this study sought to incorporate the current state of scientific knowledge on the contribution of the ice sheets by means of a formal expert elicitation protocol or structured expert judgement called the Classical Model.

Direct comparison of the different projections is difficult as the studies use different external forcings. The KNMI'14 climate change scenarios G and W and the projections of Bamber et al. (2019) are based on temperature pathways rather than the RPCs of the IPCC, which are used for the projections by Kopp et al. (2017) and Le Bars et al. (2017). For reference, the G scenario of KNMI'14 overlaps with the intermediate scenario RCP4.5 and the W scenario is roughly comparable to the high emission scenario RCP8.5. Similarly, the L scenario of Bamber et al. (2019) lies between RCP2.6 and RCP4.5, and the H scenario more or less matches RCP8.5. Hence, the projections were grouped into low-to-medium temperature/emission scenarios and high temperature/emission scenarios (see Figure 5.1 and Figure 5.2).

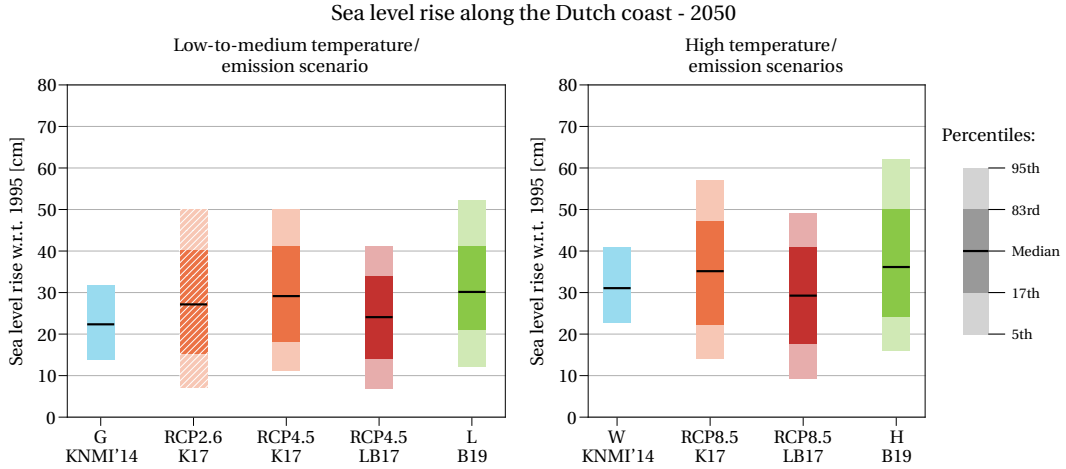

Figure 5.1: Projections of the sea level rise along the Dutch coast by 2050 for both low-to-medium temperature/emission scenarios and high temperature/emission scenarios. The bars show the 5th-95th percentile ranges and median values of the studies KNMI'14 (Van den Hurk et al., 2014), K17 (Kopp et al., 2017), LB17 (Le Bars et al., 2017), and B19 (Bamber et al., 2019). Note that the projections of Kopp et al. (2017) and Bamber et al. (2019) were corrected for the sea level rise between 1995 and 2000 by assuming a rate of 2.3 mm/year, in accordance with the *Zeespiegelmonitor 2018* (Baart et al., 2019).

There is little difference in the projections for 2050 under both the low-to-medium temperature/emission scenarios and high temperature/emission scenarios. The median values are very similar, and only the 90% probability ranges of the KNMI'14 projections are significantly smaller. In contrast, large differences can be observed in the projections for 2100. The median values show notable differences, especially under the high temperature/emission scenarios. Again, the probability ranges of the KNMI'14 projections are considerably smaller. This discrepancy results from different interpretations of the IPCC's likely range as demonstrated by A. M. R. Bakker et al. (2017). In the KNMI'14 scenarios, this likely range is implicitly interpreted as the 90% probability range, whereas the other studies consider the likely range to be the 66% probability range.

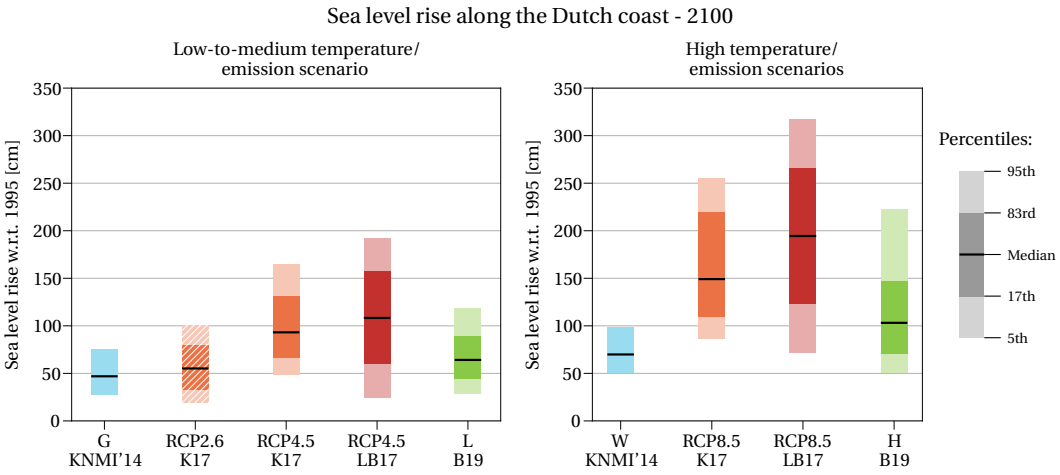

Figure 5.2: Projections of the sea level rise along the Dutch coast by 2100 for both low-to-medium temperature/emission scenarios and high temperature/emission scenarios. The bars show the 5th-95th percentile ranges and median values of the studies KNMI'14 (Van den Hurk et al., 2014), K17 (Kopp et al., 2017), LB17 (Le Bars et al., 2017), and B19 (Bamber et al., 2019). Note that the projections of Kopp et al. (2017) and Bamber et al. (2019) were corrected for the sea level rise between 1995 and 2000 by assuming a rate of 2.3 mm/year, in accordance with the *Zeespiegelmonitor 2018* (Baart et al., 2019).

In addition, Figure 5.2 shows the differences in the shapes of the probability distributions. The projections of Kopp et al. (2017) and Bamber et al. (2019) seem to exhibit a more skewed distribution, which follows from the heavy-tailed distributions of the contribution of the Antarctic ice sheet reported by DeConto and Pollard (2016) and the structured expert judgement in Bamber et al. (2019). This skewness is lacking in the projections of the KNMI'14 climate change scenarios and Le Bars et al. (2017) as the KNMI'14 projections include a significantly smaller contribution of the ice sheets, while Le Bars et al. (2017) assumed a normal distribution for the contribution of the Antarctic ice sheet. These heavy-tailed distributions of the sea level rise projections by Kopp et al. (2017) and Bamber et al. (2019) also illustrate that the use of the likely range leads to conservative estimates of sea level rise, which may provide insufficient information in situations with a high risk, i.e. low probability, yet severe consequences.

5.2 From sea level rise projections to an estimate of the remaining life

The previous chapter (Chapter 4) described how the functional performances could be related to sea level rise. Where possible, the requirements for each function (category) were linked to a critical amount of sea level rise, resulting in tables with the required performance levels and corresponding sea level rise values (see Table 5.1). Together with the sea level rise projections introduced in Section 5.1, these values can be used to estimate the remaining life of the Hollandsche IJssel barrier (expressed in years).

Table 5.1: Sea level rise values corresponding to the requirements for each function (category). The values were corrected for the sea level rise between 1995 and 2017 using a rate of 2.3 mm/year, as mentioned in the *Zeespiegelmonitor 2018* (Baart et al., 2019).

Function category	Indicator	Functional requirement	Performance requirement	Sea level rise w.r.t. 2017 [cm]	Sea level rise w.r.t. 1995 [cm]
Flood protection	Non-closure probability [per closure]	Assessment level NAP +3.04 m	1/1,000	46	51
			1/2,000	64	70
			1/5,000	87	92
			1/10,000	103	108
		Assessment level NAP +2.90 m	1/2,000	19	24
			1/5,000	45	50
			1/10,000	60	65
Navigation	Number of closures [per year]	–	9	22	27
			15	34	39
			30	51	56
	Unavailability	NAP +2.10 m	175.2 hours	61	66
		NAP +2.50 m	175.2 hours	111	116

Typically, the remaining life of a structure is dependent on multiple parameters, each with its own probability distribution, and techniques like Monte Carlo simulation have to be used to generate probabilistic outcomes, i.e. the probability distribution of the remaining life of the structure. However, in this case, the remaining life is largely governed by a single stochastic variable (sea level rise), and as a result, the probability distribution of the remaining life can be determined directly from the probability distributions of sea level rise. For example, if the critical amount of sea level rise x equals the 90th percentile of sea level rise in year y, then there is a 10% probability that the actual sea level rise will be greater than x in year y, and thus there is a 10% probability that the end of life of the structure is earlier than year y. In other words, the cumulative distribution function tied to a specific amount of sea level rise equals the survival function of the remaining life of the storm surge barrier. The procedure for deriving the survival function of the remaining life is depicted in Figure 5.3.

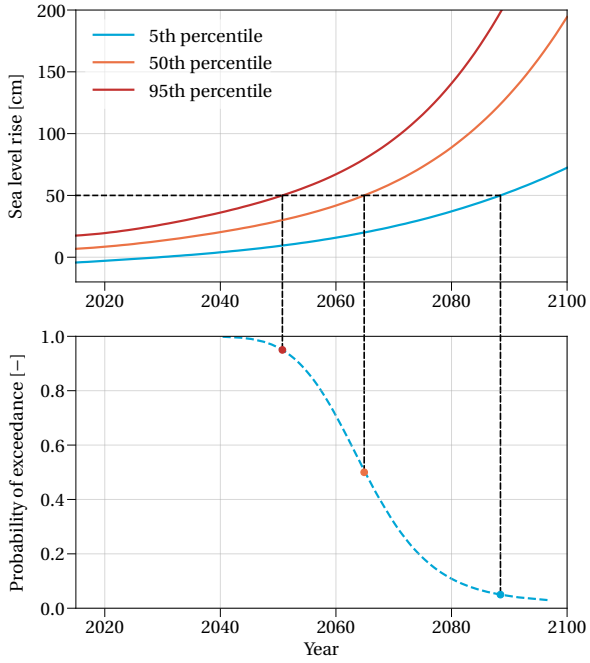

Figure 5.3: Illustration of the procedure to derive the probability distribution of the remaining life of the storm surge barrier for an arbitrary sea level rise scenario. The end of life of the barrier occurs when the critical amount of sea level rise is reached. The probability distribution of the remaining life can be obtained by determining the year in which the critical amount of sea level rise is exceeded for each percentile of the sea level rise projection. In this example, the critical amount of sea level rise is 50 cm. The figure shows that the median value of the end of life estimate is about 2065 with a 90% probability range of 2050-2090.

The KNMI'14 scenarios (Van den Hurk et al., 2014) and Le Bars et al. (2017) provide projections up to 2100. These projections were linearly extrapolated to obtain values for the probability distribution of the remaining life beyond 2100. The estimates that follow from this linear extrapolation should be interpreted with caution, especially when the projections exhibit accelerated sea level rise. As an example, the extrapolated projections for the W scenario of KNMI'14 and the scenario RCP8.5 of Le Bars et al. (2017) are shown in Figure 5.4.

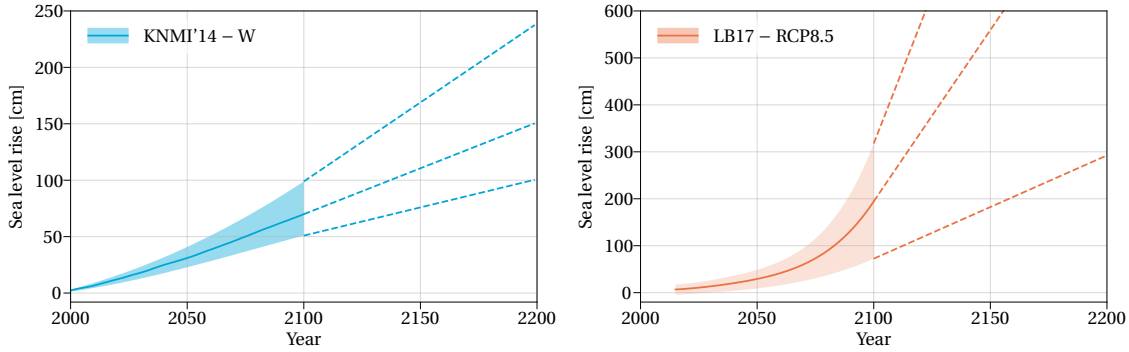

Figure 5.4: Linear extrapolation of the KNMI'14 climate change scenarios (Van den Hurk et al., 2014) and LB17 (Le Bars et al., 2017) projections. The left figure shows the extrapolation of the sea level rise projections for the W scenario of KNMI'14. The figure on the right shows the extrapolation of the projection of Le Bars et al. (2017) for RCP8.5. The bandwidth depicts the 5th-95th percentile range.

The figure illustrates that the linear extrapolation generates better results for the KNMI'14 projection. Linear extrapolation of the projection of Le Bars et al. (2017) probably results in too optimistic values for the end of life estimates. As an alternative for Le Bars et al. (2017), the projections of Kopp et al. (2017) could be used. These projections also include the results of the study by DeConto and Pollard (2016) for the contribution of the Antarctic ice sheet and go out to 2300 instead of 2100. The differences in the approaches for Antarctica's contribution become strongly apparent only after 2090, as shown in Figure 5.5.

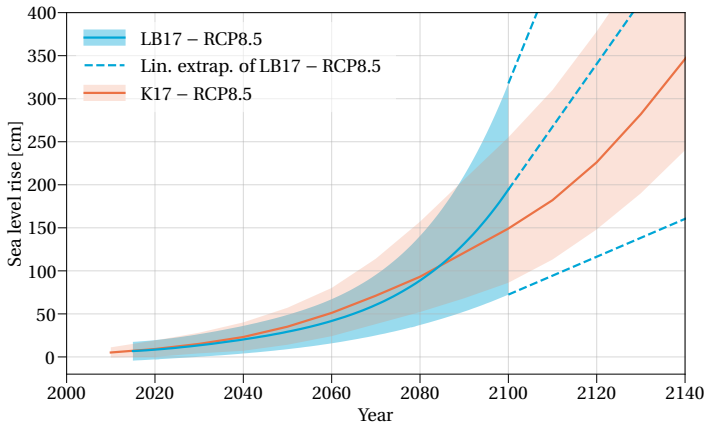

Figure 5.5: Comparison of the sea level rise projections at the Dutch coast under RCP8.5 from Kopp et al. (2017) and Le Bars et al. (2017). The bandwidth depicts the 5th-95th percentile range.

By performing the calculation steps described above, probability distributions of the remaining life with respect to each function of the storm surge barrier can be obtained. The produced probability distributions are discussed in the next section.

5.3 Resulting estimates of the remaining life

The estimates of the remaining life of the Hollandsche IJssel barrier that were obtained by combining the critical sea level rise values listed in Table 5.1 with the sea level rise projections discussed in Section 5.1 are presented in this section. The findings regarding the flood protection function are discussed first (in Section 5.3.1). The results for the other considered function category, navigation, are presented and discussed in Section 5.3.2.

5.3.1 Flood protection

For the flood protection function, the remaining life was estimated using two different assessment levels, NAP +3.04 m and NAP +2.90 m. The first level was based on the current non-closure probability of 1/200 per closure, whereas the latter corresponds to a non-closure probability of 1/1,000 per closure (both for a return period of 30,000 years). In the following paragraphs, the results for both assessment levels are discussed.

Assessment level NAP +3.04 m

The 66% and 90% probability ranges of the estimated end of life are shown in Figure 5.6 and Figure 5.7. The probability ranges for the low-to-medium temperature/emission scenarios are significantly wider than the ones for the high temperature/emission scenarios. This difference is the result of the overall smaller sea level rise values for the low-to-medium scenarios. Hence, the critical amount of sea level rise is attained later in time, and as the time scale increases, the uncertainty in the projections grows and the probability ranges widen. This behaviour also explains why the probability ranges based on the projections of Kopp et al. (2017) and Le Bars et al. (2017) are generally smaller. The rate of sea level rise is higher under those scenarios, and thus the critical amount of sea level rise is reached earlier in time so that the differences in the 5th and 95th percentiles are smaller in comparison with the other projections. And similarly, the 95th percentiles of the estimates of the end life diverge more than the 5th percentiles or median values for both the low-to-medium and high scenarios. The later in time the critical amount of sea level rise is reached, the more the results for the various projections deviate. However, the disparity between the 95th percentiles estimates is less relevant because these values indicate a remaining life of 100 years or more and correspond to a situation with low risk,

i.e. low probability and minor consequences. The 5th percentiles, on the other hand, represent a high-risk situation, with low probability but severe consequences, which are more relevant from a risk management point of view.

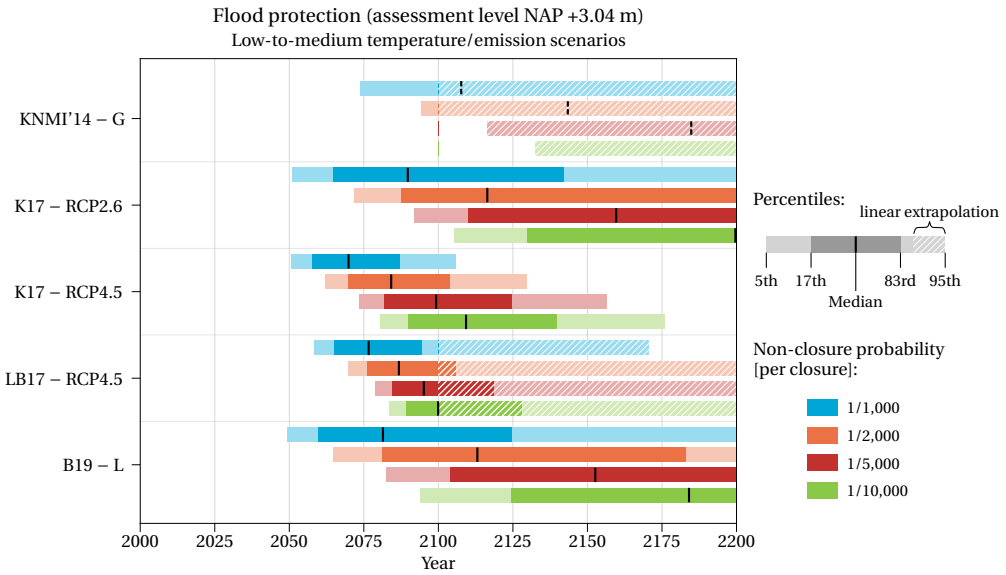

Figure 5.6: Estimates of the end of life of the Hollandsche IJssel barrier with respect to flood protection (assessment level NAP +3.04 m) for the low-to-medium temperature/emission scenarios. White hatched areas imply linear extrapolation of the sea level rise projections.

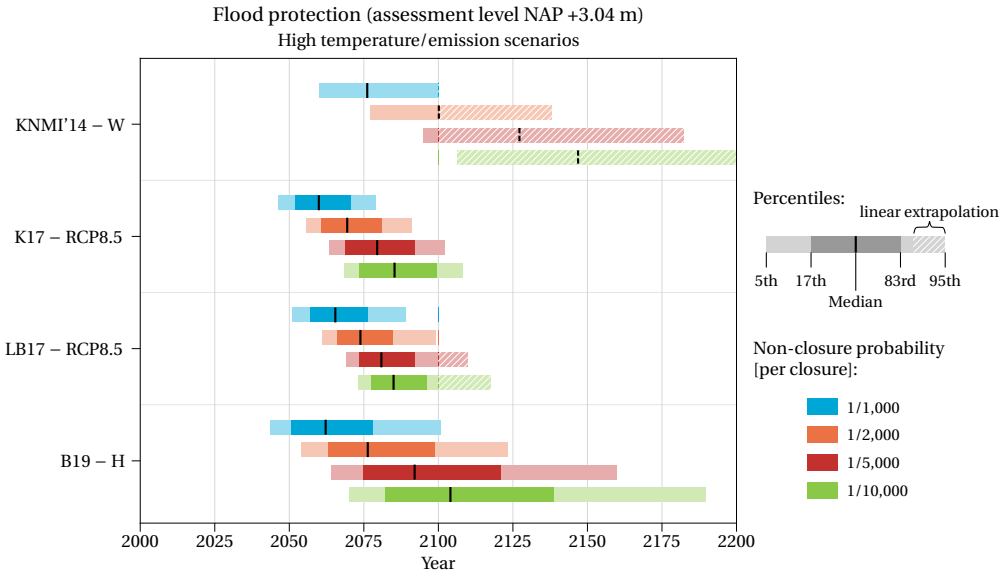

Figure 5.7: Estimates of the end of life of the Hollandsche IJssel barrier with respect to flood protection (assessment level NAP +3.04 m) for the high temperature/emission scenarios. White hatched areas imply linear extrapolation of the sea level rise projections.

It can also be seen that for both the low and high scenarios, the lower bounds (5th percentiles) of the various studies differ less than the upper bounds (95th percentiles). This can be explained by the fact that differences in the projected sea level rise of the various studies are small up to 2050, and thus if the end of life moment is around this moment in time, the choice for a specific scenario is less significant for the estimates of the remaining life (see Figure 5.1 and Figure 5.2).

Finally, one can see that in spite of the large uncertainty in the remaining life, there is a 95% probability that the Hollandsche IJssel barrier does not need to be replaced before the end of its design life (2058) if the non-closure probability is reduced to 1/2,000 per closure, irrespective of the climate change scenario.

Assessment level NAP +2.90 m

The same probability ranges as for the assessment level NAP +3.04 m are plotted in Figure 5.8 and Figure 5.9. In this case, the end of life with respect to the flood protection function can be expected considerably sooner than for the assessment level NAP +3.04 m. The figures suggest that the end of life could be reached within 5 years for a non-closure probability of 1/2,000 per closure. In fact, the lifespan has already ended for the L scenario of Bamber et al. (2019). Although incorrect, this result is possible because of the way the projections were made. The sea level rise projections use 1995 (or 2000) as the reference year, and the projected sea level rise has an uncertainty range for the years thereafter. For example, Bamber et al. (2019) projected a sea level rise of 1 to 25 cm (90% range) in 2020 under the L scenario. As a result, the critical amount of sea level rise could be reached in the years between 1995 and now (2021) if the critical value is relatively low, e.g. 20 cm. Therefore, the values in the nearest decade should be interpreted with caution, and, if desired, sea level rise measurements and extrapolations thereof could be examined to draw conclusions for the near term.

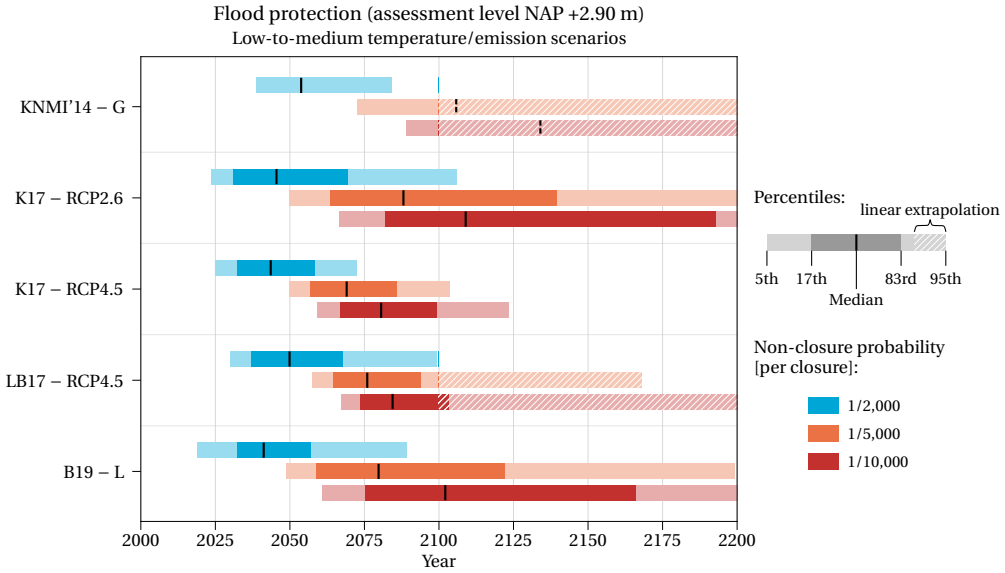

Figure 5.8: Estimates of the end of life of the Hollandsche IJssel barrier with respect to flood protection (assessment level NAP +2.90 m) for the low-to-medium temperature/emission scenarios. White hatched areas imply linear extrapolation of the sea level rise projections.

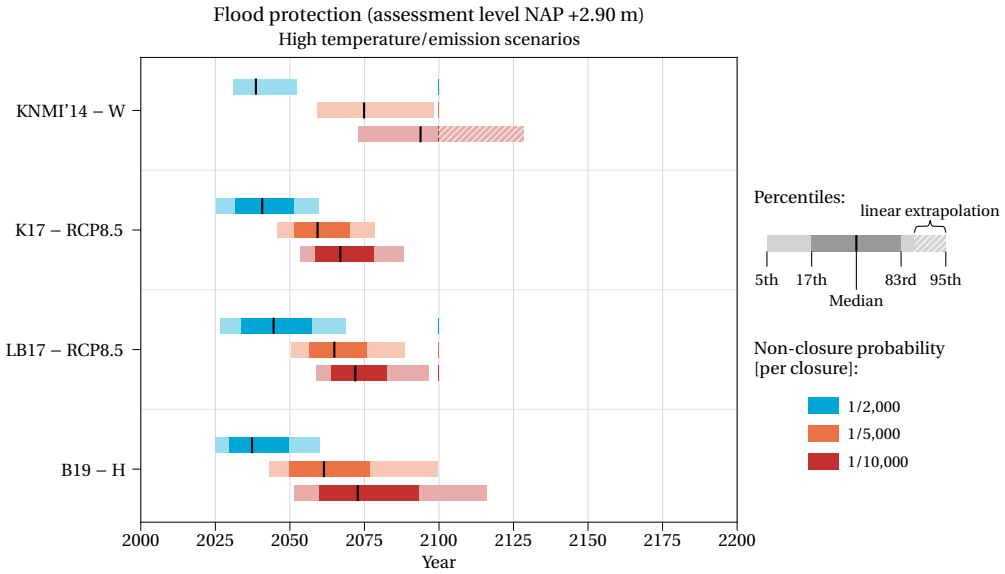

Figure 5.9: Estimates of the end of life of the Hollandsche IJssel barrier with respect to flood protection (assessment level NAP +2.90 m) for the high temperature/emission scenarios. White hatched areas imply linear extrapolation of the sea level rise projections.

Besides a shorter remaining life compared with the results for an assessment level of NAP +3.04 m, differences in the effectiveness of a decrease in the non-closure probability can be observed. The figures show that the reduction from 1/2,000 to 1/5,000 per closure results in a greater extension of the lifespan than the reduction from 1/5,000 to 1/10,000 per closure, in contrast to the situation with an assessment level of NAP +3.04 m where the reduction from 1/2,000 to 1/5,000 per closure and the reduction from 1/5,000 to 1/10,000 per closure are almost equally effective. The explanation for this behaviour lies in the shape of the projections. The projections suggest an approximately exponential trend which implies that the increase in the remaining life is greater when the critical sea level rise is raised from, say, 20 to 30 cm than when this critical level is raised from 60 to 70 cm (see Figure 5.10). As the critical amounts of sea level rise are higher for an assessment level of NAP +3.04 m, the differences in the rates in sea level rise are less clear, and so are the differences in the extensions of the remaining life.

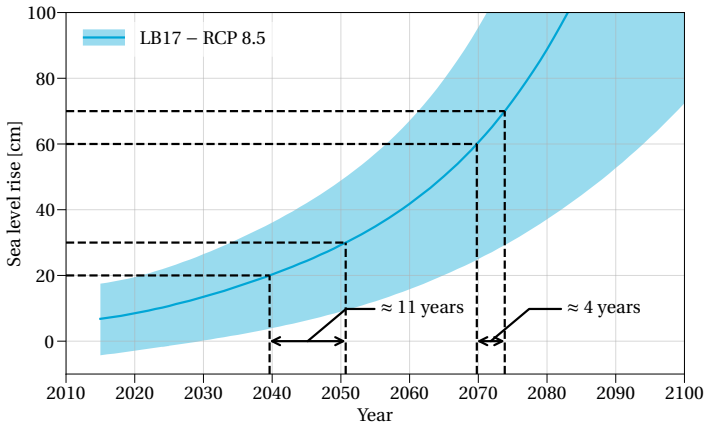

Figure 5.10: Illustration of how the same increment in sea level rise leads to different time shifts due to the trend in the projection.

As a last observation, there is a 95% probability that the barrier does not need to be replaced before the end of its design life (2058) for almost every climate change scenario if the non-closure probability is reduced to 1/10,000 per closure. The difference of 14 cm in the assessment level (NAP +2.90 m vs NAP +3.04 m) thus has quite a large impact on the required non-closure probability if one wishes to ensure that the end of the design life is reached.

5.3.2 Navigation

Two performance indicators were adopted for the navigation function: the number of closures and the total yearly duration of closures of the barrier. The first indicator provides an indication of the frequency of hindrance to shipping, while the second one represents a measure of the unavailability of the waterway. The probability ranges of the functional end of life for both indicators are presented in the following paragraphs.

Number of closures

Figure 5.11 and Figure 5.12 show the end of life estimates based on the acceptable number of closures. The figures suggest that the end of life regarding the number of closures of the storm surge barrier could be reached within 5 to 10 years if the acceptable number of closures is assumed to be nine closures per year (based on the 5th percentiles). The short remaining life is due to the relatively small critical amount of sea level rise, which is in the order of 20-30 cm, and the uncertainty in the sea level rise at the start of the projections as discussed in Section 5.3.1.

Again, the figures indicate that the probability ranges for the low-to-medium temperature/emission scenarios are significantly wider than the ones for the high temperature/emission scenarios for the same reason as described in Section 5.3.1. Moreover, the differences between the values for the individual studies within the set of low-to-medium temperature/emission scenarios are also substantially larger than the spread between the values for the high temperature/emission scenarios. For the low-to-medium scenarios, the differences between the lowest and highest median values are about 14 years and 23 years for 9 and 15 closures per year, respectively. Whereas these differences are about 7 and 8 years for the high scenarios. Part of the large differences for the low-to-medium scenarios can be explained by the fact that the end of life is reached later

this century when the uncertainty ranges in the individual projections are greater. Another cause of the variation is the different amounts of radiative forcing used in the projections for these scenarios. For instance, the results based on the projections by Kopp et al. (2017) for RCP2.6 and RCP4.5 are both included in the same figure. The individual projections for the high scenarios, on the other hand, are all based on external forcings comparable to RCP8.5.

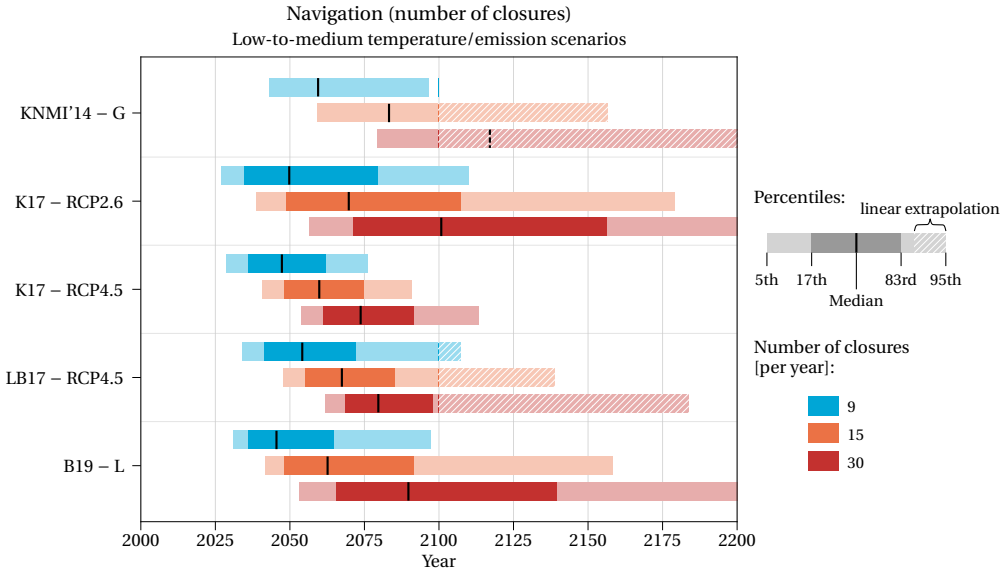

Figure 5.11: Estimates of the end of life of the Hollandsche IJssel barrier with respect to navigation (number of closures) for the low-to-medium temperature/emission scenarios. White hatched areas imply linear extrapolation of the sea level rise projections.

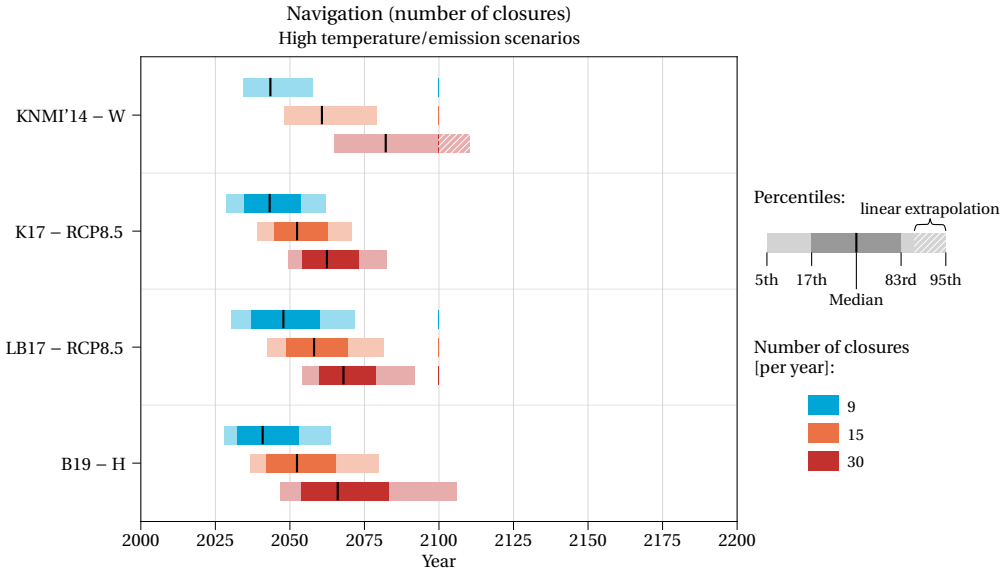

Figure 5.12: Estimates of the end of life of the Hollandsche IJssel barrier with respect to navigation (number of closures) for the high temperature/emission scenarios. White hatched areas imply linear extrapolation of the sea level rise projections.

With regard to the effectiveness of an increase in the acceptable number of closures, the increase in the 5th percentile of the end of life estimates varies between 9 (B19 - H) and 16 years (KNMI'14 - G) if the acceptable closure frequency is increased from 9 to 15 closures and between 10 (K17 - RCP8.5 and B19 - H) and 20 years (KNMI'14 - G) if the frequency is doubled from 15 to 30 closures. The changes in the estimates are slightly larger for the median values. For an increase from 9 to 15 closures, the median values shift between 9 (K17 - RCP8.5) and 24 years (KNMI'14 - G) and for 15 to 30 closures, the figures suggest an increase of 10 (K17 - RCP8.5 and LB17 - RCP8.5) to 34 years (KNMI'14 - G). These changes suggest that more tolerant requirements regarding the number of closures could extend the remaining life of the storm surge barrier substantially. The

most stringent requirement, 9 closures a year, was roughly based on the current number of closures (storm closures and test closures combined). Adopting this criterion implies that the navigation function would be governing for the remaining life of the barrier, assuming that the assessment level NAP +3.04 m is used for the flood protection function. If the requirement is changed to 30 closures a year, the 5th percentiles of the end of life estimates near the end of the design life (2058) and the median values are all well beyond this year.

Unavailability

The probability ranges for the end of life of the Hollandsche IJssel barrier in terms of unavailability (max. 175.2 hours per year) are depicted in Figure 5.13 and Figure 5.14. These figures show that the end of life is reached later in time compared with the estimates determined by the acceptable number of closures. The earliest year in which the end of life is reached, regardless of the scenario or critical level, is 2052 (5th percentile for the H scenario of Bamber et al. (2019)), which is 6 years before the end of the design life of the barrier. This result is not surprising as Figure 4.11 in Section 4.4.2 already indicated that the amounts of sea level rise corresponding to the requirements are substantially higher than the amounts for the other indicators.

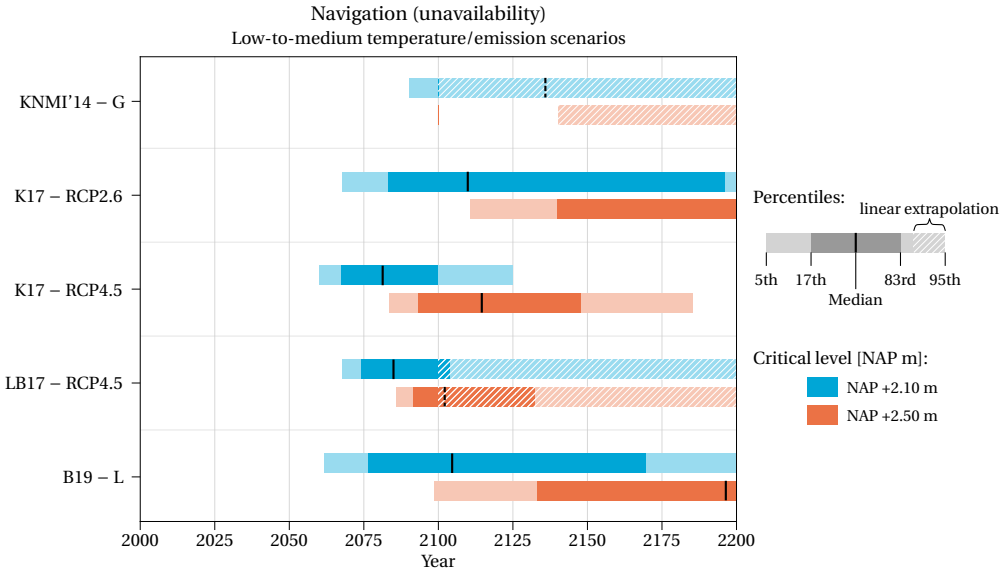

Figure 5.13: Estimates of the end of life of the Hollandsche IJssel barrier with respect to navigation (unavailability) for the low-to-medium temperature/emission scenarios. White hatched areas imply linear extrapolation of the sea level rise projections.

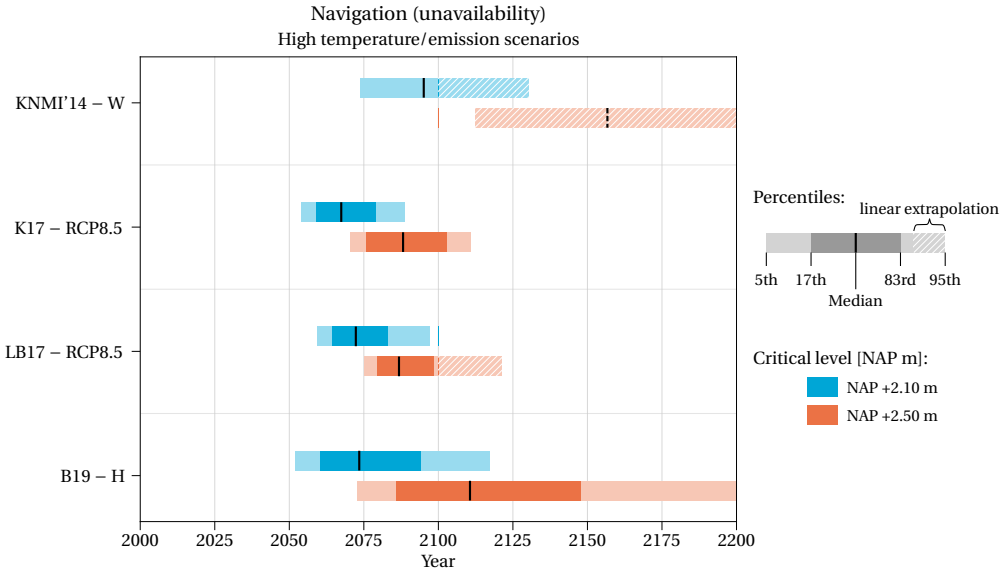

Figure 5.14: Estimates of the end of life of the Hollandsche IJssel barrier with respect to navigation (unavailability) for the high temperature/emission scenarios. White hatched areas imply linear extrapolation of the sea level rise projections.

Lastly, it can be concluded that the total average yearly duration of closures, i.e. unavailability, is not governing for the remaining life of the Hollandsche IJssel barrier. For all of the considered scenarios/projections and both critical water levels, the 5th percentiles of the end of life estimates suggest either a slightly shorter remaining life (K17 - RCP8.5 and B19 - H) or considerably longer remaining life than the design life of the storm surge barrier.

5.4 Estimates of the remaining life for one scenario of sea level rise

The use of several sea level rise projections in combination with multiple requirements for each of the functions of the storm surge barrier may complicate the interpretation of the implications for the remaining life of the Hollandsche IJssel barrier. This section therefore presents the estimates of the remaining life for a single scenario of sea level rise. The sea level rise scenario for which the estimates are presented is the W scenario of the KNMI'14 climate change scenarios. This scenario was chosen as it is one of the scenarios that is used within the Dutch Delta Programme and because the projected sea level rise under this scenario falls in between the low-end and high-end projections. The results for the functions flood protection and navigation are shown in Figure 5.15 and Figure 5.16, respectively.

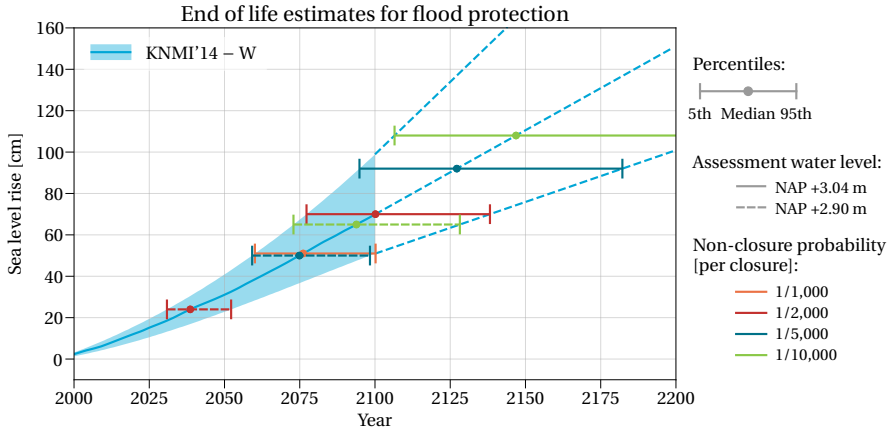

Figure 5.15: Estimates of the end of life of the Hollandsche IJssel barrier with respect to flood protection for scenario W of KNMI'14.

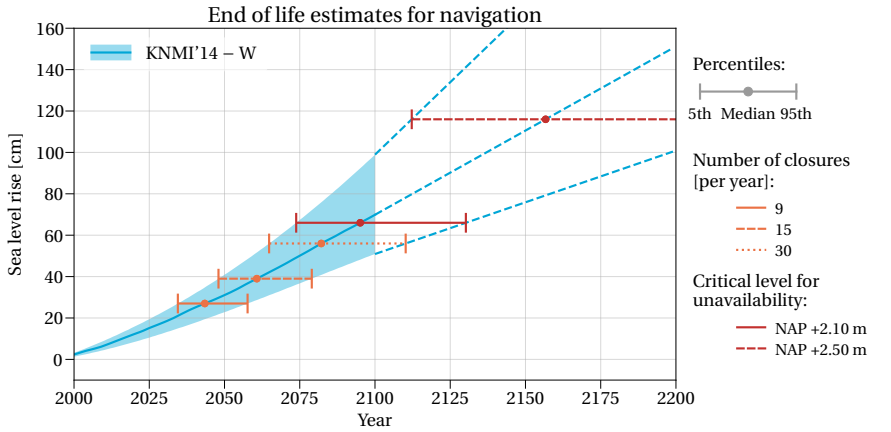

Figure 5.16: Estimates of the end of life of the Hollandsche IJssel barrier with respect to navigation for scenario W of KNMI'14.

The figures confirm what was already stated in the previous section: the navigation function (the number of closures) is the most critical aspect except when the least stringent assessment level NAP +3.04 m is adopted for the flood protection function. Based on the median values, the end of the functional life could be reached in 2043 if nine closures per year is the maximum acceptable number of closures. If the assessment level is set to NAP +2.90 m, 2038 is the earliest moment the storm surge barrier reaches the end of its functional life. However, the figures also clearly illustrate that reducing the non-closure probability (flood protection) or accepting more closures a year (navigation) may be effective measures to extend the lifespan. Extensions

in the order of 10 to 20 years are no exception. As a final remark concerning the navigation function, Figure 5.16 shows that unavailability, i.e. the total yearly duration of closures, will likely not be governing for the functional life of the Hollandsche IJssel barrier; either the performance with respect to flood protection or the number of closures will become inadmissible before the total duration of the closures becomes problematic.

5.5 Conclusions

This chapter has shown how sea level rise projections can be used to estimate the end of life or remaining life of the Hollandsche IJssel barrier. Several sea level rise studies have been discussed to illustrate the deep uncertainty in the projections and characterise the impact on the end of life estimates of the storm surge barrier. The tables in Chapter 4 that link sea level rise to the functional performances of the Hollandsche IJssel barrier were combined with the sea level rise projections to produce estimates of the end of life for each of the considered functions.

The results indicate that, irrespective of the function, the end of life estimates are characterised by wide uncertainty ranges. In particular, the percentiles of the estimates for the low-to-medium temperature scenarios are spread out. A difference of more than 200 years between the 5th and 95th percentile is not uncommon for the low-to-medium scenarios. The 5th percentiles and median values, on the other hand, usually lie 20 to 40 years apart. The large spread in the values is caused by the large uncertainty in the sea level rise projections, but also by the differences between all the projections, which demonstrates the deep uncertainty in the end of life estimates. In some cases, the results imply that the end of the functional life has already been reached. This outcome is the result of a relatively low critical amount of sea level rise in combination with the large variability in the projections. This issue is thus related to the sea level rise projections themselves and arises when the extreme percentiles of some of these projections are considered.

As expected from the critical amounts of sea level rise that were determined in Chapter 4, the flood protection function and the number of closures lead to the shortest remaining life. Based on the median values, the end of life with respect to flood protection (assessment level NAP +2.90 m) could be reached within 20 years. Similar values were found for the end of life in terms of the number of closures. Interestingly, extreme scenarios of sea level rise are not even a prerequisite for a shorter than anticipated lifespan. The low-to-medium scenarios also feature remaining life estimates of 20-25 years (median values) for the assessment level NAP +2.90 m and the number of closures. Unavailability of the waterway, on the other hand, is less of a concern. The lowest median value for the year in which the performance is insufficient, was found to be 2067, about seven years later than the largest median value for the other navigation indicator, the number of closures.

Despite the large uncertainty in the estimates, the results suggest that there are options to extend the remaining life. Three relevant steering variables that influence the remaining life estimates can be discerned. These are the assessment level, the non-closure probability, and the acceptable number of closures. The preference for one of the two assessment levels has a significant impact on the end of life estimates. This impact can best be illustrated by comparing the non-closure probability that is required to make sure that the Hollandsche IJssel barrier does not need to be replaced before the end of its design life (2058). For an assessment level of NAP +3.04 m, the end of the design life could be reached if the non-closure probability is reduced to 1/2,000 per closure, whereas a reduction to 1/10,000 or more would be required for the assessment level NAP +2.90 m. The second parameter, the non-closure probability, could also be modified to prolong the remaining life of the barrier. For example, a reduction of the non-closure probability from 1/2,000 to 1/5,000 per closure leads to an extension of the remaining life of eight to 40 years (median values) for the assessment level NAP +3.04 m. For the assessment level NAP +2.90 m, the same reduction results in an extension of 20 to 40 years. The third parameter, the acceptable number of closures, is governing when it comes to the functional performance for navigation. Increasing the acceptable closure frequency from nine to 15 or even 30 closures a year could result in an extension of the remaining life of dozens of years. For reference, the design life of 100 years (1958-2058) may be attained for every considered sea level rise projection if 30 closures a year becomes acceptable.

In summary, there is a significant probability that even for moderate sea level rise scenarios, the end of life of the Hollandsche IJssel barrier could be reached within 20 years. The estimates of the remaining life of barrier are, however, uncertain, and a considerably longer lifespan cannot be ruled out. Moreover, the results in this chapter indicate that the remaining life could be extended substantially by deciding on the assessment level, reducing the non-closure probability of the barrier, and by accepting more frequent closures. These results are put in a broader context in the next chapter. Limitations of this study are discussed in the same chapter.

6

Discussion

This chapter begins with a reflection on the methodology of this study. The assumptions and limitations of the methodology are discussed. Then the current research is placed in a broader context by reviewing the applicability of the approach to other storm surge barriers and describing the implications for the replacement strategies of the Delta Programme.

6.1 Methodology (assumptions and limitations)

This study has shown that it is worthwhile to start with identifying external drivers or factors and assess the influence of those factors on the functional performance or technical state of the storm surge barrier before attempting to develop a model to estimate the remaining life of a structure. This approach enables one to discern the most important drivers and disregard other less important ones. For instance, sea level rise stood out as the main driver affecting the remaining life in this study. This finding meant that the quantification of the remaining life became considerably easier as the interaction between or combination of multiple uncertain factors, e.g. sea level rise and increasing river discharges, could be neglected. Still, the method is subject to several limitations as elements or aspects were excluded from the research and assumptions were made throughout this study. These assumptions and limitations are addressed in this section.

6.1.1 Assumptions

External drivers

The following remarks could be made regarding the evaluation of the external drivers:

- Climate change scenarios

  The KNMI'14 climate change scenarios were used as a starting point for the evaluation of most of the physical drivers. These scenarios do not cover the entire range of possible futures but only consider the RCP4.5 and RCP8.5 scenarios. Including the low emission scenario (RCP2.6) would increase the uncertainty in the climate variables. However, the exclusion of RCP2.6 will likely have little consequences for the evaluation of the external drivers as the projected changes will be smaller. Furthermore, the semi-quantitative analysis of Chapter 3 showed that even for the most extreme scenario (RCP8.5), the effects of climate variables other than sea level rise are limited. Another climate change related development that could affect the evaluation of the external drivers is the release of a new version of the climate change scenarios. The new scenarios, called KNMI'23, will be published in the coming years. Changes in these new scenarios could lead to a shift in the importance of certain variables. Significant changes in the variables would imply that the effects have to be re-evaluated. Nevertheless, sea level rise is expected to remain the dominant driver due to the relatively small tolerance of the storm surge barrier towards sea level rise.
- Socio-economic developments

  The assessment of the likelihood of changes in the flood protection standards of the dikes along the Hollandsche IJssel was based on the national economic growth projections. Developments on a regional scale, such as strong population growth in the areas protected by the dikes, could result in deviations from the nationwide figures. Moreover, it was assumed that the ratio between economic damage and

societal damage remains constant. Strong population growth in the area could lead to a different criterion becoming governing or even result in higher flood protection standards. However, the approach described in this study could still be used for higher flood protection standards since a rough indication of the consequences of higher standards could be obtained by adjusting the assessment water level.

Quantification of the remaining life

The applied methods to estimate the end of life or remaining life of the Hollandsche IJssel barrier also include several assumptions and simplifications that should be addressed. An overview of these points is given below.

- Assessment of the flood protection function

  The evaluation of the flood protection function is solely based on the exceedance of a critical level. This is quite a rough approximation because the actual performance requirements should ideally follow from the failure probabilities of the dikes in the hinterland. These failure probabilities are estimated by examining failure mechanisms such as overtopping and piping. An alternative approach could be the use of fragility curves corresponding to the failure mechanisms, see for example the study by De Bruijn et al. (2014). These fragility curves can be used to express the failure probability for a specific failure mechanism as a function of the water level. This way, the sea level rise can be translated into an increase in the failure probabilities. The disadvantage of this method is that it first requires a detailed analysis of the dikes to derive the fragility curves.

- Adjustment of the closure level

  A remark related to the previous simplification is that the option to lower the closure water level was not considered in the assessment of the functional end of life. Closing the barrier at a lower water level leads to a decrease in the water levels behind the storm surge barrier after closure and reduces the impact of sea level rise. The effect, however, is limited. The water level statistics behind the barrier are dominated by the open situation (failed storm surge barrier), for which the closure level is of little significance. If one seeks to minimise the water damage to areas outside the dikes, the option is relevant.

- Static relationship between shipping intensity and hindrance

  The hindrance to shipping was based on two criteria: the number of closures and unavailability. Both criteria were considered independent of the shipping intensity on the Hollandsche IJssel, whereas it could be possible that if the barrier closes too often, the Hollandsche IJssel becomes less attractive for inland waterway transport. This loss of value could, in turn, lead to less stringent requirements in terms of the number of closures or unavailability. Whether such a scenario is realistic is difficult to assess. It will depend on future developments in the navigation sector and requires a cost-benefit analysis on a network scale.

- Interaction between road traffic and navigation

  On a similar note, the complex interaction between road traffic and shipping was not studied in detail. It may be relevant to investigate how a change in the number of closures causes hindrance to road traffic. As the lock next to the storm surge barrier could be used up to a water level of NAP +2.50 m, the probability of situations in which the storm surge barrier is closed and the lock is still available could increase if the number of closures increases. The result is then more frequent openings of the Algera bridge. This interaction was not examined in this study since, based on the operating hours of the bridge, it was assumed that road traffic is given priority. This assumption is justifiable given the fact that the Algera Bridge is the only direct connection between the Krimpenerwaard and Rotterdam.

- Hydra-NL

  The probabilistic model Hydra-NL plays an important role in this research. There are, however, several assumptions that are either included in this model or that were made while using the model:

  - The Hollandsche IJssel barrier is modelled as a weir with an infinite height, which means that overtopping/overflow is not included in the calculation of the water levels behind the Hollandsche IJssel barrier. Sustained periods of overtopping/overflow could raise the water levels behind the barrier. This assumption is less relevant for the Hollandsche IJssel barrier since the calculated overtopping quantities suggested that the increase in the water levels due to overtopping is negligible compared to the discharge of the pumping stations, but, if a similar study is performed for another storm surge barrier, one should check whether overtopping is also neglected and whether the increase in the water levels due to overtopping could be significant.

- Sea level rise is modelled as an additional storm surge under daily conditions instead of a rise in all water levels. This approach means that the results of Hydra-NL become less accurate as more extreme sea level rise scenarios are considered. Currently, there are no alternatives to Hydra-NL to calculate the effects of sea level rise on the local water level statistics. The introduced error therefore has to be accepted until alternative models have been developed.
- Model uncertainty was not included in any of the calculations of the water levels behind the Hollandsche IJssel barrier because uncertainty parameters related to the state (open or closed) of the Hollandsche IJssel barrier have not yet been established (Rongen & Maaskant, 2019). The consequences of neglecting the model uncertainty for the flood protection results are limited because both the occurring water levels and the assessment water levels are determined using Hydra-NL. Adding model uncertainty would increase both these water levels. Of course, the increase in the assessment level is not unbounded. An assessment water level higher than the height of the dikes can impossibly be used to assess the flood protection function. The impact on the results for the water management function, on the other hand, may be significant because of the small margin between the closure water level and the "maalstoppeil". The impact of including model uncertainty can be illustrated by calculating the frequency of a “maalstop” using two different values for the model uncertainty in the water levels. From the results in Table 6.1, it can be seen that the frequency of a “maalstop” under the current climate and a standard deviation of 20 cm is already higher than the frequency after 75 cm sea level rise (W2100) and without model uncertainty. If the standard deviation is 10 cm, the scenario in which the critical frequency (once every 200 years) is exceeded is the same as for the calculations without model uncertainty. These calculations clearly demonstrate the need for accurate estimates of the model uncertainty parameters. Correct values for the model uncertainty are not only needed to improve the results of this study but also for future studies in which the flood protection assessment is not merely based on critical water levels, e.g. safety assessments of the dike trajectories.

Table 6.1: Return period of the "maalstoppeil" for three values of the standard deviation in the water levels.

Scenario	Return period [years]		
	0 cm	10 cm	20 cm
Current climate, $P_{Q_{pump}} = 1/3$	17 921	6012	196
Current climate, $P_{Q_{pump}} = 1$	5914	1984	65
W2050, $P_{Q_{pump}} = 1/3$	2211	1089	102
W2050, $P_{Q_{pump}} = 1$	730	359	34
W2100, $P_{Q_{pump}} = 1/3$	455	214	13
W2100, $P_{Q_{pump}} = 1$	150	71	4

6.1.2 Limitations

Storm surge barrier is part of a larger system

The study focuses on the asset or object itself, while the structure is actually part of a larger interrelated and interacting system. Modification to other objects within that system could affect the remaining life of the Hollandsche IJssel barrier. Two examples of relevant objects are:

- Dikes behind the storm surge barrier

  The remaining life with respect to flood protection will be affected if the dikes behind the storm surge barrier are raised. According to the safety assessments, the dikes are susceptible to slope instability and insufficient in height over large stretches. Hence, dike reinforcement programmes have been carried out or have been proposed (Hoogheemraadschap van Schieland en de Krimpenerwaard, 2018; HWBP, 2018). It would be relevant to include dike reinforcements in the assessment of the remaining life of the storm surge barrier. However, the decision to raise the dikes will not be made in isolation as there is a trade-off between the costs of decreasing the non-closure probability of the storm surge barrier and the costs of heightening the dikes. Incorporating the possibility to raise the dikes would require a cost-benefit analysis that is beyond the scope of this study. A second reason to exclude this factor is that raising the dikes is purely a measure to extend the lifespan of the barrier, whereas this study focuses on estimating the remaining life of the barrier. Options to prolong the remaining life are only examined

briefly, for example, by presenting end of life estimates for various non-closure probabilities. The full range of measures or strategies to extend the remaining life could be explored in future research.

- Maeslant barrier

As the Hollandsche IJssel barrier is located more inland, other hydraulic structures may influence the water levels at the barrier, and thereby the functional performance of the storm surge barrier. The Maeslant barrier is the most apparent structure affecting these water levels. The Maeslant barrier has little effect on the navigation function of the Hollandsche IJssel barrier since the Hollandsche IJssel barrier closes earlier, but the flood protection function may be affected.

The analysis of the external drivers in Chapter 3 concluded that changes in river discharges have a limited effect on the water levels at the Hollandsche IJssel barrier for the current non-closure probability of the Maeslant barrier. If this probability is reduced, this conclusion will no longer apply since the relative influence of river discharge increases. Yet, the overall extreme water levels will decrease due to the higher closure reliability of the Maeslant barrier, as can be seen in Figure 6.1. This decrease implies that the already irrelevant failure mechanisms overtopping, piping, and structural failure remain negligible in terms of the effect on the remaining life of the storm surge barrier. Figure 6.1 also shows that the reduction of the non-closure probability of the Maeslant barrier hardly affects the water levels with a return period shorter than 1,000 years. This observation suggests that improvements to the Maeslant barrier also have little effect on the water levels behind the Hollandsche IJssel barrier. Calculations of the water level statistics behind the Hollandsche IJssel barrier indicate that the water levels are indeed only affected to a limited extent by the reduced non-closure probability (see Figure 6.2).

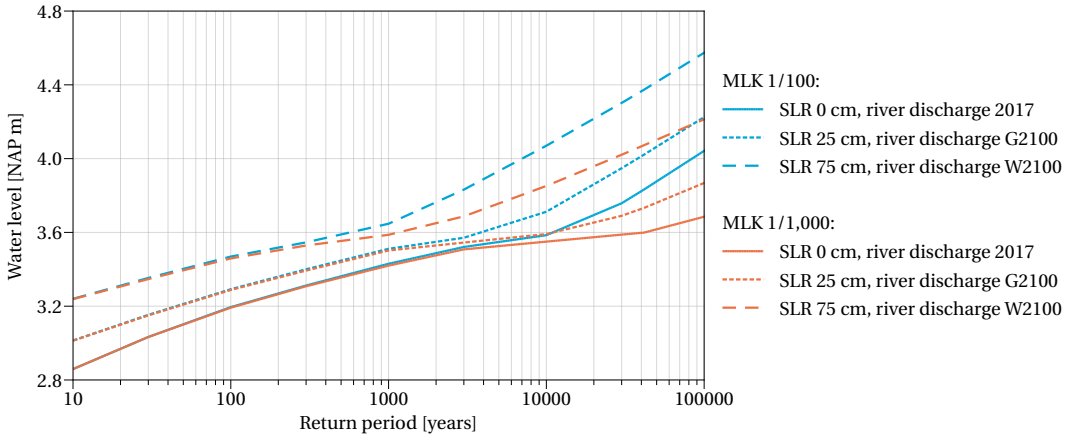

Figure 6.1: Comparison of the water level statistics in front of the Hollandsche IJssel barrier for two non-closure probabilities [per closure] of the Maeslant barrier (MLK). Default parameters for the Hollandsche IJssel barrier were used (non-closure probability of 1/200 per closure).

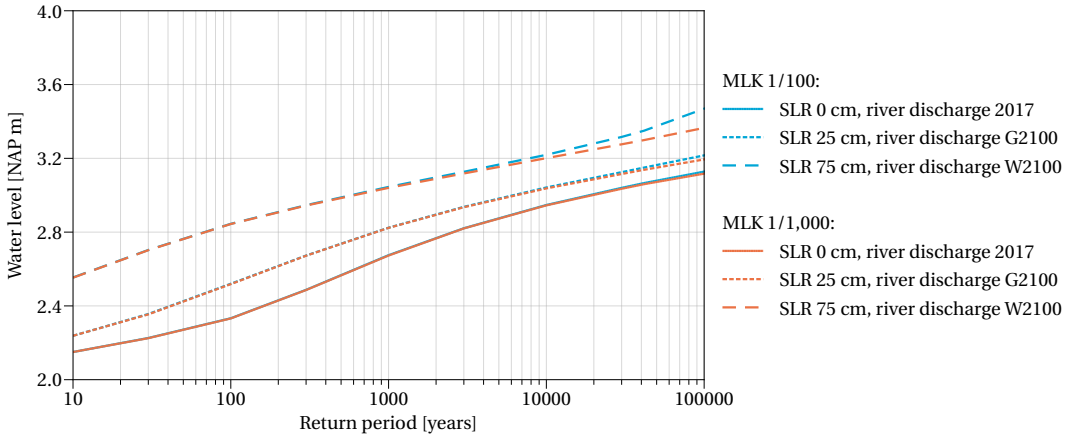

Figure 6.2: Comparison of the water level statistics behind the Hollandsche IJssel barrier for two non-closure probabilities [per closure] of the Maeslant barrier (MLK). Note that these statistics do not include model uncertainty, as was the case for any other calculation of the water levels behind the Hollandsche IJssel barrier. Default parameters for the Hollandsche IJssel barrier were used (non-closure probability of 1/200 per closure).

Apart from improvements to the Maeslant barrier, early replacement by another type of structure is also a possibility. Consider, for example, the *Plan Sluizen* which proposes to replace the Maeslant barrier by a navigation lock (Van Waveren et al., 2015). It is difficult, if not impossible, to predict if or when this option will be considered without carrying out a similar study for the Maeslant barrier. Hence, replacement of the Maeslant barrier was not considered in this study. Besides, replacement of the Maeslant barrier will be beneficial for the lifespan of the Hollandsche IJssel barrier. After replacement by a navigation lock, the effects of sea level rise or storm surges will hardly be observed in the Hollandsche IJssel and high water levels are mostly the result of extreme river discharges.

Other less prominent objects or assets include the numerous pumping stations along the Hollandsche IJssel and the upstream navigation locks (Juliana lock complex). Modifications to these assets could also indirectly affect the performance of the storm surge barrier. Entirely new structures or plans, such as Delta21, may also play a role. The actively discussed Delta21 plan proposes to construct an energy storage lake and tidal basin at the mouth of the Haringvliet (Berke & Lavooij, 2019). The plan improves the current flood protection system by pumping water from the Haringvliet into the storage lake. This discharge of water from the Haringvliet into the new lake leads to a reduction in the hydraulic loads across the entire Rhine-Meuse delta (Oerlemans, 2020). Strategies to improve the freshwater supply or cope with droughts and salt intrusion may also affect the Hollandsche IJssel barrier since the structure is located in an area where drought and salt intrusion are matters of concern. The interrelations of all these assets or strategies argues in favour of a system approach.

Economic considerations

This study defines economic life as the time period over which the costs of owning and operating an asset are still less than the costs of equivalent alternatives. This definition resulted in the exclusion of the economic life in the remainder of the research as replacement of infrastructure assets of this size will almost always be significantly more expensive than carrying out maintenance. As a consequence, the decision to focus on the technical and functional life is reasonable, but it does not mean that economic considerations do not play a role. The impact on the performance with respect to the navigation function, for example, could be expressed as costs to the shipping sector. Another example is improvements to the storm surge barrier. This study suggested that the remaining life of the storm surge barrier can be extended considerably by reducing the non-closure probability. The costs of such improvements to the barrier could be weighed against the expected benefits for flood protection to decide to what degree such measures should be taken. These examples show that such assessments could help determine what degree of hindrance to shipping should be accepted or to what extent measures to improve the storm surge barrier are economically feasible. However, such a cost-benefit analysis requires a broader definition of economic life and involves a study of the system as a whole since the incurred costs and compensating benefits apply to the system and not just individual assets such as the storm surge barrier. In that respect, this limitation is closely related to the previous one.

6.2 Applicability and implications

Although the scope of this research was limited to the Hollandsche IJssel barrier due to the complexity and uniqueness of the storm surge barriers, knowledge about the remaining life is of importance for all storm surge barriers (and hydraulic structures in general). Therefore, the applicability of the presented approach to other storm surge barriers is reviewed in this section. Subsequently, the results are discussed in light of the broader challenge of future-proofing the Dutch infrastructure.

6.2.1 Applicability of the method to other storm surge barriers

The first steps, or the first phase, of the research includes the identification of the functions and structural components of an asset (Chapter 2), and the evaluation of the impact of external drivers (Chapter 3). These steps provide a structured approach to map the effects of external drivers, such as climate change, on infrastructure assets. The analysis of the functions and decomposition into different components enables one to assess the impact of the drivers in a systematic manner while seeking to minimise the possibility of overlooking aspects. As these are general steps, they are applicable to any type of hydraulic structure, including other storm surge barriers. The results of the assessment of the external drivers will, of course, be different because of the local characteristics of each infrastructure asset.

The second phase of the research, the quantification of the remaining life, is more difficult to implement directly into the assessment of other storm surge barriers since the applied methods follow from the results

of the first phase. In this study, for example, the approaches to quantify the performance only focused on the functional life of the barrier because the technical life, as defined in Section 1.2, could be disregarded. For other storm surge barriers, however, the technical life could be governing. In addition, sea level rise was the only considered external driver as it appeared to be the most important driver. Different drivers may be important for other storm surge barriers, though it is expected that sea level rise will also affect these barriers as most of the storm surge barriers are located closer to the coast; the area that experiences the effects of sea level rise directly. In case sea level rise is the most important driver, the adopted approaches for evaluating the flood protection and navigation functions may still be suitable. The analysis of the flood protection function is based on the WBI2017 guidelines, which apply to hydraulic structures in general. Huijsman (2021), for instance, analysed the influence of sea level rise on the lifespan of sea locks in terms of flood protection in a similar way and by using these guidelines. Another example is the study by Von Meijenfeldt et al. (2017) in which the WBI2017 guidelines were applied to identify sea level rise induced tipping points for the current flood protection system of the Eastern Scheldt. The assessment of the functional performance with respect to navigation only uses the measured water levels. So the described approach could be adopted for other storm surge barriers provided that a sufficiently long time series of water level measurements at the storm surge barrier is available. Since only methods related to these two functions were described, new methods should be explored to be able to quantify the remaining life for other functions.

6.2.2 Implications for the replacement strategies of the Delta Programme

This study was carried out in the context of the replacement and renovation programme of Rijkswaterstaat (Klatter et al., 2019). But since the results show that sea level rise is the most important factor, there is also a link with the Sea Level Rise Knowledge Programme, which is a joint research programme of the Ministry of Infrastructure and Water Management, the Delta Commissioner, the KNMI, Rijkswaterstaat, the water authorities, and several research institutes (Ministerie van Infrastructuur en Waterstaat, 2019). This knowledge programme is strongly linked to the Delta Programme. The programme aims to gain better insight into sea level rise and the associated uncertainties, assess the impact of a rising sea level on flood risk management (coastal zone, flood defence structures) and freshwater supply in the Netherlands, and explore long-term strategies to ensure the Netherlands is well-prepared to cope with the consequences of sea level rise. The programme consists of five tracks, which focus on the influence of Antarctica on sea level rise (track 1), resilience of current strategies and decisions developed for the Delta Programme (track 2), development of methods to monitor sea level rise and detect signals of accelerated sea level rise (track 3), exploration of long-term solutions or strategies for climate change adaptation (track 4), and implementation strategies (track 5).

The results of the current research are particularly relevant to track 2 of the knowledge programme. The current Preferential Strategy for the Rhine Estuary-Drechtsteden region states that replacement of the Hollandsche IJssel barrier is expected to take place between 2050 and 2100 (DRPD, 2020). However, the results of this study suggest that, without improvements to the storm surge barrier, earlier replacement cannot be ruled out. Even for relatively moderate sea level rise scenarios, the performance with respect to flood protection could become insufficient within 20 years (median value). A plan to reduce the non-closure probability of the storm surge barrier from 1/200 to 1/1,000 by 2030 is included in the Preferential Strategy, but more serious reductions may be required to pursue the current strategy. Non-closure probabilities in the order of 1/2,000 or even 1/10,000 per closure may be needed according to this study. The required reduction of the probability of non-closure depends on the conservatism in the evaluation, but it is also affects the required amount of dike reinforcements. Reinforcing the dikes could also be a measure to improve the flood protection levels but this option is generally more costly than reducing the probability of non-closure of the storm surge barrier. An equally relevant aspect that could lead to a shorter lifespan is the functional performance with respect to navigation. Without accepting more hindrance to shipping or raising the closure level of the barrier alternative solutions have to be explored sooner than expected as replacement would also be required within 20 years (median value). Raising the closure level may be considered the most appealing measure as the hindrance to shipping is reduced, but one should realise that a higher closure level increases the risk of flooding of the outer dike areas and the probability of a "maalstop". These issues illustrate the conflicting demands for flood protection and navigation. From the perspective of flood protection, an ideal situation would perhaps be to close off the river during the storm season, whereas it would be in the interest of the navigation sector to keep the barrier open as much as possible. These interests have to be weighed against each other to determine the best measures. Eventually, there comes a moment that the suggested measures to extend the lifespan of the current structure are no longer sufficient and alternatives have to be investigated.

The conclusion that alternatives to the current storm surge barrier may be required sooner than expected is also input to track 4 of the Sea Level Rise Knowledge Programme. The solutions that are being investigated as part of knowledge programme can broadly be categorised into four concepts: (Haasnoot et al., 2019):

- Protect-closed: coastline is protected by a closed system of flood defences, river water is discharged using pumping stations.
- Protect-open: coastline is protected by a system of flood defences, but rivers remain in open connection with the sea. This strategy builds on the current practice.
- Advance: reclamation of new land in sea that serves as a protection for the current coastline.
- Accommodate: elevation of certain parts of the country, building of floating houses, and retreat from other areas. This strategy differs from the other three in the sense that it is focused on minimising the damage of flooding rather than preventing it.

None of the four strategies is currently preferred and given the great uncertainty and costs involved in making the Netherlands climate-proof, it is important to keep open as many options as possible. High-regret decisions should therefore be avoided. This may, however, be a major challenge considering the results of this study. Tipping points could occur considerably sooner in time, which means that important decisions may already have to be made within a period of a few years from now, while the uncertainty about sea level rise and, therefore, the remaining life of structures is still large. The shorter time before tipping points are reached also suggests that the shift from one strategy to another may be required earlier than expected, which raises the question of whether it would be better to bypass certain options. For instance, options that include new closable barriers, a serious option within the concept protect-open, should be critically reviewed, especially when facilitating navigation without too much hindrance remains part of the policy.

7

Conclusions and recommendations

7.1 Conclusions

The work described in this thesis is concerned with the estimation of the remaining life of the Hollandsche IJssel barrier. More specifically, the research focused on the remaining functional and technical life of the storm surge barrier. The study set out to identify the dominant factors affecting the remaining life and to provide a method for the estimation of the remaining life of the barrier. The main conclusions of this study are translated into four key findings to remember from this study. A more elaborate discussion of the findings is provided in the form of answers to the research questions that were formulated for this study.

7.1.1 Five key insights from this study

The following key findings emerge from this research:

- **There is a significant probability that the end of life of the Hollandsche IJssel barrier could be reached within 20 years. The estimates of the remaining life of the storm surge barrier are, however, uncertain, and a considerably longer lifespan cannot be ruled out.**
  The results (median values) show that even for moderate scenarios of the sea level rise, the lifespan of the Hollandsche IJssel may end in the 2040s due to inadequate performance in terms of flood protection (assessment level NAP +2.90 m) and number of closures (nine closures a year). At the same time, a remaining life of more than 60 years is not uncommon according to the 90% probability ranges for various scenarios of sea level rise.

- **The functional life is the dominant type of lifespan for the remaining life of the Hollandsche IJssel barrier.**
  Functional aspects, such as the required flood protection levels or the number of closures, govern the remaining life of the storm surge barrier. The technical life of the storm surge barrier is not governing because virtually all dominant deterioration mechanisms lead to (increased) maintenance of components. The deterioration processes and associated maintenance activities are therefore more relevant in the context of developing maintenance strategies or appraisal of investments to improve the flood protection system.

- **Sea level rise is the dominant physical driver for the remaining life of the Hollandsche IJssel barrier.**
  A semi-quantitative analysis of the impact of physical drivers, socio-economic developments, and policy changes showed that the remaining life of the Hollandsche IJssel barrier is largely dominated by sea level rise. In part, this is because of the potentially large future changes in sea level, but also due to the widespread consequences of sea level rise (see Table 3.3 and Table 3.4).

- **There are three steering variables with a direct impact on the remaining life of the Hollandsche IJssel barrier: the assessment level, the non-closure probability, and the acceptable number of closures.**
  Although exploring options to extend the remaining life was not part of this study, the results suggest that the remaining life is influenced considerably by the choice for a specific assessment water level, the non-closure probability, and the acceptable number of closures. The current research presents end of life estimates for two assessment water levels, NAP +3.04 m and NAP +2.90 m. The assessment level

NAP +3.04 m corresponds to the 1/30,000-year water level and a non-closure probability of the Hollandsche IJssel barrier of 1/200 per closure. For the latter level, a non-closure probability of 1/1,000 per closure was adopted, i.e. the non-closure probability that is set to be achieved in 2030. The choice for one of the two assessment levels depends on the desired conservatism in the evaluation of the remaining life. However, the choice may also have practical implications since extensive reinforcement works are currently required to comply with the flood protection standards of the dike trajectories along the Hollandsche IJssel if the non-closure probability remains 1/200 per closure. Lowering the non-closure probability could be a measure to reduce the required dike reinforcements. As an indication, a reduction of the non-closure probability from 1/2,000 to 1/5,000 per closure lengthens the remaining life by eight to 40 years (median values) for the assessment level NAP +3.04 m and by 20 to 40 years for the assessment level NAP +2.90 m. Similar extensions of the lifespan with respect to the navigation function could be obtained by accepting 15 or 30 closures a year instead of nine, though this would imply more hindrance to shipping.

7.1.2 Answers to the research questions

1. What are the main functions of the Hollandsche IJssel barrier and their desired performance level?
The main functions of the Hollandsche IJssel barrier and the associated requirements can be found in Table 2.7 in Section 2.2. The function categories include:

- Flood protection: reduce extreme water levels in the hinterland.
- Navigation: facilitate navigation.
- Water management: provide storage capacity for and discharge polder water from pumping stations, supply fresh water to the polders.
- Ecology: allow tidal flow in the Hollandsche IJssel.
- Road traffic: provide a road connection between Krimpen a/d IJssel and Capelle a/d IJssel.
- Monument: provide iconic value.

Requirements suitable for the evaluation of the remaining life could not always be formulated for each of these functions, for example, due to the abstract nature of the function or because the function is not restrictive for the remaining life of the storm surge barrier. Moreover, it is important to stress that most of the drawn up performance requirements are not formal requirements. In fact, only the requirements for the flood protection function are stipulated in a law, the *Waterwet* (Slootjes & Van der Most, 2016a). The requirements for other functions were based on requirements for structures with similar functions, e.g. navigation locks, or followed from the presumption that the current situation is deemed acceptable.

2. What are the main physical components of the barrier and their mechanisms of deterioration?
A similar analysis was carried out to identify the main physical components of the storm surge barrier. Based on their technical life, these components were classified into fixed structures, movable parts, and electrical installations. For each of the components, the dominant deterioration processes and the consequences of (accelerated) deterioration were described. The results of this analysis, which forms the answer to the second research question, are summarised in Table 2.8 in Section 2.3.

A second interesting finding that followed from the analysis is that virtually all dominant deterioration mechanisms lead to (increased) maintenance. Structural deterioration is thus a matter of concern for the economic life and less important to the technical life of the barrier. For this reason, the focus should mainly be on the functional life rather than the technical life when assessing the remaining life of the Hollandsche IJssel barrier.

3. What are the major external drivers affecting the functional performance and deterioration mechanisms, and thereby the residual life of the barrier?
A semi-quantitative analysis was carried out to identify the dominant external drivers. The considered drivers were categorised into two main groups, physical drivers and societal developments. The physical drivers comprise climate change related drivers and land subsidence. Societal developments were subdivided into socio-economic developments and policy changes. Scenarios were studied to assess the future changes and potential impact on the functional performance or the technical state of the barrier. This assessment showed

that most of the physical drivers could be neglected for the estimation of the remaining life as future changes of the variable are small, the impact on the functional performance or technical state of the barrier is limited, or the consequences could be resolved relatively easily or are already accounted for. The summary of the evaluation of the drivers in Table 3.3 and Table 3.4 shows that sea level rise is the most important factor due to the potentially large future changes and extensive consequences, including an increase in the probability of extreme water levels, more hindrance to shipping, and an increase in the frequency of a “maalstop”.

The societal developments were subdivided into policy changes and socio-economic changes. Regarding policy changes, the likelihood of new flood protection standards was examined. New standards were not expected since the current standards were introduced recently, in 2017, and the dike trajectories must comply with these standards by 2050. Hence, the conclusion was drawn that policy changes do not have to be considered for the assessment of the remaining life. Changes in the flood protection standards were also studied as part of the socio-economic developments, but now the likelihood of more stringent flood protection standards as a result of economic growth was considered. This development could be disregarded as well since the damages have to increase to such a degree that the current standards can be maintained. Developments in the inland waterway transport sector were included as a second type of socio-economic development. However, these developments were not studied in detail as they mainly serve as input for the analysis of the costs associated with the hindrance to shipping, which is not part of this study. In addition, the formulated functional requirements with respect to navigation are independent of the shipping intensity.

Overall, it can be concluded that sea level rise is the most important driver to include when developing methods or models to estimate the remaining life of the Hollandsche IJssel barrier. Compared to all other drivers that were considered, the future changes in sea level rise are significant, and the consequences of sea level rise are widespread.

4. What methods can be deployed to estimate the residual life of the barrier?

Methods to relate the functional performance to the most important driver, sea level rise, were developed to estimate the remaining life of the barrier. The technical life was no longer considered since the analysis in Chapter 2 showed that the deterioration processes are mainly of importance to the economic life instead of the technical life. Methods were introduced for the three functions (or function categories) flood protection, navigation, and water management. The remaining functions (ecology, road traffic, and monument) were not included because of a lack of quantitative requirements that are necessary for the estimation.

For the flood protection function, an approach in which the occurring water levels ("prestatiepeilen") are compared with an assessment water level ("beoordelingspeil") was used. By comparing the 1/30,000-year water levels behind the storm surge barrier for various amounts of sea level rise and closure reliabilities with two assessment levels (NAP +2.90 m and NAP +3.04 m), the critical amount of sea level rise could be estimated. These 1/30,000-year water levels follow from the probabilistic model Hydra-NL and a simple relationship between the water levels in front of and behind the Hollandsche IJssel barrier (Equation (4.3)). This relationship had to be used because of the coupling between wind speed and sea level for the Hollandsche IJssel in Hydra-NL. For navigation, water level measurements at the barrier were used to derive the closure frequency and unavailability (total average duration of closures per year) of the storm surge barrier as a function of sea level rise. The performance of the water management function was evaluated by calculating the probabilities of a “maalstop” for several scenarios using Hydra-NL. However, this function was also disregarded in the further analysis of the remaining life since it turned out not to be governing.

Ultimately, relationships between the performance of two functions (flood protection and navigation) and sea level rise were established. For flood protection, critical amounts of sea level rise were determined for two assessment levels (NAP +2.90 m and NAP +3.04 m). For navigation, critical amounts of sea level rise were presented for the number of closures and unavailability of the waterway. The advantage of this approach, in which the performance is expressed in terms of sea level rise, is that the performance can be evaluated for any scenario of sea level rise. Moreover, different values for the requirements can easily be implemented by adjusting the critical amount of sea level rise.

5. What is the remaining life of the Hollandsche IJssel barrier?

By combining the tables with the required performance levels as a function of sea level rise with probabilistic projections of sea level rise, estimates of the remaining life of the Hollandsche IJssel barrier were obtained. Multiple scenarios or projections were included to account for the deep uncertainty associated with sea level rise projections. This deep uncertainty manifests itself in the divergent projections of future sea level rise; different yet all reasonable methods or assumptions result in probabilistic projections that differ considerably. This uncertainty is also reflected in the end of life estimates of the Hollandsche IJssel barrier as these

estimates are directly derived from the sea level rise projections. Although the estimates are characterised by large uncertainties, there is a significant probability that the remaining life of the Hollandsche IJssel barrier will be shorter than the design life (2058). Regardless of the sea level rise scenarios, a remaining life of less than 20 years may be expected based on the median values for the flood protection function (assessment level NAP +2.90 m) and the number of closures (nine closures a year). On the other hand, the large uncertainty in the estimates implies that the barrier could last significantly longer than the design life.

While an analysis of the options to extend the remaining life was not part of this study, three steering variables that affect the estimates of the remaining life of the barrier could be recognised from the results. First, the decision to use one of the two assessment water levels influences the end of life estimates significantly. For example, a non-closure probability of 1/2,000 per closure is required to reach the end of the design life (2058) for the assessment level NAP +3.04 m, whereas a probability of 1/10,000 per closure is required for the assessment level NAP +2.90 m. Based on these findings, using the assessment level NAP +3.04 m may seem to be more attractive. However, extensive dike reinforcements will then have to be executed to comply with the flood protection standards because this assessment level is based on a non-closure probability of 1/200 per closure for which these dike reinforcements are currently required. The second variable is the non-closure probability itself. A reduction of the non-closure probability from 1/2,000 to 1/5,000 per closure results in an extension of the remaining life of eight to 40 years and 20 to 40 years (median values) for the assessment level NAP +3.04 m and the assessment level NAP +2.90 m, respectively. The third and last variable is the acceptable number of closures. The results suggest that the functional life with respect to navigation could be extended by several years or even decades if the acceptable closure frequency changes from nine to 15 or 30 closures a year. Adjustments to the unavailability requirements, i.e. total yearly duration of closures, are not necessary since the shortest remaining life (median value) is about seven years longer than the longest remaining life (median value) for the other navigation indicator, the number of closures.

7.2 Recommendations

The current research is a step forward in the development of methods to gain more insight into the remaining life of structures. More research needs to be done on this broad and complex issue. Several ideas for potential directions for future research are described below.

Similar studies for other storm surge barriers

One of the most important recommendations is to perform a similar study for other storm surge barriers. The Maeslant barrier would probably be the most urgent storm surge barrier for which such an analysis needs to be performed. The design of this storm surge barrier accounts for a sea level rise of 0.25 m over a period of 50 years (Ministerie van Verkeer en Waterstaat & Bouwkombinatie Maeslant kering, 1989), but this value is based only on the structural capacity of the barrier; functional aspects have not yet been considered. More knowledge of the remaining life of this barrier is especially relevant as other structures in the hinterland, such as the Hartel barrier and Hollandsche IJssel barier, are directly affected by any replacement or renovation decisions for the Maeslant barrier. Moreover, not only structures are affected, the freshwater supply strategy is also impacted by such decisions. For example, investments aimed at establishing a sustainable freshwater supply may not be necessary if the Maeslant barrier is replaced by navigation locks in the near future. The far-reaching consequences of replacement of the Maeslant barrier make information about the remaining life of this storm surge barrier highly relevant.

Possible measures to extend the lifespan and best moments to intervene

The current research is primarily focused on estimating the remaining life of the Hollandsche IJssel barrier. The next step would be to look at possible measures to extend the lifespan of the storm surge barrier. This will probably require a system approach because adaptations to a certain object could impact other elements or objects within the system, as described in the discussion (Chapter 6). The study showed that the performance with respect to flood protection and navigation are the most critical. Hence, measures to improve the performance of these two functions should be investigated. Examples of measures to extend the lifespan with respect to flood protection include reducing the non-closure probability of the storm surge barrier, strengthening the dikes behind the storm surge barrier, or closing off the river during the storm season. Regarding the navigation function, one could think of raising the closure level of the barrier. However, these two functions generally have conflicting demands, which means that these demands or interests have to be weighed against each other. Therefore, information on the costs and benefits of specific measures would also be needed to determine which measures can best be taken.

Following a study of the possible measures, it would also be interesting to determine the best time for improvements to the system in order to optimise the lifespan of the storm surge barrier. Such an optimisation challenge would probably require advanced optimisation methods for which one needs to resort to the field of operations research (Van den Boomen, 2020).

Formal requirements for infrastructure assets

Most of the requirements used in this study were based on the current situation or requirements for hydraulic structures with similar functions. This is because the functional aspects of structures have traditionally been overlooked when it comes to the replacement and renovation of structures. As a result, appropriate functional or performance requirements are sometimes lacking. Examples of requirements that were assumed are the acceptable number of closures (nine per year) and the acceptable frequency of a "maalstop" (1/200 per year). It may be challenging to establish proper requirements because input from various research fields is required. For example, ecologists may have to be consulted to obtain requirements related to the ecology of a system. Nevertheless, clearly defined requirements are needed since they could enhance the usefulness of the results of the current research and studies alike.

Advanced socio-economic scenarios and development of scenarios for policy changes

The evaluation of the impact of socio-economic developments in this study relies on two discrete scenarios, the WLO scenarios Hoog and Laag. These scenarios may not cover a sufficiently wide range of alternative futures because the scenarios were intentionally developed as moderate scenarios (CPB/PBL, 2015). In addition, these scenarios look at generic regional developments and provide descriptions of future states for only two moments in time, 2030 and 2050. This way, radical changes along the pathways to these states or unpredictable developments that could occur at other moments in time and shift future pathways are overlooked. With respect to this study, these shortcomings of the scenarios are less problematic since socio-economic aspects were not dominant, and the formulated requirements were independent of socio-economic changes. However, in future studies where economic considerations play a role, e.g. evaluation of lifespan-extending measures, or the shipping intensity is relevant, tailored scenarios that account for specific regional changes and cover a broader range of potential futures would improve the evaluation of the impact of socio-economic developments.

For the policy changes, the evaluation was performed without any type of scenarios as none have been developed yet. Therefore, it is recommended to generate policy-related scenarios to deal with policy changes and to be able to address the impact of policy actions properly.

Possible extension of the probabilistic model Hydra-NL and alternative models

The probabilistic model Hydra-NL was used for a substantial part of the methods to estimate the remaining life of the Hollandsche IJssel barrier. This model may also be applied for other storm surge barriers as most of these barriers are implemented in the model. It would therefore be interesting to investigate the possibility to incorporate probabilistic sea level rise projections in the model. This would entail adding an option to specify a probability distribution of future sea level rise for a certain scenario or year when calculating the hydraulic loads. Such an extension of the model would also be useful for the design or assessment of flood defences, for which deterministic values of sea level rise are currently used.

Besides the possible extension of Hydra-NL, the development of an alternative and more suitable model should be considered if one wishes to study the effects of extreme sea level rise (in the order of metres) on the local water levels. One of the limitations of Hydra-NL is that sea level rise is modelled as an additional storm surge under daily conditions instead of a rise in all water levels. This approach introduces an error whose magnitude grows as more extreme scenarios of sea level rise are considered. In order to account for sea level rise more accurately, alternative approaches should be developed. The development of a new model could be addressed in track 2 of the Sea Level Rise Knowledge Programme.

References

Agtersloot, R., & Paarlberg, A. J. (2016). *WAQUA Productieberekeningen IJssel- Vechtdelta: Wettelijk Beoordelingsinstrumentarium 2017* (No. 1220082-001-HYE-0014). Delft, Netherlands. Retrieved from https://www.helpdeskwater.nl/onderwerpen/waterveiligheid/primaire/beoordelen/@205777/waqua-ijvd/

Alexander, M. G., Bentur, A., & Mindess, S. (2017). Chapter 4: Concrete deterioration. In *Durability of Concrete: Design and Construction* (Vol. 53). Boca Raton, FL: CRC Press.

Alonso, C., & Andrade, C. (1994). Life time of rebars in carbonated concrete. In J. M. Costa & A. D. Mercer (Eds.), *Progress in the understanding and prevention of corrosion* (Vol. 1, pp. 634–641). London, England: Institute of Materials.

Ammerlaan, D., Buchi, H., Cats, M., Jenniskens, L., Luimes, R., Ruiter, M., … Vellinga, B. (2019). *Beter Bereikbaar Gouwe: Deel B: Bereikbaarheidsscenario's* (No. BG1636). Nijmegen, Netherlands: Royal HaskoningDHV. Retrieved from https://www.beterbereikbaargouwe.nl/documenten/

Angst, U. (2011). *Chloride induced reinforcement corrosion in concrete: Concept of critical chloride content – methods and mechanisms* [PhD thesis]. Norwegian University of Science and Technology.

Angst, U. (2018). Challenges and opportunities in corrosion of steel in concrete. *Materials and Structures*, *51*(1). https://doi.org/10.1617/s11527-017-1131-6

Baart, F., Rongen, G., Hijma, M., Kooi, H., De Winter, R., & Nicolai, R. (2019). *Zeespiegelmonitor 2018: De stand van zaken rond de zeespiegelstijging langs de Nederlandse kust* (No. 11202193-000-ZKS-0004). Delft, Netherlands: Deltares.

Bakker, A. M. R., Louchard, D., & Keller, K. (2017). Sources and implications of deep uncertainties surrounding sea-level projections. *Climatic Change*, *140*, 339–347. https://doi.org/10.1007/s10584-016-1864-1

Bakker, J., Roebers, J. H., & Knoops, J. (2016). Economic End of Life Indicator (EELI). In *Proceedings of the 5th International Symposium on Life Cycle Civil Engineering (IALCCE 2016)*. Delft.

Bamber, J. L., Oppenheimer, M., Kopp, R. E., Aspinall, W. P., & Cooke, R. M. (2019). Ice sheet contributions to future sea-level rise from structured expert judgement. *Proceedings of the National Academy of Sciences of the United States of America*, *166*(23), 11195–11200. https://doi.org/10.1073/pnas.1817205116

Beersma, J., Hakvoort, H., Jilderda, R., Overeem, A., & Versteeg, R. (2019). *Neerslagstatistiek en -reeksen voor het waterbeheer 2019*. Amersfoort, Netherlands: STOWA.

Bereiter, B., Eggleston, S., Schmitt, J., Nehrbass-Ahles, C., Stocker, T. F., Fischer, H., … Chappellaz, J. (2015). Revision of the EPICA Dome C CO2 record from 800 to 600-kyr before present. *Geophysical Research Letters*, *42*(2), 542–549. https://doi.org/10.1002/2014GL061957

Berke, L., & Lavooij, H. (2019). *Update 2019: DELTA21. Een actualisering van het plan.* Retrieved from https://www.delta21.nl/het-plan/

Bertolini, L., Elsener, B., Pedeferri, P., Redaelli, E., & Polder, R. (2013). *Corrosion of Steel in Concrete: Prevention, Diagnosis, Repair* (2nd ed.). Weinheim, Germany: Wiley-VCH.

Bijl, W. (2006). *Achterlandstudie Maeslantkering: Hoofdrapport* (Tech. Rep.). Rijkswaterstaat. Retrieved from https://puc.overheid.nl/rijkswaterstaat/doc/PUC_125106_31/

Binnenvaartcijfers. (n.d.). *Aantal passages van binnenvaartschepen per sluis.* Retrieved 21-05-2021, from https://binnenvaartcijfers.nl/aantal-passages-van-binnenvaartschepen-per-sluis

Bles, T., Breedeveld, J., & Peelen, W. (2015). *Natte Kunstwerken van de Toekomst: Verlichten vervangingsopgave natte kunstwerken door monitoring.* Retrieved from https://www.nattekunstwerkenvandetoekomst.nl/upload/documents/tinymce/NKvdT-TL-VerlichtendoorMonitoring.pdf

Bosboom, J., & Stive, M. (2015). *Coastal Dynamics 1 - Lecture notes CIE4305.* Delft, Netherlands: VSSD.

Brasser, E. (2021). *Mulitwaterwerk: Standaardisatie van Sluisdeuren.* Rijkswaterstaat.

Breedeveld, J., & Kramer, N. (2019). *Kennisprogramma Natte Kunstwerken Functionele levensduur (final)* (No. 11200741-079-HYE-0001). Delft, Netherlands: Deltares.

Breysse, D. (2010). 3 - deterioration processes in reinforced concrete: an overview. In C. Maierhofer, H.-W. Reinhardt, & G. Dobmann (Eds.), *Non-destructive evaluation of reinforced concrete structures* (Vol. 1, p. 28-56). Cambridge, England: Woodhead Publishing. https://doi.org/10.1533/9781845699536.1.28

Brolsma, J. U. (2012). *Containervervoer per binnenschip: beschrijving van een transportrevolutie te water.* Delft, Netherlands: Rijkswaterstaat Dienst Verkeer en Scheepvaart.

Brolsma, J. U. (2013). *Rapportage containerhoogtemetingen.* Driebergen, Netherlands: Brolsma Advies.

Broomfield, J. P. (2007). *Corrosion of Steel in Concrete: Understanding, investigation and repair* (2nd ed.). Weinheim, Germany: Wiley-VCH.

Bruggeman, W., Haasnoot, M., Hommes, S., Te Linde, A., Van der Brugge, R., Rijken, B., ... Van den Born, G. (2011). *Deltascenario's: Verkenning van mogelijke fysieke en sociaaleconomische ontwikkelingen in de 21ste eeuw op basis van KNMI'06 en WLO-scenario's, voor gebruik in het Deltaprogramma 2011 - 2012* (No. 1205747-000-VEB-0005). Delft, Netherlands: Deltares.

Buck Consultants International, Witteveen+Bos, & Henk van Laar advies en projectbureau. (2014). *Effectberekening verbetermaatregelen rond De Gouwe.*

Chbab, H. (2015). *Basisstochasten WTI-2017: Statistiek en statistische onzekerheid* (No. 1209433-012-HYE-0007). Delft, Netherlands: Deltares.

Chbab, H., & Groeneweg, J. (2015). *Modelonzekerheid belastingen: Wettelijk Toetsinstrumentarium WTI-2017* (No. 1209433-008-HYE-0007). Delft, Netherlands: Deltares.

Clarke, L., Edmonds, J., Krey, V., Richels, R., Rose, S., & Tavoni, M. (2009). International climate policy architectures: Overview of the EMF 22 International Scenarios. *Energy Economics, 31*(SUPPL. 2), S64–S81. https://doi.org/10.1016/j.eneco.2009.10.013

CLO. (2020a). *Neerslagextremen in Nederland, 1910-2019.* Klimaatverandering. Compendium voor de Leefomgeving. Retrieved 28-05-2020, from https://www.clo.nl/indicatoren/nl0590-neerslag-extremen

CLO. (2020b). *Temperatuurextremen in Nederland, 1907-2019.* Klimaatverandering. Compendium voor de Leefomgeving. Retrieved 28-05-2020, from https://www.clo.nl/indicatoren/nl0589-temperatuur-extremen

Coles, S. (2001). *An Introduction to Statistical Modeling of Extreme Values.* London, England: Springer.

CPB/PBL. (2015). *Nederland in 2030 en 2050: twee referentiescenario's.* The Hague, Netherlands: Planbureau voor de Leefomgeving/Centraal Planbureau.

Daniel, R., & Paulus, T. (2019). *Lock Gates and Other Closures in Hydraulic Projects.* Oxford, England: Butterworth-Heinemann. https://doi.org/10.1016/C2015-0-05399-0

De Bruijn, K. M., Diermanse, F. L. M., & Beckers, J. V. L. (2014). An advanced method for flood risk analysis in river deltas, applied to societal flood fatality risk in the Netherlands. *Natural Hazards and Earth System Sciences, 14*(10), 2767–2781. https://doi.org/10.5194/nhess-14-2767-2014

De Deugd, H. (2007). *Waterloopkundige berekeningen TMR2006 Benedenrivierengebied.* RWS RIZA rapport 2007.017. Lelystad, Netherlands.

DeConto, R. M., & Pollard, D. (2016). Contribution of Antarctica to past and future sea-level rise. *Nature, 531*(7596), 591–597. https://doi.org/10.1038/nature17145

De Goederen, S. (2014). *Een verbeterde classificering van de hoogwaterbedreigingen in de Rijn-Maasmonding* [Memo]. Rotterdam, Netherlands: Rijkswaterstaat West-Nederland Zuid.

de Graaf, F., & Steensma, R. (2019). *Netwerktoets Toervaartnetwerk "Rijn- en Veenstreek / Midden-Holland"* (No. BG3775-RHD-ZZ-XX-RP-Z-002). Amersfoort, Netherlands.

de Groot-Wallast, I., & Van Twuiver, H. (2019). *Kennisprogramma Natte Kunstwerken: Functionele levensduur: Inventarisatie relevante projecten* (No. 11200741-020-HYE-0001). Delft, Netherlands: Deltares.

de Jong, M. (2021). *Levensduurstormvloedkeringen - casestudy Hollandse IJsselkering - Interview 1* [Memo]. Delft, Netherlands: Deltares.

de Jonge, H., den Heijer, A. C., Van de Putte, H. J. M., Vijverberg, G., & Van der Voordt, D. J. M. (2018). *Vastgoedmanagement.* Delft, Netherlands: Publikatieburo Faculteit Bouwkunde TU Delft.

Deltaprogramma. (2020). *Deltaprogramma 2021. Koersvast werken aan een klimaatbestendig Nederland.* The Hague, Netherlands: Ministerie van Infrastructuur en Milieu en Ministerie van Economische zaken. Retrieved from https://www.deltaprogramma.nl/deltaprogramma/publicaties-per-deltaprogramma

Deltares, I-Storm, & Rijkswaterstaat. (2018). *Overview storm surge barriers.* Retrieved from http://www.masterpiece.dk/UploadetFiles/10852/25/ Deltares_2018_Overview_storm_surge_barriers_komprimeret.pdf

de Nijs, T. (2008). *De Delta in Wording.* Rijkswaterstaat.

de Ronde, J., Mulder, J., van Duren, L., & Ysebaert, T. (2013). *Eindadvies ANT Oosterschelde.* Delft. Retrieved from https://puc.overheid.nl/rijkswaterstaat/doc/PUC_146003_31/

DRPD. (2020). *Synthesedocument van herijking Voorkeurstrategie Deltaprogramma Rijnmond-Drechtsteden.* Deltaprogramma Rijnmond-Drechtsteden. Retrieved from https://www.deltaprogramma.nl/documenten/publicaties/2020/09/15/ dp2021-h6-synthesedocument-rijnmond-drechtsteden

Duits, M. (2019). *Hydra-NL Gebruikershandleiding versie 2.7* (No. PR4022.10). Delft, Netherlands: HKV.

Duits, M. (2020). *Hydra-NL Gebruikershandleiding versie 2.8* (No. PR4315.10). Delft, Netherlands: HKV.

Dyer, T. (2014). *Concrete Durability* (1st ed.). Boca Raton, FL: CRC Press.

Emond, D., Engels, B. W. R., & Anema, L. S. A. (2018). *Natuurverkenning Krachtige IJsseldijken Krimpenerwaard: Bureaustudie en veldonderzoek in het kader van de Wet natuurbescherming en Natuurnetwerk Nederland* (No. 17-004b). Culemborg, Netherlands.

Erkens, G., Kooi, H., & Melman, R. (2021). *Actualisatie bodemdalingsvoorspellingskaarten* (No. 11206724-002-BGS-0001). Utrecht, Netherlands.

Erkens, G., Van Der Meulen, M. J., & Middelkoop, H. (2016). Double trouble: Subsidence and CO2 respiration due to 1,000 years of Dutch coastal peatlands cultivation. *Hydrogeology Journal, 24*(3), 551–568. https://doi.org/10.1007/s10040-016-1380-4

Ferguson, H., Blokland, P., & Kuiper, H. (1970). *Rijkswaterstaat Communications - The Haringvliet Sluices.* The Hague, Netherlands: Rijkswaterstaat.

Ferry, D. J. O., & Flanagan, R. (1991). *Life cycle costing: A radical approach.* London, England: Construction Industry Research and Information Association (CIRIA).

Gaal, G. C. M. (2004). *Prediction of Deterioration of Concrete Bridges* [PhD thesis]. Delft University of Technology.

Garner, A. J., Weiss, J. L., Parris, A., Kopp, R. E., Horton, R. M., Overpeck, J. T., & Horton, B. P. (2018). Evolution of 21st Century Sea Level Rise Projections. *Earth's Future*, *6*(11), 1603–1615. https://doi.org/10.1029/2018EF000991

Gaslikova, L., Grabemann, I., & Groll, N. (2013). Changes in North Sea storm surge conditions for four transient future climate realizations. *Natural Hazards*, *66*(3), 1501–1518. https://doi.org/10.1007/s11069-012-0279-1

Gehlen, C., Von Greve-Dierfeld, S., & Osterminski, K. (2010). 4 - modelling of ageing and corrosion processes in reinforced concrete structures. In C. Maierhofer, H.-W. Reinhardt, & G. Dobmann (Eds.), *Non-destructive evaluation of reinforced concrete structures* (Vol. 1, p. 57-81). Cambridge, England: Woodhead Publishing. https://doi.org/10.1533/9781845699536.1.57

Gemeente Krimpen aan den IJssel. (n.d.). *Praktische informatie.* Retrieved 03-03-2021, from https://www.krimpenaandenijssel.nl/KRY/algeracorridor/Praktische-informatie.html

Gemeente Rotterdam, Provincie Zuid-Holland, Metropoolregio Rotterdam Den Haag, & Ministerie van Infrastructuur en Waterstaat. (2020). *Notitie Reikwijdte en Detailnivea: MIRT-verkenning Oeververbindingen regio Rotterdam.* Retrieved from https://oeververbindingen.nl/publicaties/

Glerum, A., & Vrijburcht, A. (2000). *Ontwerpen van schutsluizen.* Utrecht, Netherlands: Rijskwaterstaat Bouwdienst.

Gulikers, J. (2016). 12 - Coastal protection structures in the Netherlands. In M. G. Alexander (Ed.), *Marine Concrete Structures* (p. 321-337). Cambridge, England: Woodhead Publishing. https://doi.org/10.1016/B978-0-08-100081-6.00012-X

Haarsma, R. J., Hazeleger, W., Severijns, C., De Vries, H., Sterl, A., Bintanja, R., … Van Den Brink, H. W. (2013). More hurricanes to hit western Europe due to global warming. *Geophysical Research Letters*, *40*(9), 1783–1788. https://doi.org/10.1002/grl.50360

Haasnoot, M., Diermanse, F., Kwadijk, J., De Winter, R., & Winter, G. (2019). *Strategieën voor adaptatie aan hoge en versnelde zeespiegelstijging. Een verkenning.* (No. 11203724-004). Delft, Netherlands: Deltares. Retrieved from https://www.deltaprogramma.nl/documenten/publicaties/2019/09/30/verkenning-deltares---strategieen-voor-adaptatie-aan-hoge-en-versnelde-zeespiegelstijging

Haasnoot, M., Kwadijk, J. C., Van Alphen, J., Le Bars, D., Van Den Hurk, B., Diermanse, F., … Mens, M. (2020). Adaptation to uncertain sea-level rise; how uncertainty in Antarctic mass-loss impacts the coastal adaptation strategy of the Netherlands. *Environmental Research Letters*, *15*(3). https://doi.org/10.1088/1748-9326/ab666c

Hallegatte, S. (2009). Strategies to adapt to an uncertain climate change. *Global Environmental Change*, *19*(2), 240–247. https://doi.org/10.1016/j.gloenvcha.2008.12.003

Hegnauer, M., Kwadijk, J., & Klijn, F. (2015). *The plausibility of extreme high discharges in the river Rhine* (No. 1220042-004-ZWS-0008). Delft, Netherlands: Deltares. Retrieved from http://publications.deltares.nl/1220042_004a.pdf

Hermans, M. H. (1999). Building performance starts at hand-over: The importance of life span information. In M. A. Lacasse & D. J. Vanier (Eds.), *Durability of building materials and components 8: Service life and durability of materials and components* (pp. 1867–1873). Ottawa, Canada: NRC Research Press.

Hertogh, M. J., Bakker, J., Van der Vlist, M., & Barneveld, A. (2018). Life cycle management in upgrade and renewal of civil infrastructures. *Organization, Technology and Management in Construction: an International Journal*, *10*(1), 1735–1746. https://doi.org/10.2478/otmcj-2018-0005

Heutink, A., Van Beek, A., Van Noortwijk, J. M., Klatter, H. E., & Barendregt, A. (2004). Maintenance of Protective Paint Systems At Lowest Costs. In *27th fatipec congress* (pp. 351–364). Paris, France: Association Francaise des Techniciens des Peintures.

Hinkel, J., Church, J. A., Gregory, J. M., Lambert, E., Le Cozannet, G., Lowe, J., … van de Wal, R. (2019). Meeting User Needs for Sea Level Rise Information: A Decision Analysis Perspective. *Earth's Future, 7*(3), 320–337. https://doi.org/10.1029/2018EF001071

Hinkel, J., Jaeger, C., Nicholls, R. J., Lowe, J., Renn, O., & Peijun, S. (2015). Sea-level rise scenarios and coastal risk management. *Nature Climate Change, 5*(3), 188–190. https://doi.org/10.1038/nclimate2505

Hoek, J. (2012, Februay 28). *Scheepswerf Jooren bouwt eerste Gouwenaar.* Retrieved from https://onlinekrant.binnenvaartkrant.nl/2012-05/59382031/19

Hoek, J. (2019, May 9). *Alphenaar: elektrisch en emissieloos over Gouwe en IJssel.* Retrieved from https://binnenvaartkrant.nl/alphenaar-elektrisch-en-emissieloos-over-gouwe-en-ijssel

Hoogheemraadschap van Schieland en de Krimpenerwaard. (2018). *Verkenning Krachtige IJsseldijken Krimpenerwaard: Eindrapport Verkenning* (No. D2018-09-001736). Rotterdam, Netherlands.

Hoogheemraadschap van Schieland en de Krimpenerwaard. (2019). *Toelichting peilbesluit polder Capelle aan den IJssel.* Rotterdam, Netherlands. Retrieved from https://www.schielandendekrimpenerwaard.nl/wat-doen-we/het-hoogheemraadschap-beheert-het-water-de-dijken-en-de-wegen-in-onze-regio/peilbesluiten-schieland-en-de-krimpenerwaard

Hoogheemraadschap van Schieland en de Krimpenerwaard. (2021). *Toelichting peilbesluiten Krimpenerwaard.* Rotterdam, Netherlands. Retrieved from https://www.schielandendekrimpenerwaard.nl/wat-doen-we/het-hoogheemraadschap-beheert-het-water-de-dijken-en-de-wegen-in-onze-regio/peilbesluiten-schieland-en-de-krimpenerwaard

Horton, B. P., Kopp, R. E., Garner, A. J., Hay, C. C., Khan, N. S., Roy, K., & Shaw, T. A. (2018). Mapping sea-level change in time, space, and probability. *Annual Review of Environment and Resources, 43*, 481–521. https://doi.org/10.1146/annurev-environ-102017-025826

Howard, T., Pardaens, A. K., Bamber, J. L., Ridley, J., Spada, G., L. Hurkmans, R. T., … Vaughan, D. (2014). Sources of 21st century regional sea-level rise along the coast of northwest Europe. *Ocean Science, 10*(3), 473–483. https://doi.org/10.5194/os-10-473-2014

Huijsman, D. (2021). *Adaptation of marine locks against sea level rise* [MSc thesis]. Delft University of Technology. Retrieved from https://repository.tudelft.nl/islandora/object/uuid%3A8861b136-c686-4085-85a7-870a96888f08

HWBP. (2018). *Projectenboek HWBP 2021.* Hoogwaterbeschermingsprogramma. Retrieved from https://www.hwbp.nl/documenten/publicaties/2018/11/01/projectenboek-2019

HydroLogic. (2016). *Slim Watermanagement Hollandsche IJssel.* Amersfoort, Netherlands.

HydroLogic. (2020). *Rijn-Maasmonding: Slim Watermanagement Redeneerlijn Watertekort.* Amersfoort, Netherlands.

IPCC. (2013). *Climate Change 2013: The Physical Science Basis. Contribution of Working Group I to the Fifth Assessment Report of the Intergovernmental Panel on Climate Change* (T. Stocker et al., Eds.). Cambridge, United Kingdom and New York, NY, USA: Cambridge University Press.

IPCC. (2014). *Climate Change 2014: Synthesis Report. Contribution of Working Groups I, II and III to the Fifth Assessment Report of the Intergovernmental Panel on Climate Change* (Core Writing Team, R. Pachauri, & L. Meyer, Eds.). Cambridge, United Kingdom and New York, NY, USA: Cambridge University Press.

IPCC. (2019). Summary for Policymakers. In H.-O. Pörtner et al. (Eds.), *Special Report on the Ocean and Cryosphere in a Changing Climate.* Cambridge, United Kingdom and New York, NY, USA: Cambridge University Press.

IPCC. (2021). *Climate Change 2021: The Physical Science Basis. Contribution of Working Group I to the Sixth Assessment Report of the Intergovernmental Panel on Climate Change* (V. Masson-Delmotte et al., Eds.). Cambridge University Press, In Press.

ISO. (2019). *Asset management - Guidance on the alignment of financial and non-financial functions in asset management.* Retrieved from https://www.iso.org/standard/72700.html (ISO/TS 55010:2019)

Jaffer, S. J., & Hansson, C. M. (2009). Chloride-induced corrosion products of steel in cracked-concrete subjected to different loading conditions. *Cement and Concrete Research*, *39*(2), 116–125. https://doi.org/10.1016/j.cemconres.2008.11.001

Jansen, P. C., Raadgever, G. T., & Van den Ouden, A. O. (2010). *Een stormvloedkering bij Gouda: Een alternatief voor dijkverbetering?* (Tech. Rep. No. T&M-1023394-AvdO/hh). De Bilt: Grontmij.

Jevrejeva, S., Frederikse, T., Kopp, R. E., Le Cozannet, G., Jackson, L. P., & van de Wal, R. S. (2019). Probabilistic Sea Level Projections at the Coast by 2100. *Surveys in Geophysics*, *40*(6), 1673–1696. https://doi.org/10.1007/s10712-019-09550-y

Jongeling, T. (2005). *Hydraulische aspecten van balgstuwen en balgkeringen.* Retrieved from https://repository.tudelft.nl/islandora/object/uuid:19ca0715-7364-4587-b9a6-aefbe2c78ecd?collection=research

Jonkman, S. N., Jorissen, R. E., Schweckendiek, T., & Van den Bos, J. P. (2018). *Flood defences Lecture notes CIE5314 3rd edition 2018.* Delft University of Technology.

Jonkman, S. N., Voortman, H. G., Klerk, W. J., & Van Vuren, S. (2018). Developments in the management of flood defences and hydraulic infrastructure in the Netherlands. *Structure and Infrastructure Engineering*, *14*(7), 895–910. https://doi.org/10.1080/15732479.2018.1441317

Kallen, M. J., Nicolai, R. P., Van der Wiel, W. D., Willems, A., Van Den Dungen, E. L., & Klatter, H. E. (2014). Functional and technical end-of-service estimates for hydraulic Structures. *Safety, Reliability and Risk Analysis: Beyond the Horizon - Proceedings of the European Safety and Reliability Conference, ESREL 2013*, 679–685. https://doi.org/10.1201/b15938-106

Keeling, C. D., Stephen, C., Piper, S. C., Bacastow, R. B., Wahlen, M., Whorf, T. P., … Meijer, H. a. (2005). Exchanges of atmospheric CO_2 and $^{13}CO_2$ with the terrestrial biosphere and oceans from 1978 to 2000. In J. R. Ehleringer, T. E. Cerling, & M. D. Dearing (Eds.), *A History of Atmospheric CO_2 and Its Effects on Plants, Animals, and Ecosystems* (pp. 83–113). New York, NY: Springer. https://doi.org/10.1007/0-387-27048-5_5

Kind, J., De Bruijn, K., Diermanse, F., Wojciechowska, K., Klijn, F., Van der Meij, R., … Sloff, K. (2019). *Invloed Hoge Scenario's voor Zeespiegelstijging voor Rijn-Maas Delta* (No. 11203724-008-BGS-0002). Delft, Netherlands: Deltares. Retrieved from https://www.deltaprogramma.nl/documenten/publicaties/2019/10/11/invloed-hoge-scenarios-voor-zeespiegelstijging-voor-rijn--maas-delta

Klatter, H. E., Roebers, H., Slager, J., & Hooimeijer, H. (2019). *Prognoserapport Vervanging en Renovatie (VenR) 2019.* The Hague, Netherlands: Rijkswaterstaat.

Klatter, H. E., & Van Noortwijk, J. M. (2003). Life-cycle cost approach to bridge management in the Netherlands. In *Proceedings 9th international bridge management conference, orlando, florida, usa, april 28-30, 2003* (pp. 179–188). Washington DC: Transportation Research Board (TRB).

Klein Tank, A., Beersma, J., Bessembinder, J., van den Hurk, B., & Lenderink, G. (2015). *KNMI'14 climate scenarios for the Netherlands.* De Bilt, Netherlands: KNMI. Retrieved from http://projects.knmi.nl/publications/showAbstract.php?id=10756

Klijn, F., Asselman, N., & Mosselman, E. (2019). Robust river systems: On assessing the sensitivity of embanked rivers to discharge uncertainties, exemplified for the netherlands' main rivers. *Journal of Flood Risk Management*, *12*(S2), e12511. https://doi.org/10.1111/jfr3.12511

Klimaateffectatlas. (n.d.). *Bodemdalingsvoorspellingskaarten.* Retrieved 10-09-2021, from https://www.klimaateffectatlas.nl/nl/bodemdalingsvoorspellings-kaarten

KNMI. (n.d.). *Extreme neerslag.* Retrieved 28-04-2021, from https://www.knmi.nl/kennis-en-datacentrum/uitleg/extreme-neerslag

Kopp, R. E., DeConto, R. M., Bader, D. A., Hay, C. C., Horton, R. M., Kulp, S., … Strauss, B. H. (2017, dec). Evolving Understanding of Antarctic Ice-Sheet Physics and Ambiguity in Probabilistic Sea-Level Projections. *Earth's Future*, *5*(12), 1217–1233. https://doi.org/10.1002/2017EF000663

Kopp, R. E., Gilmore, E. A., Little, C. M., Lorenzo-Trueba, J., Ramenzoni, V. C., & Sweet, W. V. (2019). Usable Science for Managing the Risks of Sea-Level Rise. *Earth's Future, 7*(12), 1235–1269. https://doi.org/10.1029/2018EF001145

Kraaijenbrink, P. (2010). *Toetsrapportage Waterkeringen Hollandsche IJssel - Toetsronde 3.* Delft, Netherlands: Deltares.

Kst-30300-A-55. (2006, feb 20). *Vaststelling van de begrotingsstaat van het Infrastructuurfonds voor het jaar 2006: Brief van de staatssecretaris van Verkeer en Waterstaat.* Retrieved from https://zoek.officielebekendmakingen.nl/kst-30300-A-55.html

Kst-31409-239. (2019, June 6). *Vervolg Kosten-batenanalyse brughoogtes (4 kansrijke vaarwegcorridors).* Brief van de de minister van Infrastructuur en Waterstaat. Kamerstuk 31409 nr. 239. The Hague, Netherlands. Retrieved from https://zoek.officielebekendmakingen.nl/kst-31409-239.html

Le Bars, D., De Vries, H., & Drijfhout, S. (2019). *Sea level rise and its spatial variations* (Tech. Rep. No. 372). Retrieved from http://bibliotheek.knmi.nl/knmipubTR/TR372.pdf

Le Bars, D., Drijfhout, S., & De Vries, H. (2017). A high-end sea level rise probabilistic projection including rapid Antarctic ice sheet mass loss. *Environmental Research Letters, 12*(4). https://doi.org/10.1088/1748-9326/aa6512

Lemer, A. C. (1996). Infrastructure Obsolescence and Design Service Life. *Journal of Infrastructure Systems, 2*(4), 153–161. https://doi.org/10.1061/(asce)1076-0342(1996)2:4(153)

Lempert, R. J., Popper, S. W., & Bankes, S. C. (2003). *Shaping the Next One Hundred Years: New Methods for Quantitative, Long-Term Policy Analysis* (1st ed.). Santa Monica, California: RAND Corporation. Retrieved from https://www.rand.org/pubs/monograph_reports/MR1626.html

Levermann, A., Winkelmann, R., Nowicki, S., Fastook, J. L., Frieler, K., Greve, R., … Bindschadler, R. A. (2014). Projecting Antarctic ice discharge using response functions from SeaRISE ice-sheet models. *Earth System Dynamics, 5*(2), 271–293. https://doi.org/10.5194/esd-5-271-2014

Liefveld, W., & Postma, R. (2007). *Twee rivieren: Rijn en Maas.* Rijkswaterstaat. Retrieved from https://puc.overheid.nl/rijkswaterstaat/doc/PUC_127490_31/

Louters, T., van den Berg, J. H., & Mulder, J. P. (1998). Geomorphological changes of the oosterschelde tidal system during and after the implementation of the Delta project. *Journal of Coastal Research, 14*(3), 1134–1151. Retrieved from https://journals.flvc.org/jcr/article/view/80700

Marcotte, T. D. (2001). *Characterization of chloride-induced corrosion products that form in steel-reinforced cementitious materials* [PhD thesis]. University of Waterloo.

Maronier, V. A. (2014). *Dijkversterking Oosteinde Moordrecht: Projectplan* (No. 263820). Almere, Netherlands: Antea Group.

McCafferty, E. (2010). *Introduction to Corrosion Science.* New York, NY: Springer.

Ministerie van Infrastructuur en Milieu. (2016). *Regeling veiligheid primaire waterkeringen 2017: Bijlage I Procedure.* Retrieved from https://www.helpdeskwater.nl/onderwerpen/waterveiligheid/primaire/beoordelen/@205738/regeling-veiligheid/

Ministerie van Infrastructuur en Waterstaat. (2019). *Kennisprogramma Zeespiegelstijging* [Brochure]. Retrieved from https://www.deltaprogramma.nl/deltaprogramma/documenten/publicaties/2019/09/17/brochure-kennisprogramma-zeespiegelstijging

Ministerie van Verkeer en Waterstaat, & Bouwkombinatie Maeslant kering. (1989). Geeiste prestaties en randvoorwaarden. Bijlage 1 bij overeenkomst BD 001. In *Overeenkomst bouw stormvloedkering nieuwe waterweg.*

Ministerie van Verkeer en Waterstaat, Rijkswaterstaat Midden Nederland, Hoogheemraadschap van Delfland, Hoogheemraadschap van Rijnland, Hoogheemraadschap van Schieland en de Krimpenerwaard, & Hoogheemraadschap De Stichtse Rijnlanden. (2005). *Waterakkoord Hollandsche IJssel en Lek*. Retrieved from https://www.rijnland.net/regels/waterakkoorden

Ministerie van Verkeer en Waterstaat, Rijkswaterstaat Midden Nederland, Hoogheemraadschap van Delfland, Hoogheemraadschap van Rijnland, Hoogheemraadschap van Schieland en de Krimpenerwaard, & Hoogheemraadschap De Stichtse Rijnlanden. (2006). *Draaiboek waterbeheer Hollandsche IJssel en Lek*. Rijkswaterstaat Zuid-Holland.

Ministerie van Verkeer en Waterstaat, Rijkswaterstaat Midden Nederland, Hoogheemraadschap van Delfland, Hoogheemraadschap van Rijnland, Hoogheemraadschap van Schieland en de Krimpenerwaard, & Hoogheemraadschap De Stichtse Rijnlanden. (2017). *Waterakkoord Kleinschalige Wateraanvoervoorzieningen Midden-Holland*. Retrieved from https://www.rijnland.net/regels/waterakkoorden

Mooyaart, L. F., & Jonkman, S. N. (2017). Overview and Design Considerations of Storm Surge Barriers. *Journal of Waterway, Port, Coastal, and Ocean Engineering*, *143*(4). https://doi.org/10.1061/(asce)ww.1943-5460.0000383

Mooyaart, L. F., Jonkman, S. N., De Vries, P., Van der Toorn, A., & Van Ledden, M. (2014). Storm Surge Barrier: Overview and Design Considerations. *Coastal Engineering Proceedings*, *1*(34), 45. https://doi.org/10.9753/icce.v34.structures.45

Moss, R. H., Edmonds, J. A., Hibbard, K. A., Manning, M. R., Rose, S. K., Van Vuuren, D. P., … Wilbanks, T. J. (2010). The next generation of scenarios for climate change research and assessment. *Nature*, *463*(7282), 747–756. https://doi.org/10.1038/nature08823

Nederlandse Gemalen Stichting. (n.d.). *Inventarisatie*. Retrieved 22-02-2021, from https://gemalen.nl/inventarisatie.asp

Nicolai, R. P., Dekker, R., & Van Noortwijk, J. M. (2007). A comparison of models for measurable deterioration: An application to coatings on steel structures. *Reliability Engineering and System Safety*, *92*(12), 1635–1650. https://doi.org/10.1016/j.ress.2006.09.021

Nicolai, R. P., & Klatter, H. E. (2015). Long-term budget requirements for the replacement of bridges and hydraulic structures. *Safety and Reliability of Complex Engineered Systems - Proceedings of the 25th European Safety and Reliability Conference, ESREL 2015*, 969–974. https://doi.org/10.1201/b19094-129

NOAA. (2021, April 7). *Despite pandemic shutdowns, carbon dioxide and methane surged in 2020*. NOAA Research News. Retrieved 28-05-2021, from https://research.noaa.gov/article/ArtMID/587/ArticleID/2742/Despite-pandemic-shutdowns-carbon-dioxide-and-methane-surged-in-2020

Oerlemans, C. (2020). *The missing link in adaptive delta management. Insights on the potential of pumps in reducing flood risk under sea level rise and adaptive social learning to improve decision-making in the Rhine-Meuse estuary* [MSc thesis]. Delft University of Technology. Retrieved from https://repository.tudelft.nl/islandora/object/uuid%3Aebc4c396-97f7-42ad-ba0f-72af97eebb35

Op 't Landt, M. R. (2018). *Impact of high-end sea level rise scenarios on storm surge barriers in the Netherlands* [MSc thesis]. Delft University of Technology.

PCA. (2002). *Types and Causes of Concrete Deterioration*. Skokie, IL: Portland Cement Association. Retrieved from https://www.cement.org/docs/default-source/fc_concrete_technology/durability/is536-types-and-causes-of-concrete-deterioration.pdf?sfvrsn=4&sfvrsn=4

PIANC. (2008). *Life Cycle Management of Port Structures Recommended Practice for Implementation* (No. MarCom WG103). Brussels, Belgium: Author.

PIANC. (2020). *Fatigue of Hydraulic Steel Structures* (No. InCom WG189). Brussels, Belgium.

Polder, R. B., & De Rooij, M. R. (2005). Durability of marine concrete structures - Field investigations and modelling. *Heron*, *50*(3), 133–154.

Popov, B. N. (2015). *Corrosion Engineering: Principles and Solved Problems.* Amsterdam, Netherlands: Elsevier.

Prinsen, G., Van den Boogaard, H., & Hegnauer, M. (2015). *Onzekerheidsanalyse hydraulica in GRADE* (No. 1220082-010-HYE-0001). Delft, Netherlands: Deltares. Retrieved from http://publications.deltares.nl/1220082_010.pdf

Provincie Zuid-Holland. (2018). *Kleinschalige wateraanvoervoorzieningen - route waterloop* [Dataset]. Retrieved 08-09-2021, from https://opendata.zuid-holland.nl/geonetwork/srv/dut/catalog.search#/metadata/36C4CD95-77E6-443A-B374-1E2B87A2ECB3

Revie, R. W., & Uhlig, H. H. (2008). *Corrosion and Corrosion Control: An Introduction to Corrosion Science and Engineering.* Hoboken, NJ: John Wiley & Sons.

RICS. (2016). *Life cycle costing: RICS guidance note, UK* (1st ed.). London, England: Royal Institution of Chartered Surveyors (RICS).

Rijksdienst voor Cultureel Erfgoed. (2018, September 20). *Besluit aanwijzen Rijksmonument (Monumentnummer: 532245).*

Rijksdienst voor Cultureel Erfgoed. (2020a, November 20). *Monumentnummer: 517584 Julianasluis te Gouda* [Monument registry]. Retrieved 2021-02-15, from https://monumentenregister.cultureelerfgoed.nl/monumenten/517584

Rijksdienst voor Cultureel Erfgoed. (2020b, November 20). *Monumentnummer: 517620 te Gouda* [Monument registry]. Retrieved 2021-02-15, from https://monumentenregister.cultureelerfgoed.nl/monumenten/517620

Rijkswaterstaat. (n.d.-a). *Fairway Information Services.* Retrieved 11-02-2021, from https://vaarweginformatie.nl/frp/main/

Rijkswaterstaat. (n.d.-b). *Hollandsche IJsselkering.* Retrieved 26-02-2021, from https://www.rijkswaterstaat.nl/water/waterbeheer/bescherming-tegen-het-water/waterkeringen/deltawerken/hollandsche-ijsselkering

Rijkswaterstaat. (2003). *Ontwerpnota Stormvloedkering Oosterschelde, Boek 4: De sluitingsmiddelen.* Retrieved from https://repository.tudelft.nl/islandora/object/uuid{%}3A16aa14dc-2fbe-4def-ab4d-04fc9f74f5a0

Rijkswaterstaat. (2008). *Verslag van de stormvloed van 21 maart 2008 SR(90).* Lelystad, Netherlands: Watermanagementcentrum Nederland.

Rijkswaterstaat. (2009a). *Scheepvaartinformatie Hoofdvaarwegen Editie 2009.* The Hague, Netherlands: Ministerie van Verkeer en Waterstaat.

Rijkswaterstaat. (2009b). *Systeemanalyse Rijn-Maasmonding: Analyse levensduur primaire waterkeringen bij 1/200 kans niet sluiten Maeslantkering.* Rijkswaterstaat Zuid-Holland. Retrieved from https://puc.overheid.nl/rijkswaterstaat/doc/PUC_132642_31/

Rijkswaterstaat. (2011). *WaterStand Zuid-Holland: Actualisatie op basis van meetgegevens 2009/2010* (No. RWS/DZH/ARA/2011-02). Rijkswaterstaat dienst Zuid-Holland.

Rijkswaterstaat. (2017a). *Prestatiepeilenmodel Oosterscheldekering 2017* (Versie 3.0 ed.). Goes, Netherlands: RWS Zee en Delta District Noord.

Rijkswaterstaat. (2017b). *Richtlijnen Ontwerp Kunstwerken.* The Hague, Netherlands: RWS GPO. Retrieved from https://standaarden.rws.nl/link/set/S0027

Rijkswaterstaat. (2018a, October 22). *Hollandsche IJsselkering bestaat 60 jaar.* Retrieved 25-02-2021, from https://www.rijkswaterstaat.nl/nieuws/2018/10/hollandsche-ijsselkering-bestaat-60-jaar.aspx

Rijkswaterstaat. (2018b). *Our flood defences: working on storm safety.* Retrieved from https://puc.overheid.nl/rijkswaterstaat/doc/PUC_160821_31

Rijkswaterstaat. (2019). *Objectbeheerregime Stormvloedkeringen.* Rijkswaterstaat GPO-ICO.

Rijkswaterstaat. (2020a). *Richtlijnen Vaarwegen 2020.* The Hague, Netherlands: Author. Retrieved from https://puc.overheid.nl/rijkswaterstaat/doc/PUC_167730_31/

Rijkswaterstaat. (2020b). *Staat van de Infra RWS.* The Hague, Netherlands: Author. Retrieved from https://www.rijksoverheid.nl/documenten/rapporten/2020/12/17/bijlage-4-rapport-staat-van-de-infra-rws-netwerken

Rijkswaterstaat. (2020c). *Stormvloedrapport 9 tot 12 februari 2020 (SR98)* (Vol. 2020; Tech. Rep.). Lelystad, Netherlands: Watermanagementcentrum Nederland.

Rijkswaterstaat Deltadienst. (1957). De stormvloedkering in de mond van de Hollandsche lJssel (detailbeschrijving). In *Driemaandelijks bericht deltawerken: Nummer 2.* Rijkswaterstaat Deltadienst. Retrieved from https://repository.tudelft.nl/islandora/object/uuid%3A8afaa246-aa9d-4d10-9552-7aef5e7d2433?collection=research

Rijkswaterstaat WVL. (2017). *Deelrapportage Vaarwegen voor de Nationale Markt en Capaciteits Analyse (NMCA).* Rijkswaterstaat Water Verkeer en Leefomgeving.

Rijkswaterstaat WVL. (2021). *Schematiseringshandleiding hoogte kunstwerk: WBI 2017.* The Hague, Netherlands: Ministerie van Infrastructuur en Waterstaat.

Roberge, P. R. (2008). *Corrosion Engineering: Principles and Practice.* New York, NY: McGraw-Hill.

Rongen, G., & Botterhuis, T. (2018). *Mini-systeemanalyse Hollandsche IJssel* (No. PR3757.10). Delft, Netherlands: HKV.

Rongen, G., & Maaskant, B. (2019). *Systeemanalyse Hollandsche IJssel: Uitwerking conform BOI uitgangspunten* (No. PR3925.10). Delft, Netherlands.

Schießl, P., & Mayer, T. F. (2007). Lebensdauermanagementsystem - Teilprojekt A2. In *Schlussberichte zur ersten Phase des DAfStB/BMBF-Verbundforschungsvorhabens „Nachhaltig Bauen mit Beton“.* DAfStb Heft 572. Berlin, Germany: Deutscher Ausschuss für Stahlbeton.

Schijve, J. (2009). *Fatigue of Structures and Materials* (2nd ed.). Dordrecht, Netherlands: Springer.

Schoemaker, M. (2016). *Flood Risk Assessment Investment Framework - a framework for flood risk reduction strategies in the Hollandsche IJssel* [MSc thesis]. Delft University of Technology. Retrieved from http://repository.tudelft.nl/islandora/object/uuid:5137a7e4-1397-4b86-80ca-c9d0ae69226d/?collection=research

Siemens. (2021, 01 27). *Siemens Mobility past besturing van Hollandsche IJsselkering aan.* Retrieved 04-05-2021, from https://mobilitymatters.siemens.nl/its/hijk/

Slangen, A. B., Carson, M., Katsman, C. A., Van de Wal, R. S., Köhl, A., Vermeersen, L. L., & Stammer, D. (2014). Projecting twenty-first century regional sea-level changes. *Climatic Change, 124*(1-2), 317–332. https://doi.org/10.1007/s10584-014-1080-9

Slootjes, N., & Van der Most, H. (2016a). *Achtergronden bij de normering van de primaire waterkeringen in Nederland: Hoofdrapport.* The Hague, Netherlands: Ministerie van Infrastructuur en Milieu.

Slootjes, N., & Van der Most, H. (2016b). *Technisch-inhoudelijke uitwerking van eisen aan primaire keringen: Bijlagen.* The Hague, Netherlands: Ministerie van Infrastructuur en Milieu.

Slootjes, N., & Wagenaar, D. (2016). *Factsheets normering primaire waterkeringen: Getalsinformatie per normtraject.* The Hague, Netherlands: Ministerie van Infrastructuur en Milieu.

Sperna Weiland, F., Hegnauer, M., Bouaziz, L., & Beersma, J. (2015). *Implications of the KNMI'14 climate scenarios for the discharge of the Rhine and Meuse: comparison with earlier scenario studies* (No. 1220042-000-ZWS-0004). Delft, Netherlands: Deltares. Retrieved from https://www.knmi.nl/kennis-en-datacentrum/publicatie/implications-of-the-knmi-14-climate-scenarios-for-the-discharge-of-the-rhine-and-meuse-comparison-with-earlier-scenario-studies

Sterl, A., Van Den Brink, H., De Vries, H., Haarsma, R., & Van Meijgaard, E. (2009). An ensemble study of extreme storm surge related water levels in the North Sea in a changing climate. *Ocean Science*, *5*(3), 369–378. https://doi.org/10.5194/os-5-369-2009

Stewart, M. G., Wang, X., & Nguyen, M. N. (2011). Climate change impact and risks of concrete infrastructure deterioration. *Engineering Structures*, *33*(4), 1326–1337. https://doi.org/10.1016/j.engstruct.2011.01.010

Stouthamer, E., Erkens, G., Cohen, K., Hegger, D., Driessen, P., PeterWeikard, H., … Van Rijswick, M. (2020). Dutch national scientific research program on land subsidence: Living on soft soils subsidence and society. *Proceedings of the International Association of Hydrological Sciences*, *382*, 815–819. https://doi.org/10.5194/piahs-382-815-2020

Strehblow, H. H., & Marcus, P. (2011). 7 - Mechanisms of Pitting Corrosion. In P. Marcus (Ed.), *Corrosion Mechanisms in Theory and Practice* (3rd ed., p. 349-394). Boca Raton, FL: CRC press.

Studio Bereikbaar. (2019). *Eindrapportage probleemanalyse en oplossingsrichtingen Algeracorridor* (Versie 3.3 ed.). Retrieved from https://oeververbindingen.nl/publicaties/

Sullivan, W. G., Wicks, E. M., & Koelling, C. P. (2019). *Engineering Economy* (17th ed.). Boston, MA: Pearson.

't Hart, R., De Bruijn, H., & De Vries, G. (2018). *Fenomenologische beschrijving: Faalmechanismen WBI* (No. 11200574-007-GEO-0005). Delft, Netherlands: Deltares.

fib. (2006). *fib Bulletin 34 - Model Code for Service Life Design*. Lausanne, Switzerland: International Federation for Structural Concrete (fib).

Tosserams, M. (2014). *Vervangingsopgave Natte Kunstwerken Gevoeligheidstest Natte Kunstwerken*. The Hague, Netherlands: Rijkswaterstaat. Retrieved from https://www.deltaprogramma.nl/documenten/publicaties/2013/09/17/deltaprogramma-2014-bijlage-c

Tuutti, K. (1982). *Corrosion of steel in concrete*. Stockholm: Swedish Cement and Concrete Research Institute.

Van den Born, G., Kragt, F., Henkens, D., Rijken, B., Van Bemmel, B., & Van der Sluis, S. (2016). *Dalende bodems, stijgende kosten: Mogelijke maatregelen tegen veenbodemdaling in het landelijk en stedelijk gebied*. The Hague, Netherlands: PBL. Retrieved from https://www.pbl.nl/sites/default/files/downloads/pbl-2016-dalende-bodems-stijgende-kosten-1064.pdf

Van der Geest, W., & Kindt, M. (2018). *Vervolgonderzoek containeroverslag in de regio Midden-Holland: Onderzoek naar nut en noodzaak*. Zoetermeer, Netherlands: Panteia.

Van Balen, W., Slootjes, N., Van Haaren, D., & Vermeij, E. (2010). *Verkenning effecten faalkansen en faalkanseis Hollandse IJsselkering: Technische achtergrondrapportage* (No. PR1847). Delft, Netherlands: HKV.

van Breem, B., Delhez, R., Jongejan, R., & Casteleijn, A. (2018). *Werkwijzer Ontwerpen Waterkerende Kunstwerken – Ontwerpverificaties voor de hoogwatersituatie*. Rijkswaterstaat-WVL Waterkeringen.

Van den Boomen, M. (2020). *Replacement optimisation for public infrastructure assets: Quantitative optimisation modelling taking typical public infrastructure related features into account* [PhD thesis]. Delft University of Technology. https://doi.org/10.4233/uuid:3cef9da8-d432-4d6a-8805-4c094440bd56

Van den Boomen, M., Leontaris, G., & Wolfert, A. R. (2019). Replacement optimization of ageing infrastructure under differential inflation. *Construction Management and Economics*, *37*(11), 659–674. https://doi.org/10.1080/01446193.2019.1574977

Van den Hurk, B., & Geertsema, T. (2020). *An assessment of present day and future sea level rise at the Dutch coast* (No. 11204868-002-ZWS-0001). Delft, Netherlands: Deltares. Retrieved from https://www.deltares.nl/nl/publication/assessment-present-day-future-sea-level-rise-dutch-coast/

Van den Hurk, B., Siegmund, P., & Klein Tank, A. (2014). *KNMI'14: Climate Change scenarios for the 21st Century–A Netherlands perspective* (No. WR2014-01). De Bilt, Netherlands: KNMI.

Van der Graaf, H. J., & Van Voorst, J. (2016). *Hoofdrappport Faalkansanalyse Stormvloedkering Hollandsche IJssel 2013* (Versie 5.1 ed.). Capelle aan den IJssel: Rijkswaterstaat Zuid-Holland.

Van der Vlist, M., Roovers, G., & Barneveld, A. (2016). Vervangingsopgave natte kunstwerken in het hoofdwatersysteem en hoofdvaarwegennet in Nederland. *Water Governance*(2), 76–83. Retrieved from http://edepot.wur.nl/430752

Van de Sandt, T. (2014, June 20). *Tweede sluiskolk Julianasluis geopend.* Retrieved 15-02-2021, from https://www.maritiemnederland.com/nieuws/tweede-sluiskolk-julianasluis-geopend

Van Dorsser, J. (2012). *Scheepvaartscenario's voor Deltaprogramma: 100 jaar later...* Delft, Netherlands: Rijkswaterstaat-DVS.

Van Dorsser, J. (2015). *Very Long Term Development of the Dutch Inland Waterway Transport System: Policy Analysis, Transport Projections, Shipping Scenarios, and a New Perspective on Economic Growth and Future Discounting* [PhD thesis]. Delft University of Technology.

van Gelder, P. (2000). *Statistical methods for the Risk-Based Design of Civil Structures* [PhD thesis]. Delft University of Technology.

van Groningen, C. L. (1996). *De Krimpenerwaard.* Zeist, Netherlands / Zwolle, Netherlands: Rijksdienst voor de Monumentenzorg / Waanders Uitgevers.

Van Houdt, J. (2008, April 9). *Capelle aan den IJssel stormvloedkering en Algerabrug ID317941.* Retrieved 08-03-2021, from https://beeldbank.rws.nl/MediaObject/Details/317941

Van Veelen, P. C. (2016). *Adaptive planning for resilient coastal waterfronts: Linking flood risk reduction with urban development in Rotterdam and New York City* [PhD thesis]. Delft University of Technology.

Van Voorst, J., & Van der Graaf, H. J. (2016). *Systeembeschrijving Hollandsche IJsselkering 2016* (Versie 5.1 ed.). Capelle aan den IJssel: Rijkswaterstaat Zuid-Holland.

Van Vuuren, D. P., & Carter, T. R. (2014). Climate and socio-economic scenarios for climate change research and assessment: Reconciling the new with the old. *Climatic Change*, *122*(3), 415–429. https://doi.org/10.1007/s10584-013-0974-2

Van Vuuren, D. P., Edmonds, J., Kainuma, M., Riahi, K., Thomson, A., Hibbard, K., … Rose, S. K. (2011). The representative concentration pathways: an overview. *Climatic Change*, *109*(1), 5–31. https://doi.org/10.1007/s10584-011-0148-z

Van Waveren, H., Kors, A., Labrujere, A., & Osmanoglu, D. (2015). *Motie Geurts, Deltaprogramma: onderzoek naar de effecten van sluizen in de Nieuwe Maas en Oude Maas op de waterveiligheid en de zoetwatervoorziening.* Rijkswaterstaat. Retrieved from https://www.eerstekamer.nl/overig/20160217/motie_geurts_deltaprogramma/document

Vellinga, N. E., Hoitink, A. J., Van der Vegt, M., Zhang, W., & Hoekstra, P. (2014). Human impacts on tides overwhelm the effect of sea level rise on extreme water levels in the Rhine-Meuse delta. *Coastal Engineering*, *90*, 40–50. https://doi.org/10.1016/j.coastaleng.2014.04.005

Visser, H. (2004). Estimation and detection of flexible trends. *Atmospheric Environment*, *38*(25), 4135–4145. https://doi.org/10.1016/j.atmosenv.2004.04.014

Von Meijenfeldt, N., Bouw, R., van Tol, P., Smit, M., Nieuwkamer, R., van Ek, R., … Smit, A. (2017). *Integrale veiligheid Oosterschelde: MIRT onderzoek - knikpunten, oplossingsrichtingen en effecten.* (No. RW1929-201/17-004.991). Deventer, Netherlands: Witteveen+Bos.

Von Greve-Dierfeld, S., & Gehlen, C. (2016a). Performance based durability design, carbonation part 1: Benchmarking of European present design rules. *Structural Concrete*, *17*(3), 309–328. https://doi.org/10.1002/suco.201600066

Von Greve-Dierfeld, S., & Gehlen, C. (2016b). Performance-based durability design, carbonation part 2: Classification of concrete. *Structural Concrete*, *17*(4), 523–532. https://doi.org/10.1002/suco.201600067

Von Greve-Dierfeld, S., & Gehlen, C. (2016c). Performance-based durability design, carbonation, part 3: PSF approach and a proposal for the revision of deemed-to-satisfy rules. *Structural Concrete*, *17*(5), 718–728. https://doi.org/10.1002/suco.201600085

Voortman, H. G., & Veendorp, M. (2011). Robust flood defences in a changing environment. In *Applications of statistics and probability in civil engineering* (pp. 2176–2183). Boca Raton, FL: CRC Press.

Vousdoukas, M. I., Voukouvalas, E., Annunziato, A., Giardino, A., & Feyen, L. (2016). Projections of extreme storm surge levels along Europe. *Climate Dynamics*, *47*(9-10), 3171–3190. https://doi.org/10.1007/s00382-016-3019-5

Vroon, J. (1994). Hydrodynamic characteristics of the Oosterschelde in recent decades. *Hydrobiologia*, *282-283*(1), 17–27. 10.1007/BF00024618

Walker, W. E., Harremoes, P., Rotmans, J., van der Sluijs, J. P., van Asselt, M. B. A., Janssen, P., & Krayer Von Krauss, M. P. (2003). Defining Uncertainty: A Conceptual Basis for Uncertainty Management in Model-Based Decision Support. *Integrated Assessment*, *4*(1), 5–17. https://doi.org/10.1076/iaij.4.1.5.16466

Welsink, M. W. J. (2013). *Adaptation of the Hollandsche IJssel storm surge barrier* [MSc thesis]. Delft University of Technology.

Wilkinson, S. J., Remøy, H., & Langston, C. (2014). 5 Building Obsolescence and Reuse. In *Sustainable building adaptation: Innovations in decision-making* (1st ed., pp. 95–120). Somerset, United Kingdom: John Wiley & Sons, Incorporated.

Willems, J. J., Busscher, T., Woltjer, J., & Arts, J. (2018). Planning for Waterway Renewal: Balancing Institutional Reproduction and Institutional Change. *Planning Theory and Practice*, *19*(5), 678–697. https://doi.org/10.1080/14649357.2018.1542504

Willett, K. M., Dunn, R. J., Thorne, P. W., Bell, S., De Podesta, M., Parker, D. E., … Williams, C. N. (2014). HadISDH land surface multi-variable humidity and temperature record for climate monitoring. *Climate of the Past*, *10*(6), 1983–2006. https://doi.org/10.5194/cp-10-1983-2014

Witteveen+Bos. (2010). *Stormvloedkering en sluis Hollandsche IJssel (VWK 10): Toetsing verbindende waterkering 10 conform VTV2006*. Rotterdam, Netherlands: Rijkswaterstaat Zuid-Holland.

Wolters, H. A., Van den Born, G., Dammers, E., & Reinhard, S. (2018). *Deltascenario's voor de 21e eeuw, actualisering 2017*. Utrecht, Netherlands: Deltares. Retrieved from https://media.deltares.nl/deltascenarios/Deltascenarios_actualisering2017_hoofdrapport.pdf

Woodward, D. G. (1997). Life cycle costing: Theory, information acquisition and application. *International Journal of Project Management*, *15*(6), 335–344. https://doi.org/10.1016/S0263-7863(96)00089-0

Zeeman, M. (2019). *Memo (korte termijn) maatregelen Algeracorridor* [Memo]. Rotterdam, Netherlands: Rijkswaterstaat West-Nederland Zuid. Retrieved from https://oeververbindingen.nl/publicaties/

A

Storm surge barriers in the Netherlands

The Netherlands have been protecting themselves from flooding for centuries. This battle against the water has shaped the Dutch landscape, and one of the most prominent features are the storm surge barriers. These structures are vital for the flood protection of the Netherlands as a significant part of the country is indirectly protected by one or more barriers, see Figure A.1. Most of these storm surge barriers belong to the Delta Works, an enormous flood-control project that partially closed off and protected the south-western part of the country. As part of this project five storm surge barriers were built: the Hollandsche IJssel barrier, the Eastern Scheldt barrier, the Haringvliet sluices, the Hartel barrier, and the Maeslant barrier. The sixth storm surge barrier, the Ramspol barrier, is not part of the Delta Works but was built to protect the north-eastern part of the country against flooding due to high water levels in the IJsselmeer (Lake IJssel) (Deltares et al., 2018). This appendix provides a small overview of these storm surge barriers. The Kromme Nol barrier is the seventh storm surge barrier in the Netherlands, but it is not discussed any further as the structure is operated by the local water authority.

Figure A.1: Parts of the Netherlands for which the storm surge barriers provide flood protection, adapted from Rijkswaterstaat (2018b).

Hollandsche IJssel barrier

The Hollandsche IJssel barrier was the first structure to be constructed as part of the Delta Works. The barrier was completed and brought into operation in 1958 (Mooyaart & Jonkman, 2017). The barrier consists of two 80 metres wide vertical lifting gates of which one is closed when the forecasted water level at Krimpen aan de IJssel exceeds NAP +2.25 m (Rijkswaterstaat, 2018b). A movable barrier was chosen to allow for navigation and river discharge of the Hollandsche IJssel. Damming the river would lead to a reduction in the availability of fresh water in the Rijnland area and loss of the flushing effect of the tide. Next to the barrier, a ship lock was constructed for ships that are too large or in case the gates are closed. The bridge that is part of the barrier complex connects the Krimpenerwaard to the city of Rotterdam.

The structure has its own prescribed flood protection standards. The barrier has a retaining height of NAP +5.0 m, and failure of the barrier is expressed in terms of probabilities. The failure of a storm surge barrier is defined as the loss of the water-retaining function. For the Hollandsche IJssel barrier, the probability of failure is 1/30,000 per year (signal value is 1/100,000 per year) (Slootjes & Van der Most, 2016b). Other than fixed flood defences, such as dams and dikes, storm surge barriers have an additional requirement regarding the closure reliability. The *Waterwet* prescribes an additional probability of failure of the closure operation. The Hollandsche IJssel barrier is allowed to fail once every 200 closures (Slootjes & Van der Most, 2016b).

Haringvliet sluices

It is debatable whether the Haringvliet sluices can be considered a storm surge barrier. The main function of the sluices is to regulate the inland water levels and discharge water from the Rhine and Meuse into the North Sea. Hence, one could argue that the structure is strictly speaking not a storm surge barrier. However, Rijkswaterstaat added the Haringvliet sluices to their portfolio of storm surge barriers in 2018 and therefore the structure is also mentioned here.

The Haringvliet sluices were commissioned in 1971. The structure has a total length of more than 1 km and consists of 17 discharge openings with sector gates on both sides (sea and river side). The construction of the barrier had a significant impact on the ecosystem of the Haringvliet as the Haringvliet became a freshwater lake and the tidal influence disappeared (Deltares et al., 2018). Since 2018, the sluices are set ajar to allow migratory fish to pass the structure (Rijkswaterstaat, 2019). In case of storm surges, the barrier will still be closed if the forecasted water level is NAP +2.2 m.

The retaining height of the sluices is NAP +5.0 m. This height is insufficient to prevent overtopping during severe storms, but there is enough storage capacity in the hinterland. The prescribed failure probability is 1/1,000 per year (signal value is 1/3,000 per year) (Slootjes & Van der Most, 2016b). Requirements regarding the non-closure probability of the sluices have not yet been defined after the decision to set the sluices ajar (Rijkswaterstaat, 2019).

Eastern Scheldt barrier

The Eastern Scheldt barrier is the largest storm surge barrier in the Netherlands. The 9 km long structure includes 62 gates with a cumulative length of 2,600 m (Mooyaart & Jonkman, 2017). The barrier is considered to be the pinnacle of the Delta Plan and was completed in 1986 (Rijkswaterstaat, 2018b). Once the expected water level at sea exceeds +3.0 m, the vertical lifting gates are closed and the area around the Eastern Scheldt is protected against storm surges from the North Sea. The entire structure consists of two auxiliary dams on islands in the Eastern Scheldt, three gated sections, and a shipping lock (Deltares et al., 2018). The barrier is an important road connection between two islands of Zeeland; Noord-Bevenland and Schouwen-Duiveland.

The initial design consisted of a dam that closed of the entire Eastern Scheldt estuary, but a structure with moveable gates was opted instead to preserve the unique ecosystem of the estuary. Nevertheless, the construction of the Delta Work has had a significant impact on the tidal system. The wet cross-sectional area of the inlet has reduced by 80% from 80,000 m^2 to 17,900 m^2, the tidal prism has been reduced by 30% (from 1,230 Mm^3 to 880 Mm^3), and the mean tidal range of 3.70 m at Yerseke has decreased by about 12% to 3.24 m (Louters et al., 1998; Vroon, 1994). These reductions transformed the estuary into a sedimentation basin with a severe sediment deficit commonly referred to as "sand hunger". This sediment demand leads to erosion of the intertidal areas and loss of important habitats for several bird species and seals. The rise in sea level will further accelerate the shrinkage of the intertidal flats, making the restoration of the original morphological equilibrium unfeasible (de Ronde et al., 2013).

The design water level at the seaside is NAP +5.5 m, but the actual height of the structure in closed condition varies between NAP +5.6 m at Hammen and NAP +5.8 m at Roompot and Schaar (Rijkswaterstaat, 2003). The prescribed probability of failure is 1/10,000 years (signal value is 1/30,000 per year) (Slootjes & Van der Most, 2016b). Non-closure probabilities are not prescribed due to the complexity of the barrier.

Hartel barrier

The Hartel barrier (completed in 1997) is located in the Hartel Canal, a waterway that connects the Europoort, a more inland part of the Port of Rotterdam, to the North Sea. With the Maeslant barrier in the Nieuwe Waterweg, a second storm surge barrier was needed to limit the water inflow from the North Sea to the Europoort area under extreme conditions. The Hartel barrier consists of two sliding gates with an elliptical shape that are hanging between the side towers. The gates have different sizes (98 m width and 49.3 m width) and are placed side-by-side instead of behind each other as was done at the Hollandsche IJssel barrier (Mooyaart & Jonkman, 2017). The Hartel barrier is part of the Europoort barrier, a system of flood defences that comprises the Maeslant barrier, the Hartel barrier, and the dikes situated between these two structures. Hence, the barrier closes at the same time as the Maeslant barrier. Both barriers close when the forecasted water level is NAP +3.0 m in Rotterdam or NAP +2.9 m in Dordrecht (Rijkswaterstaat, 2018b). The barrier has been integrated in the already existing bridge across the Hartel Canal and a navigation lock was constructed next to the barrier to let ships for which the clearance height is insufficient pass.

The Hartel barrier has a relatively low retaining height of NAP +3.0 m but was designed for overtopping conditions (Daniel & Paulus, 2019). The failure probability defined as the loss of the water-retaining function is 1/30,000 years (signal value is 1/100,000 per year) and the non-closure probability is 1/10 per closure (Slootjes & Van der Most, 2016b). This requirement for the closure reliability of the Hartel barrier is relatively low, about a factor 10 or 20 lower compared with the requirements for the other barriers. The reason being that a higher closure reliability does not have a significant impact on the water levels in the area behind the Europoort barrier (Bijl, 2006).

Maeslant barrier

The Maeslant barrier consists of two enormous sector gates that are both connected to a ball-and-socket joint on the abutments (Rijkswaterstaat, 2018b). The design with floating sector gates was chosen due to the importance of the Nieuwe Waterweg for the Port of Rotterdam; shipping should not be hindered during normal weather conditions. The barrier was constructed between 1989 and 1997, around the same time as the Hartel barrier. The gates close automatically when the water level in Rotterdam or Dordrecht is expected to exceed NAP +3.0 m or NAP +2.9 m, respectively (Rijkswaterstaat, 2018b).

The gates have a height of 22 m and are lowered to the sill at -17.0 m during the closure procedure, which implies a retaining height of NAP +5.0 m (Deltares et al., 2018). The probability of failure is 1/30,000 years (signal value is 1/100,000 per year) and the prescribed non-closure probability is 1/100 per closure (Slootjes & Van der Most, 2016b). Initially, the barrier was designed with a non-closure probability of 1/1,000, but soon after the Maeslant barrier was completed, research showed that this probability could not be obtained (Rijkswaterstaat, 2009b). The probability has been as low as 1/10 in the past (Kst-30300-A-55, 2006).

Ramspol barrier

The Ramspol barrier (1996-2002) is the most recent storm surge barrier in the Netherlands. It differentiates itself from the other barriers by both design and location. The Ramspol barrier is made of three inflatable rubber membrane sheets that can be filled with air and water to protect the hinterland against flooding. Once inflated, the barrier's height increases to 8.2 m above the sill and each dam attains a width of approximately 78 m (Jongeling, 2005). The rubber dam is the only storm surge barrier that is not located in the south-western part of the country. It was built to protect the areas in the northwest of Overijssel against storm surges from the IJsselmeer (Lake IJssel). The option of an inflatable dam was chosen as this type of structure makes it possible to realise large spans without intermediate abutments, minimises the hindrance of shipping, limits the impact on the landscape, and because it had lower expected construction, operation, and maintenance costs (Deltares et al., 2018; Jongeling, 2005). The closure procedure of the storm surge barrier starts as soon as the water level directly west of the dam reaches NAP +0.5 m and the current is directed eastward (Agtersloot & Paarlberg, 2016).

The retaining height of the dam is +3.55 m, the probability of failure (loss of water-retaining function) is 1/10,000 years (signal value is 1/30,000 per year), and the allowed number of non-closures is 1 per 100 closures (Slootjes & Van der Most, 2016b).

B

Deterioration mechanisms

The three types of components (fixed, movable, and electrical) distinguished in Chapter 2 suffer from various material or element specific deterioration processes. Concrete structures are subject to different processes than steel structures. The most important deterioration mechanisms of both materials are discussed in the following sections.

B.1 Concrete deterioration

B.1.1 Description of processes

The deterioration of concrete has been described extensively in scientific literature and each author prefers his own classification of the deterioration processes. A common approach is to differentiate between physical and chemical deterioration mechanisms (Alexander et al., 2017; Breysse, 2010; Dyer, 2014). Another option is to split the processes into direct mechanisms that affect the concrete itself and indirect mechanisms that describe the deterioration of concrete caused by volume increase of the reinforcement (Bertolini et al., 2013; Gaal, 2004; Gehlen et al., 2010). The latter classification system is also adopted in this discussion since it also describes the deterioration mechanisms from the perspective of the materials.

Direct mechanisms

The direct processes include sulfate attack, alkali-aggregate reaction, exposure to acids, deterioration by salts, and freeze-thaw action (Gaal, 2004). Other authors (Alexander et al., 2017; Dyer, 2014; Breysse, 2010; PCA, 2002) also include mechanical abrasion/erosion and restraint to volume changes next to freeze-thaw action as physical deterioration mechanisms.

Sulfate ions originating from external sources such as soil, groundwater, and seawater may react with other compounds in the hardened cement resulting in expansion and cracking or loss of strength. When the sulfate ions come from the outside environment the process is referred to as external sulfate attack. Internal sulfate attack occurs when sulfate from endogenous sources react with the compounds. For instance, the use of recycled concrete or delayed formation of a mineral called ettringite could be the cause of internal sulfate attack (Gaal, 2004). Another type of expansive reactions is alkali-aggregate reactions. Alkali hydroxides in the cement can react with certain aggregates forming a gel that swells as it absorbs water. The reaction comes in two forms: alkali-silica reaction (ASR) and alkali-carbonate reaction (ACR). ASR is the dominant form since aggregates containing reactive silica materials are more common (Gaal, 2004; PCA, 2002). Acids attack concrete through chemical reactions with the cement. These processes increase the porosity and weaken the concrete (Dyer, 2014; Gaal, 2004; PCA, 2002). Salts such as ammonium chloride have similar effects on the concrete; soluble compounds are formed and leached away or cement hydrates are replaced by weaker ones. Salts can also affect concrete through a physical deterioration process called salt crystallisation. When water rich in salt evaporates on the surface, the dissolved salts crystallise, generating pressures that could cause cracking (PCA, 2002). Another mechanical weathering process is freeze-thaw action. The expansion of frozen water causes the build-up of pressures in the pores and if the pressure exceeds the tensile strength, the concrete gets damaged. The accumulated effect of repeated cycles of freezing and thawing could lead to growing cracks or even scaling or spalling of the concrete (Alexander et al., 2017; Dyer, 2014; PCA, 2002).

Cracks could also arise due to restraints to volume changes. Plastic shrinkage, drying shrinkage, and autogenous shrinkage are three types of processes in which the volume changes are restrained. Plastic shrinkage takes place in fresh concrete before hardening when water evaporates from the surface, whereas drying shrinkage occurs when more water than required for the hydration of cement is added during mixing and the remaining water in the hardened concrete evaporates. Autogenous shrinkage is the chemical shrinkage of concrete due to cement hydration during the hardening (Alexander et al., 2017). Cracking because of expansion and contraction following temperature changes is another type of deterioration due to restrained volume changes. Finally, the progressive loss of material on the concrete surface due to abrasion or erosion by particles such as sand or stones deteriorates the concrete directly.

Indirect mechanisms

The indirect deterioration of concrete is caused by corrosion of the reinforcement. Corrosion reduces the cross-sectional area of the steel and thus the load capacity of the structure. At the same time, corroding steel expands and this expansion creates tensile stresses in the concrete, which could lead to cracking and spalling. The volume increase of steel is due to the formation of rust, a mixture of iron oxides and hydroxides. Figure B.1 shows the relative volume of common corrosion products of iron (Fe). The volume increase can be up to six times for hydrous ferric oxide ($Fe_2O_3 \cdot 3H_2O$), the major component of ordinary rust that gives it its red-brown colour. The exact composition of the rust varies with temperature, pressure, moisture, pH value, and oxygen availability (Alexander et al., 2017; Dyer, 2014; Gaal, 2004). How rust is formed and a basic introduction to the corrosion process is given in Section B.2 on the deterioration processes of steel. Here, the processes relevant to the corrosion of the reinforcement are described.

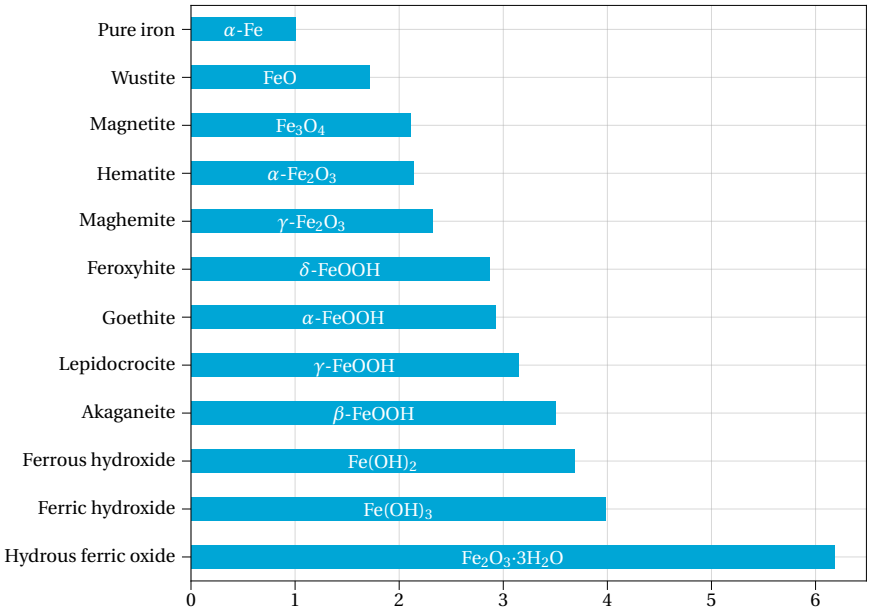

Figure B.1: Relative volume of iron corrosion products, adapted from Jaffer and Hansson (2009) and originally from Marcotte (2001).

Normally, concrete is highly alkaline. The pH value of the pore solution varies between 13 and 14. Under these conditions, the reinforcement is protected by a passive film of stable iron oxides of only a few nanometres thick (Bertolini et al., 2013) . This passive film reduces the corrosion rate to about 0.1 µm per year (Bertolini et al., 2013; PCA, 2002) . The dependency of passivation on the alkaline conditions of the concrete can be visualised in a so-called Pourbaix diagram, which shows the thermodynamic conditions for corrosion, immunity, and passivity of iron (Figure B.2). Typical conditions in concrete were obtained from Bertolini et al. (2013).
As apparent from the figure, iron oxides are formed under alkaline conditions. As explained before, these iron oxides form of a thin passive layer on the steel that prevents further dissolution of the underlying reinforcement. This passive layer has to be damaged for corrosion to start. Two processes could lead to the destruction of the passive film: carbonation and chloride ingress.

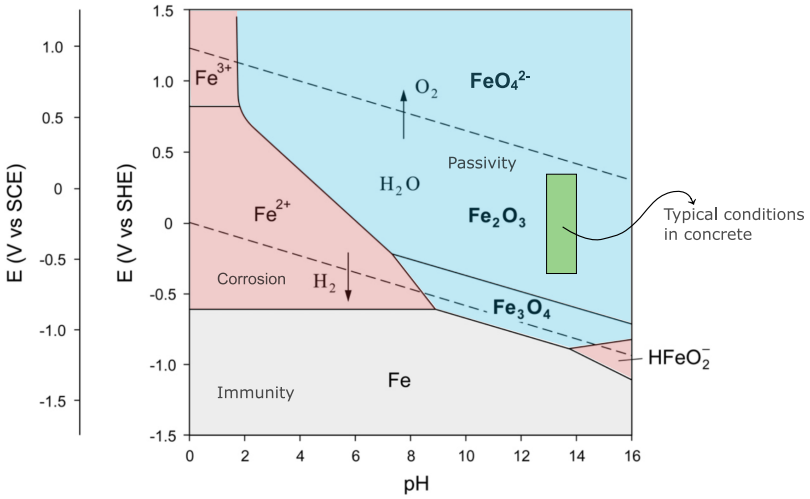

Figure B.2: Pourbaix diagram for iron in water at 25 °C (for ion concentration 10^{-6} mol/l and considering Fe, Fe_3O_4, Fe_2O_3 as the only solid substances), adapted from Angst (2011).

Carbonation is a process in which carbon dioxide (CO_2) from the atmosphere reacts with the compounds that give the concrete its alkaline character, i.e. hydroxides. The reactions result in a lowering of the pH value to less than 9, where the passive film is no longer stable and breaks down (Alexander et al., 2017; Bertolini et al., 2013) . Carbonation is a two-step process, where CO_2 first dissolves in water to form carbonic acid (H_2CO_3), which then reacts with cement hydrates, mainly calcium hydroxide ($CaOH_2$), to form carbonates, e.g. $CaCO_3$. The process starts at the concrete surface and advances into the concrete creating a low pH front. Once this front reaches the reinforcement, the passive layer is disrupted and corrosion of the steel starts. The process is highly dependent on environmental factors, such as CO_2 concentration, relative humidity and temperature, and the concrete composition, e.g. type of cement, water/cement ratio, and porosity (Bertolini et al., 2013; Dyer, 2014; Gaal, 2004; PCA, 2002). The rate of carbonation is about 0.5-1.0 mm per year. Carbonation induced corrosion can generally be prevented by applying sufficient concrete cover, using a low water/cement ratio and proper curing (Bertolini et al., 2013; Gaal, 2004; PCA, 2002).

Chloride ingress is a process in which chloride ions from the environment penetrate the concrete and destroy the passive film locally. There is no wide consensus among researchers about the mechanism of how the penetration of chloride ions leads to the depassivation of the steel. For reference, Strehblow and Marcus (2011) describe three possible mechanisms. These mechanisms are not discussed in this thesis since a simpler explanation is often adopted. Namely, the passive film is destroyed and corrosion starts when the concentration of chloride ions exceeds a certain threshold level (Alexander et al., 2017; Bertolini et al., 2013; Gaal, 2004; PCA, 2002) . The local breakdown of the passive layer results in a type of corrosion which is called pitting (Bertolini et al., 2013). At the location of the pit, the anode, the solid iron dissolves and ions (Fe^{2+}) are formed. Inside the pit, the iron ions hydrolyse (reaction with water) which increases the acidity and accelerates the corrosion. It should be noted that only free chloride ions are responsible for the initiation of corrosion. Chlorides can also be bound to the cement paste and these are assumed not to be actively involved in the corrosion reaction. However, equilibrium conditions exist between bound and free chlorides and bound chloride ions might be released and subsequently increase the corrosion risk under certain conditions. Therefore, the total chloride content, given as a percentage of the cement mass, is mostly used to represent the critical chloride concentration (Bertolini et al., 2013). This threshold level, and thus the chloride-induced corrosion, is influenced by several environmental factors and properties of the steel/concrete. Environmental factors include exposure to chlorides, temperature, relative humidity, and oxygen availability. Important characteristics of the steel and concrete are: pH in the concrete, quality of the steel/concrete interface (presence of voids), concrete resistivity, cement type, and water/cement ratio (Bertolini et al., 2013; Gaal, 2004; PCA, 2002). The critical chloride concentration for atmospherically exposed reinforced concrete structures varies between 0.2% and 0.6% of chloride content by cement mass. This threshold level is often higher for submerged structures due to the reduced oxygen availability at the steel surface (Bertolini et al., 2013). A value of 0.4% is often taken for practical purposes (Broomfield, 2007). This value is also adopted in the Dutch standards (Gaal, 2004).

Of all mechanisms that lead to the deterioration of concrete structures, reinforcement corrosion is the dominate one. Several reviews concluded that premature deterioration of concrete structures could be attributed to corrosion of the reinforcement in 70-90% of the cases according to Angst (2018). Similar figures were reported for the concrete bridges in Germany, see Figure B.3. Chloride ingress, mainly caused by exposure to seawater and the use of deicing salts, is considered to be the most important cause of reinforcement corrosion and deterioration of concrete structures in many countries (Bertolini et al., 2013). Chloride-induced corrosion was also the only concrete deterioration mechanism studied during the design of the Eastern Scheldt barrier. Interestingly, it was one of the earliest applications of a mathematical model describing the chloride ingress over time for the design of a new structure (Gulikers, 2016).

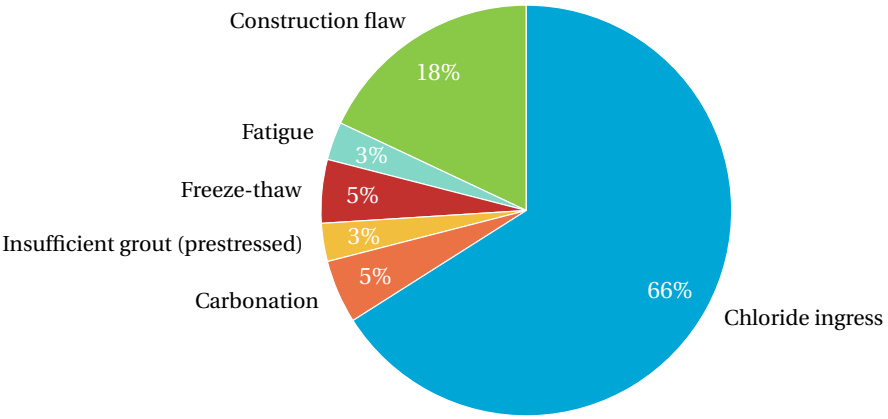

Figure B.3: Causes of bridge deterioration in Germany, adapted from Schießl and Mayer (2007).

B.1.2 Carbonation modelling

As was discussed in the previous section, corrosion of the reinforcement is the main cause of concrete deterioration. Two main mechanisms that lead to reinforcement corrosion can be distinguished: carbonation and chloride ingress. Chloride-induced corrosion is probably the most important mechanisms for the storm surge barriers near the coast, e.g. Eastern Scheldt barrier and Hartel barrier. For the Hollandsche IJssel barrier, carbonation is expected to be more significant for the deterioration of the concrete because of its more inland location.

One of the first and widely adopted models for the reinforcement corrosion process was developed by Tuutti (1982). Tuutti (1982) suggested that the deterioration of the reinforcement can be split into two phases: the initiation phase and the propagation phase. In the initiation phase, aggressive agents such as carbon dioxide (carbonation) and chloride ions (chloride ingress) penetrate through the concrete cover until the reinforcement is reached and the passive layer of iron oxides on the steel reinforcement is broken down. This process is referred to as depassivation. The propagation phase describes the actual reinforcement corrosion process. The corrosion products formed in this stage could lead to cracking, spalling of the concrete, and eventually collapse of the structure due to the loss of cross-section of the reinforcement (Alexander et al., 2017; Bertolini et al., 2013; *fib*, 2006). This phase ends when a limit state is reached. This limit state can either be an acceptable degree of corrosion after which repair activities have to be performed or the end of life of the structure. Because of the different mechanisms occurring in the propagation phase, this stage is sometimes further subdivided into three stages (see Figure B.4b).

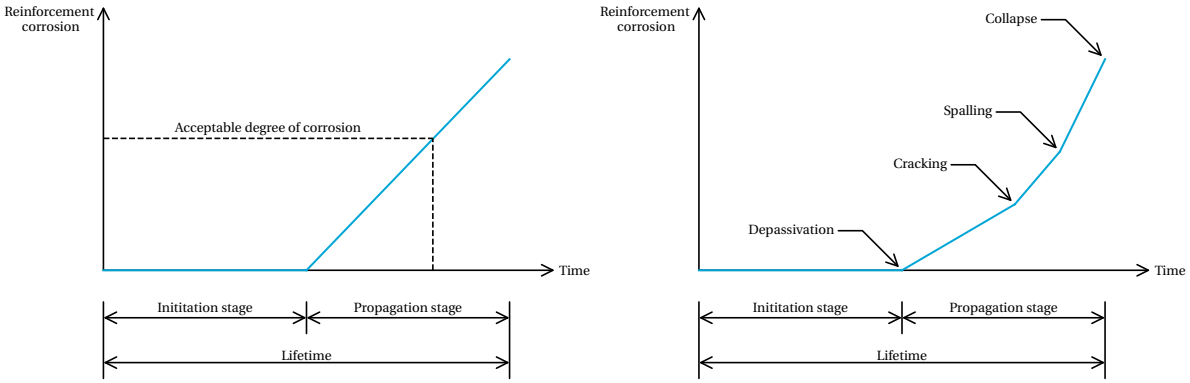

(a) Two-phase model, adapted from Tuutti (1982).

(b) Updated two-phase model, adapted from *fib* (2006).

Figure B.4: Conceptual model for reinforcement corrosion.

Initiation phase

For the carbonation process, different methods can be applied to estimate the duration of the initiation stage and the propagation time. The initiation time is a function of the concrete properties, environmental factors, and the concrete cover thickness, whereas the propagation period is related to the rate of corrosion of the reinforcement. A commonly used model for the initiation period of carbonation-induced corrosion assumes a linear relationship between the carbonation depth x and the square root of time. This model considers diffusion as the governing transport mechanism within the concrete using Fick's first law of diffusion (Alexander et al., 2017; Bertolini et al., 2013):

$$x = K \cdot t^{1/2} \tag{B.1}$$

The carbonation coefficient K incorporates the effects environmental conditions (CO_2 concentration, relative humidity, temperature) and the concrete properties (alkaline conditions, diffusion coefficient). Estimates of the factor K can be obtained from measurements of the carbonation depth after a certain period of time. These measurements can be performed in a straightforward fashion by spraying a pH indicator solution, such as thymolphthalein or phenolphthalein, on the freshly broken concrete. The transition from natural coloured concrete (carbonated) to coloured concrete (uncarbonated) represents the carbonation depth (Bertolini et al., 2013; Dyer, 2014). In wet or dense concrete, the carbonation rate is slower than the one from Equation (B.1) and the exponent $1/2$ is changed to $1/n$ where $n > 2$.

Another, yet similar model was suggested by the International Federation for Structural Concrete (*fib*). This model, based on knowledge obtained within the European research project DuraCrete, is one the most accepted carbonation models that aims to provide a more explicit account of the effects of several parameters on the carbonation rate (Alexander et al., 2017; Bertolini et al., 2013; *fib*, 2006).

$$x_c(t) = \sqrt{2 \cdot k_e \cdot k_c \cdot \left(k_t \cdot R_{ACC}^{-1} + \varepsilon_t\right) \cdot C_S} \cdot W(t) \cdot \sqrt{t} \tag{B.2}$$

where:

$x_c(t)$ = carbonation depth at the time t [mm]
k_e = environmental function [−]
k_c = execution transfer parameter [−]
k_t = regression parameter [−]
R_{ACC}^{-1} = inverse effective carbonation resistance of concrete [(mm^2/year)/(kg/m^3)]
ε_t = error term
C_S = CO_2 concentration in the air [kg/m^3]
$W(t)$ = weather function [−]
t = time [year]

The environmental function incorporates the influence of the humidity on the diffusion coefficient:

$$k_e = \left(\frac{1 - \left(\frac{RH_{real}}{100}\right)^{f_e}}{1 - \left(\frac{RH_{ref}}{100}\right)^{f_e}} \right)^{g_e} \tag{B.3}$$

where:

k_e = environmental function [−]
RH_{real} = relative humidity (of the carbonated layer) [%]
RH_{ref} = reference relative humidity, constant value of 65 [%]
f_e = exponent, empirically determined to be 5.0 [−]
g_e = exponent, empirically determined to be 2.5 [−]

The execution parameter takes into account the curing process of the concrete. The following formula was derived by regression:

$$k_c = \left(\frac{t_c}{7}\right)^{b_c} \tag{B.4}$$

where:

k_c = execution transfer parameter [−]
b_c = exponent of regression [−]
t_c = period of curing [days]

The carbonation resistance of the concrete is determined by accelerated carbonation tests (ACC). To transform the results of such tests to the carbonation resistance under normal or natural conditions, the regression parameter k_t and error term ε_t were introduced (*fib*, 2006):

$$R_{NAC}^{-1} = k_t \cdot R_{ACC}^{-1} + \varepsilon_t \tag{B.5}$$

The weather function accounts for wetting events of the concrete surface, such as rain. The function is defined as:

$$W(t) = \left(\frac{t_0}{t}\right)^{\frac{(p_{SR}\cdot ToW)^{b_w}}{2}} \tag{B.6}$$

where:

$W(t)$ = weather function [−]
t_0 = reference time, usually 28 days (0.0767 year) [year]
p_{SR} = probability of driving rain [−]
ToW = time of wetness, defined as $\frac{\text{days with rainfaill} \geq 2.5 \text{ mm/yr}}{365}$ [−]
b_w = exponent of regression [−]

As part of ongoing research on how to implement the methodology of the *fib* into the next generation of European concrete standards, Von Greve-Dierfeld and Gehlen (2016a, 2016b, 2016c) presented an alternative formula in which R_{NAC}^{-1} has been replaced by k_{NAC}, which is the carbonation rate under standardised test conditions. The full equation for calculating the carbonation depth is:

$$x_c(t) = k_{NAC} \cdot \sqrt{k_e \cdot k_c \cdot k_a} \cdot W(t) \cdot \sqrt{t} \tag{B.7}$$

where:

$x_c(t)$ = carbonation depth at the time t [mm]
k_{NAC} = carbonation rate for standard test conditions [mm/year^2]
k_e = environmental function, as defined by Equation (B.3) [−]
k_c = execution transfer parameter, as defined by Equation (B.4) [−]
k_a = parameter for the effect of CO_2 concentration in the ambient air, defined as $CO_{2,\,air}/CO_{2,\,ref}$ [−]
$W(t)$ = weather function, as defined by Equation (B.6) [−]
t = time [year]

The value of the carbonation rate k_{NAC} was determined by collecting and analysing data on the carbonation rates of concrete mixes from Germany, the Netherlands, Switzerland, and Finland. The data were used to classify concrete mixes with different cement types and water/cement ratios based on the carbonation rates under standardised environmental conditions (65% RH, 20 °C, natural CO_2 concentration). The values of the

carbonation coefficient were found to be varying between 2 and 7 mm/year$^{1/2}$, following a normal distribution with a standard deviation of 1.1 mm/year$^{1/2}$, which is virtually independent of the concrete composition (Von Greve-Dierfeld & Gehlen, 2016b).

The method proposed by Von Greve-Dierfeld and Gehlen (2016a, 2016b, 2016c) was used to estimate the carbonation depth at the Hollandsche IJssel barier because of its complete overview of carbonation rates for different European regions and concrete mixes. To estimate the properties of the concrete elements at the Hollandsche IJssel barrier, published information on the construction of the Haringvliet sluices was used. The construction of this Delta Work started around the same time (1958), which makes it reasonable to assume that similar practices were followed when it comes to the concrete procurement. According to Ferguson et al. (1970), blast furnace cement (CEM III, class B to be conservative) and a w/c ratio of 0.47 were used for the piers of the Haringvliet sluices. Assuming similar characteristics for the Hollandsche IJssel barrier results in a carbonation coefficient of 5 mm/year$^{1/2}$. A complete overview of the input parameters is presented in Table B.1. The values were obtained from Von Greve-Dierfeld and Gehlen (2016c). For the CO_2 concentration a slightly different value of 412 ppm was used instead of the suggested 465 ppm since the latter value is used as a value for the next 50 years and the carbonation depth is calculated for the current climate conditions. The predicted carbonation depth is shown in Figure B.5. The concrete cover depth is estimated to be 40 mm based on the cover depths of the structural elements of six concrete structures in the Netherlands included in the study by Polder and De Rooij (2005).

Table B.1: Input parameters for the calculation of the carbonation depth.

Parameter	Sub-parameter	Unit	Distribution	Mean	Standard deviation
k_{NAC}		mm/years$^{1/2}$	normal	5	1.1
k_c	b_c	–	normal	-0.567	0.25
	t_c	–	constant	7	–
k_e	RH_{air}	% RH	Weibull (max) loc. parameter = 100	80	12
	RH_{ref}	% RH	constant	65	–
	g_e	–	constant	2.5	–
	f_e	–	constant	5	–
$W(t)$	ToW	–	constant	0.2	–
	p_{SR}	–	constant	0.1	–
	b_w	–	normal	0.446	0.163
	t_0	years	constant	0.0767	–
k_a	$CO_{2,\,air}$	vol. %	normal	0.0412	0.005
	$CO_{2,\,ref}$	vol. %	constant	0.04	–

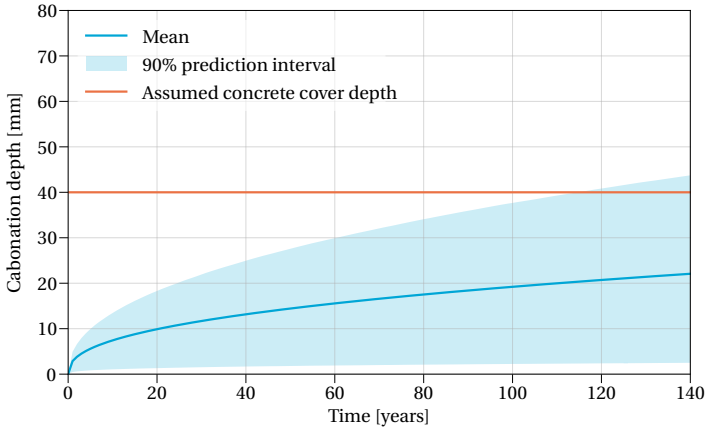

Figure B.5: Mean value and 90% prediction interval of the carbonation depth under the current climate.

Propagation phase

A common approach for the determination of the duration of the propagation period is to assume a linear relationship between the corrosion rate v_{corr} and a predefined acceptable degree of corrosion or penetration depth of the reinforcement:

$$t_p = \frac{x_{crit}}{v_{corr}} \tag{B.8}$$

where:

t_p = duration of propagation period [years]
x_{crit} = initial chloride content of the concrete [% by mass of cement]
v_{corr} = corrosion rate [mm/year]

The corrosion rate varies with temperature and humidity, provided there is sufficient oxygen available. Typical corrosion rates under various conditions are presented by Bertolini et al. (2013) and are shown in Figure B.6.

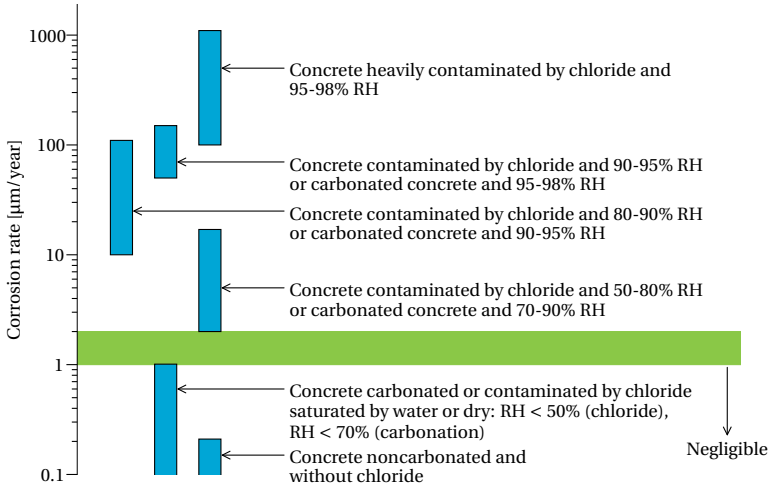

Figure B.6: Typical corrosion rates of steel under different environmental conditions, adapted from Bertolini et al. (2013).

From the values shown Figure B.6, it becomes clear that while the carbonation rate is highest for modest values of relative humidity, the corrosion process thrives under opposite conditions. As a result, carbonation-induced corrosion poses a major risk in areas characterised by periodic wetting and drying of concrete, especially long dry periods alternated by long wet periods are unfavourable. For carbonated concrete, the corrosion rate can be as high as 100-200 µm/year under extremely wet conditions. Similar values were found from large sets of measurements of which most were taken in Spain (Alonso & Andrade, 1994). The results of these measurements were given in current density (mA/m^2) and were converted to µm/year using the relation 1 mA/m^2 ≈ 1.17 µm/year (Bertolini et al., 2013). The converted results are shown in Figure B.7. Based on both figures, an average corrosion rate of 25 µm/year seems to be a conservative and appropriate estimate for the calculation of the propagation period. The maximum corrosion rate is approximately 5-10 times larger than the average value (Bertolini et al., 2013).

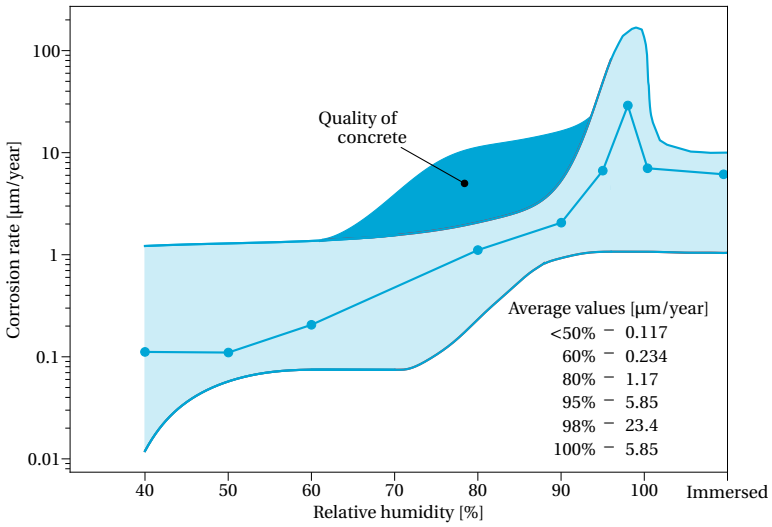

Figure B.7: Range of values of the corrosion rate in carbonated concrete as a function of environmental humidity, adapted from Bertolini et al. (2013).

The initiation phase lasts for a substantial period of time (in the order of multiple decades) and intermediate repair works could be performed to mitigate the carbonation of concrete. Therefore, the propagation period is not considered any further in this study.

B.2 Steel deterioration

The two main deterioration mechanisms of steel are corrosion and fatigue. These mechanisms work very differently, corrosion is a electrochemical process whereas fatigue is a mechanical phenomenon. Nevertheless, the effect is similar: a loss in material strength.

Corrosion

Corrosion is generally defined as the destruction or deterioration of a material, usually metal, by chemical or electrochemical reactions with its environment (McCafferty, 2010; Revie & Uhlig, 2008; Roberge, 2008; Popov, 2015). For corrosion to take place four elements are required: an area/element where the corroding metal is oxidised to its ionic form and electrons are released (anode), an area/element where the electrons are consumed in a reduction reaction (cathode), a substance to transport the ions between the electrodes (electrolyte), and a conductor to facilitate the flow of electrons from the anode to the cathode (the metal itself).

In the context of steel deterioration, the formation of rust is implied when one speaks of corrosion. Rusting is the corrosion of iron or its alloys, such as steel, which only occurs in the presence of oxygen. Rust is a mixture of iron oxides, hydroxides, and oxide-hydroxides. The typical reactions that lead to the formation of rust are (under neutral or alkaline conditions):

At anodic areas:

$$Fe \rightarrow Fe^{2+} + 2e^{-}$$

At cathodic areas:

$$2H_2O + O_2 + 4e^{-} \rightarrow 4OH^{-}$$

The hydroxide ions (OH^{-}) will react with the ferrous ions (Fe^{2+}) to form ferrous hydroxide ($Fe(OH)_2$):

$$2Fe^{2+} + 4OH^{-} \rightarrow 2Fe(OH)_2$$

The ferrous hydroxide is usually further oxidised to (hydrated) forms of Fe_2O_3 and Fe_3O_4, see Figure B.1 for common types of corrosion products. The process is illustrated in Figure B.8a, and a real-life example is given in Figure B.8b. In essence, the corrosion of steel (rusting) requires the compounds iron, water and oxygen, and the effect is loss of metal at the anode, see Figure B.8a. This process leads to a reduction in the strength and ductility of the steel. In some cases, the corrosion of a structural element is tolerated, but that would lead

to frequent replacements of the element, which can be costly. So to prevent or delay the corrosion of steel some sort of protection is applied to steel structures. These protections act as an inhibitor of the process. The most widely used protection method for hydraulic gates is the application of a paint coating system (Daniel & Paulus, 2019).

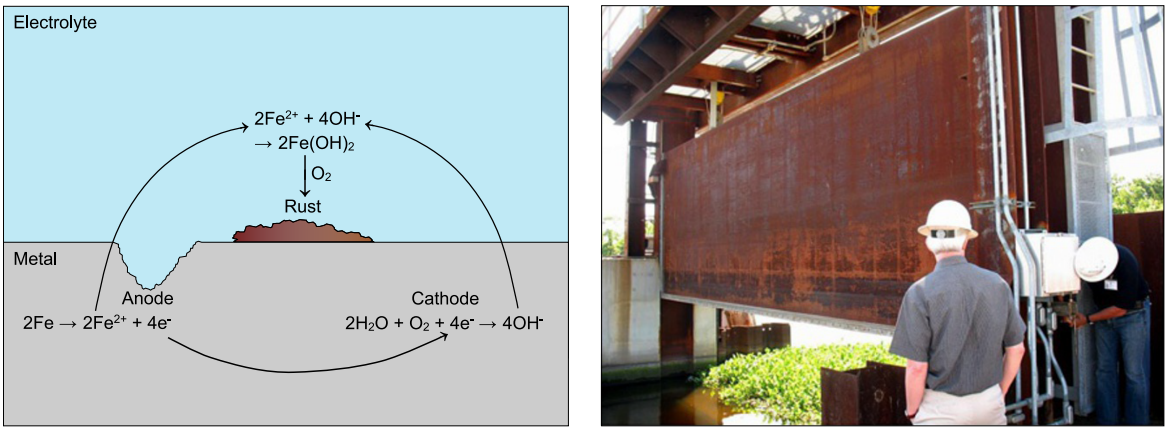

(a) Schematisation of corrosion process.

(b) Rust formation on a lock gate (Daniel & Paulus, 2019).

Figure B.8: Rust formation process.

Fatigue

Fatigue is the cumulative damage caused by cyclic loading of a material or structure. A small crack is initiated due to repetitive loading, followed by crack growth with each loading cycle, and finally complete failure of the structure (Schijve, 2009). The process already starts at stresses below the yield stress. It may start very early on in the life of a structure and almost immediately if the cyclic stress exceeds the fatigue limit, which is the cyclic stress below which fatigue failure does not occur. The process starts with the formation of slip bands, localised bands of plastic deformation, when the resolved shear stress is large enough. These slip bands are in fact intrusions and extrusions at the surface where microcracks can initiate due to stress concentrations. Subsequently, the microcracks can grow, turn into macrocracks, and lead to structural failure. This process is usually split into two phases: crack initiation and crack growth (Figure B.9).

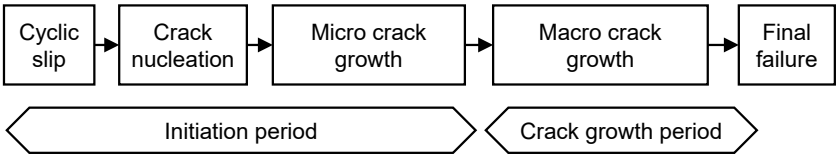

Figure B.9: Phases of the fatigue life of a structural component (Schijve, 2009).

The main factors influencing the fatigue process are the stress/load amplitude and the number of load cycles. Critical elements for fatigue cracks are connections, such welds, joints, and notches, i.e. locations of potential stress concentrations. Furthermore, the process of corrosion and fatigue could interact with each other. Corrosion could affect the fatigue process in several ways. Corrosion leads to surface damage and thus potential locations of stress concentrations, and it reduces the cross-section of the element which increases the stress in the element and thereby shorten the fatigue life (PIANC, 2020; Schijve, 2009). It is beyond the scope of this thesis, to study the fatigue of the steel gates and the interaction with corrosion in detail. If considered, the impact of fatigue on the end of life calculation could be included by assuming a maximum number of load cycles after which the gates of the barrier have to be replaced.

C

Developments in the waterway transport sector

This appendix explores the possible developments in the navigation sector. First, national developments are discussed as the scenarios comprise projections on a national scale. Next, these national projections are translated into regional developments by considering location-specific characteristics. These regional projections are used to draw conclusions in relation to the navigation function of the Hollandsche IJssel barrier.

C.1 National developments

The developments in the inland waterway transport sector are largely driven by economic growth. Strong economic growth results in a higher transport demand. The developments in transport demand for different modes of transport are considered in the National Market and Capacity Analysis (NMCA). This recurring study on behalf of the Ministry of Infrastructure and the Environment (Ministry of Infrastructure and Water Management as of 2017) tries to provide projections of these transport developments for the years 2030, 2040, and 2050. The analysis is based on the WLO scenarios of CPB and PBL. The scenarios take into account the following specific socio-economic developments that can have a major impact on cargo transport:

- modal shift agreements for container transport (reduction of the road transport's share, in favour of rail and inland waterway transport).
- geographical shifts in sand and gravel extraction (decrease in extraction in the south of the country).
- closure/opening of several coal-fired power stations.
- opening of various new inland container terminals.
- emergence of biomass as an alternative to coal and petroleum (products).
- CO_2 levy on the inland waterway transport sector for scenario Hoog.

The projected developments in the inland waterway transport (IWT) sector are depicted in Figure C.1. In both scenarios, the IWT continues to grow. The difference in average growth between the scenarios is smaller than for other modes of transport, but major differences can be observed when the transport flows are broken down by type of transport (transit, import, export, and domestic), see Table C.1.

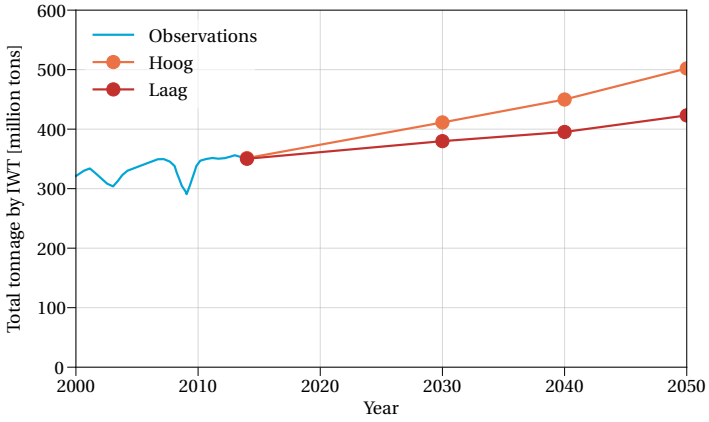

Figure C.1: Development of the total tonnage by IWT (Rijkswaterstaat WVL, 2017).

Table C.1: Developments IWT per type of transport (Rijkswaterstaat WVL, 2017).

Type of transport	Tonnage 2014 [mln. tonnes]	Increase 2014-2040		Average annual growth 2014-2040	
		Scenario Laag	Scenario Hoog	Scenario Laag	Scenario Hoog
Domestic	112	−4%	+10%	−0.2%	+0.4%
Import	64	+44%	+64%	+1.4%	+1.9%
Export	128	+6%	+20%	+0.2%	+0.7%
Transit	46	+26%	+49%	+0.9%	+1.5%
Total	350	+13%	+28%	+0.5%	+1.0%

Table C.1 shows that the growth of the IWT sector is largely due to international transport, especially import. This is a consequence of the fact that, in the WLO scenarios, Dutch export and consumption will grow faster than the production. For this to be possible, the import of goods has to increase significantly. A second interesting trend is the shrinkage of domestic transport in the scenario Laag. This trend can be explained by the limited economic growth in this scenario (+1%) in combination with dematerialisation (Rijkswaterstaat WVL, 2017).

Another interesting development, especially for the Hollandsche IJssel, is the strong growth of container transport (Table C.2). Container transport is still a growth market and the realisation of the 2nd Maasvlakte in 2014 will contribute to a further increase in the container transport volume (Van Dorsser, 2015). A second development in container shipping described earlier is the emergence of high cube containers, see Section 2.2.2. The increasing use of this type of container is very relevant in view of the vertical clearance at fixed bridges.

Table C.2: Developments in IWT per type of cargo: container or others (Rijkswaterstaat WVL, 2017).

Type of transport	Tonnage 2014 [mln. tonnes]	Increase 2014-2040		Average annual growth 2014-2040	
		Scenario Laag	Scenario Hoog	Scenario Laag	Scenario Hoog
Containers	47	+47%	+73%	+1.5%	+2.1%
Others	304	+7%	+22%	+0.3%	+0.8%
Total	350	+13%	+28%	+0.5%	+1.0%

The NMCA is a useful tool for identifying future bottlenecks based on several socio-economic developments. However, the analysis has several limitations that are relevant for determining the residual life of the storm surge barrier. First of all, the projections do not extend beyond the year 2050. The design life of all storm surge barriers, including the Hollandsche IJssel barrier, will end in the decades thereafter, so longer-term developments are also important. A second limitation arises from the fact that the analysis has been performed to determine future bottlenecks. Because the analysis serves to determine where capacity problems will arise, shifts in transport flows due to limited capacities of locks or other structures are not considered. Finally, and

perhaps most importantly, climate change. The NMCA does not include climate change in its projections, while changes in the climate could have a major impact. For example, long periods of low discharge and subsequent periods of low water could limit the loading capacity of vessels. Higher water levels as a result of sea level rise can lead to more frequent closure of storm surge barriers resulting in an increased unavailability of the waterway. Subsidence is also an important factor. Large stretches of the river bed could experience vertical movements while other areas, e.g. near locks, do not settle as much due to their foundation. This unequal movement of the river bed could have a negative impact on the available draught for vessels.

Developments in the IWT sector are thus driven by socio-economic developments as well as climate change. Because this also holds for other uses of land and water, the earlier described Delta Scenarios were developed. Van Dorsser (2015) and Wolters et al. (2018) use these scenarios to describe the developments in the IWT sector for the long term, up to 2100. In addition to the four Delta Scenarios, Van Dorsser (2015) developed two other scenarios as a sensitivity analysis for the four official Delta Scenarios. The first extra scenario, DOORSTOMEN, represents strong - but unsustainable - economic growth and moderate climate change. The second scenario, WATERDRUK, relates to strong and sustainable economic growth combined with rapid and substantial climate change. These two scenarios are not discussed any further here since they are not part of the official Delta Scenarios presented by Wolters et al. (2018). The key developments of the IWT system for each scenario are (Van Dorsser, 2015; Wolters et al., 2018):

DRUK

The economic prosperity has resulted in a significant increase in transport volumes and transhipment at the seaports. In addition, technological developments ensure the consolidation of cargo flows and the development of multi- and intermodal transport, enabling the use of larger and/or better vehicles and vessels, and creating a dense network of inland terminals. This growth can partly take place due to limited climate change and a strong focus on sustainable developments. The share of bulk shipments decreases due to the relocation of heavy industry to the countries where the raw materials are mined. Yet, in absolute numbers the transport of bulk goods remains relatively stable since the traditional bulk goods such as crude oil and coals are replaced by hydrogen and biomass. The share of container transport, on the other hand, continues to grow. The increase in container transport and multimodal transport also means that continental 45 ft containers will be used more and more. These 45 ft, pallet wide, high cube containers were developed because the (American) 20 ft or 40 ft deep sea containers are not compatible with the standard-sized pallets used in the European transport system. The continental containers have now become the new European standard for continental road, short-sea-shipping, and rail transport (Van Dorsser, 2015).

STOOM

Transhipment volumes increase due to strong economic growth, but the IWT sector does not follow this trend entirely. The limited interest in the transition to a sustainable society and severe climate change have adverse effects on the IWT system. Inland navigation remains and important mode for the transport of goods in the coming decades, but the sector loses its market share in the second half of the century and multi-/intermodal transport with continental containers develops moderately. The share of bulk shipments is maintained as fossil fuels remain a dominant source of energy and heavy industry remains in Europe. Despite the economic prosperity, the growth of the shipping industry is not as strong as in DRUK because of the poor navigability of the river Rhine during the summer in the second half of the century, which results in a loss of market share of Dutch ports to other ports in Europe.

RUST

The limited economic growth is reflected in the moderate growth of transhipments and inland navigation. The desire for more sustainable modes of transport together with moderate climate change has a positive effect on the IWT sector. The inland navigation sector is able to maintain its market share compared to the other modes of transport due to the relatively low costs and impact on the environment. Athough the importance of the port of Rotterdam declines on a global scale after 2050, the port remains valuable to Northwestern Europe. Similar to the scenario DRUK, heavy industry moves to the countries where the raw materials are mined, and the share of container transport increases at the cost of bulk shipments. Intermodal transport and the use of continental containers increase to a reasonable extent. The overall growth of container transport is limited.

WARM

Transhipments at the ports and inland transport grow moderately, in line with the limited economic growth. These developments cease around 2050 as severe climate change results in a substantial drop in the market share of the IWT sector in the second half of the century. The heavy industry remains in Europe, contributing to a continued, yet reduced supply of bulk goods, whereas container transport barely increases due to limited growth in transport volumes and fierce competition with other ports. Development of multi- and intermodal transport is practically absent, and continental cargo is almost exclusively transported by road.

The qualitative descriptions of the developments in the IWT sector for each Delta Scenario are summarised in Table C.3. Van Dorsser (2015) also made quantitative projections of the IWT volumes for each scenario. These results can be compared with the estimated total volumes presented by Wolters et al. (2018), see Figure C.2.

Table C.3: Developments in IWT for the Delta Scenarios (Van Dorsser, 2015; Wolters et al., 2018).

Aspect	DRUK	STOOM	RUST	WARM
Economic growth	High	High	Low	Low
Climate change	Moderate	Severe	Moderate	Severe
Sustainability	High interest	Low interest	High interest	Low interest
Transport demand	Large increase	Large increase	Moderate increase (decrease after 2050)	Moderate increase (decrease after 2050)
Market share seaports	Increase	Decrease	Increase	Decrease
Transport of bulk goods	Unchanged	Unchanged	Decrease	Decrease
Conventional container transport	Large increase	Considerable increase	Moderate increase (decrease after 2050)	Moderate increase (decrease after 2050)
Continental container transport	Large increase	Moderate increase	Moderate increase	Unchanged

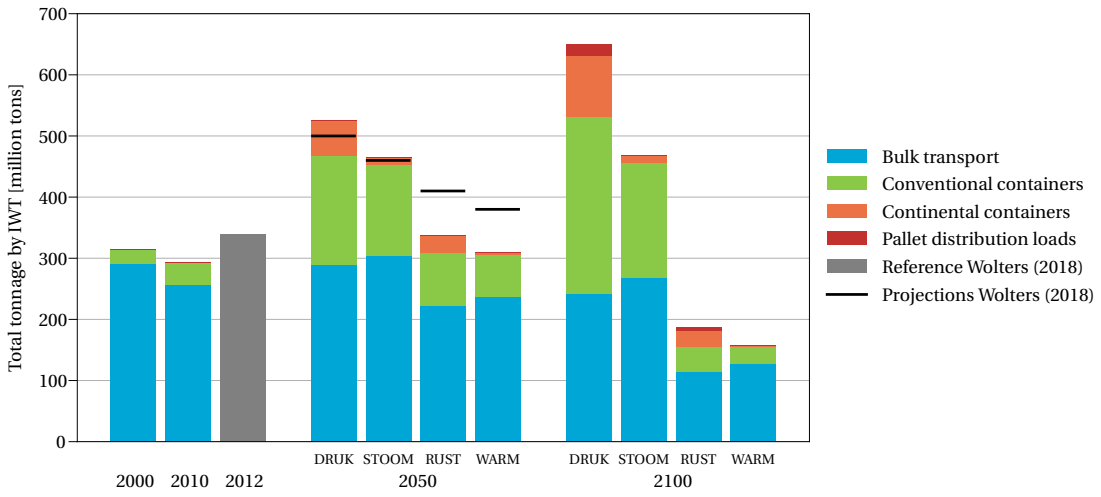

Figure C.2: Developments of the volumes by IWT for each Delta Scenario (Van Dorsser, 2015; Wolters et al., 2018).

The projections by Van Dorsser (2015) differ considerably from the ones by Wolters et al. (2018). For all the Delta Scenarios, the projections by Van Dorsser (2015) are more extreme. The total volumes are higher for the scenarios with strong economic growth and lower for the low economic growth scenarios. A possible explanation for these differences lies in the fact that the predictions of Van Dorsser (2015) were based on a previous version of the Delta Scenarios. These scenarios use the WLO scenarios of 2006 and the climate change scenarios KNMI'06 (Bruggeman et al., 2011). The former socio-economic scenarios predict higher and lower economic growth compared to the current WLO scenarios. The KNMI'06 scenarios do not differ substantially from the KNMI'14 scenarios. The overall trends in the climate change scenarios are similar. The

sea level rise projections are lower in the old scenarios, but summer warming and drying are more severe (Klein Tank et al., 2015). Low summer discharges are more extreme in the old scenarios, which results in more draught restrictions for vessels. These factors could cause the differences in the predictions of the total volume by IWT for 2050. The WLO scenarios do not look beyond 2050 and, in the past, later developments were deduced from expert opinions (Bruggeman et al., 2011). This approach was not adopted when the new Delta Scenarios were drafted. Quantitative predictions were performed only for the first half of the century (Wolters et al., 2018).

Even though the projections of Van Dorsser (2015) and Wolters et al. (2018) differ to a certain extent, the results are comparable in a qualitative sense. The scenario DRUK (high economic growth, moderate climate change) exhibits the greatest growth and WARM (low economic growth, severe climate change) the smallest. Hence, the results of the study by Van Dorsser (2015) are also included in the evaluation of the scenarios by Wolters et al. (2018).

C.2 Regional developments

The Delta Scenarios are nationwide scenarios and applying these scenarios to the Hollandsche IJssel barrier requires translation to a regional scale taking into account regional characteristics. As mentioned in Section 2.2.2, data on the number or types of vessels on the Hollandsche IJssel were not available. As an alternative, data on the passages at the Juliana lock near Gouda were used. These data show that recreational boating exhibits a strong seasonal variation with a very small number of boats during the storm season, in which the storm surge barrier closes most often and hindrance to shipping can be expected. Therefore, developments in recreational navigation were not considered in the following paragraphs.

Container vessels and bulk carriers are the main types of vessels navigating the Hollandsche IJssel. Container vessels make up 22% of the commercial vessels and the other 78% are bulk carriers. The total amount of tonnage transported is roughly 3.5-3.6 million tonnes a year, of which about 2 million tonnes concerns bulk goods (Ammerlaan et al., 2019; Buck Consultants International et al., 2014). The figures in Section 2.2.2 show that neither the absolute number of commercial vessels nor the amount of tonnage has changed significantly since the opening of the container terminal Alpherium in 2009. This indicates a shift in transport flows rather than an increase. Despite the relatively constant transport of cargo over the past years, the number of ships may increase in the future since container transport is still a growth market and all Delta Scenarios show some increase in container transport. A second development affecting the number of container vessels is the idea of constructing a second container terminal in the region (Van der Geest & Kindt, 2018). This second terminal could lead to an additional transport of about 45,000 TEU. Whether this second terminal will actually be built depends on the future economic situation.

Based on the current situation, both the changes in bulk transport and container transport are important for future shipping activities on the Hollandsche IJssel. However, according to the projections of Van Dorsser (2015), bulk transport hardly grows in the future, there is even a slight shrinkage for the scenarios with low economic growth (WARM and RUST). Container transport, on the other hand, will experience very strong growth and gain a larger market share in the case of DRUK and STOOM. For the other two scenarios, the number of container ships will increase in the coming decades but then fall back to the current level. Consequently, the increase in shipping activities on the Hollandsche IJssel is mainly determined by container transport.

The predictions of Van Dorsser (2015) indicate that container transport will grow by a factor of 5.0 and 1.5 compared to the current volume of 47 million tonnes (2014) for the DRUK and WARM scenarios, respectively. These numbers translate into an average annual growth of 4.6% and 1.2%, respectively. The calculated volumes for the scenarios with high economic growth (DRUK and STOOM) are relatively on the high side, while the volumes for the RUST and WARM scenarios are underestimated compared with the predictions of Wolters et al. (2018). The growth figures for the scenarios DRUK and STOOM are therefore reduced and the figures for the other two scenarios increased, see Table C.4. The chosen corrections are to some extent based on the differences between the projections of Van Dorsser (2015) and Wolters et al. (2018). However, it is not the objective to make accurate predictions for the future with the chosen growth figures. The numbers rather indicate the wide range of possible developments and their consequences.

Table C.4: Estimated growth in the total volume of container transport by IWT.

Scenario	Containers [mln. tonnes]	Growth factor	Average annual growth 2014-2050	Corrected average annual growth 2014-2050
Reference (2014)	47	1		
DRUK 2050	237	5.0	+4.6%	+4.0%
STOOM 2050	161	3.4	+3.5%	+3.2%
RUST 2050	115	2.4	+2.5%	+2.8%
WARM 2050	72	1.5	+1.2%	+1.5%

The corrected growth figures from Table C.4 were used to estimate the developments in the total transport volume on the Hollandsche IJssel. The calculated volumes are shown in Table C.5.

Table C.5: Estimated growth in the total volume of container transport by IWT on the Hollandsche IJssel, reference figures are from Buck Consultants International et al. (2014).

Scenario	Bulk goods [mln. tonnes]	Containers [mln. tonnes]	Total [mln. tonnes]	Growth factor	Average annual growth 2013-2050
Reference (2013)	2	1.6	3.6		
DRUK 2050	2	6.6	8.6	2.4	+2.4%
STOOM 2050	2	4.9	6.9	1.9	+1.8%
RUST 2050	2	4.3	6.3	1.8	+1.5%
WARM 2050	2	2.7	4.7	1.3	+0.7%

The figures for the Hollandsche IJssel are significantly higher than the national figures of Wolters et al. (2018). The reason being that container transport already accounts for a significant portion of total transport on the river (about 44% in terms of volume), while, on a national scale, container transport represents only 14% of the total volume (Rijkswaterstaat WVL, 2017). The high growth of container transport, in combination with the already large contribution of container vessels, means that the average growth of the cargo volume on the Hollandsche IJssel is higher than the national average.

The larger volumes in container transport do not necessarily mean a large increase in the number of vessels. By using larger vessels (more containers per vessel) and efficiency improvements (fewer empty containers), the increase in the number of vessels can be limited. Container vessels are loaded for 55 to 75% of their capacity. In addition, the number of loaded containers also varies between 50 and 70% (Brolsma, 2012). On average, ships sail with 65% of their maximum TEU capacity, of which 65% loaded and 35% unloaded (Brolsma, 2013). In theory, a considerable efficiency improvement can be made before the number of vessels increases. If one considers the vessel type *Gouwenaar* with a capacity of 104 TEU, an average of 67.6 TEU is transported, of which 65% comprises loaded containers. Assuming 12.5 tonnes/TEU for the total weight of a loaded container and 2.1 tonnes for the weight of an unloaded container, a *Gouwenaar* will transport around 600 tonnes, while a total of 1,300 tonnes could be transported when fully loaded. The capacity utilisation of container vessels on the Hollandsche IJssel is slightly different from these average values. According to the data of 2013, vessels sail fully loaded towards the container terminal Alpherium and for 20% loaded in the other direction (Buck Consultants International et al., 2014). The number of containers is the same in both directions and so the capacity utilisation is assumed to be 60% (100% utilisation of which 60% loaded). As a result, an average of 870 tonnes is transported per vessel. This value corresponds well with the calculated volume of 830-890 tonnes that follows from the combination of the total volume of 1.5-1.6 million tonnes and about 1,800 container vessels per year (Buck Consultants International et al., 2014). The changes in the number of vessels can now be calculated by combining the increases in volume of Table C.5 with the average 870 tonnes per vessel. The number of bulk carriers was kept constant compared to the reference year. The results are shown in Table C.6.

Table C.6: Estimated growth in the number of vessels on the Hollandsche IJssel.

Scenario	Bulk carriers	Container vessels (870 tonnes/vessel)	Total	Growth factor	Average annual growth 2013-2050
Reference (2013)	6380	1803[a]	8183		
DRUK 2050	6380	7539	13 919	1.7	+1.4%
STOOM 2050	6380	5675	12 055	1.5	+1.1%
RUST 2050	6380	4999	11 379	1.4	+0.9%
WARM 2050	6380	3134	9514	1.2	+0.4%

[a] actual number of container vessels, not based on estimated volume per vessel.

The calculations were also performed for a capacity utilisation of 80% (100% utilisation of which 80% loaded) to estimate how a further efficiency gain influences the number of vessels. This results in an average volume of about 1,080 tonnes per vessel. The effect of this increased efficiency on the number of vessels is shown in Table C.7. The reduction is in the order of 10%, indicating that container transport on the Hollandsche IJssel is already reasonably efficient.

Table C.7: Estimated growth in the number of vessels on the Hollandsche IJssel with an increase in efficiency to 1,080 tonnes per container vessel.

Scenario	Bulk carriers	Container vessels (1080 tonnes/vessel)	Total	Growth factor	Average annual growth 2013-2050
Reference (2013)	6380	1803[a]	8138		
DRUK 2050	6380	6073	12 453	1.5	+1.1%
STOOM 2050	6380	4571	10 951	1.3	+0.8%
RUST 2050	6380	4027	10 407	1.3	+0.7%
WARM 2050	6380	2525	8905	1.1	+0.2%

[a] actual number of container vessels, not based on estimated volume per vessel.

The derived figures can be used to quantify the impact of the changing functionality of the storm surge barrier on navigation. However, the presented figures only serve as an indication of possible developments in shipping. The reality is more complicated and uncertain. For instance, any interaction between the IWT sector and the functional performance of the barrier has not been taken into account. More frequent closures of the barrier may have consequences for the cargo transport on the river. The industry might shift to more road or rail when the hindrance becomes too large, or possibly to other inland container terminals. Both changes result in a devaluation of the importance of the Hollandsche IJssel for the IWT sector.

Another important factor is the capacity of the waterway and the structures in the waterway. Container vessels sail between the Port of Rotterdam and the container terminal Alpherium. Bulk carriers mainly transport sand and cement to the concrete plants that are also located in Alphen aan den Rijn (de Graaf & Steensma, 2019). As most vessels are destined for Alphen aan den Rijn, the vessels also navigate the Gouwe. This waterway is CEMT class IV, whereas the Hollandsche IJssel is CEMT class Va. Moreover, the vertical clearance at several bridges across the Gouwe is less than at the Hollandsche IJssel barrier. The bridge deck of the highest bridge across the Gouwe, the railway bridge near Gouda, is at NAP +7.0 m, while the deck of the Algera bridge is at NAP +8.5 m (Rijkswaterstaat, n.d.-a). Yet, both waterways are part of the *staande mast route Vlissingen-Delfzijl* and thus, strictly speaking, there are no height restrictions. The only adverse effect of these structures is long waiting times when the bridges have to be opened. Because of the smaller dimensions of the Gouwe, capacity problems will arise on the Gouwe first before the storm surge barrier complex becomes a potential bottleneck for navigation. However, with the previously predicted number of vessels, capacity problems are not expected for the Gouwe. The estimated figures do not differ significantly from the high number of passages (11,639) in 2018, and back then no issues were reported.

The number of passages in 2018 also sheds new light on the estimated figures in Table C.7. If the number of passages in 2018 is not an outlier, the projections may soon be outdated. It is therefore advised to monitor the passages in the next years to determine if 2018 was indeed an outlier.

D

Hydra-NL: probabilistic modelling of hydraulic loads

The water levels and wave conditions for dikes and other hydraulic structures in the Netherlands can be calculated using the software package Hydra-NL. This program is included in the Wettelijk Beoordelingsinstrumentarium (WBI2017), a set of tools and guidelines used for the assessment of flood defences in the Netherlands (Ministerie van Infrastructuur en Milieu, 2016). The probabilistic model Hydra-NL calculates the hydraulic loads at a specific location and with a certain return period by combining the statistical properties of the global load variables (river discharge, sea level, wind speed, etc.) with databases in which the influence of those variables on the local hydraulic loads is collected. These databases that serve as input for the probabilistic model are created using hydrodynamic models (WAQUA or SOBEK) and wave models (SWAN).

This appendix elaborates on several aspects relevant to this study. Section D.1 elaborates on some of the parameters that could be adjusted in Hydra-NL by the user. In Section D.2, the latest versions of the model are compared since halfway through this study, a new version of Hydra-NL (version 2.8.2) was released. This comparison was necessary to assess whether calculations performed with the older version had to be redone.

D.1 User defined settings Hydra-NL

The Hydra-NL model requires several user defined parameters which need to be clarified in order to guarantee the reproducibility of the results of this study. These variables include the non-closure probabilities of the storm surge barriers, uncertainties in the hydraulic loads, sea level rise, and whether or not the river discharge should be capped at a certain value.

Storm surge barriers

The Maeslant barrier and Hartel barrier are assumed to be fully dependent in the model since they have one and the same operating system and the same closure criteria. These barriers are included in Hydra-NL as the Europoort barrier with a joint failure probability of 1/100 per closure. The Europoort barrier closes when the expected water level at Rotterdam or Dordrecht exceeds NAP +3.00 m or NAP +2.90 m, respectively. One of the parameters determining the water levels at these two locations is the sea water level at Hoek van Holland. The operating system of the barriers uses the predicted water level at Hoek van Holland to decide whether the water levels at Rotterdam or Dordrecht will exceed the closure levels. This process is also simulated in Hydra-NL where the uncertainty in the predictions of the water level at Hoek van Holland is modelled by a normal distribution. The recommended parameters for the normal distribution are a mean of -0.09 m and a standard deviation of 0.18 m. This implies that the predictions underestimate the water levels consistently by 9 cm (Chbab, 2015).

Uncertainties

Uncertainties can generally be classified as aleatory or epistemic. Aleatory uncertainties are related to the intrinsic randomness of nature, whereas epistemic uncertainties arise from a lack of knowledge (van Gelder, 2000; Walker et al., 2003). The natural variability of, for instance, sea water level and river discharge cannot be reduced, yet they can be modelled by probability distributions instead. This is also how Hydra-NL treats the aleatory uncertainties. Epistemic uncertainty follows from a limited amount of data to estimate the probability distributions and corresponding parameters or from uncertainties and simplifications in the models used

to simulate processes. In the past, epistemic uncertainty was not taken into account in the safety assessments of the flood defences (Chbab, 2015). However, in the current version of Hydra-NL, epistemic uncertainties can be included if desired or prescribed.

The first type of epistemic uncertainty is referred to as statistical uncertainty (van Gelder, 2000). In Hydra-NL, datasets of the stochastic variables with or without statistical uncertainties can be selected. For the calculations in this study, the datasets with statistical uncertainty were used since this is also required in the current assessment round with the WBI2017.

Model uncertainty is the second type of epistemic uncertainty (van Gelder, 2000). These uncertainties are location specific. Chbab and Groeneweg (2015) estimated the model uncertainties in the calculated water levels and wave conditions for different regions. For the region of the Rhine-Meuse delta, in which the Hollandsche IJssel barrier is located, the model uncertainty in the water level is included as a standard deviation of 0.15 m in case of an open Europoort barrier and 0.25 m for a closed Europoort barrier. Model uncertainties in the wave conditions are represented by a relative bias and a relative standard deviation. For the Hollandsche IJssel, the model uncertainties for the significant wave height and wave periods are shown in Table D.1.

Sea level rise

The sea level rise scenarios presented in Chapter 3 are relative to 1995 (1986-2005 average) and the datasets in Hydra-NL were constructed for the WBI2017. This means that the future sea level rise scenarios have to be corrected for the value that is used in Hydra-NL. According to Table M-1 of the user manual of Hydra-NL (Duits, 2020), the sea level rose by 10 cm at Hoek van Holland between 1990 and 2017. Between 1990 and 1995, the sea level increased by about 1.15 cm (follows from the 2.3 mm/year rise reported in the *Zeespiegelmonitor 2018* (Baart et al., 2019)). So, about 9 cm has to be deducted from the sea level scenarios used in the Hydra-NL calculations to obtain the correct water levels.

River discharge capping

The extreme river discharges increase with time due to climate change, but this increase is not unlimited. The discharges have a maximum because at a certain moment upstream areas in the Rhine basin will start to flood and the discharge peaks are reduced. Sperna Weiland et al. (2015), who looked at the implications of the KNMI'14 climate change scenarios on the river discharges, estimated the maximum Rhine discharge to be between 17,500 and 18,000 m^3/s in case upstream flooding is taken into account. Hydra-NL offers the option to include the capping of the Rhine discharge to a maximum value but since the effects of the river discharges on the water levels at the Hollandsche IJssel barrier were already small, the effects of upstream flooding are neglected and the river discharges are not capped. Moreover, Schoemaker (2016) showed quantitatively using the model Hydra-BS, a model similar to Hydra-NL, that the influence of capping the discharges is negligible for the water levels in the Hollandsche IJssel.

Summary of the user defined settings

The settings in Hydra-NL used for this study are summarised in Table D.1.

Table D.1: User defined settings in Hydra-NL used in this study.

Parameter	Value	Remark
Non-closure probability Europoort barrier	1/100 per closure	Maeslant barrier and Hartel barrier are included as a single barrier with a joint failure probability
Non-closure probability Hollandsche IJssel barrier	1/200 per closure	
Statistical uncertainties	Included in the databases	Can be opted out
Uncertainty in the predicted water level	μ = -0.09 m, σ = 0.18 m	Uncertainty in the predictions of the water level at Hoek van Holland is modelled by a normal distribution $N(\mu,\sigma)$
Model uncertainty water level	At New Meuse: Open barrier: σ = 0.15 m, Closed barrier: σ = 0.25 m	
Significant wave height (H_{m0})	Relative bias μ = -0.04, Relative std σ = 0.27	
Mean wave period ($T_{m-1,0}$)		Not applicable to the relatively small Hollandsche IJssel, peak period is used instead
Peak period (T_p)	Relative bias μ = +0.03, Relative std σ = 0.13	
River discharge capping	No capping	Effect of capping is limited

D.2 Comparison of Hydra-NL versions

During the course of this study, a new version (version 2.8.2) of the probabilistic model Hydra-NL was released. Several calculations that were performed in relatively early stages of this study (shown in Figure 3.15, Figure 4.2, Figure 4.4, and Figure 4.5) made use of an older version (version 2.7.1). These calculations did not have to be revised, as the effects of using the new version proved to be small for the Rhine-Meuse delta. The opposite applies to the water levels in the Hollandsche IJssel, as shown in the next sections.

D.2.1 Modifications impacting the results in front of the Hollandsche IJssel barrier

The new version, and the associated databases with the results from the hydrodynamic models, included only minor changes for the Rhine-Meuse delta. According to the impact analysis of this new version, the way of implementing the model uncertainty of the wave conditions has been adjusted. An option to include correlations between the wave conditions has been included as well. Although those adjustments are not relevant to the water levels in front of the barrier, there are still small differences when the results calculated with version 2.8.2 and version 2.7.1 are compared. However, these differences were so small that the calculations did not have to be reproduced with the new version of Hydra-NL (Figure D.1).

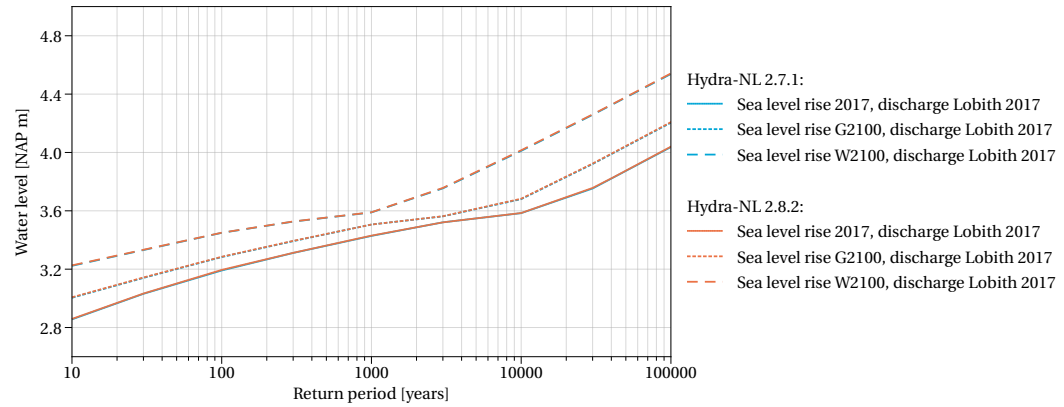

(a) Comparison for various amounts of sea level rise with the river discharge for the current climate.

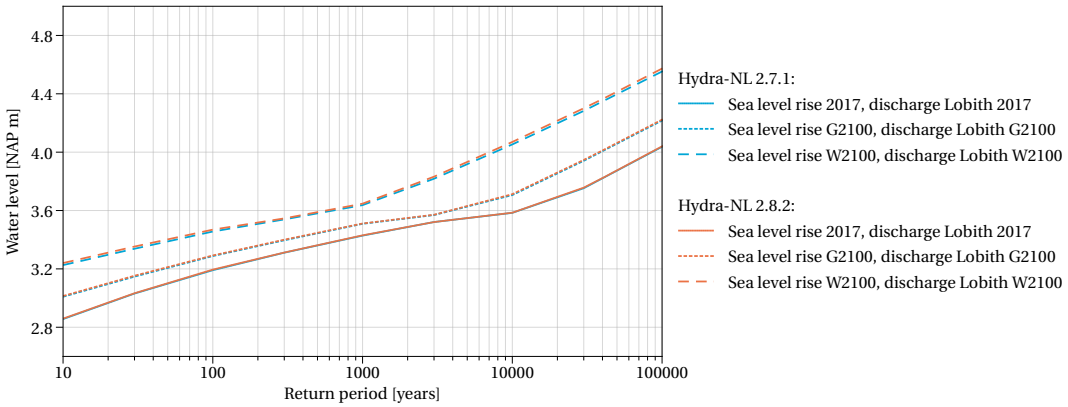

(b) Comparison for various amounts of sea level rise and corresponding river discharges.

Figure D.1: Comparison of the water levels in front of the Hollandsche IJssel barrier calculated with Hydra-NL version 2.7.1 and version 2.8.2 for various amounts of sea level rise and river discharges.

D.2.2 Modifications impacting the results behind the Hollandsche IJssel barrier

For the water levels behind the Hollandsche IJssel barrier, it is a different story due to several assumptions that were made in the hydrodynamic modelling. For example, the database for the Hollandsche IJssel was made under the assumption of open water wind conditions. This assumption is very conservative since the Hollandsche IJssel is not a wide river and there are quite a few buildings along the river. These factors prevent the wind from reaching open water wind speeds. A second assumption is related to the modelling of the closure operation of the barrier. It was assumed that the storm surge barrier closes at NAP +2.0 m and closures at slack water were not considered. Thirdly, the discharge of water from the polders was not explicitly included in the database. If the water levels in closed condition are lower than the "maalstoppeil", then these water levels are raised to the "maalstoppeil" of NAP +2.60 m (Rongen & Botterhuis, 2018).

The effects of those assumptions can be illustrated by comparing the water levels calculated with Hydra-NL version 2.7.1 with the results of two other studies. The first study, by Rongen and Botterhuis (2018), was a first step in improving the modelling of the water levels in the Hollandsche IJssel. This study still uses open water wind conditions and assumes that the barrier closes at NAP +2.0 m but includes improvements to the modelling of the translatory waves caused by lowering the lifting gate. The second study, performed by Rongen and Maaskant (2019), uses the the potential wind speed instead of open water wind speed, includes a closure level of NAP +1.80 m, improvements to the modelling of translatory waves, and accounts for the occurrence of closures at slack water. Rongen and Maaskant (2019) assume that on average 1/3 of the closures are closures at slack water with a discharge of 75 m^3/s from the polders into the river. The results are shown in Figure D.2.

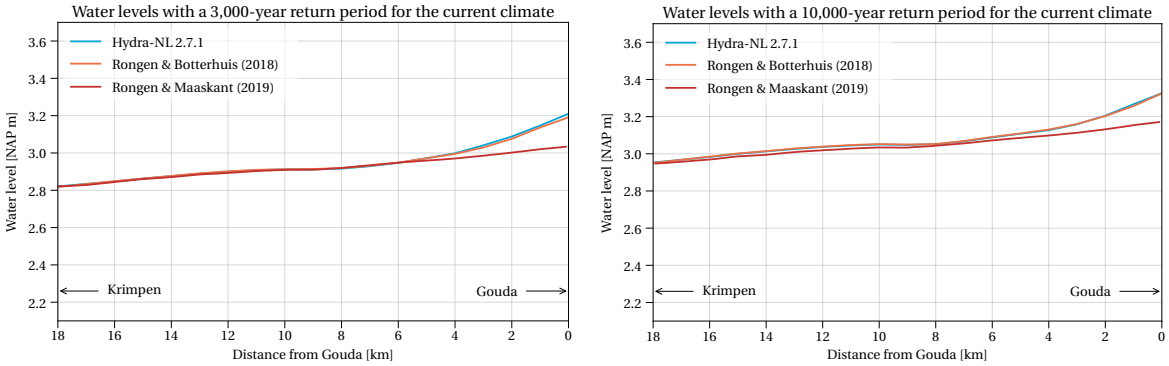

Figure D.2: Water levels in the Hollandsche IJssel for the current climate and closure reliability 1/200 per closure.

The adjustments by Rongen and Botterhuis (2018) are only related to the closed situation and the closed situation only starts to play a role near Gouda, where the wind set-up is strong. Hence, the differences between Hydra-NL version 2.7.1 and the results of the study by Rongen and Botterhuis (2018) in Figure D.2 are small in the current climate.

The difference between the results of Hydra-NL version 2.7.1 and the other two studies become more pronounced under future climate scenarios. The main reason is that in Hydra-NL the wind speed is coupled to the sea water level. As a result, sea level rise leads to higher wind speeds in the model. In the studies by Rongen and Botterhuis (2018) and Rongen and Maaskant (2019), additional SOBEK simulations were performed for the W+ scenario of KNMI'06 for the years 2050 and 2100. In those simulations, the sea level was raised and the same wind speeds as in the current situation were used. The impact of the coupling between wind speed and sea level is clearly visible in Figure D.3. The effect is strongest near Gouda where the wind set-up is greatest. An additional benefit of using the simulations for 2050 and 2100 is the correct modelling of closures, especially low water slack closures. When sea level rise is added to the calculation using a database based on the current climate, the rise is modelled as an additional storm surge under daily conditions instead of an increase in all water levels. This means that the simulated moments of closure are not entirely correct. However, the impact of this model shortcoming is of minor importance compared to the effect of the coupling between wind speed and sea level (Rongen & Maaskant, 2019).

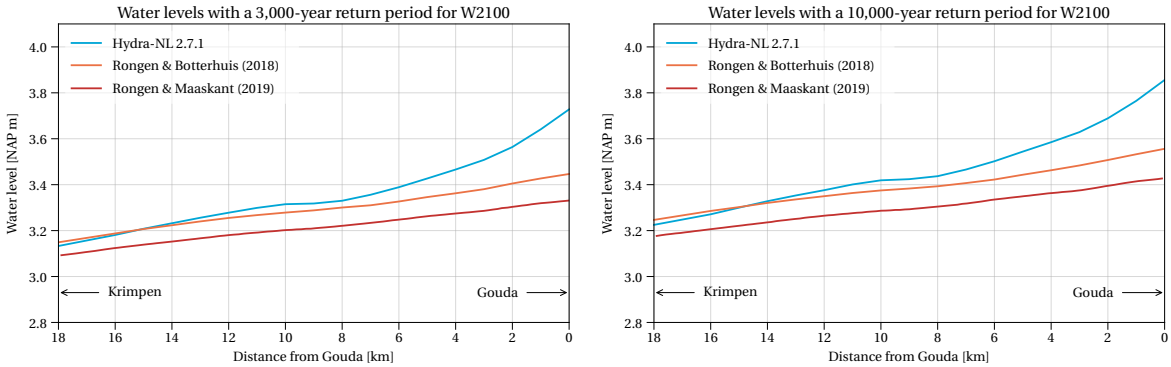

Figure D.3: Water levels in the Hollandsche IJssel for climate scenario W+ in 2100 and closure reliability 1/200 per closure.

The differences between Hydra-NL version 2.7.1 and the results of the study by Rongen and Maaskant (2019) are of such magnitude that the adjustments by Rongen and Maaskant (2019) were implemented in the latest version of Hydra-NL (version 2.8.2). This version was also used in this study to determine the water levels behind the Hollandsche IJssel barrier.

E

Sea level rise and the water levels behind the Hollandsche IJssel barrier

This appendix describes the analysis of how sea level rise translates into an increase in the local water levels behind the Hollandsche IJssel barrier. This analysis was performed with Hydra-NL (version 2.8.2). The results were used in Section 4.2 to derive a simple relationship between the increase in the local water levels behind the storm surge barrier and sea level rise.

E.1 Impact of sea level rise on the water levels in the Hollandsche IJssel

The water levels in the Hollandsche IJssel were visualised for various return periods and two scenarios of sea level rise to study how sea level rise impacts these water levels, see Figure E.1. The scenarios are the W+ scenario of KNMI'06 for the years 2050 and 2100. These scenarios are the only scenarios for which additional SOBEK simulations were performed to overcome the issue of coupling between wind speed and sea water level. These scenarios correspond to a sea level rise of 25 cm and 75 cm, respectively. The river discharge distribution of 2017 was used for all scenarios to include only the impact of sea level rise.

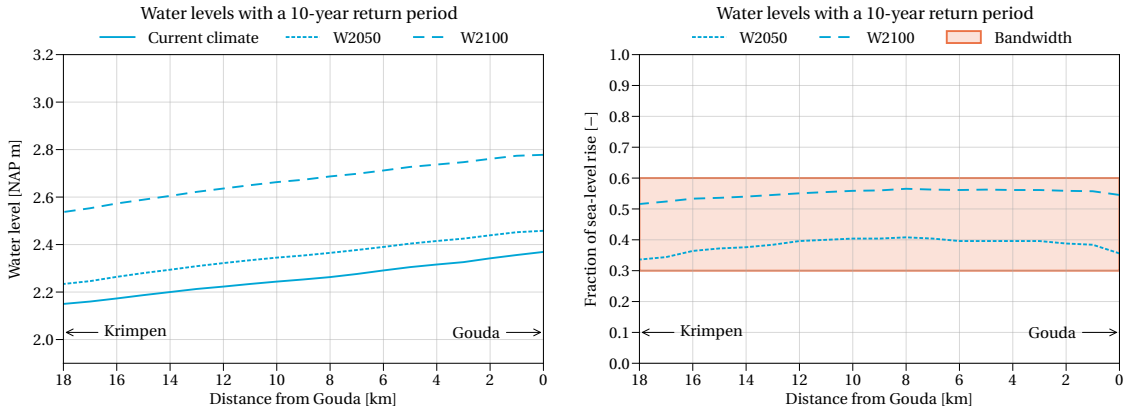

Figure E.1: Water levels in the Hollandsche IJssel (left) and increase in local water levels as a fraction of sea level rise (right) for various return periods and two scenarios of sea level rise. The bandwidth shown in the right figure follows from rounding up the first decimal place for the maximum values and rounding down the first decimal place for the minimum values.

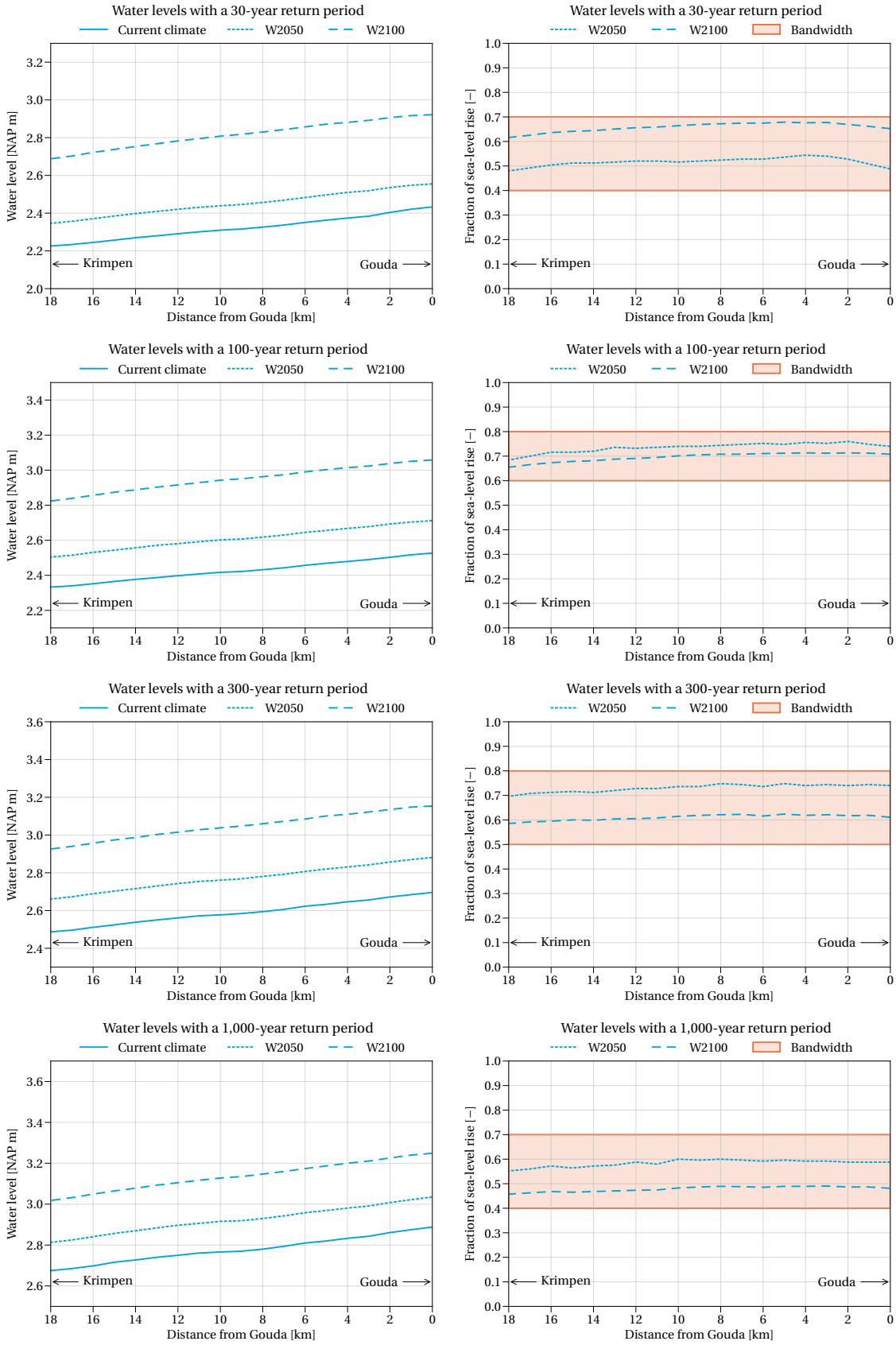

Figure E.1 (Cont.): Water levels in the Hollandsche IJssel (left) and increase in local water levels as a fraction of sea level rise (right) for various return periods and two scenarios of sea level rise. The bandwidth shown in the right figure follows from rounding up the first decimal place for the maximum values and rounding down the first decimal place for the minimum values.

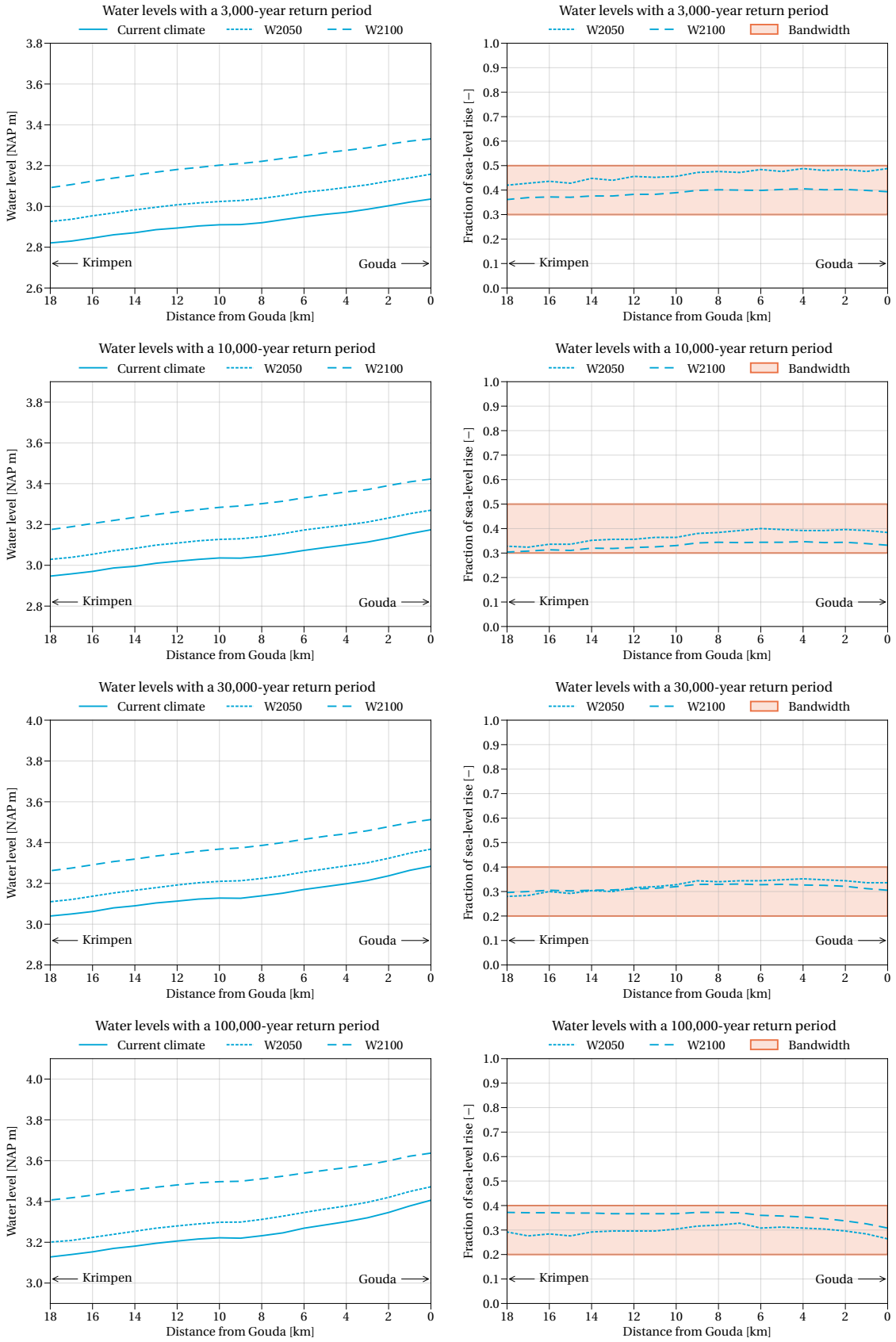

Figure E.1 (Cont.): Water levels in the Hollandsche IJssel (left) and increase in local water levels as a fraction of sea level rise (right) for various return periods and two scenarios of sea level rise. The bandwidth shown in the right figure follows from rounding up the first decimal place for the maximum values and rounding down the first decimal place for the minimum values.

The results in Figure E.1 display a wide variation in the impact of sea level rise. For shorter return periods, the water levels may increase by up to 0.8 times the sea level rise, while the increase can be as low as 0.2 times the sea level rise for the longer return periods. The reason for this large variability could be sought in the functioning of the storm surge barriers since these structures have a strong effect on the water levels. The relative contribution of different states of the Maeslant barrier and Hollandsche IJssel barrier to the water levels at 10 km from the Waaier lock are shown in Table E.1. The values in Table E.1 were examined for trends that could explain the behaviour observed in Figure E.1. The results were obtained for the location 10 km from the Waaier lock because this point is about midway of the river, where wind set-up is important but not expected to dominate the results.

Table E.1: Relative contribution of an open or closed Maeslant barrier (MLK) and open or closed Hollandsche IJssel barrier (HIJK) to the increase in water levels for different return periods and sea level rise scenarios. The relative contribution is based on the results for a location about halfway the Hollandsche IJssel (at 10 km from the Waaier lock).

Return period [years]	Sea level rise scenario	Fraction at 10 km	Relative contribution of the state of the storm surge barriers [MLK-HIJK]				Relative contribution of the state of the HIJK	
			Op-Op	Op-Cl	Cl-Op	Cl-Cl	Open HIJK	Closed HIJK
10	Current climate		94.7%	3.6%	1.5%	0.2%	96.2%	3.8%
	W2050	0.4	94.8%	3.5%	1.3%	0.4%	96.1%	3.9%
	W2100	0.56	98.8%	0.2%	0.4%	0.6%	99.2%	0.8%
30	Current climate		95.9%	2.1%	1.6%	0.3%	97.5%	2.4%
	W2050	0.52	73.5%	18.1%	1.5%	6.8%	75.0%	24.9%
	W2100	0.66	99.4%	0.0%	0.6%	0.0%	100.0%	0.0%
100	Current climate		77.3%	9.4%	5.2%	8.0%	82.5%	17.4%
	W2050	0.74	94.5%	0.8%	0.9%	3.8%	95.4%	4.6%
	W2100	0.7	99.0%	0.0%	1.0%	0.0%	100.0%	0.0%
300	Current climate		97.0%	0.5%	0.4%	2.0%	97.4%	2.5%
	W2050	0.74	98.8%	0.0%	1.2%	0.0%	100.0%	0.0%
	W2100	0.61	98.5%	0.0%	1.5%	0.0%	100.0%	0.0%
1000	Current climate		99.5%	0.0%	0.5%	0.0%	100.0%	0.0%
	W2050	0.6	98.6%	0.0%	1.4%	0.0%	100.0%	0.0%
	W2100	0.48	99.2%	0.0%	0.8%	0.0%	100.0%	0.0%
3000	Current climate		99.2%	0.0%	0.8%	0.0%	100.0%	0.0%
	W2050	0.46	97.9%	0.0%	2.1%	0.0%	100.0%	0.0%
	W2100	0.39	98.7%	0.0%	1.3%	0.0%	100.0%	0.0%
10 000	Current climate		98.9%	0.0%	1.1%	0.0%	100.0%	0.0%
	W2050	0.37	96.8%	0.0%	3.2%	0.0%	100.0%	0.0%
	W2100	0.33	97.7%	0.0%	2.3%	0.0%	100.0%	0.0%
30 000	Current climate		99.2%	0.0%	0.8%	0.0%	100.0%	0.0%
	W2050	0.33	96.7%	0.0%	3.3%	0.0%	100.0%	0.0%
	W2100	0.32	96.2%	0.0%	3.8%	0.0%	100.0%	0.0%
100 000	Current climate		99.0%	0.0%	1.0%	0.0%	100.0%	0.0%
	W2050	0.3	96.9%	0.0%	3.1%	0.0%	100.0%	0.0%
	W2100	0.37	95.1%	0.0%	4.9%	0.0%	100.0%	0.0%

Op stands for Open, Cl stands for Closed. So Op-Cl means open Maeslant barrier and closed Hollandsche IJssel barrier.

The analysis presented in Table E.1 reveals some interesting findings about the variation in the increase in the local water level due to sea level rise. As mentioned before, this variation may be the result of the different contributions of the two states of both storm surge barriers. The data in Table E.1 indicates that the water levels for all return periods are dominated by the situation with a open Maeslant barrier and open Hollandsche IJssel barrier. The situation with an open Hollandsche IJssel barrier and open or closed Maeslant barrier even completely determines the water levels for return periods longer than 1,000 years. Since the failure to close the storm surge barriers dominates the water levels in the hinterland, the exceedance probability of water levels behind the storm surge barrier $P_{bb}(h)$ may be approximated by multiplying the exceedance probability of

the water levels in front the barrier $P_{fb}(h)$ by the non-closure probability of the barrier P_{nc}:

$$P_{bb}(h) = P_{nc} \cdot P_{fb}(h) \tag{E.1}$$

Together with the characteristic values of the water level measurements at Hoek van Holland (the measuring station in front of the Maeslant barrier), Equation (E.1) was used to estimate the water levels behind the Maeslant barrier and Hollandsche IJssel barrier. The resulting frequency curves are shown in Figure E.2.

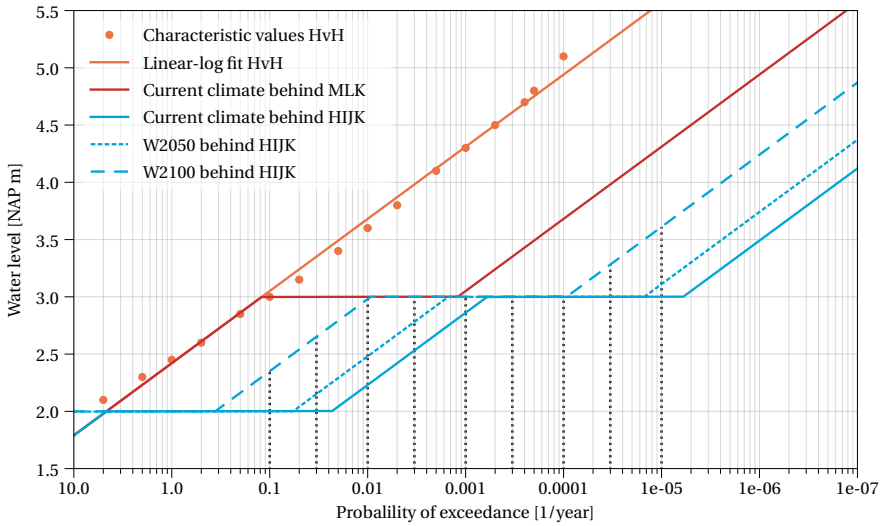

Figure E.2: Simplified illustration of the water levels behind the Maeslant barrier and Hollandsche IJssel barrier, based on the water levels at Hoek van Holland and Equation (E.1) with a non-closure probability of 1/100 and 1/200 per closure for the Maeslant barrier and Hollandsche IJssel barrier, respectively.

The frequency curves of the water levels behind the storm surge barriers in Figure E.2 are highly simplified. Other factors such as the prediction error for the closure of the barriers, wind set-up, and in the case of the Hollandsche IJssel barrier, extreme river discharges also influence these water levels. Nevertheless, the figure illustrates reasonably well why the influence of sea level rise varies so much for the different return periods. If one compares the water levels for different return periods in Figure E.1 with the lines for the water levels behind the Hollandsche IJssel barrier in Figure E.2, it becomes apparent that the increase due to sea level rise is greatest for the return periods that lie on the sloped parts of the curve. The effect of sea level rise is not entirely nil for the flat sections of the curves as the influence of sea level rise decreases land inwards, while the effects of river discharge and wind set-up increase. Hence, the calculated increase in water levels varies between 0.3 and 0.8 times the sea level rise.

E.2 Validation of the water levels with sea level rise

The analysis in the previous section demonstrates the large variability in the influence of sea level rise on the water levels in the Hollandsche IJssel, which makes it difficult to obtain a good relationship between sea level rise and the water levels in the Hollandsche IJssel for a range of sea level rise scenarios. Yet, the analysis also shows that the extreme water levels are dominated by the situation with an open Hollandsche IJssel barrier (and open Maeslant barrier). Given this fact, the water levels directly behind the Hollandsche IJssel barrier may be approximated by Equation (E.1) in which P_{nc} is the non-closure probability of the barrier and $P_{fb}(h)$ the exceedance probability of the water levels in front of the barrier.

The validity of Equation (E.1) was verified through comparison with the frequency curves for the current climate and the two scenarios of sea level rise obtained from Hydra-NL. Because Hydra-NL only generates frequency curves for return periods longer than 10 years, the shortest return period that could be calculated with Equation (E.1) is $10/P_{nc}$. This limitation is not of major concern for the specific application of the equation as only the water levels with return periods in the order of 10,000 years are of interest. Although shorter return periods are not important, the frequency curves determined using with Equation (E.1) were linearly extrapolated to a return period of 100 years for the comparison with the curves obtained from Hydra-NL. The results are depicted in Figure E.3.

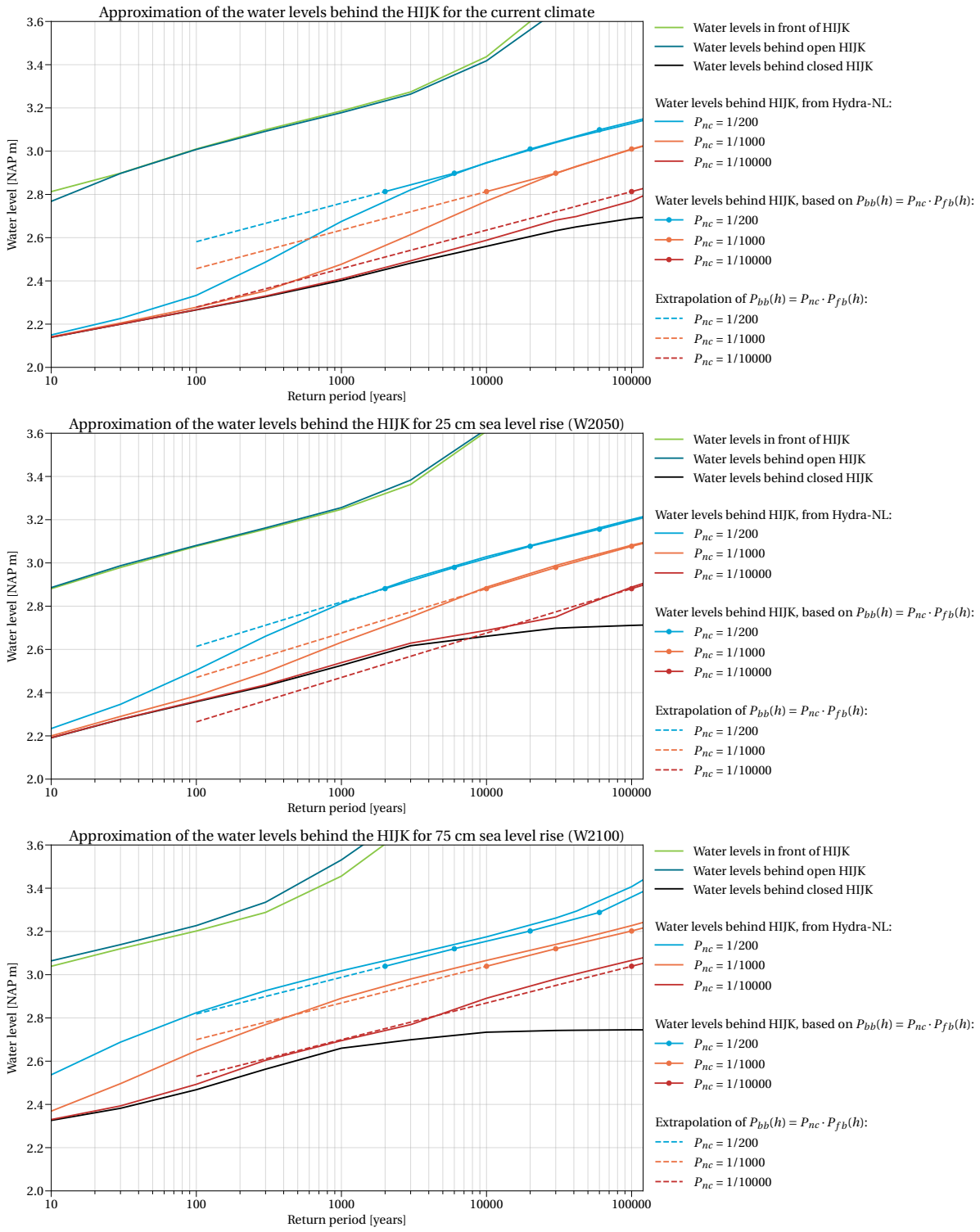

Figure E.3: Comparison of the approximation of the water levels behind the Hollandsche IJssel barrier (HIJK) using Equation (E.1) and the frequency curves obtained from Hydra-NL.

As becomes apparent from Figure E.3, using Equation (E.1) results in reasonably good approximations of the actual water levels behind the Hollandsche IJssel barrier. The estimated frequency curves show similar trends as the curves calculated with Hydra-NL, though the water levels are overestimated as the return period decreases. This inaccuracy for shorter return periods is due to the open condition becoming less dominant for shorter return periods. However, as sea level rises, the relative contribution of the open situation increases, and the disparity between the approximated water levels and actual water levels reduces.

Besides the good agreement between the estimated frequency curves and frequency curves from Hydra-NL for the three climates, the estimated curves also show good fitness for various closure reliabilities of the barrier. This result implies that the Equation (E.1) could also be used to estimate the water levels for other non-closure probabilities than the current 1/200 per closure.

Equation (E.1) may be useful when approximating the water levels directly behind the Hollandsche IJssel barrier, but for the more upstream locations, wind set-up becomes of importance. The curves in Figure E.1, however, indicate that the effect of wind set-up is almost constant for all return periods and sea level rise scenarios. In order to verify this impression, the increase in the water levels along the Hollandsche IJssel with respect to the water level at Krimpen (directly behind the barrier) are plotted in Figure E.4.

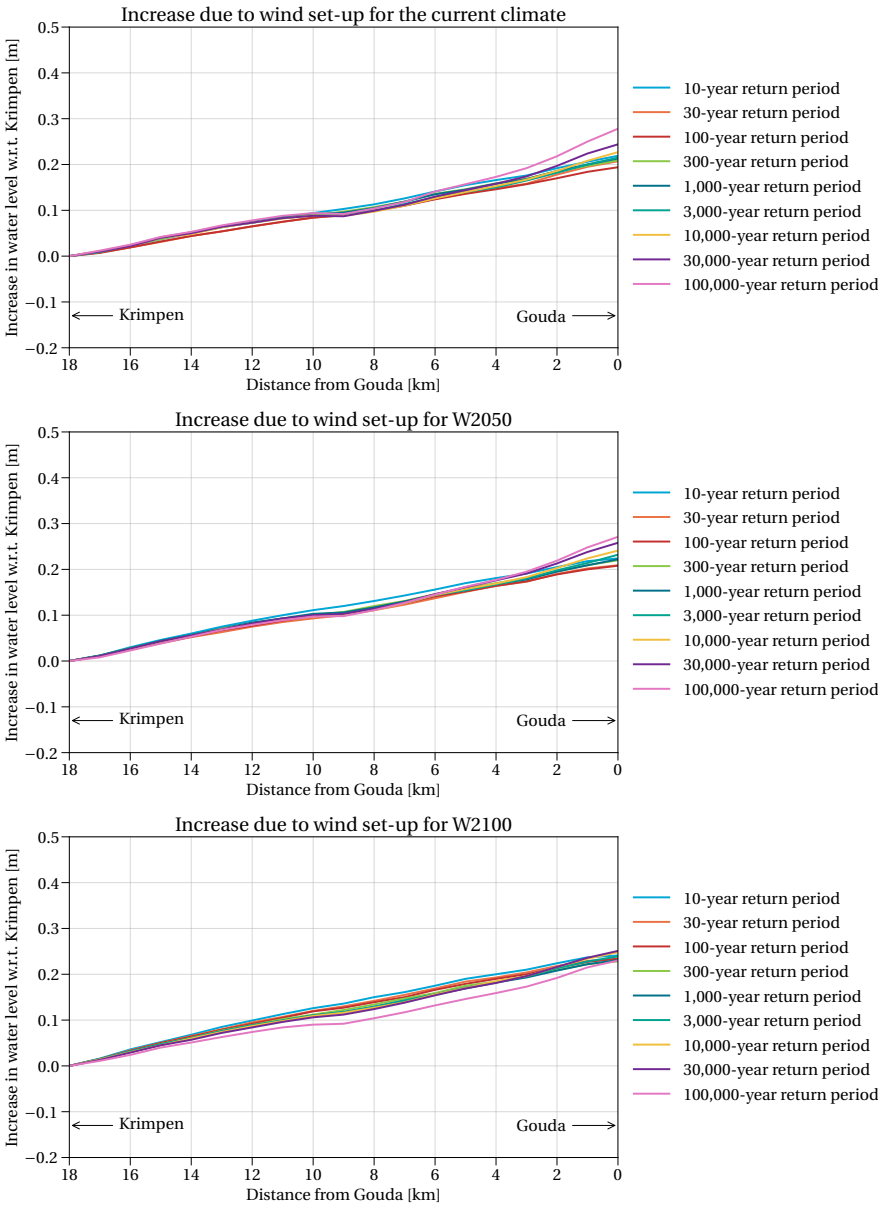

Figure E.4: Increase in the water levels in the Hollandsche IJssel with respect to the water levels at Krimpen a/d IJssel due to wind set-up.

As can be seen in Figure E.4, the increase in the upstream water levels due to wind set-up is indeed fairly constant. This stable increase in the upstream water levels implies that it is sufficient to compute the water level at a single location to assess the functional performance with respect to flood protection. For that reason, the water levels directly behind the barrier, calculated with Equation (E.1), were used in the assessment of the remaining life in Chapter 4.